Remarks/Argument

This paper is being filed in response to the Office Action mailed September 8, 2004, and is being submitted along with a Request for Continued Examination (RCE). Per the petition and fee submitted herewith, the Applicants have extended the time for responding by three months, to March 8, 2005. The fee for the Request for Continued Examination is also submitted herewith. The Commissioner is hereby authorized to charge any additional fees required for filing of this paper or the RCE, or credit any overpayments, to deposit account no. 50-2719.

Claim 1 has been amended to indicate that the claimed ASIC channel protein constitutes some or all of a mammalian neuronal cationic channel. Support for this amendment is found on page 4, lines 7-17, which disclose that the ASIC channels can be hybrids constituted by different proteins of the invention. No new matter has been added by these amendments.

Claims 12, 13 and 15 have been amended to more clearly indicate that the claimed nucleic acid sequence includes the recited nucleotides by which the claimed sequence is bounded. No new matter has been added by these amendments.

Claims 22 and 28 have been amended to correct minor errors and to fix their dependencies. Claims 23 and 29 have been amended to correct minor grammatical errors. No new matter has been added by these amendments.

Based on the above changes and the following remarks, the Applicants respectfully request reconsideration of the claims.

Response to the Section 101 rejection

Claims 1, 11-13, 15, 17-23 and 26-29 are rejected under 35 U.S.C. § 101 as allegedly lacking utility, and are also rejected under § 112, 1st paragraph because one skilled in the art would allegedly not know how to use the invention if an appropriate utility has not been established. The Applicants respectfully traverse these rejections.

A claimed invention meets the utility requirements of § 101 if one skilled in the art would appreciate why such invention is useful and if the utility is specific, substantial and credible. *Utility Examination Guidelines*, 66(4) F.R. 1092, 1098, January 5, 2001. Where the applicant has asserted that a claimed invention is useful for any particular practical purpose (*i.e.*, it has a "specific and substantial utility"), and the assertion would be considered credible by a person of

ordinary skill in the art, then a rejection based on lack of utility should not be imposed. *Id.* Here, the application explicitly asserts several specific, substantial and credible utilities. Claims 1, 11-13, 15, 17-23 and 26-29 therefore satisfy the requirements of § 101.

This application asserts, among other utilities, that the claimed channels are useful in identifying drugs for the prevention or treatment of pain (pg. 8, lines 25-26), especially acid-induced pain associated with ischemia (pg. 9, lines 8-11), treatment of neurodegenerative disorders (pg. 9, lines 2-3), and the identification of agents that modulate taste (pg. 9, line 1 and pg. 11, lines 1-4). The neurodegenerative disorders that can be treated by targeting ASIC channels constituted by proteins of the invention include Alzheimer's disease, Huntingdon's disease, Parkinson's disease, amyotrophic lateral sclerosis and cerebellar ataxia (pg. 10, lines 3-9).

A claimed invention need not accomplish every asserted utility. As long as the claimed invention meets at least one stated utility, the utility requirement is satisfied. *Stiftung v. Renishaw PLC*, 20 USPQ2d 1094, 1100 (Fed. Cir. 1991). The Revised Interim Utility Guidelines Training Materials (http://www.uspto.gov/web/menu/utility.pdf) ("Training Materials") teach that an asserted utility for treating a disease is specific and substantial.

Example 3 of the Training Materials is particularly pertinent. Example 3 reads, in relevant part, as follows:

> The specification discloses a protein having the amino acid sequence of SEQ ID NO: 1 and discloses that the protein can be made by protein synthesis techniques well known in the art. The only disclosed utility for the protein is for curing Alzheimer's disease. There is no other disclosure of any chemical, physical, or biological properties of the protein. There are 98 pages of specification which disclose alternate administration techniques and dosages that are very specific, conventional techniques for protein administration. There are no working examples that demonstrate the specifically asserted utility.
>
> Claim: 1. The isolated protein consisting of the amino acid sequence set forth in SEQ ID NO: 1.
>
> Analysis: The following analysis includes the questions that need to be asked according to the guidelines and the answers to those questions based on the above facts:
>
> * * *

2) Has the applicant made any assertion of utility for the specifically claimed invention? Here, there is an asserted utility, *i.e.*, curing Alzheimer's disease.

3) Is the asserted utility specific? Curing Alzheimer's disease, a well known disease, clearly defines a use that depends upon the particular protein disclosed. Therefore, the utility is specific.

4) Is the asserted utility "substantial"? Since a cure for Alzheimer's disease is a desirable outcome based upon a need in the art, the disclosed use of the claimed protein is substantial and "real world".

Thus, Example 3 of the Training Materials makes clear that an asserted utility involving the treatment of a disorder (such as Alzheimer's disease) with the claimed protein is both specific and substantial.

Here, the Applicants have made an assertion of utility for the specifically claimed invention; namely, that the claimed ASIC channels can be used to diagnose and cure specific neurodegenerative diseases, including Alzheimer's disease. The Applicants also assert that the claimed ASIC channels can be used in the treatment of pain (especially pain associated with ischemia) and to alter the taste perception. Questions 2 through 4 presented in Example 3 of the Training Materials can therefore be answered in the affirmative with respect to the presently claimed invention:

2) Has the applicant made any assertion of utility for the specifically claimed invention?

Yes, there is an asserted utility, *i.e.*, treating Alzheimer's disease and other neurodegenerative diseases such as Huntingdon's disease, Parkinson's disease, amyotrophic lateral sclerosis and cerebellar ataxia. A utility of treating pain (for example from ischemia) is also made.

3) Is the asserted utility specific?

Yes. Treating Alzheimer's disease, Huntingdon's disease, Parkinson's disease, amyotrophic lateral sclerosis and cerebellar ataxia, which are all well known diseases, clearly defines a use that depends upon the particular channels disclosed and claimed. Treating pain, a well-known and well-characterized phenomenon, also clearly defines a use that depends upon the particular channels disclosed and claimed. Therefore, these asserted utilities are specific.

4) Is the asserted utility "substantial"?

> ***Yes***. Since a treatment for Alzheimer's disease, Huntingdon's disease, Parkinson's disease, amyotrophic lateral sclerosis, cerebellar ataxia and pain are desirable outcomes based upon a need in the art, the disclosed uses of the claimed protein are substantial and "real world."

The application thus presents the same situation as that shown in Example 3 of the Training Materials, for a number of asserted utilities. Indeed, the present disclosure goes beyond Example 3, as the present application also contains ample disclosure regarding the chemical, physical and biological properties of the claimed ASIC channel and the proteins constituting it. (In Example 3, utility was found even though "[t]here is no other disclosure of any chemical, physical, or biological properties of the protein.") The asserted utilities of diagnosing and treating specific neurodegenerative diseases, such as Alzheimer's disease, and of treating pain (such as ischemic pain) are therefore specific and substantial.

Where one or more uses for an invention are set forth in the specification, a rejection for lack of utility should not be made or maintained unless an Examiner has reason to doubt the objective truth of the asserted utility. A reason to doubt an invention's asserted utility may be established when the written description suggests an inherently unbelievable undertaking or involves implausible scientific principles. *In re Cortright*, 49 USPQ2d 1464, 1466 (Fed. Cir. 1999). However, the use of the claimed proteins constituting the ASIC channels for the diagnosis or treatment of neurodegenerative diseases or pain is not inherently unbelievable, nor does it involve implausible scientific principles. See, *e.g.*, the working examples of the application, which begin on pg. 15.

In particular, the experiments presented in the working examples show that the claimed proteins constituting the ASIC proton-activated cationic channels are expressed not only in the sensory neurons, but also in the neurons of the central nervous system (see Figs. 7a and 7b). Figs. 8a and 8b show that mRNA for proteins constituting the ASIC channels is expressed by the small neurons of the dorsal root ganglion, which supports the fact that ASIC is the rapidly desensitizing proton-activated cationic channel expressed in the nociceptive sensory neurons. The results of the *in-situ* hybridization shown in Fig. 8c show a broad and heterogeneous expression of proteins constituting the ASIC channel throughout the brain, with the highest

levels of expression observed in the principal olfactory bulb, the cerebral cortex, the hippocampus, the habenula, the basolateral amygdaloid nucleus and the cerebellum.

Several post-filing publications support the utilities disclosed in this application for the claimed proteins constituting the ASIC channels. For example, Pan et al., J. Phys. (1999), 518: 857 and Benson et al., Circ. Res. (1999), 84: 921 (copies enclosed) report that acidic conditions during myocardial ischemia contribute to afferent fiber sensitization through ASIC channel activity. Askwith et al., Neuron (2000), 26: 133 (copy enclosed) states in the abstract that acidosis is associated with inflammation and ischemia, and that this acidosis activates cation channels in sensory neurons. Askwith et al. also show that certain neuropeptides modulate pain by inducing sustained currents in neuronal ASIC channels, which implicates such channels in nociception.

From the data presented in the present application, and from the post-filing studies discussed above, one skilled in the art would find the asserted utilities for the claimed ASIC channels to be credible.

The Examiner has made specific comments in the Office Action regarding the credibility of the asserted utilization. For example, the Examiner considers that the specification and the art of record do not provide any specific function or biological significance of the claimed cationic ASIC channel. The Examiner considers that the functions of the claimed cationic ASIC channel are based entirely on conjecture from homologous polypeptides such as MDEG. However, the specification discloses at page 19, lines 1-3 that the ASIC channel protein exhibits approximately 67% sequence homology with the degenerine ionic channel referred to as MDEG (Reference 14: Waldmann and al., 1996, *J. Biol. Chem.*). The specification also discloses that the electrophysiological properties of MDEG in *Xenopus* oocytes are clearly different by comparison with ASIC. More particularly:

- The MDEG channel is not activated by the same pH changes as the ASIC channel (see Fig. 5). MDEG requires much more acidic pH (<pH5) for activation than ASIC1 (<pH7).

- The substitution of the glycine residue in position 430 of MDEG by an acid-inhibiting amino acid such as valine or phenylalanine activates the MDEG channel. Analogous mutations of ASIC (glycine residue in position 431 replaced by valine or phenylalanine) do not lead to

increased ASIC channel activity, as these ASIC mutants can not be activated by protons (pg. 19, lines 7-12).

- ASIC channels (ASIC1a and ASIC1b) are modulated by neuropeptide FF, whereas MDEG is not affected by this neuropeptide (see Askwith et al., *supra*; and Deval et al., Neuropharmacology (2003), 44: 662; copy enclosed).

- ASIC channels containing the MDEG subunit are potentiated by Zn2+, whereas homomeric ASIC1 channels are not affected by Zn2+ (see Baron et al. (2001), J Biol Chem, 276: 35361; copy enclosed).

- ASIC1a activity is blocked by tarantula toxin PcTx1, whereas MDEG is not affected by this toxin (see Escoubas et al. (2000), J Biol Chem, 275: 25116; copy enclosed).

Thus, the Applicants are not basing the asserted utilities of the claimed peptides on comparisons with the MDEG channel, but rather have shown a specific, substantial and credible utility based on the disclosure and data of the present application.

The Examiner also considers that the specification and the art of record do not describe any diseases directly related to ASIC channel dysfunction. The Examiner further considers that the role of ASIC channel function in brain is obscure, based on the Berdiev et al. reference.

Berdiev et al. concerns ASIC channels in tumor cells and gliomas, and not in untransformed glia. Extensive genetic recombinations of chromosome 17, where the MDEG gene is located, occur frequently in brain tumors such as neuroblastoma (Lastowska et al. (2002), Genes Chromosomes Cancer 34: 428; abstract enclosed). The MDEG gene spans more than 1% of chromosome 17 (this can be verified on http://genome.ucsc.edu), and the unusual ASIC currents recorded by Berdiev et al. could well be caused by rearrangement of the MDEG gene. The ASIC currents reported by Berdiev et al. in malignant glioma were never recorded, either by them or by others, in native neurons or glia. The article by Berdiev et al. is thus not an adequate reference for describing the properties or the role of ASIC channels in native neurons or glia.

The Applicants have also enclosed an article by Zhi-Gang Xiong et al. (*Cell*, 2004, 118: 687) and comments on this article (The Lancet Neurology, 2004, vol. 3 ; and N. Engl. J. Med., 2005, vol. 352). The article and comments show that both a ASIC1a blockers (such as PcTX1) or ASIC1a gene knock-out reduce neuronal damage due to ischemia in the brain. As a

consequence, blockers of ASIC1a activity would become relevant drugs for the prevention of brain damage after ischemia.

Thus, diseases directly related to ASIC channels are described in the literature. The present application also details many diseases and disorders directly linked to ASIC channels, as discussed above, including neurodegenerative disorders and pain due to ischemia

In light of the foregoing, it is submitted that the utility asserted in the specification is credible, as well as specific and substantial. It is respectfully requested that the rejection based on 35 U.S.C. § 101 be reconsidered and withdrawn.

Response to the section 112, 1st paragraph rejection

Claims 1, 11-13, 15, 17-23 and 26-29 are rejected under 35 U.S.C. §112, first paragraph. This rejection follows from and is dependent upon the §101 rejection discussed above; stating, in essence, that one skilled in the art would not know how to use the claimed invention because an appropriate utility has allegedly not been established. For the reasons set forth above, the application does, in fact, set forth sufficient, specific, substantial and credible utilities for the claimed proteins constituting the ASIC channels. Thus, one skilled in the art would know how to make and use the claimed invention. The Applicants therefore respectfully requested that the §112, 1st paragraph enablement rejection of claims 1, 11-13, 15, 17-23 and 26-29 be withdrawn.

Conclusion

Based on the foregoing, the Applicants respectfully submit that the Application is now in a condition for allowance, which is respectfully requested.

Respectfully submitted,

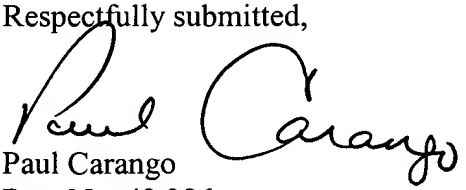

Paul Carango
Reg. No. 42,386
Attorney for Applicants

PC:rb
(215) 656-3320

Role of protons in activation of cardiac sympathetic C-fibre afferents during ischaemia in cats

Hui-Lin Pan *†, John C. Longhurst ‡, James C. Eisenach * and Shao-Rui Chen *

*Department of Anesthesiology and †Department of Physiology & Pharmacology, Wake Forest University School of Medicine, Winston-Salem, NC 27157 and ‡Division of Cardiovascular Medicine, Department of Internal Medicine, University of California School of Medicine, Davis, CA 95616, USA

(Received 22 March 1999; accepted after revision 30 April 1999)

1. Chest pain caused by myocardial ischaemia is mediated by cardiac sympathetic afferents. The mechanisms of activation of cardiac afferents during ischaemia remain poorly understood. Increased lactic acid production is associated closely with myocardial ischaemia. The present study examined the role of protons generated during ischaemia in activation of cardiac sympathetic C-fibre afferents.

2. Single-unit activity of cardiac afferents innervating both ventricles was recorded from the left sympathetic chain in anaesthetized cats. Epicardial tissue pH was measured within 1–1·5 mm of the surface by a pH-sensitive needle electrode. Responses of cardiac afferents to myocardial ischaemia, lactic acid, sodium lactate, acidic phosphate buffer and hypercapnia were determined.

3. Occlusion of the coronary artery for 5 min decreased epicardial tissue pH from 7·35 ± 0·21 to 6·98 ± 0·22 ($P < 0·05$). Epicardial placement of isotonic neutral phosphate buffer, but not saline, prevented the ischaemia-induced decrease in epicardial pH. This manoeuvre significantly attenuated the response of 16 afferents to 5 min of ischaemia (1·56 ± 0·23 pre-treatment *vs.* 0·67 ± 0·18 impulses s^{-1}). Topical application of 10–100 $\mu g\ ml^{-1}$ of lactic acid, but not sodium lactate, concentration-dependently stimulated 18 cardiac afferents. Inhalation with high-CO_2 gas failed to activate 12 separate cardiac afferents. Furthermore, lactic acid stimulated cardiac afferents to a greater extent than acidic phosphate buffer solution, applied at a similar pH to the same afferents.

4. Collectively, this study provides important *in vivo* evidence that protons contribute to activation/sensitization of cardiac sympathetic C-fibre afferents during myocardial ischaemia.

Chest pain, or angina pectoris, is one of the hallmarks of myocardial ischaemia although 'silent' ischaemia (lack of pain perception) also occurs in some patients with coronary artery disease. Sympathetic and vagal nerves innervating the heart contain not only autonomic efferent axons but also afferent fibres that transmit signals generated by cardiac sensory receptors (White, 1957; Cervero, 1994). Cardiac primary afferents running in the sympathetic nerves, especially finely myelinated Aδ- and unmyelinated C-fibre afferents, generally are considered to be the essential pathways for transmission of cardiac nociception to the central nervous system during myocardial ischaemia (White, 1957; Baker *et al.* 1980; Cervero, 1994). In this regard, removal of both stellate ganglia and excision of the first to the fifth thoracic sympathetic ganglia relieves cardiac pain in patients with ischaemic heart disease (White, 1957). Occlusion of coronary arteries also produces severe pain and pseudaffective reactions in dogs and cats, which can be abolished by thoracic sympathectomy but not vagotomy (Moore & Singleton, 1935; Brown, 1967). There is ample evidence demonstrating that myocardial ischaemia excites a subgroup of cardiac sympathetic afferents, namely, ischaemically sensitive afferents, which transmit nociceptive information to the central nervous system to elicit cardiac pain perception (Brown, 1967; Nishi *et al.* 1977; Bosnjak *et al.* 1979; Chandler *et al.* 1989, 1998; Pal *et al.* 1989). Furthermore, activation of cardiac sympathetic afferents during ischaemia is known to initiate neural reflexes, which lead to haemodynamic alterations and arrhythmias (Malliani *et al.* 1969). Although adenosine was initially considered as the metabolite responsible for activation of cardiac afferents during ischaemia (Thames *et al.* 1993; Gnecchi-Ruscone *et al.*

1995), several recent studies have failed to demonstrate that adenosine is capable of stimulating cardiac sympathetic afferents (Pan & Longhurst, 1995; Veelken *et al.* 1996; Abe *et al.* 1998). Thus, the mechanisms of activation of cardiac nociceptors during ischaemia remain unclear.

Under physiological conditions, extracellular hydrogen ion concentrations are regulated within a very narrow range, and buffering of protons in the extracellular space minimizes changes in pH around sensory nerve endings (Poole-Wilson, 1978). It has long been recognized that myocardial ischaemia is associated with local acidosis, and that both intracellular and extracellular pH fall markedly during ischaemia (Opie *et al.* 1973; Poole-Wilson, 1978). Protons have been known to play a dominant role in excitation/sensitization of cutaneous nociceptors, pulmonary vagal afferents and abdominal sympathetic afferents (Steen *et al.* 1992, 1995; Stahl & Longhurst, 1992; Hong *et al.* 1997). Furthermore, intracoronary injection of lactic acid elicits a pseudaffective response in lightly anaesthetized animals (Guzman *et al.* 1962). However, the contribution of endogenously accumulated protons to activation of cardiac sympathetic afferents during ischaemia has not been studied directly. In the present study, by directly recording single-unit activity of cardiac sympathetic C-fibre afferents, we tested the hypothesis that protons produced during myocardial ischaemia play a role in activation of ischaemia-sensitive cardiac afferents.

METHODS

Surgical preparations

The surgical preparations and experimental protocols were approved by the Animal Care and Use Committee at Wake Forest University School of Medicine and the University of California at Davis. Adult cats of either sex were anaesthetized with ketamine (30 mg kg^{-1}, I.M.) and anaesthesia was maintained with α-chloralose (60–80 mg kg^{-1}, I.V.). Supplemental doses of α-chloralose (5–10 mg kg^{-1}) were given as necessary to maintain an adequate depth of anaesthesia, assessed by lack of nociceptive reflexes and fluctuation of blood pressure and heart rate. A femoral artery and vein were cannulated for measurement of pressure and administration of fluids and drugs, respectively. The trachea was intubated and respiration maintained artificially with an animal ventilator (model CIV-101, Columbus Instruments, Columbus, OH, USA). The left carotid artery was cannulated with a Millar catheter (catheter-tip pressure transducer), which was passed retrogradely into the left ventricle for monitoring the left ventricular pressure. A PE 60 catheter was also introduced into the left atrium through the left atrial appendage for intracardiac injection of drugs. Arterial blood pressure was measured with a pressure transducer (model PT300, Grass Instruments). Arterial blood gases were analysed with a blood gas analyser and maintained within physiological limits ($P_{O_2} > 100$ mmHg, P_{CO_2} 35–40 mmHg, pH 7·35–7·45). When necessary, arterial P_{O_2} was increased by enriching the inspired O_2 supply; pH was corrected by administering $NaHCO_3$ (1 M, I.V.) and/or adjusting ventilation. The haemodynamic parameters were monitored and maintained stable (mean arterial pressure: 70–99 mmHg; heart rate: 110–130 beats min^{-1}; left ventricular end-diastolic pressure: 3–4 mmHg) throughout the experiment. Blood from a donor cat or 6% dextran was infused when necessary to keep the haemodynamics in the above range. Body temperature was maintained in the range 37–38 °C with a circulating water heating pad and heat lamps. Animals were killed at the end of experiments by an intravenous injection of an overdose of sodium pentobarbital.

Recording of cardiac sympathetic afferents

A midline sternotomy was performed and the first to seventh left ribs and the upper lobe of the left lung were removed. The fascia overlying the left paravertebral sympathetic chain from T2 to T6 was removed. The chain and rami communicantes were then draped over a plastic platform and covered with warm mineral oil. Small nerve filaments were teased gently from the chain or rami communicantes between T2 and T5 under an operating microscope (model M900, D.F. Vasconcellos S.A., São Paulo, Brazil). The rostral end was placed across a recording electrode, which was connected to a high impedance probe. The nerve filaments were dissected gradually until single-unit activity of a cardiac afferent nerve was isolated (Pan & Longhurst, 1995; Huang *et al.* 1995; Tjen-A-Looi *et al.* 1998). The action potential of the afferent was amplified and processed through an audioamplifier (model AM8, Grass Instruments) and displayed on an oscilloscope (model 450, Gould). The neurogram, blood pressure and left ventricular pressure were simultaneously monitored on a recorder (model K2G, Astro-Med, W. Warwick, RI, USA). In addition, afferent nerve activity was fed into a Pentium computer through an analog-to-digital interface card for subsequent off-line quantitative analysis. Discharge frequency was quantified by using a data acquisition and analysis software (DataWave Technology, Inc., Longmont, CO, USA) and a histogram was created for each afferent nerve. Accurate counting of the afferent nerve discharge frequency was verified for each afferent by comparing the constructed histogram with the original neurogram. The precise location of afferent nerve endings was confirmed using a stimulating electrode placed directly on the receptive field of the afferent to electrically evoke the action potential of the afferent fibre. We have found that this method is the most accurate means of locating afferent nerve endings on the beating heart (Pan & Longhurst, 1995; Tjen-A-Looi *et al.* 1998). Conduction time was determined by measuring the time interval from the signal of electrical stimulation to the recording of the action potential from the evoked afferent. Conduction distance was estimated from the receptive field along the course of the inferior cardiac nerve through the left stellate ganglion, and to the recording electrode following the course of the sympathetic chain (Kuo *et al.* 1984; Pan & Longhurst, 1995). C- and Aδ-fibre afferent nerves were classified as those with a conduction velocity $< 2{\cdot}5$ and 2·5–30 m s^{-1}, respectively (Pan & Longhurst, 1995; Huang *et al.* 1995; Tjen-A-Looi *et al.* 1998).

Measurement of epicardial pH

Epicardial tissue pH was measured with a pH-sensitive needle electrode (20 gauge, 0·9 mm o.d., model 401, Micro Probe, Hamden, CT, USA), which has a response time of < 3 s. The needle electrode was connected to an ATI Orion digital pH meter (model 330, Boston, MA, USA) and was calibrated *in vitro* using standard pH solutions (7·40, 6·85 and 6·40), as described previously (Stahl & Longhurst, 1992). The electrode was then inserted into the myocardium within 1–1·5 mm of the surface. The pH electrode was inserted into the region of epicardium perfused by the left anterior descending coronary artery or the left circumflex coronary artery since most ischaemically sensitive afferent nerve endings are located in these two areas when recording of afferent nerve activity is performed with fibres in the left sympathetic chain from T2 to T5

(Pan & Longhurst, 1995; Tjen-A-Looi *et al.* 1998). The output voltage signal from the pH meter was recorded continuously on the chart recorder.

Experimental protocols

Epicardial pH during myocardial ischaemia. This protocol was utilized to determine the epicardial pH changes during ischaemia since most cardiac sympathetic afferent nerve endings are distributed near the epicardial surface (Baker *et al.* 1980; Barber *et al.* 1984; Pan & Longhurst, 1995). This protocol was also used to evaluate the effect of topical placement of neutral phosphate buffer on ischaemia-induced epicardial pH changes. The pH electrode was allowed to stabilize for at least 45 min to minimize pH changes due to tissue damage caused by insertion of the electrode (Stahl & Longhurst, 1995). Regional myocardial ischaemia was induced by constricting the corresponding coronary vessel with a thread placed around the coronary artery. In six animals, epicardial pH in the ischaemic and non-ischaemic zones was measured continuously during 5 min of control, 5 min of ischaemia and 2 min of reperfusion. Repeat myocardial ischaemia was induced 30–45 min after the first period of ischaemia in the presence of a topical application of saline to ensure that the ischaemia-induced pH changes were reproducible. In another seven animals, after the first period of myocardial ischaemia, a 2 cm^2 filter paper patch pre-immersed in a solution of isotonic neutral phosphate buffer was placed directly on the epicardium where the pH electrode was inserted. Isotonic neutral phosphate buffer was prepared by combining 140 mM Na_2HPO_4 and 135 mM NaH_2PO_4. The pH (7·4) and osmolarity (290 mosmol $(l\ H_2O)^{-1}$) of the phosphate buffer were measured and adjusted with use of an ATI Orion digital pH meter and a μOSMETER (Precision Systems, Inc., Natick, MA, USA), respectively. Five minutes of myocardial ischaemia was reinduced 30 min later to determine the changes in epicardial pH during ischaemia in the presence of buffer solution.

Effects of exogenous protons on cardiac sympathetic afferents. This protocol examined the effect of protons derived from various sources on ischaemically sensitive cardiac sympathetic afferents. The effect of the acidic phosphate buffer on cardiac afferents was compared with the response of afferents to lactic acid, sodium lactate and hypercapnia. The differential effect of various sources of protons on ischaemically sensitive and insensitive cardiac afferents was also investigated. After the location of the receptive field of the afferent nerves was confirmed, the ischaemically sensitive or insensitive afferent fibres were identified following 5 min of regional myocardial ischaemia. Myocardial ischaemia was induced by constricting the coronary artery supplying the receptive field of cardiac ventricular afferent nerves with a thread placed around the vessel. Under an operating microscope, ligatures were placed around the proximal left anterior descending or left circumflex coronary artery, with care being taken not to disrupt nerve fibres that course along the vessel. Lactic acid (10–100 $\mu g\ ml^{-1}$, Sigma), acidic phosphate buffer (pH = 5·42), or vehicle (normal saline) was applied, in random order, to the receptive field of afferent nerves using a cotton-tipped applicator soaked with these solutions or injected (2 ml) into the heart through the left atrial catheter (Pan & Longhurst, 1995). Allowing for dilution during application of lactic acid from the epicardial surface into the interstitial space where the nerve endings are located, the concentrations of lactic acid are approximately within the range occurring during tissue ischaemia (Stahl & Longhurst, 1992). Sodium lactate (100–300 $\mu g\ ml^{-1}$, Sigma) was applied or injected into the heart to determine if afferents respond to lactic acid rather than to the dissociated lactate ions. Receptive fields were washed with saline and blood pH was corrected after each chemical had been administered. Furthermore, since high tissue CO_2 during myocardial ischaemia also constitutes a source of protons (Opie *et al.* 1973), we studied the effect of hypercapnia on cardiac afferents. After ischaemically sensitive cardiac afferents were identified, the animal was ventilated with gas containing a high percentage of CO_2 (12% CO_2, 21% O_2, and N_2 balance) for 5 min while the impulse activity of the afferent was recorded continuously (Stahl & Longhurst, 1992). In addition, to investigate further the possible differential effect of protons on ischaemically sensitive *versus* ischaemically insensitive cardiac afferents, the latter group of cardiac afferents was subjected to topical application or intracardiac injection of lactic acid. The epicardial pH was measured during hypercapnia and during topical application of the test solutions.

Role of endogenously produced protons in activation of cardiac sympathetic afferents during myocardial ischaemia. In 18 animals, after the receptive fields of the afferents were located precisely, ischaemically sensitive cardiac afferents were identified following 5 min of myocardial ischaemia. A 2 cm^2 filter paper patch was immersed in solution of isotonic neutral phosphate buffer and then placed directly on the epicardium where the afferent nerve ending was located. We have found in our previous studies that ischaemically sensitive afferents usually have one receptive field, and the size of the receptive field of cardiac afferent nerves is generally $< 0{\cdot}5$–1 cm (Pan & Longhurst, 1995; Huang *et al.* 1995; Tjen-A-Looi *et al.* 1998). Five minutes of myocardial ischaemia was repeated 30–45 min later to assess the response of the afferent nerve fibre to ischaemia in the presence of saline on the receptive field of the afferent. In a separate group of animals ($n = 14$ animals), the response of cardiac sympathetic afferents to 5 min of ischaemia was determined before and after application of a 2 cm^2 filter paper patch saturated with normal saline on the receptive field of the afferent. This procedure was used to establish a proper vehicle control to show that alteration of the afferent response to ischaemia following application of phosphate buffer was not caused simply by dilution of other metabolites. We have documented that two 5 min periods of myocardial ischaemia, separated by 30–45 min, induce reproducible responses from cardiac afferents without damaging or sensitizing the nerve endings (Pan & Longhurst, 1995; Tjen-A-Looi *et al.* 1998). We did not measure epicardial pH and afferent nerve activity at the same time due to the interfering electrical noise from the pH meter. In addition, dichloroacetate has been reported to decrease myocardial lactic acid accumulation by stimulating pyruvate dehydrogenase during partial occlusion of the coronary artery in dogs (Sakai *et al.* 1990). Thus, we evaluated the effect of systemic administration of dichloroacetate (200–600 mg, I.V.) on myocardial lactic acid concentrations and epicardial pH in our feline model of myocardial ischaemia in nine cats.

Data analysis

Results are given as means ± S.E.M. The discharge activity of afferents was averaged during a 5 min pre-ischaemic control period, a 5 min period of myocardial ischaemia and a 2 min period after reperfusion (Pan & Longhurst, 1995; Huang *et al.* 1995; Tjen-A-Looi *et al.* 1998). Afferents were considered to be ischaemically sensitive if their discharge frequency during 5 min of myocardial ischaemia was increased and was sustained at least twofold above baseline activity (Pan & Longhurst, 1995; Tjen-A-Looi *et al.* 1998). The response of afferents to lactic acid, hypercapnia, acidic phosphate buffer and sodium lactate was measured by averaging discharge rates during the entire period of the response of afferents. Comparisons between control and experimental interventions were

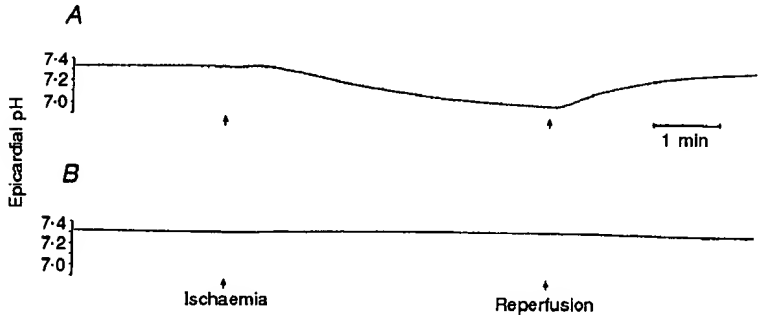

Figure 1. Effect of isotonic neutral buffer on changes in epicardial pH induced by myocardial ischaemia

Original record showing the epicardial pH changes during 5 min of myocardial ischaemia in the presence of saline (*A*) and isotonic neutral phosphate buffer (*B*) in one animal.

made either by Student's paired t test or a repeated measures analysis of variance followed by Duncan's *post hoc* test. Differences were considered to be statistically significant when $P < 0{\cdot}05$.

RESULTS

Acid–base status and haemodynamic profiles

The acid–base balance (arterial blood gas) was kept in the following range during the experiments: P_{CO_2}, 35–40; HCO_3^-, 22–28 mmol l^{-1}; and pH, 7·36–7·42. The haemodynamic parameters throughout the experiments were as follows: mean arterial pressure, 78 ± 15 mmHg; heart rate, 117 ± 11 beats min^{-1}; left ventricular end-diastolic pressure, 3 ± 1 mmHg. Afferent recordings from three animals were eliminated due to ventricular fibrillation during the 5 min period of ischaemia. Inhalation of hypercapnic gases significantly increased mean arterial blood pressure from 78 ± 15 to 158 ± 22 mmHg.

Epicardial pH during myocardial ischaemia

In seven animals, 5 min of myocardial ischaemia significantly decreased the epicardial pH (Fig. 1*A*). Topical application of phosphate buffer effectively prevented ischaemia-induced decreases in epicardial pH (Fig. 1*B*). In six other animals, topical placement of saline solution did not attenuate the decrease in epicardial pH caused by ischaemia, compared with that during the initial ischaemic period (Fig. 2). There was no significant difference between changes in epicardial pH induced by occlusion of the left anterior coronary artery (6·98 ± 0·21, $n = 7$ animals) or the left circumflex coronary artery (7·03 ± 0·23, $n = 5$ animals). In five additional animals, we measured epicardial interstitial pH in the right ventricle during 5 min of ischaemia. Epicardial pH decreased from 7·32 ± 0·14 during control to 6·98 ± 0·08 during 5 min of ischaemia, similar to that observed in the left ventricle (see Fig. 2).

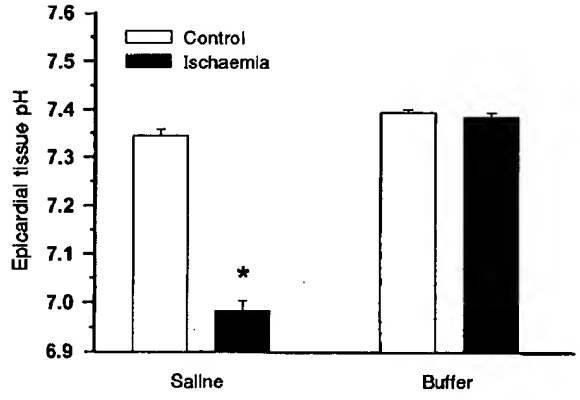

Figure 2. Bar graph summarizing changes in epicardial pH during control and 5 min of ischaemia in the presence of saline and phosphate buffer

Columns and error bars represent means ± S.E.M. * $P < 0{\cdot}05$ compared with pre-ischaemia control.

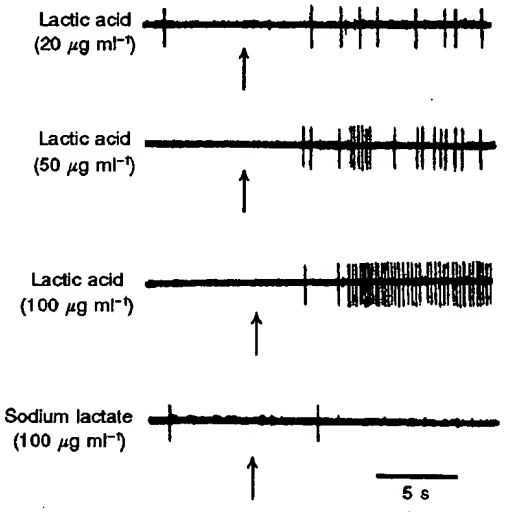

Figure 3. Original representative tracings showing responses of an ischaemically sensitive cardiac afferent to topical application (↑) of lactic acid or sodium lactate

The afferent ending was located in the anterior left ventricle and had a conduction velocity of 0·46 m s^{-1}. During topical applications of lactic acid at 20, 50 and 100 μg ml^{-1} and of sodium lactate at 100 μg ml^{-1}, the epicardial pH values measured by the tissue electrode were 7·18, 7·03, 6·83 and 7·34, respectively.

Exposure to hypercapnic gases decreased the arterial pH to 6·97 ± 0·23 and the epicardial pH to 6·95 ± 0·26 in six animals. Intracardiac injection of 2 ml of lactic acid decreased epicardial pH to 7·01 ± 0·27 ($n = 9$ animals), which was comparable to that measured during topical applications of lactic acid and during 5 min of ischaemia.

Effects of exogenous protons on cardiac sympathetic afferents

Five minutes of myocardial ischaemia increased the discharge frequency of 18 cardiac C-fibre afferent nerves from 0·22 ± 0·08 to 1·63 ± 0·24 impulses s^{-1}. Topical application or intracardiac injection of lactic acid stimulated these afferent nerve fibres in a concentration-dependent fashion (Figs 3 and 4). However, topical application or intracardiac injection of sodium lactate failed in all cases to stimulate the same afferents. The impulse discharge activity of these afferent fibres was 0·23 ± 0·08 and 0·22 ± 0·07 impulses s^{-1} before and after administration of sodium lactate, respectively.

We observed that inhalation of hypercapnic gases for 5 min in four animals effectively decreased the epicardial pH to 6·96 ± 0·21, which was similar to the values observed during 5 min of ischaemia. In 12 separate ischaemically sensitive afferents, inhalation of hypercapnic gases for 5 min did not activate any of these afferent nerve endings (Fig. 5) although the arterial blood pressure was increased significantly. The response of eight other ischaemically sensitive afferent nerves to acidic phosphate buffer was significantly less than their response to 50 μg ml^{-1} of lactic acid (Fig. 6), although the pH of these two solutions was identical (pH = 5·42). The epicardial interstitial pH was measured when lactic acid and acidic phosphate buffer at a similar pH (5·42) were topically applied. These two solutions

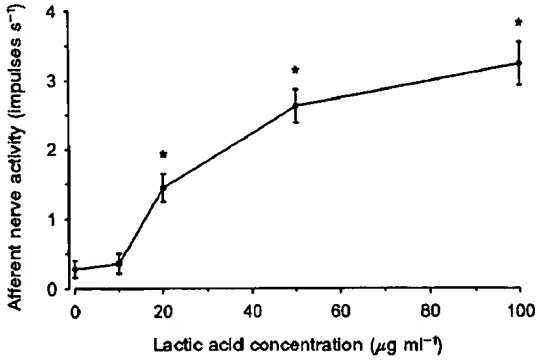

Figure 4. Concentration-dependent responses of 18 ischaemically sensitive cardiac afferents to topical (epicardial) application of lactic acid

Data are presented as means ± S.E.M. * $P < 0·05$ compared with the discharge activity during control. During topical applications of lactic acid at 20, 50 and 100 μg ml^{-1}, the epicardial pH values were 7·20 ± 0·04, 7·00 ± 0·04 and 6·80 ± 0·06, respectively.

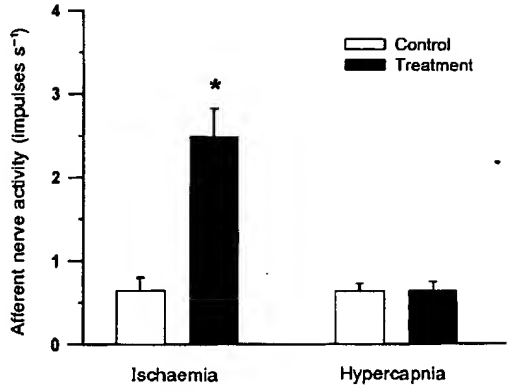

Figure 5. Bar graph showing responses of 12 ischaemically sensitive cardiac afferents to 5 min of ischaemia and inhalation of high-CO_2 gas

Columns and error bars represent means ± S.E.M. * $P < 0·05$ compared with pre-ischaemia control. Tissue pH values during ischaemia and hypercapnia were 6·98 ± 0·21 and 6·96 ± 0·21, respectively.

caused an identical decrease in epicardial interstitial pH (7·0 ± 0·08 for lactic acid *vs.* 6·9 ± 0·08 for acidic phosphate buffer, $n = 6$ afferents). The locations of these 38 C-fibre afferent nerve endings are shown in Table 1.

Topical application of 100 μg ml^{-1} of lactic acid only weakly activated 3 of 16 ischaemically insensitive cardiac afferent nerve fibres (increase in afferent nerve activity from 0·32 ± 0·11 to 0·56 ± 0·14 impulses s^{-1}). The remaining 13 afferent nerves were unresponsive to topical application or intracardiac injection of lactic acid.

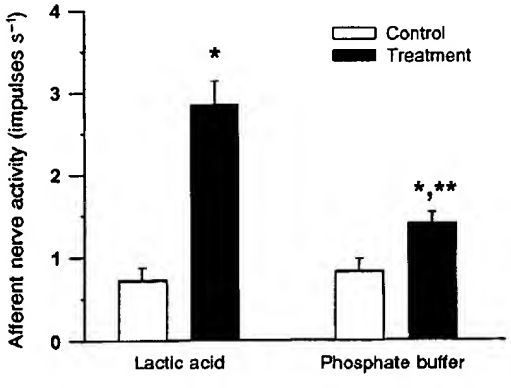

Figure 6. Bar graph showing responses of 8 ischaemically sensitive cardiac afferents to topical application of lactic acid or isotonic phosphate buffer

With both lactic acid (50 μg ml^{-1}), and isotonic phosphate buffer, pH = 5·42 . Columns and error bars represent means ± S.E.M. * $P < 0·05$ compared with the afferent activity during control. ** $P < 0·05$ compared with afferent response to lactic acid. The epicardial interstitial pH was 7·0 ± 0·08 during topical application of lactic acid and 6·9 ± 0·08 during application of acidic phosphate buffer.

Table 1. Location of nerve endings of ischaemically sensitive cardiac sympathetic afferents

	Lactic acid ($n=18$)	Hypercapnia ($n=12$)	Acidic phosphate ($n=8$)	Phosphate buffer ($n=16$)	Saline ($n=14$)
Left ventricle					
Anterior	7	3	2	6	5
Posterior	4	6	5	2	2
Right ventricle					
Anterior	3	1	—	5	3
Posterior	3	2	1	1	2
Apex	1	—	—	2	2

Role of endogenously produced protons in activation of cardiac sympathetic afferents during myocardial ischaemia

Figure 7 shows the response of an ischaemically sensitive cardiac afferent nerve to 5 min of ischaemia in the absence and presence of isotonic neutral phosphate buffer solution. The response of the afferent to ischaemia was reduced after placement of the buffer solution. For 16 cardiac sympathetic afferent fibres recorded in 15 animals, the initial 5 min of myocardial ischaemia led to a significant increase in discharge activity. Buffering the pH changes in the receptive field of these afferents with isotonic neutral phosphate buffer significantly attenuated the response of these afferents to repeated 5 min periods of ischaemia (Fig. 8*A*). In 14 other animals, the response of 14 cardiac afferent nerves to repeated 5 min periods of ischaemia was not significantly altered in the presence of saline solution, compared with that during the initial period of ischaemia (Fig. 8*B*). The epicardial pH was $7{\cdot}02 \pm 0{\cdot}23$ during 5 min of ischaemia in the absence of saline, and topical application of saline did not significantly change the epicardial tissue pH during ischaemia ($7{\cdot}02 \pm 0{\cdot}22$, $n=6$ afferents). The locations of these 30 C-fibre afferent nerve endings are shown in Table 1.

In an attempt to determine more specifically the role of endogenous lactic acid in cardiac afferent activation during myocardial ischaemia, we measured both epicardial pH and lactic acid sampled from the coronary vein before and after treatment with dichloroacetate (600 mg, I.V., $n=9$ animals). Before treatment with dichloroacetate, the epicardial pH decreased from $7{\cdot}34 \pm 0{\cdot}11$ during pre-ischaemic control to $6{\cdot}96 \pm 0{\cdot}08$ during 5 min of coronary artery occlusion. The lactic acid in coronary venous samples increased from $3{\cdot}3 \pm 0{\cdot}6$ during control to $7{\cdot}5 \pm 1{\cdot}2$ mM during 5 min of myocardial ischaemia. Treatment with dicholoracetate did not significantly attenuate ischaemia-induced changes in epicardial pH (from $7{\cdot}32 \pm 0{\cdot}11$ to $6{\cdot}94 \pm 0{\cdot}07$) and coronary venous lactic acid (from $3{\cdot}2 \pm 0{\cdot}6$ to $7{\cdot}8 \pm 1{\cdot}3$ mM). Thus, we were unable to use this approach to study further the role of endogenous lactic acid in ischaemia-induced cardiac afferent activation.

DISCUSSION

We focused our current study on C-fibre afferents because the heart is innervated predominantly by sympathetic C-fibre afferents (Pan & Longhurst, 1995; Huang *et al.* 1995; Tjen-A-Looi *et al.* 1998). In the present study, we only recorded three Aδ-fibre afferents whose nerve endings were

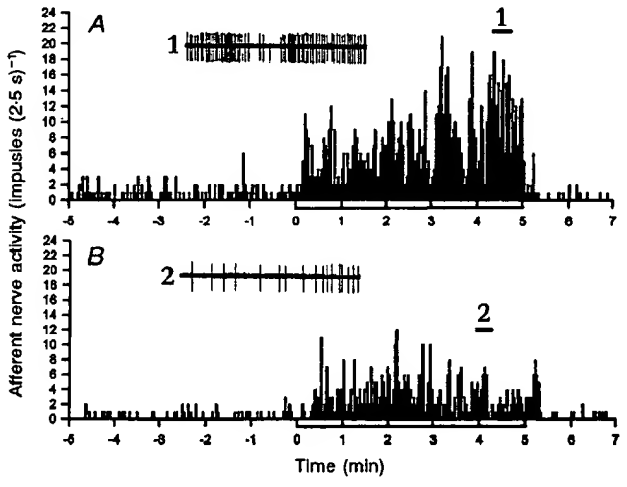

Figure 7. Representative histograms showing the discharge activity of a cardiac afferent during control, ischaemia and reperfusion before (*A*) and after (*B*) treatment with isotonic neutral phosphate buffer

The afferent ending was located in the anterior left ventricle and had a conduction velocity of 0·64 m s^{-1}. Traces 1 and 2: original tracings of this afferent recorded at the times indicated by bars above histograms.

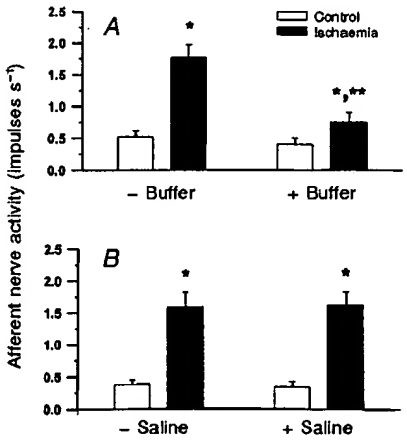

Figure 8. Bar graphs showing the response of cardiac sympathetic afferents to repeated 5 min periods of ischaemia in the absence and presence of isotonic neutral phosphate buffer (*A*) or saline (*B*)

Columns and error bars represent means ± S.E.M. * $P<0{\cdot}05$ compared with respective pre-ischaemic control. ** $P<0{\cdot}05$ compared with the initial afferent response to ischaemia.

in the heart. None of these fibres was responsive to 5 min of myocardial ischaemia or administration of lactic acid.

There are two important findings in the present study. First, we found that protons, probably derived from lactic acid, stimulated ischaemically sensitive cardiac afferent fibres in a concentration-dependent fashion. In this regard, hypercapnia, sodium lactate and acidic phosphate buffer either had no effect on ischaemically sensitive cardiac afferent endings or only slightly increased the discharge activity of these fibres. Furthermore, our data demonstrate that buffering the receptive field of afferents, which stabilizes epicardial pH, significantly attenuated the increase in discharge activity of cardiac sympathetic afferents induced by ischaemia. Therefore, the present electrophysiological study provides *in vivo* evidence for the first time that endogenously produced protons, most probably those derived from lactic acid, play an important role in activation of cardiac sympathetic C-fibre afferents during ischaemia.

Increased production of some metabolites during myocardial ischaemia has been proposed to contribute to excitation of nerve endings of primary cardiac sympathetic afferents (Nishi *et al.* 1977; Baker *et al.* 1980). For example, we have shown that bradykinin and free radicals, but not adenosine, contribute to activation of ischaemically sensitive cardiac sympathetic afferents (Pan & Longhurst, 1995; Huang *et al.* 1995; Tjen-A-Looi *et al.* 1998). However, *in vivo* myocardial ischaemia is a complex entity and many metabolites probably act in concert to activate cardiac sympathetic afferents. In this regard, elimination of the action of free radicals or blockade of kinin B_2 receptors generally does not eliminate completely ischaemia-induced activation of cardiac sympathetic afferents (Huang *et al.* 1995; Tjen-A- Looi *et al.* 1998). Thus, we believe that other mechanisms are still present which account for activation/sensitization of cardiac afferents during ischaemia. Since lactic acid is produced in large quantities during myocardial ischaemia and because exogenous lactic acid elicits nociceptive responses in conscious animals (Guzman *et al.* 1962; Opie *et al.* 1973; Nishi *et al.* 1977), this metabolite has been long suspected of playing a role in myocardial ischaemia-induced chest pain. However, there is little *in vivo* evidence supporting the hypothesis that endogenously produced protons contribute to activation of cardiac nociceptors during ischaemia. Evidence that outward proton flux from myocytes occurs rapidly during ischaemia has been presented by Yan & Kleber (1992), who found that proton efflux during ischaemia, coupled with the poor buffering capacity of the extracellular *versus* the intracellular milieu, is sufficient to lower extracellular pH more than intracellular pH. Although it has been established previously that myocardial pH decreases during ischaemia (Poole-Wilson, 1978), epicardial pH changes during myocardial ischaemia have not been examined in particular. In the present study, we found that epicardial pH decreased progressively during 5 min of ischaemia. Because the nerve endings of cardiac sympathetic afferents are distributed near the epicardial surface (Baker *et al.* 1980), we measured the epicardial tissue pH changes, which are most relevant to the environment of cardiac sympathetic afferents during ischaemia. In preliminary studies, we performed extensive experiments using several approaches, including treatments with dichloroacetate (200–600 mg kg^{-1}, I.V.) and acetazolamide (60–100 mg kg^{-1}, I.V.) (data not shown) in an attempt to define further the role of lactic acid in activation of cardiac afferents during ischaemia. However, we could not demonstrate significant attenuation of ischaemia-induced alterations in epicardial pH and lactic acid by either dichloroacetate or acetazolamide. A previous study has shown that dichloroacetate effectively attenuated myocardial acidosis in a canine model of partial occlusion of the coronary artery (Sakai *et al.* 1990). We were unable to demonstrate such an effect in our feline model of complete occlusion of the coronary artery, and therefore the present study is limited by the lack of a suitable protocol to restrict the accumulation of lactic acid in our feline model of myocardial ischaemia.

Taking advantage of the anatomical distribution of the nerve endings of cardiac sympathetic afferents, we observed that epicardial application of isotonic phosphate buffer prevented the decrease in pH during ischaemia. Thus, buffering the epicardium pH provided a useful means of evaluating the role of endogenously produced protons in the activation of cardiac afferents during ischaemia. The role of protons from lactate ions and other sources in the activation of ischaemically sensitive cardiac afferents was determined in our study. The cause of acidosis during myocardial ischaemia is mainly due to the retention of acid metabolites. The major sources of protons during myocardial ischaemia are glycolysis associated with the production of lactic acid, generation of CO_2, and abnormal lipid metabolism (Opie *et al.* 1973; Poole-Wilson, 1978). Steen *et al.* (1995) found that, at pathophysiologically relevant concentrations, protons played a dominant role in activating cutaneous afferents. Uchida & Murao (1975) reported that application of low concentrations (7·5–75 $\mu g\ ml^{-1}$) of lactic acid preferentially stimulated cardiac unmyelinated C-fibre afferents but not myelinated afferents (the afferent response to ischaemia was not tested in this study). We have shown previously that exogenous lactic acid is capable of activating ischaemically sensitive afferent nerve endings innervating abdominal viscera (Stahl & Longhurst, 1992). The present study indicates that protons are primarily important in the activation of ischaemically sensitive afferents since sodium lactate (lactate ions) alone had no direct effect on this group of afferents. Our results also suggest that protons derived from lactic acid, but not from hypercapnia, stimulate cardiac sympathetic afferents in a concentration-dependent fashion. Unlike results from *in vitro* studies on cutaneous afferents (Steen *et al.* 1992, 1995), we found that, although hypercapnia caused a similar reduction in epicardial pH to ischaemia, it did not stimulate cardiac afferents. This finding is consistent with our previous studies showing that hypercapnia has no effect on abdominal visceral afferents (Stahl &

Longhurst, 1992). It is unclear why the response of visceral afferents to protons derived from hypercapnia differs from that of cutaneous afferents. This discrepancy may be due to the difference in the biochemical transduction mechanism of the afferent nerve endings (i.e. the generator potential of receptors) and/or the tissue type in which the nerve endings reside. Furthermore, it remains uncertain why protons from different sources have a different effect on the cardiac nociceptors. This disparity has been demonstrated in other visceral afferents, including abdominal sympathetic afferents and pulmonary afferents (Stahl & Longhurst, 1992; Hong *et al.* 1997). The lactate and proton exchange in the nerve endings may be important in activation of cardiac afferents during ischaemia (Schneider *et al.* 1993). Thus, the combination of lactic ions and protons is probably a stronger stimulus for cardiac afferent endings, as has been demonstrated for pulmonary afferents (Hong *et al.* 1997). This notion is supported by our finding that lactic acid stimulated cardiac sympathetic afferents to a much greater extent than acidic phosphate buffer solution, although both solutions caused a similar decrease in epicardial pH when applied to the surface of the heart.

We observed that lactic acid stimulates ischaemically sensitive C-fibre afferent nerves but has a rare mild effect on ischaemically insensitive cardiac afferent nerves. The reason behind this unique action of lactic acid is not clear. A proton-induced current has been discovered in a subpopulation of rat dorsal root ganglion neurons, which is specifically gated by downward steps in extracellular pH (Bevan & Yeats, 1989; Peterson & LaMotte, 1993). Indeed, the acid-sensing ionic channel expressed in the dorsal root ganglion and central neurons has been cloned recently (Waldmann *et al.* 1997). This channel type may exist mainly in ischaemically sensitive sensory nerve endings (Rang *et al.* 1991; Peterson & LaMotte, 1993), and could provide a molecular basis for activation of this group of cardiac afferents.

In contrast to previous electrophysiological studies on cardiac afferents, our study assessed directly the role of endogenous protons in excitation of cardiac sympathetic afferents during ischaemia. Since the nerve endings of cardiac sympathetic afferents are mainly located near the epicardial surface and the isotonic neutral phosphate buffer was demonstrated to effectively prevent the epicardial pH change caused by ischaemia, this intervention was used to explore the role of protons in activation of cardiac afferents during ischaemia. Because topical saline application did not alter the response of cardiac afferents to ischaemia, it is unlikely that dilution of other metabolites contributed to the attenuating effect of the buffer on cardiac afferents. Although no histological measurements were made, we were confident that both the pH electrode and the receptive field of the afferents were located in the ischaemic zone for the following reasons. First, regional ischaemia was clearly indicated by visible cyanosis of the ischaemic zone during occlusion of the coronary artery. Furthermore, occlusion of the corresponding coronary artery always decreased the epicardial pH and increased the discharge frequency of afferents, confirming that the pH electrode and the afferent endings were indeed located in the ischaemic zone. In addition, in our experiments, all afferent nerve endings were precisely located on the surface of the heart using a stimulating electrode. Based on our previous experience (Pan & Longhurst, 1995; Huang *et al.* 1995; Tjen-A-Looi *et al.* 1998), the pH electrode was placed in the area in which most of the afferent endings are located (i.e. the anterior left ventricle). Thus, we believe that epicardial pH changes were closely related to afferent responses to ischaemia. This notion is also strongly supported by the data showing that buffering the epicardium (where the afferent ending was located) significantly attenuated the afferent responses to ischaemia.

We recognize that, in addition to its direct stimulating effect on cardiac afferents, accumulation of protons in the ischaemic myocardium also may sensitize cardiac afferents in response to other stimuli, as demonstrated for cutaneous afferents (Steen *et al.* 1992). Results from our study, however, cannot distinguish a stimulating *vs.* a sensitizing action of protons on cardiac afferents. It is likely that accumulating protons in ischaemic myocardium could contribute to activation of cardiac afferents through both direct and indirect actions. Furthermore, tissue ischaemia is a complex process and many ischaemic metabolites are produced during myocardial ischaemia. It is clear from the present study that endogenously produced protons are not entirely responsible for activation of cardiac sympathetic afferents during ischaemia since buffering the receptive field of afferents did not completely abolish the response of afferent endings to ischaemia. Considering the results from previous studies (Huang *et al.* 1995; Tjen-A-Looi *et al.* 1998), it is possible that protons interact synergistically with many other metabolites, such as oxygen-derived free radicals, bradykinin and prostaglandins, to fully stimulate cardiac sympathetic afferents during ischaemia. These ischaemic metabolites also may play a distinct role in afferent activation during different phases of ischaemia. For example, previous studies have shown that bradykinin is generated rapidly during brief ischaemia (Kimura *et al.* 1973), which may account for a short latency in the activation of afferent endings during ischaemia. Data shown in Figs 1 and 7 appear to suggest that protons play a more important role in activation of cardiac afferents when ischaemia is prolonged to more than 1–2 min. Further studies are warranted to determine precisely the role of their interactions in ischaemia-induced activation of cardiac afferents.

In conclusion, this study has provided important *in vivo* evidence that protons, probably derived from lactic acid but not from tissue hypercapnia, contribute to activation/sensitization of cardiac sympathetic C-fibre afferents during

myocardial ischaemia. Our data suggest that increased production of protons/lactic acid during myocardial ischaemia is responsible for stimulation of the nerve endings of cardiac sympathetic afferents, which triggers perception of chest pain and, through a reflex mechanism, evokes excitatory cardiovascular responses and tachyarrythmias.

Abe, T., Morgan, D., Sengupta, J. N., Gebhart, G. F. & Gutterman, D. D. (1998). Attenuation of ischemia-induced activation of cardiac sympathetic afferents following brief myocardial ischemia in cats. *Journal of the Autonomic Nervous System* **71**, 28–36.

Baker, D. G., Coleridge, H. M., Coleridge, J. C. G. & Nerdrum, T. (1980). Search for a cardiac nociceptor: stimulation by bradykinin of sympathetic afferent nerve endings in the heart of the cat. *Journal of Physiology* **306**, 519–536.

Barber, M. J., Mueller, T. M., Davies, B. G. & Zipes, D. P. (1984). Phenol topically applied to canine left ventricular epicardium interrupts sympathetic but not vagal afferents. *Circulation Research* **55**, 532–544.

Bevan, S. & Yeats, J. (1989). Protons activate a cation conductance in a subpopulation of rat dorsal root ganglion neurons. *Journal of Physiology* **433**, 145–161.

Bosnjak, Z. J., Zuperku, E. J., Coon, R. L. & Kampine, J. P. (1979). Acute coronary artery occlusion and cardiac sympathetic afferent nerve activity. *Proceedings of Society for Experimental Biology & Medicine* **161**, 142–148.

Brown, A. M. (1967). Excitation of afferent cardiac sympathetic nerve fibres during myocardial ischaemia. *Journal of Physiology* **190**, 35–53.

Cervero, F. (1994). Sensory innervation of the viscera: peripheral basis of visceral pain. *Physiological Reviews* **74**, 95–138.

Chandler, M. J., Garrison, D. W., Brennan, T. J. & Foreman, R. D. (1989). Effects of chemical and electrical stimulation of the midbrain on feline T2-T6 spinoreticular and spinal cell activity evoked by cardiopulmonary afferent input. *Brain Research* **496**, 148–164.

Chandler, M. J., Zhang, J. & Foreman, R. D. (1998) Cardiopulmonary sympathetic input excites primate cuneothalamic neurons: comparison with spinothalamic tract neurons. *Journal of Neurophysiology* **80**, 628–637.

Gnecchi-Ruscone, T., Montano, N., Contini, M., Guazzi, M., Lombardi, F. & Malliani, A. (1995). Adenosine activates cardiac sympathetic afferent fibers and potentiates the excitation induced by coronary occlusion. *Journal of the Autonomic Nervous System* **53**, 175–184.

Guzman, F., Braun, C. & Lim, K. S. (1962). Visceral pain and the pseudoaffective response to intra-arterial injection of bradykinin and other analgesic agents. *Archives Internationales de Pharmacodynamie et de Therapie* **136**, 353–384.

Hong, J. L., Kwong, K. & Lee, L. Y. (1997). Stimulation of pulmonary C fibers by lactic acid in rats: concentrations of H^+ and lactate ions. *Journal of Physiology* **500**, 319–329.

Huang, H., Pan, H.-L. & Longhurst, J. C. (1995). Ischemia- or reperfusion-sensitive cardiac sympathetic afferents: influence of H_2O_2 and hydroxyl radicals. *American Journal of Physiology* **269**, H888–901.

Kimura, E., Hashimoto, K., Furukawa, S. & Hayakawa, H. (1973). Changes in bradykinin level in coronary sinus blood after the experimental occlusion of a coronary artery. *American Heart Journal* **85**, 635–647.

Kuo, D., Oravitz, J. J. & DeGroat, W. C. (1984). Tracing of afferent and efferent pathways in the left inferior cardiac nerve of the cat using retrograde and transganglionic transport of horseradish peroxidase. *Brain Research* **321**, 111–118.

Malliani, A., Schwartz, P. J. & Zanchetti, A. (1969). A sympathetic reflex elicited by experimental coronary occlusion. *American Journal of Physiology* **217**, 703–709.

Moore, R. M. & Singleton, A. O. (1935). A pseudaffective reflex evoked by injections into the left coronary artery and the peripheral paths of the pain fibers which are concerned. *American Journal of Physiology* **113**, 99–100.

Nishi, K., Sakanashi, M. & Takenaka, F. (1977). Activation of afferent cardiac sympathetic nerve fibers of the cat by pain producing substances and by noxious heat. *Pflügers Archiv* **372**, 53–61.

Opie, L. H., Owen, P., Thomas, M. & Samson, R. (1973). Coronary sinus lactic measurements in assessment of myocardial ischemia. *American Journal of Cardiology* **32**, 295–305.

Pal, P., Koley, J., Bhattacharyya, S., Gupta, J. S. & Koley, B. (1989). Cardiac nociceptors and ischemia: role of sympathetic afferents in cat. *Japanese Journal of Physiology* **39**, 131–144.

Pan, H.-L. & Longhurst, J. C. (1995). Lack of a role of adenosine in activation of ischemically sensitive cardiac sympathetic afferents. *American Journal of Physiology* **269**, H106–113.

Peterson, M. & LaMotte, R. H. (1993). Effect of protons on the inward current evoked by capsaicin in isolated dorsal root ganglion cells. *Pain* **54**, 37–42.

Poole-Wilson, P. A. (1978). Measurement of myocardial intracellular pH in pathological states. *Journal of Molecular and Cellular Cardiology* **10**, 511–526.

Rang, H. P., Bevan, S. & Dray, A. (1991). Chemical activation of nociceptive peripheral neurons. *British Medical Bulletin* **47**, 534–548.

Sakai, K., Ichihara, K., Nasa, Y., Kamigaki, M. & Abiko, Y. (1990). Dichloroacetate attenuates myocardial acidosis and metabolic changes induced by partial occlusion of the coronary artery in dogs. *Archives Internationales de Pharmacodynamie et de Therapie* **307**, 92–108.

Schneider, U., Poole, R. C., Halestrap, A. P. & Grafe, P. (1993). Lactate-proton co-transport and its contribution to interstitial acidification during hypoxia in isolated rat spinal roots. *Neuroscience* **4**, 1153–1162.

Stahl, G. L. & Longhurst, J. C. (1992). Ischemically sensitive visceral afferents: importance of H^+ derived from lactic acid and hypercapnia. *American Journal of Physiology* **262**, H748–753.

Steen, K. H., Reeh, P. W., Anton, F. & Handwerker, H. O. (1992). Protons selectively induce lasting excitation and sensitization to mechanical stimulation of nociceptors in rat skin, *in vitro*. *Journal of Neuroscience* **12**, 86–95.

Steen, K. H., Steen, A. E. & Reeh, P. W. (1995). A dominant role of acid pH in inflammatory excitation and sensitization of nociceptors in rat skin, *in vitro*. *Journal of Neuroscience* **15**, 3982–3989.

Thames, M. D., Kinugawa, T. & Dibner-Dunlap, M. E. (1993) Reflex sympathoexcitation by cardiac sympathetic afferents during myocardial ischemia: role of adenosine. *Circulation* **87**, 1698–1704.

TJEN-A-LOOI, S. C., PAN, H.-L. & LONGHURST, J. C. (1998). Endogenous bradykinin stimulates ischaemically sensitive cardiac visceral afferents through kinin B_2 receptors in cats. *Journal of Physiology* **510**, 633–641.

UCHIDA, Y. & MURAO, S. (1975). Acid-induced excitation of afferent cardiac sympathetic nerve fibers. *American Journal of Physiology* **228**, 27–33.

VEELKEN, R., GLABASNIA, A., STETTER, A., HILGERS, K. F., MANN, J. F. & SCHMIEDER, R. E. (1996). Epicardial bradykinin B2 receptors elicit a sympathoexcitatory reflex in rats. *Hypertension* **28**, 615–621.

WALDMANN, R., CHAMPIGNY, G., BASSILANA, F., HEURTEAUX, C. & LAZDUNSKI, M. (1997). A proton-gated cation channel involved in acid-sensing. *Nature* **386**, 173–177.

WHITE, J. C. (1957). Cardiac pain: anatomic pathway and physiologic mechanisms. *Circulation* **16**, 644–655.

YAN, G.-X. & KLEBER, A. (1992). Changes in extracellular and intracellular pH in ischemic rabbit papillary muscle. *Circulation Research* **71**, 460–470.

Acknowledgements

This study was supported by grant GS-30 (H.-L.P.) from the American Heart Association, Mid-Atlantic Affiliate, and by grants HL-60026 (H.-L.P.) and HL-52165 (J.C.L.) from the National Institutes of Health.

Corresponding author

H.-L. Pan: Department of Anesthesiology, Wake Forest University School of Medicine, Medical Centre Boulevard, Winston-Salem, NC 27157, USA.

Email: hpan@wfubmc.edu

Author's present address

J. C. Longhurst: Department of Medicine, University of California College of Medicine, Irvine, Orange, CA 92868, USA.

Acid-Evoked Currents in Cardiac Sensory Neurons
A Possible Mediator of Myocardial Ischemic Sensation

Christopher J. Benson, Stephani P. Eckert, Edwin W. McCleskey

Abstract—Sensory neurons that innervate the heart sense ischemia and mediate angina. To use patch-clamp methods to study ion channels on these cells, we fluorescently labeled cardiac sensory neurons (CSNs) in rats so that they could later be identified in dissociated primary culture of either nodose or dorsal root ganglia (DRG). Currents evoked by a variety of different agonists imply the importance of lowered pH (≤7.0) in signaling ischemia. Acidic pH evoked extremely large depolarizing current in almost all cardiac afferent neurons from the DRG (CDRGNs). In contrast, only about half of the unlabeled DRG neurons responded to acid, and their current amplitudes were much less than that in CDRGNs. In all respects tested—kinetics, selectivity, and pharmacology—the acid-evoked current was similar to that of previously described native and cloned acid-sensing ion channels. Cardiac afferents from the nodose ganglia differed from CDRGNs in having smaller acid-evoked currents but clearly larger currents evoked by ATP. Serotonin, acetylcholine, bradykinin, and adenosine elicited currents in fewer CSNs than did ATP or lowered pH, and the currents were relatively small. Capsaicin, an activator of small nociceptive sensory neurons that innervate skin, evoked only small and rare currents in CDRGNs. The extremely large amplitude and prevalent expression of acid-evoked current in CSNs imply a critical role for acidity in sensation associated with myocardial ischemia. (*Circ Res.* **1999;84:921-928.**)

Key Words: myocardial ischemia ■ cardiac sensory neuron ■ proton ■ whole-cell patch clamp

Although much is understood about the effect of autonomic nervous system input to the heart, the cardiac sensory, or afferent, system and its role in physiological and pathological conditions are less well understood. Historically, the major impetus for research on the cardiac sensory system has been to find the source of cardiac pain, or angina. During the first half of this century, the neuroanatomical pathways of the cardiac sensory system were defined by clinical reports of surgical attempts to relieve angina and by experimental studies.[1,2] These studies revealed that the cardiac sensory neurons (CSNs) follow the sympathetic and vagal nerve tracts en route to the central nervous system (Figure 1). The cell bodies of those sensory axons following the sympathetic tracts are found in the upper thoracic dorsal root ganglia (DRG); those following the vagal tracts are located in the nodose ganglia. The sensory innervation of the fibrous and serous parietal pericardium, separate from that of the heart and epicardium, follows the phrenic nerves to the cervical DRG (C_3-C_5).[3,4]

It has long been understood that cardiac pain is associated with myocardial ischemia, which causes oxygen supply/demand insufficiency.[5] In various whole-animal preparations, occlusion of a coronary artery activates the cardiac afferent nerve fibers in the sympathetic[6-8] and vagal tracts.[9,10] Various substances released during myocardial ischemia have been implicated as chemical mediators of myocardial ischemic sensation. Several of these substances have been shown to activate CSNs: ATP,[8,10] serotonin (5HT),[11] bradykinin (BK),[12,13] and adenosine.[8,10] In turn, stimulation of sensory fibers elicits reflexes specifically mediated by the sympathetic tract[14] and by the vagal tract.[15] Still, the precise stimuli that are sensed during myocardial ischemia are incompletely understood (see Reference 16 for review).

A likely contributor is acid. The heart is an organ of high metabolic activity and is susceptible to drops in pH during ischemia or hypoxia. It has been demonstrated that pH is lowered intracellularly[17] and extracellularly[18,19] in ischemic heart models and clinically in patients with coronary artery disease.[20] In dogs, lowered pH stimulates afferent cardiac sympathetic nerve fibers.[21] In another organ system, rat skin, acid plays a dominant role in exciting sensory neurons when compared with other potential chemical mediators of inflammation.[22]

Acid evokes depolarizing currents in sensory neurons studied in primary dissociated culture,[23-26] and a variety of different components are distinguished by kinetic criteria.[27] Most components activate somewhere between pH 7 and pH 6 and desensitize in response to a maintained stimulus. These desensitizing currents all have the unusual property of selectively passing Na^+ over K^+ about as effectively as voltage-gated Na^+ channels. In addition to the desensitizing, Na^+-selective currents in DRG neurons, there is a sustained,

Received August 12, 1998; accepted February 10, 1999.

From the Vollum Institute (C.J.B., S.P.E, E.W.M.) and Division of Cardiology (C.J.B.), Oregon Health Sciences University, Portland, Ore.

Correspondence to Christopher J. Benson, Division of Cardiology, Oregon Health Sciences University, 3181 SW Sam Jackson Park Rd, UHN-62, Portland, OR 97201-3098. E-mail bensonc@ohsu.edu

Circulation Research **is available at http://www.circresaha.org**

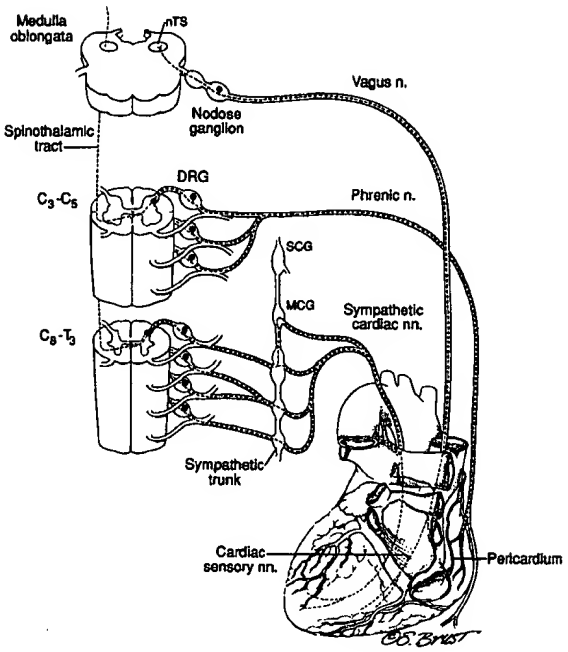

Figure 1. Illustration of the cardiac and pericardial sensory pathways. Cardiac sensory signals travel from terminals throughout the heart through both the sympathetic and the vagal nerve tracts en route to the central nervous system. Axons of some CSNs exit the heart via the sympathetic cardiac nerves and course through sympathetic ganglia (middle [MCG] and inferior cervical and upper thoracic) en route to their cell bodies, located in the lower cervical and upper thoracic DRG. Axons of other CSNs travel within the vagal nerve to their cell bodies in the nodose ganglia. Afferent neurons from the pericardium follow the phrenic nerves to their cell bodies in the DRG of the upper cervical region (C_3-C_5).

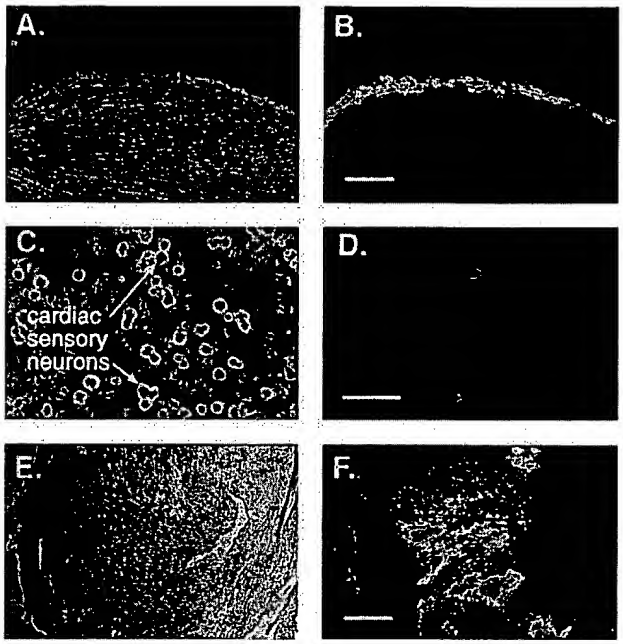

Figure 2. Fluorescent labeling of CSNs. A and B, Corresponding phase (A) and fluorescence micrograph (B) of an apical slice of myocardium 3 weeks after surgical injection of fluorescent dye into the pericardial space. C and D, Phase (C) and fluorescence micrograph (D) of 2 CSNs in primary dissociated culture of DRG neurons. E and F, Phase (E) and fluorescence micrograph (F) of a myocardial slice after an intramural injection of dye. Scale bars represent 0.5 mm for panels A, B, E, and F and 0.25 mm for panels C and D.

nonselective current that is evoked by pH below 6.0.[26] The channels underlying these currents are believed to be the recently cloned acid-sensing ion channels (ASICs), which are members of the amiloride-sensitive Na^+ channel/degenerin family of cation channels.[28]

These acid-evoked currents may play a role in mediating the pain of cardiac and skeletal muscle ischemia and perhaps also of inflammation. It is difficult to explore this possibility in culture, because the sensory modality and the site of innervation of individual neurons are not known. The first goal of the present study was to fluorescently label CSNs in the rat so that they can later be distinguished from other sensory neurons in dissociated culture; we accomplished this using a retrogradely transported dye placed in the pericardial space. We found that acid evoked extraordinarily large currents in the cardiac afferent neurons from the DRG (CDRGNs) compared with other, unlabeled DRG neurons (UDRGNs). The very high expression of these currents in cells thought to be specialized for sensing ischemia suggests an important role of acid in mediating cardiac pain.

Materials and Methods

In Vivo Labeling of CSNs

Surgical Preparation

Sprague-Dawley rats (200 to 300 g) were anesthetized by intramuscular injection of 1 mL/kg rat anesthetic (in mg/mL, ketamine 55, xylazine 5.5, and acepromazine 1.1). Each animal was intubated and respiration maintained with a rodent ventilator (Harvard model 683). The heart and thymus were exposed through a left lateral thoracotomy at the fifth intercostal space. The thymus, with the anterior superior portion of the pericardium adherent to its undersurface, was gently retracted cephalad to better delineate the pericardium and pericardial space. Twenty-five microliters of a suspension of 17 mg/mL of 1,1′-dioctadecyl-3,3′,3′-tetramethyl indocarbocyanine perchlorate (DiI; Molecular Probes) in saline solution was injected into the pericardial space. The rat pericardial membrane is thin and contains microscopic pores[29]; thus, a suspension rather than solution of the lipophilic DiI was used to decrease the potential of leakage of dye from the pericardial space. After injection, the ribs were approximated, the thoracic cavity was evacuated, and the incision was closed in layers. The animals were cared for in accordance with the current *Guide for the Care and Use of Laboratory Animals* (US Public Health Service, Department of Health and Human Services) and guidelines of the Institutional Animal Care and Use Committee of Oregon Health Sciences University.

Tissue Culture and Identification of Labeled CSNs

During the 2- to 4-week postoperative period, DiI was carried through retrograde transport back to the cell bodies of the CSNs. The rats were then sacrificed, and the right and left dorsal root (C_8-T_3) and nodose ganglia were collected. The ganglia were dissociated and cultured as previously described, except that the Percoll spin was omitted.[30] In brief, the ganglia underwent enzymatic dissociation successively in papain and collagenase/dispase solutions; this was followed by trituration in Hanks solution. The cells were then plated on polylysine- and laminin-coated plastic in F12 medium plus nerve growth factor (50 ng/mL) at 37°C in 5% CO_2. After several hours, the medium was changed to L15 plus nerve growth factor, and the cells were maintained at 22°C in air. CSNs were identified by fluorescence microscopy (Figure 2C and 2D). From the animals that underwent the pericardial space injection preparation, the following

Number of Labeled DRG Neurons Per Dye Injection Site

Injection Site	No. of Labeled DRG (C_8-T_3)
Pericardial space (n=9)	75 to 189 (mean=124)
Intramural myocardium (n=7)	0 to 7 (mean=1.86)
Left pleural space (n=1)	28
Right ventricular chamber (n=1)	4
Left ventricular chamber (n=1)	0

3 populations of sensory neurons were obtained for study: (1) labeled CDRGNs, (2) UDRGNs, and (3) labeled neurons from the nodose ganglia (CNodNs).

Control Experiments

To check for dye leakage from the pericardium and to explore the effects of labeling at different injection sites, we performed several control procedures. First, after a pericardial space injection, the heart and lungs were sectioned at the time of euthanization and viewed under a fluorescence microscope. Whereas the heart consistently displayed confluent fluorescence over the epicardium (Figure 2A and 2B), the surface of the lungs contained only an occasional isolated crystal of dye. Next, to test whether dye leakage from the pericardial space would cause significant contamination, we intentionally injected dye in the following sites in separate animals: the left pleural space, the left ventricular chamber, or the right ventricular chamber. As expected, sectioning of the lungs after injecting into the right ventricular chamber revealed confluent pulmonary vascular embolization of the dye. Next, in an effort to label sensory nerve terminals deeper within the myocardium, we stabilized the heart with sutures and made several intramural injections into the left ventricular myocardium (Figure 2E and 2F).

The numbers of labeled sensory neurons obtained in culture of the DRG after the various injection experiments are listed in the Table. The pericardial space injection resulted in a significantly greater number of labeled neurons in the DRG than the various control injection site experiments. Thus, despite the potential for dye leakage from the pericardial space, it would cause little contamination because relatively few cells were labeled with intentional injection into the pleural space. Because of the low number of neurons labeled by the intramural injections, we abandoned this experimental preparation. The number of nodose ganglion neurons labeled by the pericardial space injection was not quantified; however, there appeared to be a higher fraction of labeled cells in the nodose ganglion (≈10%) than in the DRG (≈1%) cultures.

Whole-Cell Patch-Clamp Recording

Whole-cell currents were recorded with an EPC-9 amplifier (HEKA Elektronik). For most experiments, pipettes of 2- to 4-MΩ resistance were filled with KCl internal solution containing (in mmol/L) KCl 100, EGTA 10, HEPES 40, $MgCl_2$ 5, Na_2ATP 2, and Na_3GTP 0.3, adjusted to pH 7.4 with KOH unless otherwise stated. For the monovalent permeability experiments, NaCl replaced KCl in the internal solution, and pH was adjusted with NaOH; high internal Na^+ eliminated contamination by large, outward K^+ currents. For the Ca^{2+} permeability experiments, the internal solution consisted of (in mmol/L) *N*-methyl glucamine 90 (titrated with HCl), NaCl 10, EGTA 10, HEPES 40, $MgCl_2$ 5, Na_2ATP 2, and Na_3GTP 0.3, pH adjusted with tetramethylammonium (TMA)-OH. Our strategy was to measure relative Na^+ and Ca^{2+} permeability by using similar Na^+ and Ca^{2+} activities inside and outside the cell, respectively. Standard extracellular solutions contained (in mmol/L) NaCl 130, KCl 5, $CaCl_2$ 2, $MgCl_2$ 1, HEPES 10, and MES 10, pH adjusted with TMA-OH. TMA-Cl was added to the various pH solutions to equalize the concentration of TMA. For the monovalent permeability experiments, the extracellular solutions consisted of (in mmol/L) NaCl (or KCl, $NaCH_3SO_3$, or CsCl) 130, $CaCl_2$ 2, $MgCl_2$ 1, HEPES 10, and MES 10; pH was adjusted with NaOH, KOH, or CsOH. For the Ca^{2+} permeability experiments, external solutions consisted of (in mmol/L) *N*-methyl glucamine 120 (titrated with HCl), HEPES 10, MES 10, and $CaCl_2$ 10 or 30. For experiments on Ca^{2+} block, external solutions consisted of (in mmol/L) NaCl 130; HEPES 10; MES 10; and $CaCl_2$ 1, 2, or 10. The series resistance ranged from 3 to 7 MΩ, and it was compensated by ≈50%.

All dose-response curves were made by random-order application of various concentrations at 30-second intervals. Solutions were applied through an array of 1- or 10-μL pipes positioned ≈50 μm from the cell under 40 cm of water pressure. Rapid solution exchanges were controlled via computer-driven solenoid valves and were accomplished within 5 ms as measured by an osmotically induced change in current (Figure 5A). Cells were held at −70 mV unless otherwise stated. Experiments were performed at room temperature (≈22°C). We studied most cells after 1 to 2 days in culture; however, some experiments were done on cells cultured up to 7 days. We saw no obvious difference in the responses of cells cultured for longer times.

Data Analysis

The equation $I(H^+)=1/\{1+(K_{0.5}/[H^+])^n\}$, where pH at half-maximal response is $-\log K_{0.5}$, and I is the current at a given proton concentration, $[H^+]$, was best-fit to the dose-response data using the program NFIT (University of Texas Medical Branch, Galveston, TX), a least-squares algorithm. PulseFit (HEKA Elektronik) was used to determine the time constants of current activation and desensitization, fit to a single exponential. Igor software (WaveMetrics, Inc) was used to curve-fit the time of recovery from desensitization. Permeability ratios were calculated from reversal potentials using the Goldman-Hodgkin-Katz equation.[31] $P_{Na}:P_K$ was calculated from the change in reversal potential (ΔE_{rev}) when K^+ replaced Na^+ in the external solution: $\Delta E_{rev}=(RT/F)\ln\{P_{Na^+}[Na^+]_o/P_{K^+}[K^+]_o\}$, where T is absolute temperature, R and F are gas and Faraday constants, respectively, and brackets indicate concentrations. $P_{Na}:P_{Ca}$ was calculated from the absolute reversal potential with Na^+ and Ca^{2+} as the only current carriers inside and outside the cell, respectively, using the following equation: $E_{rev}=(RT/2F)\ln\{4P_{Ca2+}[Ca^{2+}]_o/P_{Na+}[Na^+]_i\}$. Data are reported as mean±SEM. Statistical analysis was performed with an unpaired t test. A value of $P<0.01$ was considered statistically significant.

Results

Response of CSNs to Chemical Stimuli

To study the response of CSNs to potential chemical mediators of ischemia, the following chemicals were each dissolved in an external solution of pH 7.4: in μmol/L, ATP 30,[32] 5HT 30,[33] capsaicin 1,[34] acetylcholine (ACh) 200,[35] and adenosine 200,[37] as well as 500 nmol/L BK.[36] The concentrations chosen for each compound produced maximal responses in our experiments and in the references cited. The largest measured currents (8.58±1.44 nA) were consistently evoked (93%) by acid applied to CDRGNs (Figure 3). A smaller percentage of UDRGNs (54%) and CNodNs (74%) responded to acid, and the cells that responded displayed significantly smaller currents (3.48±1.10 nA in UDRGNs and 1.15±0.23 nA in CNodNs; $P<0.01$ versus pH-evoked current in CDRGNs) (Figure 3B and 3C). These differences between cell populations refer to the amplitude of transient acid-evoked current (see below); the sustained component evoked by very low pH was seen in virtually every neuron and did not distinguish different cell populations.

Another consistent and large response (4.87±0.59 nA) was evoked by ATP acting on ion channels called P2X receptors in CNodNs. The current was slow activating and only partially desensitized (data not shown), which is indicative of

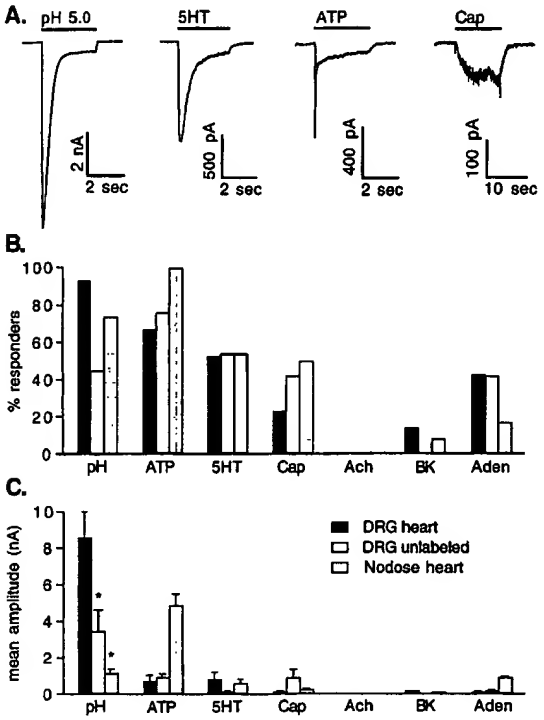

Figure 3. CSNs respond to a variety of chemical activators. A, Representative currents evoked by application of various chemicals to CDRGNs. Note the different scale bars and application times. Each of the test solutions was applied to cells, in random order, for a minimum of 3 seconds; a longer application was made if needed to see the peak current amplitude. Control solution flowed onto the cells for 30 seconds between chemical applications. B, Percentages of CDRGNs, UDRGNs, and CNodNs that responded to the following: pH 5.0; (in μmol/L) ATP 30, 5HT 30, capsaicin 1, ACh 200, and adenosine 200; and 500 nmol/L BK. A positive response was defined as an evoked current >50 pA. For pH response, the number of CDRGNs studied was 29; UDRGNs, 22; and CNodNs, 19. Not all of the cells studied were tested for all chemicals; each bar represents at least 12 cells. C, Mean current amplitudes of the responding neurons. Data are mean±SEM. *$P<0.01$ vs pH-evoked current in CDRGNs. Cap indicates capsaicin; Aden, adenosine.

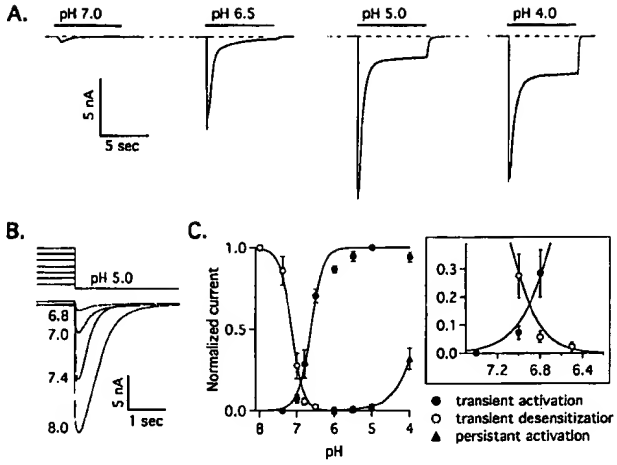

Figure 4. Activation and desensitization of acid-evoked currents in CDRGNs. A, Typical currents evoked by applying various pH solutions to a CDRGN. Note the transient, fast-activating, and fast-desensitizing current that is evoked by relatively low proton concentrations. At higher proton concentrations, a nondesensitizing, sustained current is evoked. Resting pH=8.0 at −70 mV. B, Superimposed currents evoked by pH 5.0 from varying resting pH values. The resting pH was applied for at least 3 seconds. C, Dose-response data for acid-evoked transient (●, n=6) and sustained (▲, n=6) currents. ○ indicates data obtained using the desensitization protocol shown in panel B (n=7). Transient responses are normalized to the peak current obtained from application of pH 5.0 from a resting pH of 8.0. The sustained responses are normalized to the saturation level of the curve fit. Curves are best fits of the Hill equation, $I(H^+)=1/\{1+[K_{0.5}/(H^+)]^n\}$ (activation), or $I(H^+)=1/\{1+[(H^+)/K_{0.5}]^n\}$ (desensitization). Half-activation values were pH 6.6 (transient) and pH 3.7 (sustained); half-desensitization was pH 7.2. Hill coefficients (n) were 2.5 (transient activation), 1.2 (sustained activation), and 2.6 (transient desensitization). Boxed inset magnifies the region where the transient activation and desensitization curves overlap. Points represent mean±SEM.

the heteromeric combination of P2X2 and P2X3 receptor subtypes previously described in nodose neurons.[38] In contrast, the ATP-evoked currents in CDRGNs and UDRGNs were substantially smaller and consisted primarily of a fast-activating and fast-desensitizing current (Figure 3A), which suggests either the P2X1 or P2X3 receptor subtypes.[39] CSNs sometimes responded to the other chemicals indicated in Figure 3; however, they did so inconsistently, and the amplitude of evoked currents in the responders was much smaller than with either pH or ATP (Figure 3B and 3C).

Biophysical and Pharmacological Properties of Acid-Evoked Currents in CDRGNs

The exceptionally large amplitude and prevalence of the transient acid-evoked current in CDRGNs suggests its significance in sensing cardiac ischemia. Therefore, we characterized its biophysical and pharmacological properties to see how these compared with the variety of acid-evoked currents seen in sensory neurons.[23–26] In short, we found no properties unexpected from those described in the literature.

A drop in pH to 7.0 reproducibly evoked a transient, rapidly activating and rapidly desensitizing current in CDRGNs (Figure 4A and 4C). This transient current was half-activated by a pH step to 6.6 and half-desensitized by preincubation at pH 7.2 (Figure 4C). The Hill coefficient of the activation curve was 2.5. A smaller, nondesensitizing current was evoked by more extreme decreases in pH (≤6). The activation curve for this current is fitted with a $pH_{0.5}$ of 3.7. The combination of transient and sustained components at low pH has previously been seen in unlabeled rat sensory neurons.[26,27]

Varying the pH before a test stimulus of pH 5 revealed that a significant fraction of the transient current is desensitized at a resting pH of 7.4 (Figure 4B). This is consistent with the previous demonstration that acid-evoked channels need not open to desensitize.[25] The steady-state desensitization and activation curves show clear overlap in the vicinity of pH 7 (Figure 7C and inset), suggesting that the channel can generate a standing current at pH 7.

A closer look at the time constants of activation and desensitization of the transient currents in CDRGNs revealed multiple transient components (Figure 5), as noted by Krishtal and Pidoplichko.[27] Most cells exhibited a rapidly activating and desensitizing current, but some had a current that was 10-fold slower. The fast and slow transient currents were not

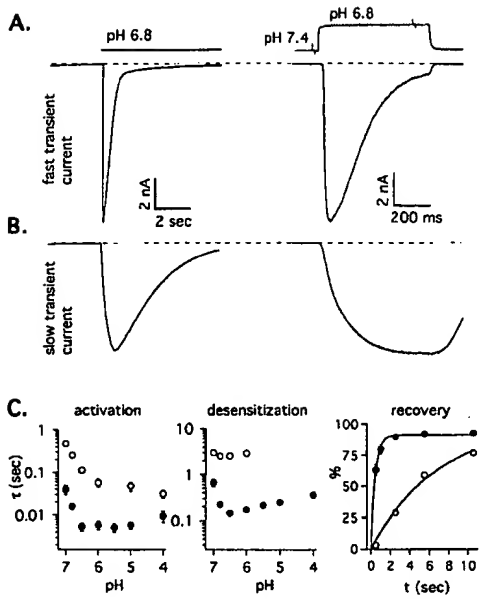

Figure 5. Kinetics of acid-evoked transient currents in CDRGNs. A, Typical transient current evoked by pH 6.8. Trace on the right is a shorter pH application to the same cell, displayed on a faster time scale to demonstrate the fast activation. Top right trace shows the measured time course of pH application (see Materials and Methods). B, In a small subpopulation of CDRGNs, acid evoked a different transient current with slower activation and desensitization. Left and right scale bars correspond to left and right traces for both panels A and B. C, Activation, desensitization, and recovery from desensitization are each faster in the fast transient (●) than the slow transient (○) current. Time constants for activation and desensitization at various pH solutions are from exponential fits to the rising and falling phase of currents, as in panels A and B. Recovery times are at pH 7.4. Horizontal axis indicates interval at pH 7.4 spent between 2 pulses to pH 6.8. The first pulse completely desensitizes the current, and the second tests the extent of recovery. Vertical axis is the relative amplitude of currents evoked by the second and first pulses. Time constants of the exponential fits are 0.44 and 6.8 seconds for the fast and slow currents, respectively.

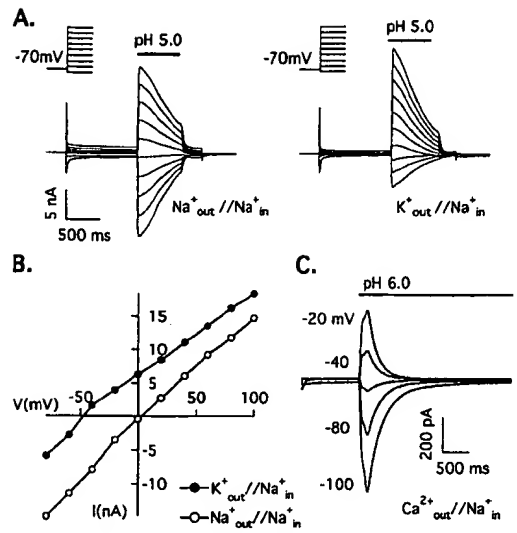

Figure 6. Fast transient acid-evoked currents in CDRGNs are Na^+ selective. A, Transient currents evoked by applying pH 5.0 during steps to various membrane potentials in an extracellular solution of NaCl (left) or KCl (right). Internal solution was NaCl. B, Current vs voltage curves from the data in panel A. Data points indicate differences between currents at pH 7.4 and 5.0. The mean shift in reversal potential was −50±1.2 mV (n=3); thus, P_{Na}/P_K=6.8. C, Currents evoked by pH 6.0 at the indicated potentials in 10 Ca^{2+} (external) and 15 Na^+ (internal). Mean reversal potential was −47.2±2.3 mV (n=7); thus, P_{Na}/P_{Ca}=105.

exclusive; a few neurons displayed both currents, which was evident as biphasic activation and/or desensitization. These cells were not included in the analysis of time constants. The rate of recovery from desensitization differed for the fast and slow transient currents in CDRGNs (Figure 5C). In a control solution of pH 7.4, the fast transient current recovered with τ=0.44 seconds, and the slow transient current recovered with τ=6.8 seconds.

The fast transient current is Na^+ selective but Ca^{2+} permeable (Figure 6). With the usual internal (high K^+) and external (high Na^+) solutions, the reversal potential was in the vicinity of +50 mV (data not shown). To quantify the evident preference for Na^+ over K^+, we measured reversal potentials with Na^+ as the internal ion (see Materials and Methods). The reversal potential shifted −50±1.2 mV when K^+ replaced Na^+, corresponding to a P_{Na}/P_K of 6.8.

Current-voltage relationships measured in 10 mmol/L extracellular Ca^{2+} with 15 mmol/L intracellular Na^+ displayed an average reversal potential of −47.2±1.2 mV (n=7), corresponding to a P_{Na}/P_{Ca} of 105 (Figure 6C). In all cells, current amplitude increased when [Ca^{2+}] was increased from 10 to 30 mmol/L (n=7; amplitude increase varied from 28% to 725%; data not shown). Thus, as previously shown,[40] the current can be carried by Ca^{2+}. To determine whether the acid-evoked currents are blocked by millimolar extracellular Ca^{2+}, as seen in some native[24,25] and cloned[41] channels, we measured Na^+ currents elicited by pH 6.0 in 1, 2, and 10 mmol/L Ca^{2+}. There was no change in amplitude (n=5; data not shown); therefore, the current was not blocked by millimolar Ca^{2+} concentrations.

The fast transient and sustained current components differ in 2 respects: ion selectivity (Figure 7A) and pharmacology (Figure 7B). Both components are cation selective, because they were unchanged when extracellular Cl^- was replaced with the impermeant anion $CH_3SO_3^-$. Replacement of extracellular Na^+ with Cs^+ revealed that the transient current does not readily pass Cs^+, whereas the sustained current does. Thus, as previously described in UDRGNs,[26] the transient current is selective for Na^+, whereas the sustained current is a nonselective cationic current.

Amiloride, a K^+-sparing diuretic that has been shown to block proton-activated currents in mouse neuroblastoma cells,[42] blocked the fast transient current (IC_{50}=9.2 μmol/L) but not the sustained current (Figure 7B). This difference is consistent with one of the ASICs.[43] The slow transient current was similarly inhibited by amiloride (data not shown). The amiloride derivative ethylisopropylamiloride inhibited the fast transient current with an IC_{50} of 37.6 μmol/L (data not shown). These blocking concentrations are ≈100-fold greater than those needed to block the epithelial amiloride-sensitive Na^+ channel[44] and are high enough to block unrelated ion channels.[42]

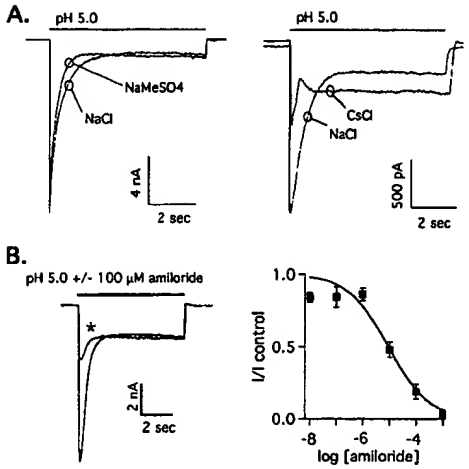

Figure 7. Fast transient and sustained acid-evoked currents in CDRGNs differ in ion selectivity and in amiloride sensitivity. A, Superimposed acid-evoked currents in NaCl and $NaCH_3SO_3$ (left). Both the transient and sustained acid-evoked currents were unchanged when extracellular Cl^- was replaced with the impermeable anion $CH_3SO_3^-$. Thus, neither current is carried by anions. Right, Currents evoked in extracellular solutions containing either NaCl or CsCl. Transient current is more permeable to Na^+ than Cs^+, whereas the sustained current is more permeable to Cs^+ than Na^+. B, Left, currents evoked by pH 5.0 and by pH 5.0 plus 100 μmol/L amiloride (*). The transient current was significantly reduced by amiloride, whereas the sustained current was unchanged. Right, dose-response curve for amiloride on current evoked by a pH change from 7.4 to 6.8. IC_{50}=9.2 μmol/L (n=5).

Discussion

There are 4 key findings in this study, as follows. (1) We describe a method to distinguish CSNs from neurons of other sensory modalities in primary dissociated tissue culture. (2) Compared with other sensory neurons, CDRGNs have extremely large currents evoked when pH drops to 7.0 or below. (3) CNodNs have smaller acid-evoked currents, but larger ATP-evoked currents than CDRGNs. (4) Other than its large amplitude, the acid-evoked current in CSNs has no biophysical or pharmacological properties that are not predicted by previous studies of acid-evoked currents in sensory neurons. The large amplitude indicates the importance of acid in mediating pain due to cardiac ischemia, but it certainly does not imply that other potential mediators are unimportant.

Isolation of CSNs

As described in Materials and Methods, considerable effort was made to validate this preparation. Each of the control injection experiments resulted in significantly fewer labeled neurons compared with the pericardial space injections; this lends support to our assertion that we have specifically labeled and isolated CSNs. Finally, the different responses between the labeled DRG neurons and UDRGNs in our whole-cell patch-clamp experiments provide further evidence that we have isolated a distinct subgroup of sensory neurons from the DRG population at large.

Although neuroanatomy was not the primary focus of this study, some anatomical information can be gleaned from our data. The number of labeled neurons we obtained was consistent with previous neuroanatomical studies in the rat in which fluorescent tracers were injected into the pericardial space.[4,45] In contrast to the large number of labeled neurons appearing after pericardial space injections, we found relatively few labeled neurons after intramural injections. This may reflect either less tissue exposure to dye compared with the pericardial space injection or a true paucity of nerve terminals within the rat intramural myocardium. The endocardial layers were not labeled in our study. Interestingly, in a dog preparation, myocardial ischemia caused cardiac sympathetic afferent firing only if the ischemia was transmural and involved the superficial epicardial layers.[10]

Chemical Activation of CSNs

Several insights arise from a comparison of responses to different agonists in the different cell populations that we isolated. Most importantly, modest decreases in extracellular pH (ie, to pH 7.0 or below) evoke exceptionally large currents in almost all epicardial CDRGNs. In contrast, and as reported previously,[26,27] only ≈50% of UDRGNs respond to acid; those that did respond had much smaller average currents than CDRGNs.[46]

Cardiac afferents with cell bodies in the DRG differed from those in the nodose ganglia. CNodNs had significantly smaller acid-evoked currents and larger ATP-evoked currents than CDRGNs. This raises the possibility that the 2 cell populations sense different chemical signals during cardiac ischemia.

There are 2 classes of molecules that are proposed to sense changes in extracellular pH in sensory neurons: ASICs and vanilloid (capsaicin) receptors. Vanilloid receptors are activated by noxious heat and by capsaicin (the compound in pepper that tastes "hot"); also, current through vanilloid receptors is strongly increased by acidic pH.[34,47] Therefore, it is considered that vanilloid receptors, in addition to sensing heat, may mediate sensory responses to acidity caused by inflammation and ischemia. The neurons we isolated detect cardiac ischemia, yet only a small fraction exhibit capsaicin-activated current, and those that do respond have small currents compared with UDRGNs. In contrast, almost all exhibit grossly large currents through ASICs. These results argue that ASICs are more important than vanilloid receptors for sensing myocardial ischemia.

5HT evoked currents that were substantial in cardiac afferents, but they were still smaller than the acid- or ATP-evoked currents. Various cells that contribute to the immune response to tissue damage release 5HT, so these currents may provide a means of communication between immune cells and CSNs.

Of the chemicals tested, protons, ATP, 5HT, and capsaicin activate ion channels (the ASICs,[28] P2X receptors,[38,39] 5HT3 receptor,[33] and vanilloid receptors,[34] respectively) that are presumed to serve as sensory transducers in sensory neurons. No current was ever evoked by ACh, but currents were occasionally seen in response to BK or adenosine. We do not infer anything from the relatively rare and small currents evoked by these compounds, because they do not directly gate ion channels in sensory neurons; in fact, adenosine inhibits a Ca^{2+}-activated K^+ channel.[37] The current we saw presumably arose from modulation of a channel by an

intracellular signaling cascade; the importance of this may be understated by simply comparing the amplitude with those of channels directly gated by protons, ATP, or 5HT.

Physiological and Pathophysiological Significance

CSNs respond to lowered pH (in the range produced by myocardial ischemia) with consistent and robust depolarizing currents; this suggests that acid is a potential mediator of myocardial ischemic sensation.

In humans, the only conscious sensation from the heart is pain or angina, which most commonly occurs during myocardial ischemia. However, objective measurements of myocardial ischemia often do not correlate with the presence or severity of chest pain. In fact, ambulatory electrocardiographic monitoring in patients with myocardial ischemia has revealed that the majority of ischemic episodes are not reported as painful.[48] Attempts to model ischemic cardiac pain in animals have produced variable results. The pseudoaffective measures of pain in these behavioral studies correlate poorly with sensory neuronal activation.[13,16,49] Thus, it is reasonable to conclude that activation of CSNs with acid does not equate with nociception. For example, in patients with "silent" ischemia (defined as objective myocardial ischemia that is painless), there is evidence of sensory activation to the level of the thalamus, whereas patients with typical angina have additional activation of the cerebral cortex.[50] Thus, the conscious perception of chest pain most certainly involves complex central processing and integration at multiple levels, and activation of CSNs is probably necessary but not sufficient to produce pain. Regardless, ischemia- or acid-induced activation of CSNs, whether painful or not, may be an important initiator of cardiovascular reflexes in pathological cardiac conditions.

A broad range of cardiovascular disease processes, including myocardial ischemia,[51] congestive heart failure,[52] and arrhythmias,[53] are precipitated or worsened by perturbations in the autonomic nervous system. Much of the current pharmacological therapies are directed toward blocking the compensatory, but often deleterious, neurohormonal systems that are activated in these diseases. In human skeletal muscle, ischemia-induced acidic pH is coupled with sympathetic efferent nerve discharge.[54] Also, abdominal visceral ischemia leads to profound cardiovascular reflex changes, the degree of which appears related to the level of the resulting acidosis.[55] A similar acid-evoked reflex loop may exist in the heart and contribute to the detrimental effect of sympathetic activation in myocardial ischemic conditions. Specific blockade of acid-evoked activation of CSNs presents a potential new therapeutic management strategy in the treatment of ischemic heart disease.

Acknowledgments

This study was supported by the following NIH grants: RO1DAO7415, Cardiovascular Signaling Training Grant T32-HL07817 (to C.J.B.), and Neuronal Signal Transduction Training Grant NS07381 (to S.P.E.). We thank G. Giraud and K. Thornburg for their comments on the manuscript and V.C. Dang for technical assistance.

References

1. Cutler EC. Summary of experiences up-to-date in the surgical treatment of angina pectoris. *Am J Med Sci.* 1927;173:613–624.
2. White JC. Cardiac pain: anatomic pathways and physiologic mechanisms. *Circulation.* 1957;16:644–655.
3. Berry M, Bannister LH, Standering SM, eds. *Gray's Anatomy.* New York, NY: Churchill Livingstone; 1995;901–1397.
4. McNeill DL, Burden HW. Convergence of sensory processes from the heart and left ulnar nerve onto a single afferent perikaryon: a neuroanatomical study in the rat employing fluorescent tracers. *Anat Rec.* 1986; 214:441–444.
5. Lewis T. Pain in muscular ischemia: its relation to anginal pain. *Arch Int Med.* 1932;49:713–727.
6. Brown AM. Excitation of afferent cardiac sympathetic nerve fibres during myocardial ischemia. *J Physiol (Lond).* 1967;190:35–53.
7. Minisi AJ, Thames MD. Activation of cardiac sympathetic afferents during coronary occlusion: evidence for reflex activation of sympathetic nervous system during transmural myocardial ischemia in the dog. *Circulation.* 1991;84:357–367.
8. Huang MH, Horackova M, Negoescu RM, Wolf S, Armour JA. Polysensory response characteristics of dorsal root ganglion neurones that may serve sensory functions during myocardial ischaemia. *Cardiovasc Res.* 1996;32:503–515.
9. Thames MD, Klopfenstein HS, Abboud FM, Allyn LM, Walker JL. Preferential distribution of inhibitory cardiac receptors with vagal afferents to the inferoposterior wall of the left ventricle activated during coronary occlusion in the dog. *Circ Res.* 1978;43:512–519.
10. Armour JA, Huang MH, Pelleg A, Sylven C. Responsiveness of in situ canine nodose ganglion afferent neurones to epicardial mechanical or chemical stimuli. *Cardiovasc Res.* 1994;28:1218–1225.
11. James TN. A cardiogenic hypertensive chemoreflex. *Anesth Analg.* 1989; 69:633–646.
12. Baker DG, Coleridge HM, Coleridge JCG, Nerdrum T. Search for a cardiac nociceptor: stimulation by bradykinin of sympathetic afferent nerve endings in the heart of the cat. *J Physiol (Lond).* 1980;306: 519–536.
13. Euchner-Wamser I, Meller ST, Gebhart GF. A model of cardiac nociception in chronically instrumented rats: behavioral and electrophysiological effects of pericardial administration of algogenic substances. *Pain.* 1994;58:117–128.
14. Malliani A, Schwartz PJ, Zanchetti A. A sympathetic reflex elicited by experimental coronary occlusion. *Am J Physiol.* 1969;217:703–709.
15. Sleight P. A cardiovascular depressor reflex from the epicardium of the left ventricle in the dog. *J Physiol (Lond).* 1964;173:321–343.
16. Meller ST, Gebhart GF. A critical review of the afferent pathways and the potential chemical mediators involved in cardiac pain. *Neuroscience.* 1992;48:501–524.
17. Jacobus WE, Taylor GT IV, Hollis DP, Nunnally RL. Phosphorus nuclear magnetic resonance of perfused working rat hearts. *Nature.* 1977;265: 756–758.
18. Cobbe SM, Poole-Wilson PA. The time of onset and severity of acidosis in myocardial ischemia. *J Mol Cell Cardiol.* 1980;12:745–760.
19. Hirsch HJ, Franz CHR, Bos L, Bissig R, Lang R, Schramm M. Myocardial extracellular K^+ and H^+ increase and noradrenaline release as possible cause of early arrhythmias following acute coronary artery occlusion in pigs. *J Mol Cell Cardiol.* 1980;12:579–593.
20. Cobbe SM, Poole-Wilson PA. Continuous coronary sinus and arterial pH monitoring during pacing-induced ischaemia in coronary artery disease. *Br Heart J.* 1982;47:369–374.
21. Uchida Y, Murao S. Acid-induced excitation of afferent cardiac sympathetic nerve fibers. *Am J Physiol.* 1975;228:27–33.
22. Steen KH, Steen AE, Reeh PW. A dominant role of acid pH in inflammatory excitation and sensitization of nociceptors in rat skin, in vitro. *J Neurosci.* 1995;15:3982–3989.
23. Krishtal OA, Pidoplichko VI. A receptor for protons in the nerve cell membrane. *Neuroscience.* 1980;5:2325–2327.
24. Konnerth A, Lux HD, Morad M. Proton-induced transformation of calcium channel in chick dorsal root ganglion cells. *J Physiol (Lond).* 1987;386:603–633.
25. Davies NW, Lux HD, Morad M. Site and mechanism of activation of proton-induced sodium current in chick dorsal root ganglion neurons. *J Physiol (Lond).* 1988;400:159–187.
26. Bevan S, Yeats J. Protons activate a cation conductance in a subpopulation of rat dorsal root ganglion neurones. *J Physiol (Lond).* 1991; 433:145–161.

27. Krishtal OA, Pidoplichko VI. A receptor for protons in the membrane of sensory neurons may participate in nociception. *Neuroscience.* 1981;6: 2599–2601.
28. Waldmann R, Lazdunski M. H^+-gated cation channels: neuronal acid sensors in the NaC/DEG family of ion channels. *Curr Opin Neurobiol.* 1998;8:418–424.
29. Nakatani T, Shinohara H, Fukuo Y, Morisawa S, Matsuda T. Pericardium of rodents: pores connect the pericardial and pleural cavities. *Anat Rec.* 1988;220:132–137.
30. Eckert SP, Taddese A, McCleskey EW. Isolation and culture of rat sensory neurons having distinct sensory modalities. *J Neurosci Methods.* 1997;77:183–190.
31. Hille B. Selective permeability: independence. In: *Ion Channels of Excitable Membranes.* Sunderland, Mass: Sinauer Associates; 1992: 344–347.
32. Cook SP, Vulchanova L, Hargreaves KM, Elde R, McCleskey EW. Distinct ATP receptors on pain-sensing and stretch-sensing neurons. *Nature.* 1997;387:505–508.
33. Maricq AV, Peterson AS, Brake AJ, Myers RM, Julius D. Primary structure and functional expression of the $5HT_3$ receptor, a serotonin-gated ion channel. *Science.* 1991;254:432–436.
34. Caterina MJ, Schumacher MA, Tominaga M, Rosen TA, Levine JD, Julius D. The capsaicin receptor: a heat-activated ion channel in the pain pathway. *Nature.* 1997;389:816–824.
35. Sucher NJ, Cheng TPO, Lipton SA. Neural nicotinic acetylcholine responses in sensory neurons from postnatal rat. *Brain Res.* 1990;533: 248–254.
36. Nicol GD, Cui M. Enhancement by prostaglandin E_2 of bradykinin activation of embryonic rat sensory neurones. *J Physiol (Lond).* 1994;480: 485–492.
37. Allen TGJ, Burnstock G. The actions of adenosine 5′-triphosphate on guinea-pig intracardiac neurones in culture. *Br J Pharmacol.* 1990;100: 269–276.
38. Lewis C, Neidhart S, Holy C, North RA, Buell G, Suprenant A. Coexpression of $P2X_2$ and $P2X_3$ receptor subunits can account for ATP-gated currents in sensory neurons. *Nature.* 1995;377:432–435.
39. Chen CC, Akopian AN, Sivilotti L, Colquhoun D, Burnstock G, Wood JN. A P2X purinoceptor expressed by a subset of sensory neurons. *Nature.* 1995;377:428–431.
40. Kovalchuk YN, Krishtal OA, Nowycky MC. The proton-activated inward current of rat sensory neurons includes a calcium component. *Neurosci Lett.* 1990;115:237–242.
41. Waldmann R, Champigny G, Bassilana F, Heurteaux C, Lazdunski M. A proton-gated cation channel involved in acid-sensing. *Nature.* 1997;386: 173–177.
42. Tang CM, Presser F, Morad M. Amiloride selectively blocks the low threshold (T) calcium channel. *Science.* 1988;240:213–215.
43. Waldmann R, Bassilana F, de Weille J, Champigny G, Heurteaux C, Lazdunski M. Molecular cloning of a non-inactivating proton-gated Na^+ channel specific for sensory neurons. *J Biol Chem.* 1997;272: 20975–20978.
44. Canessa CM, Schild L, Buell G, Thorens B, Gautschi I, Horisberger J, Rossier BC. Amiloride-sensitive epithelial Na^+ channel is made of three homologous subunits. *Nature.* 1994;367:463–467.
45. Alles A, Dom RM. Peripheral sensory nerve fibers that dichotomize to supply the brachium and the pericardium in the rat: a possible morphological explanation for referred cardiac pain? *Brain Res.* 1985;342: 382–385.
46. Bevan S, Winter J. Nerve growth factor (NGF) differentially regulates the chemosensitivity of adult rat cultured sensory neurons. *J Neurosci.* 1995; 15:4918–4926.
47. Tominaga M, Caterina MJ, Malmberg AB, Rosen TA, Gilbert H, Skinner K, Raumann BE, Basbaum AI, Julius D. The cloned capsaicin receptor integrates multiple pain-producing stimuli. *Neuron.* 1998;21:531–543.
48. Deanfield JE, Shea MJ, Selwyn AP. Clinical evaluation of transient myocardial ischemia during daily life. *Am J Med.* 1985;79(suppl 3A): 18–24.
49. Malliani A. Significance of experimental models in assessing the link between myocardial ischemia and pain. *Adv Cardiol.* 1990;37:126–141.
50. Rosen SD, Paulesu E, Nihoyannopoulos P, Tousoulis D, Prackowiak SJ, Frith CD, Jones T, Camici PG. Silent ischemia as a central problem: regional brain activation compared in silent and painful myocardial ischemia. *Ann Intern Med.* 1996;124:939–949.
51. Thamer V, Deussen A, Schipke JD, Tolle T, Heusch G. Pain and myocardial ischemia: the role of sympathetic activation. *Basic Res Cardiol.* 1990;85:253–266.
52. Francis GS, Goldsmith SR, Levine TB, Olivari MT, Cohn JN. The neurohormonal axis in congestive heart failure. *Ann Intern Med.* 1984; 101:370–377.
53. Mitrani RD, Zipes DP. Clinical neurocardiology: arrhythmias. In: Armour JA, Ardell JL, ed. *Neurocardiology.* New York, NY: Oxford University Press; 1994:365–395.
54. Victor RG, Bertocci LA, Pryor SL, Nunnally RL. Sympathetic nerve discharge is coupled to muscle cell pH during exercise in humans. *J Clin Invest.* 1988;82:1301–1305.
55. Rendig SV, Chalal PS, Longhurst JC. Cardiovascular reflex responses to ischemia during occlusion of celiac and/or superior mesenteric arteries. *Am J Physiol.* 1997;272:H791–H796.

Neuron, Vol. 26, 133–141, April, 2000, Copyright ©2000 by Cell Press

Neuropeptide FF and FMRFamide Potentiate Acid-Evoked Currents from Sensory Neurons and Proton-Gated DEG/ENaC Channels

Candice C. Askwith,* Chun Cheng,† Mutsuhiro Ikuma,* Christopher Benson,† Margaret P. Price,† and Michael J. Welsh*†‡§
*Howard Hughes Medical Institute
†Department of Internal Medicine
‡Department of Physiology and Biophysics
University of Iowa College of Medicine
Iowa City, Iowa 52242

Summary

Acidosis is associated with inflammation and ischemia and activates cation channels in sensory neurons. Inflammation also induces expression of FMRFamide-like neuropeptides, which modulate pain. We found that neuropeptide FF (Phe-Leu-Phe-Gln-Pro-Gln-Arg-Phe amide) and FMRFamide (Phe-Met-Arg-Phe amide) generated no current on their own but potentiated H^+-gated currents from cultured sensory neurons and heterologously expressed ASIC and DRASIC channels. The neuropeptides slowed inactivation and induced sustained currents during acidification. The effects were specific; different channels showed distinct responses to the various peptides. These results suggest that acid-sensing ion channels may integrate multiple extracellular signals to modify sensory perception.

Introduction

FMRFamide (Phe-Met-Arg-Phe amide) and related peptides comprise a family of neuropeptides that are abundant in many invertebrates, including *Caenorhabditis elegans* (Nelson et al., 1998), *Aplysia californica* (Greenberg and Price, 1992), and *Drosophila melanogaster* (Schneider and Taghert, 1988). In these organisms, FMRFamide-like neuropeptides act as neurotransmitters and neuromodulators. At least one gene encoding FMRFamide-related peptides is present in mammals; it produces neuropeptide FF (Phe-Leu-Phe-Gln-Pro-Gln-Arg-Phe amide) and neuropeptide AF (A18Famide) (Perry et al., 1997; Vilim et al., 1999). Although FMRFamide itself has not been discovered in mammals (Yang et al., 1985), administration of FMRFamide induces a variety of physiologic effects, including alterations in blood pressure, respiratory rate, glucose-stimulated insulin release, and behavior (Mues et al., 1982; Sorenson et al., 1984; Kavaliers and Hirst, 1985; Raffa et al., 1986; Kavaliers, 1987; Telegdy and Bollók, 1987; Thiemermann et al., 1991; Muthal et al., 1997; Nishimura et al., 2000). In mammals, FMRFamide and neuropeptide FF also modify the response to painful stimuli, and neuropeptide FF is induced by inflammation (Tang et al., 1984; Yang et al., 1985; Raffa and Connelly, 1992; Kontinen et al., 1997; Vilim et al., 1999). When FMRFamide or neuropeptide FF is injected intracerebroventricularly, it elicits hyperalgesia and a reduction in morphine-induced analgesia (Tang et al., 1984; Yang et al., 1985; Kavaliers, 1987; Raffa, 1988; Brussaard et al., 1989; Roumy and Zajac, 1998). In addition, FMRFamide-like immunoreactive material is released in mammals following chronic morphine administration, and anti-FMRFamide antibodies can enhance morphine's effects (Tang et al., 1984; Devillers et al., 1995). However, when administered intrathecally, these peptides can have an analgesic effect thought to be mediated through opioid receptors (Raffa, 1988; Raffa and Connelly, 1992; Gouardères et al., 1993; Roumy and Zajac, 1998).

Some effects of FMRFamide and neuropeptide FF appear to be mediated through opioid receptors; these effects are blocked by the opioid antagonist naloxone (Kavaliers and Hirst, 1985; Kavaliers, 1987; Raffa, 1988; Gouardères et al., 1993; Roumy and Zajac, 1998). Yet, other effects of FMRFamide and FMRFamide-related peptides are independent of opioid receptors and are insensitive to naloxone (Gayton, 1982; Raffa et al., 1986; Kavaliers, 1987; Raffa, 1988; Allard et al., 1989; Roumy and Zajac, 1998). In mammals, the nonopioid receptor(s) for FMRFamide and related peptides has not been identified, and it is not known how these peptides modulate pain sensation. However, the discovery of a FMRFamide-activated Na^+ channel (FaNaCh) in the mollusc *Helix aspersa* (Lingueglia et al., 1995) provided a clue that similar receptors might exist in mammals.

Unlike many neuropeptide receptors, FaNaCh is an ion channel gated directly by its peptide ligand, FMRFamide (Lingueglia et al., 1995). The neuropeptide receptor FaNaCh is a member of the DEG/ENaC family of channels. DEG/ENaC channels are homo- or heteromultimers composed of multiple subunits (Bassilana et al., 1997; Lingueglia et al., 1997; Coscoy et al., 1998; Waldmann and Lazdunski, 1998). Each subunit contains two transmembrane domains separated by a large, extracellular, cysteine-rich domain and cytosolic N and C termini (Waldmann and Lazdunski, 1998). DEG/ENaC channels are not voltage gated and are cation selective (usually $Na^+ > K^+$). FaNaCh is the only known DEG/ENaC channel that acts as a neuropeptide receptor. Other members of this family are involved in mechanosensation, salt taste, and epithelial Na^+ absorption (Schild et al., 1995; Snyder et al., 1995; Lindemann, 1996; Mano and Driscoll, 1999). Although a mammalian FaNaCh has not yet been isolated, mammals do possess multiple DEG/ENaC family members. Interestingly, one subset of this channel family, the acid-sensing ion channels, has been postulated to play a role in sensory perception and may, like FMRFamide, play a role in pain perception (Waldmann and Lazdunski, 1998). The acid-sensing DEG/ENaC channels respond to protons and generate a voltage-insensitive cation current when the extracellular solution is acidified.

The tissue acidosis associated with inflammation, infection, and ischemia causes pain (Reeh and Steen, 1996). Acidosis also generates proton-dependent transient and sustained Na^+ currents in cultured sensory

§ To whom correspondence should be addressed (e-mail: mjwelsh@blue.weeg.uiowa.edu).

neurons (Krishtal and Pidoplichko, 1981; Davies et al., 1988; Akaike et al., 1990; Kovalchuk Yu et al., 1990; Bevan and Yeats, 1991; Akaike and Ueno, 1994). Although the molecular identity of the channels responsible for these currents is unknown, they have been hypothesized to be acid-sensing members of the DEG/ENaC protein family based on their ion selectivity, voltage insensitivity, and expression pattern (Bassilana et al., 1997; Lingueglia et al., 1997; Waldmann et al., 1997a, 1997b; de Weille et al., 1998; Babinski et al., 1999). The acid-sensing ion channels include the brain Na^+ channel 1 (BNC1, also known as MDEG, BNaC1, and ASIC2) and its differentially spliced isoform, MDEG2 (Price et al., 1996; Waldmann et al., 1996; García-Anoveros et al., 1997; Lingueglia et al., 1997); the acid-sensing ion channel (ASICα, also known as BNaC2 and ASIC1) and its differentially spliced isoform, ASICβ (Waldmann et al., 1997b; Chen et al., 1998); and the dorsal root acid-sensing ion channel (DRASIC, also known as ASIC3) (Waldmann et al., 1997a; de Weille et al., 1998; Babinski et al., 1999). BNC1, MDEG2, ASICα, and DRASIC are expressed in the central nervous system (Lingueglia et al., 1997; Waldmann et al., 1997b; Chen et al., 1998; Olson et al., 1998). ASICα, ASICβ, DRASIC, and MDEG2 are expressed in sensory neurons of the dorsal root ganglia (DRG) (Waldmann et al., 1997a; Chen et al., 1998; Olson et al., 1998; Babinski et al., 1999).

We hypothesized that FMRFamide or FMRFamide like-neuropeptides might modulate pH-dependent currents in DRG neurons. This hypothesis was based on the ability of FMRFamide and related peptides to modulate pain perception, the potential connections between painful stimuli and the acid-gated currents in DRG neurons, and the sequence similarity between FaNaCh and the acid-sensing ion channels expressed in sensory ganglia.

Results

FMRFamide Modulates Proton-Gated Current in Rat DRG Neurons

We used whole-cell patch-clamp recordings to investigate the effect of FMRFamide on proton-gated currents in cultured rat DRG neurons. As previously reported (Krishtal and Pidoplichko, 1981; Akaike et al., 1990; Kovalchuk Yu et al., 1990; Akaike and Ueno, 1994), acidification to pH 5 produced rapidly activating and inactivating currents in the sensory neurons (Figures 1A–1D). FMRFamide added alone generated no response from any of the neurons tested. However, after FMRFamide addition (50–100 μM), the inactivation of proton-dependent currents slowed, and in many neurons there was a sustained current in the continued presence of acid (Figures 1A and 1B). The presence of the neuropeptide immediately before acidification also altered inactivation (Figures 1C and 1D); we examine this further below.

Some effects of FMRFamide are thought to be mediated through activation of opiate receptors (Raffa, 1988; Roumy and Zajac, 1998). To discern whether this might account for potentiation of the proton-gated currents, we tested the effect of naloxone, an opiate antagonist, and morphine, an opiate agonist. Naloxone did not block the effect of FMRFamide (Figure 1B), and morphine did not mimic it (Figure 1C). These results suggested that FMRFamide was not acting through opioid receptors to alter current.

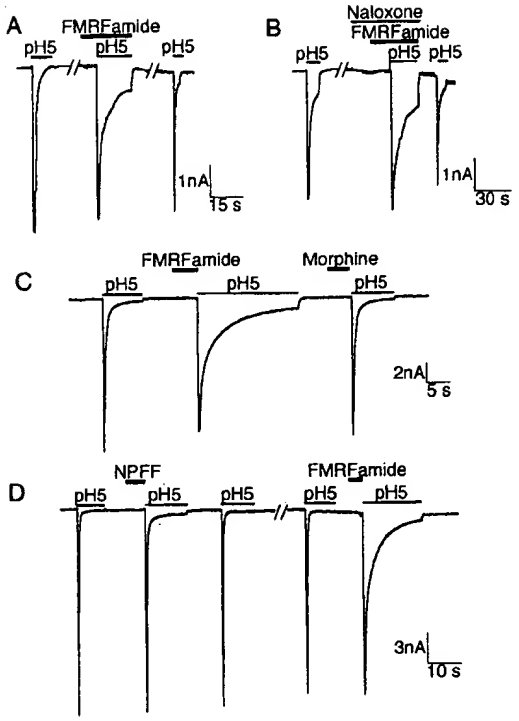

Figure 1. Proton-Gated Currents in Rat DRG Neurons Are Modulated by FMRFamide

(A) Trace of proton-gated whole-cell current; FMRFamide (100 μM) and pH 5 solution were present in bath during time indicated by bars. Unless otherwise indicated, pH was 7.4; n = 8.

(B) Naloxone (100 μM) was present during time indicated by bar; n = 3.

(C) Morphine (50 μM) and FMRFamide (50 μM) were added as indicated; n = 3.

(D) Neuropeptide FF (NPFF) (50 μM) and FMRFamide (50 μM) were present at times indicated by bar; n = 5.

We also tested the mammalian FMRFamide-like neuropeptide FF. Neuropeptide FF modulated currents in a manner similar to that of FMRFamide; it generated no current on its own, but it altered inactivation of proton-gated DRG currents (Figure 1D). The effects, however, were smaller than those generated by FMRFamide (Figure 1D).

Effect of FMRFamide on Acid-Sensing Ion Channels

Members of the DEG/ENaC family are thought to be at least partially responsible for the acid-gated currents in the DRG. This notion is based on the findings that H^+-gated currents from DRG and DEG/ENaC channels, although not identical, share similar pH sensitivity, ion selectivity, and inactivation (Davies et al., 1988; Bevan and Yeats, 1991; Bassilana et al., 1997; Lingueglia et al., 1997; Waldmann et al., 1997a, 1997b; de Weille et al., 1998; Babinski et al., 1999). The differences may be due to as yet unidentified subunits and/or heteromultimeric complexes. Because FMRFamide affected DRG

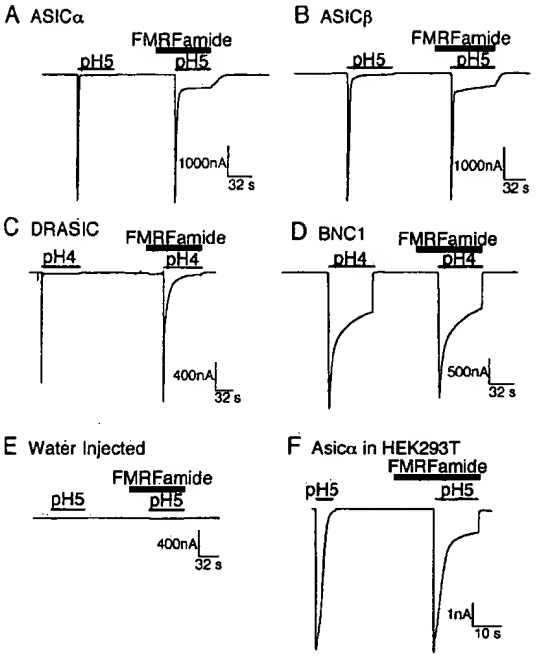

Figure 2. Effect of FMRFamide on H$^+$-Gated DEG/ENaC Family Members

Data are representative traces from *Xenopus* oocytes expressing ASICα (A), ASICβ (B), DRASIC (C), or BNC1 (D); from water-injected oocyte (E); or from HEK293T cells expressing ASICα (F). Unless otherwise indicated, extracellular pH was 7.4. FMRFamide (50 or 100 μM) and pH 5 solution were present in extracellular solution during time indicated by bars. Experiments were repeated at least seven times.

currents, we reasoned that FMRFamide might alter acid-gated DEG/ENaC channels. To test this hypothesis, we expressed mammalian acid-sensitive ion channels in *Xenopus* oocytes and measured the resulting currents. ASICα and its alternatively spliced variant, ASICβ, generated rapidly inactivating currents when the extracellular pH was lowered from 7.4 to 5 (Figures 2A and 2B). In contrast to its effect on FaNaCh, FMRFamide alone had no effect on either channel. However, subsequently lowering pH in the presence of FMRFamide potentiated the current; Figures 2A and 2B show slowing of inactivation and the appearance of a sustained current at pH 5 in both ASICα and ASICβ. DRASIC showed a similar response in the presence of FMRFamide (Figure 2C); following a reduction in pH, inactivation was slowed, and a sustained current was more apparent. In contrast, the acid-gated currents from oocytes expressing BNC1 were not discernibly altered by FMRFamide (Figure 2D). Neither pH nor FMRFamide in any combination produced current in control, water-injected oocytes (Figure 2E).

FMRFamide also altered the function of ASICα expressed in the human cell line HEK293T (Figure 2F). Acidic extracellular solutions induced rapidly inactivating whole-cell currents. In the presence of FMRFamide, inactivation slowed, and a sustained current was apparent. The effect of FMRFamide on current from acid-gated channels expressed in *Xenopus* oocytes and mammalian cells mimicked that observed in DRG neurons. This similarity suggested that these DEG/ENaC

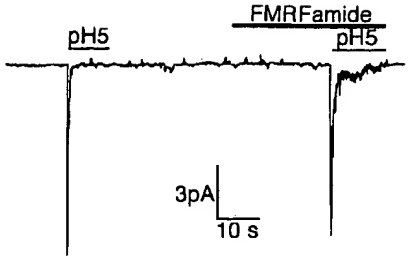

Figure 3. FMRFamide Modulates ASICα Function in Excised, Outside-Out Patches

Tracing is representative of H$^+$-dependent currents recorded from HEK293T cells transfected with ASICα. FMRFamide (100 μM) and pH 5 solution were present in extracellular solution during time indicated by bars; otherwise, pH was 7.4; n = 6.

channels may be responsible, at least in part, for proton-gated currents in neurons. For further studies, we focused on ASICα since it has been the most extensively studied, it is localized in nociceptive neurons of the DRG (Olson et al., 1998), and it produced a stable sustained current with FMRFamide addition.

We also tested the effect of FMRFamide on ASICα in excised, outside-out patches from HEK293T cells. Figure 3 shows that lowering the extracellular pH activated transient currents. In the presence of FMRFamide, inactivation was slowed substantially. These data suggest that FMRFamide interacts with ASICα.

Sequence of Adding FMRFamide and Acidification

In cells expressing ASICα, the presence of FMRFamide before and during acidification induced a sustained current (Figure 4Aiii). The continued presence of FMRFamide did not prevent channel closure when pH was returned to 7.4 (Figure 4Aiii). Thus, FMRFamide could neither activate nor sustain the current; rather, it modulated acid-activated current. This stands in sharp contrast to FaNaCh, which opens in response to FMRFamide alone and not acid (Lingueglia et al., 1995). The sequence of acid and FMRFamide application was important. The largest sustained currents required FMRFamide addition before lowering the extracellular pH; simultaneous addition of FMRFamide and acid (Figure 4Avi) or addition of FMRFamide after acid (Figure 4Aiv) was much less effective. In contrast, when we first applied FMRFamide at pH 7.4 and then washed away the FMRFamide while simultaneously lowering pH, a sustained current still ensued (Figure 4Av). With ASICα expressed in HEK293T cells, the maximal sustained current also required addition of FMRFamide prior to acidification (Figures 4Bii and 4Biii); application of FMRFamide after the pH reduction failed to induce large, sustained current (Figure 4Biv). Therefore, modulation required FMRFamide addition at pH 7.4, when the channel was closed.

It seemed surprising that FMRFamide could generate a sustained current, even when it was removed while the pH was being lowered (Figures 4Av and 4Biii). We observed similar behavior with acid-evoked currents in DRG cells (Figures 1C and 1D). To investigate this further, we examined the effect of removing FMRFamide from

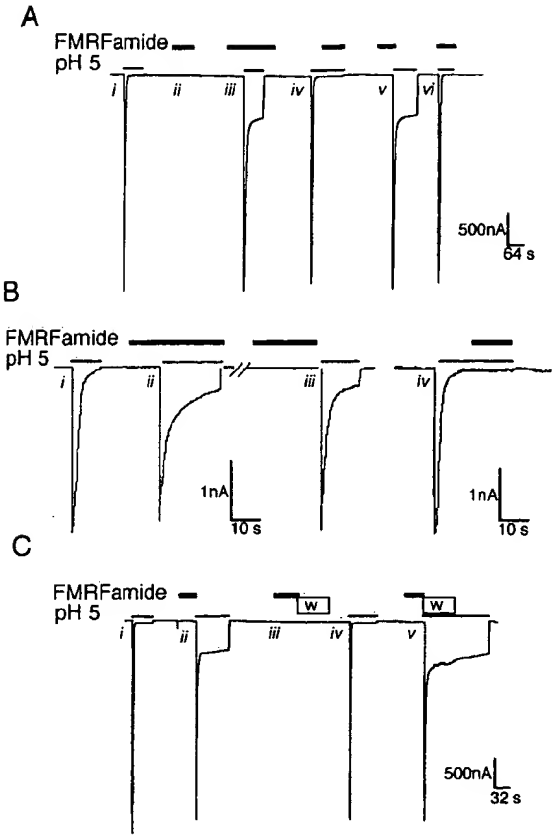

Figure 4. Effect of Order of FMRFamide and Acid Addition

Data are whole-cell currents from *Xenopus* oocytes expressing ASICα (A and C) (n = 5 each) or HEK293T cells expressing ASICα (B) (n = 8). Roman numerals indicate specific interventions referred to in text. pH was 7.4, unless otherwise indicated. FMRFamide (50 or 100 μM) and pH 5 solution were present in bath during times indicated by bars. In (C), cell was continuously perfused with solution, at pH 7.4 or pH 5, for 80 s during time indicated by box.

the bath solution at either pH 7.4 or pH 5. FMRFamide was applied at pH 7.4, and then the bath was continuously washed for 80 s (Figure 4Diii). After this time, acidification generated no sustained current (Figure 4Div). This result suggests that during the 80 s wash, the peptide dissociated or the effect reversed. However, when the pH was reduced while simultaneously removing FMRFamide, the sustained current persisted throughout an 80 s pH 5 wash and beyond (Figure 4Dv). These results suggest that the effect of FMRFamide is only reversible at pH 7.4; once the channel has been activated by acid, the effect of FMRFamide is retained until the pH is returned to 7.4.

Properties of the Current Generated by pH and FMRFamide

FMRFamide concentrations around 1 μM induced detectable sustained currents in cells expressing ASICα (Figure 5A). Maximal levels of sustained current were achieved at ~250 μM FMRFamide. The FMRFamide concentration that induced half-maximal sustained currents was ~33 μM. This concentration is higher than that reported for FaNaCh (2 μM) (Lingueglia et al., 1995).

We asked whether FMRFamide alters the properties of ASICα transient currents and whether the FMRFamide-generated sustained current has properties different from the transient current. Figures 5B and 5C show that the FMRFamide-induced sustained current was inhibited by amiloride in oocytes and HEK293 cells. Figure 5D shows that FMRFamide did not alter the pH sensitivity of the transient current. The FMRFamide-induced sustained current, however, showed sensitivity to a broader pH range compared with the transient current. This broader range of sensitivity might allow a more graded pH response of the FMRFamide-bound channel. This may have implications for the perception of acid-evoked pain, since sustained currents are thought to play a role in pH-dependent nociception (Bevan and Geppetii, 1994).

The current–voltage (I–V) relationship of the H^+-activated transient current of ASICα showed cation selectivity similar to what has been reported previously (Waldmann et al., 1997b); the relative permeabilities were $Na^+/Li^+ = 0.95 \pm 0.06$ and $Na^+/K^+ = 6.76 \pm 0.40$. The slope conductance was similar for all of the cations. The I–V relationship of the peak current was not altered in the presence of FMRFamide (Figure 5E). The sustained current showed a somewhat different ion selectivity (Figure 5F); the relative permeability was $Na^+/Li^+ = 1.05 \pm 0.07$ and $Na^+/K^+ = 1.25 \pm 0.2$, and the slope conductivity sequence was $Na^+ \geq Li^+ > K^+$. The sustained current did not show Ca^{2+} conductance. Thus, FMRFamide did not alter the ASICα response to pH or the properties of the initial transient current. However, the sustained current showed a different cation selectivity and pH response.

Effect of FMRFamide-like Neuropeptides on ASICα

Since FMRFamide itself has not been found in mammals, we asked whether other FMRFamide-like peptides would more potently affect ASICα. We tested FMRFamide-like compounds that have been identified in mammals, including neuropeptide FF and A18Famide, which terminate with the sequence PQRFamide (Yang et al., 1985; Perry et al., 1997), and MERF (met-enkephalin-Arg-Phe), which ends with FMRF but lacks the amide. Neither A18Famide nor MERF altered ASICα current, and neuropeptide FF produced only minor effects on inactivation (Figure 6; see below). We tested several of the many neuropeptides terminating with RFamide that have been discovered in invertebrates (Schneider and Taghert, 1988; Greenberg and Price, 1992; Perry et al., 1997; Nelson et al., 1998). FLRFamide also induced a sustained current in ASICα, albeit less than did FMRFamide (Figure 6). N-terminal extensions of FLRFamide and other RFamide-containing peptides identified in invertebrates did not alter ASICα currents in the presence (Figure 6) or absence of acid. FMRF-OH did not induce a response, indicating that the C-terminal amide is required. These results are similar to the neuropeptide specificity observed for FaNaCh, which has been reported to respond only to FMRFamide and FLRFamide (Cottrell, 1997). We tested morphine to determine whether it could induce a sustained current and naloxone to see if it blocked FMRFamide-induced sustained current in *Xenopus* oocytes. Consistent with our results

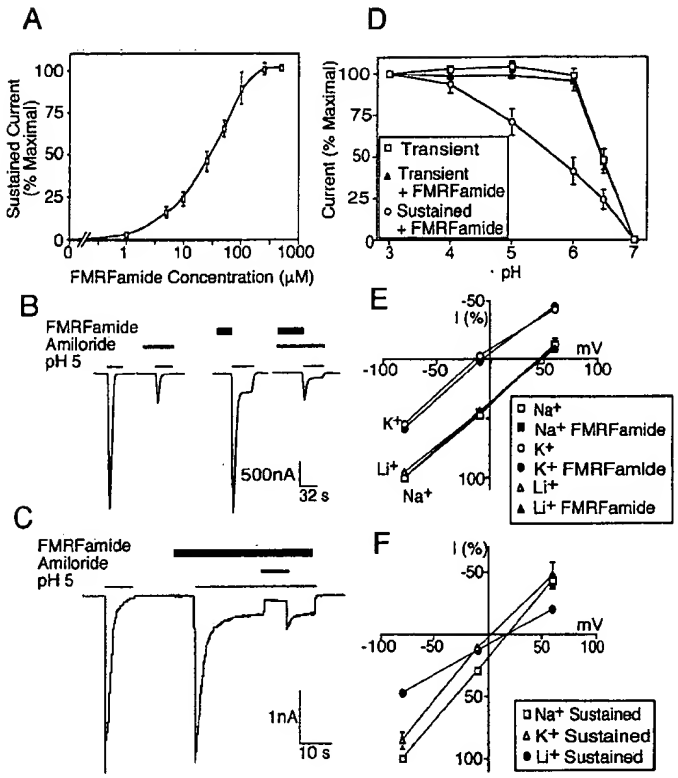

Figure 5. Properties of FMRFamide-Modulated ASICα Current

Data are from *Xenopus* oocytes (A, B, and D–F) or HEK293T cells (C) expressing ASICα.

(A) Effect of FMRFamide concentration on potentiation of H^+-dependent sustained current. Oocytes were exposed to indicated concentrations of FMRFamide prior to and during current activation with pH 5 solution. Measurements were normalized to the value of sustained current obtained with 500 μM FMRFamide. Data are mean ± SEM; n = 6–7.

(B) Effect of amiloride on FMRFamide and acid-induced sustained current. Amiloride (1 mM), FMRFamide (50 μM), and pH 5 are indicated by bars; n = 5.

(C) Amiloride (100 μM), FMRFamide (100 μM), and pH 5 are indicated by bars; n = 3.

(D) pH sensitivity of ASICα current with addition of FMRFamide. FMRFamide (50 μM) was added prior to acidification. Values were normalized to current obtained at pH 3 for the transient and the FMRFamide-modulated sustained current. Data are mean ± SEM; n = 7.

(E and F) I–V relationships of ASICα current measured at pH 5 in the presence and absence of FMRFamide (50 μM); extracellular bath solution containing 116 mM Na^+, K^+, or Li^+, as indicated. In these studies, the solution was changed from 116 mM Na^+ to the other cations ~30 s before acidification, and membrane voltage was stepped from a holding voltage of −60 mV to voltages of −80, −10, or +60 mV immediately before acidification. Currents from each cell were normalized to current obtained in the same cell at −80 mV in the Na^+ solution (100%) (E) or the sustained currents (F). Data are mean ± SEM; n = 8 cells for Na^+ solution and 4 cells for K^+ and Li^+ solutions.

in rat DRG (Figures 1B and 1C), neither morphine nor naloxone altered ASICα current (Figure 6).

Differential Effects of FMRFamide and FRRFamide

In an attempt to learn more about the peptide specificity of acid-gated channel modulation, we tested several FXRFamide peptides. One of these, FRRFamide, showed a pronounced specificity difference between acid-gated channels. With ASICα, equivalent concentrations of FRRFamide generated a sustained current similar to that produced by FMRFamide, although it was smaller in magnitude (Figure 7A). With ASICβ, FRRFamide markedly slowed the rate of inactivation without generating as large a sustained current as FMRFamide (Figure 7B). With DRASIC, both FRRFamide and FMRFamide slowed inactivation of the transient current and increased the sustained current, although equivalent concentrations of FRRFamide had larger effect on transient and sustained currents (Figure 7C).

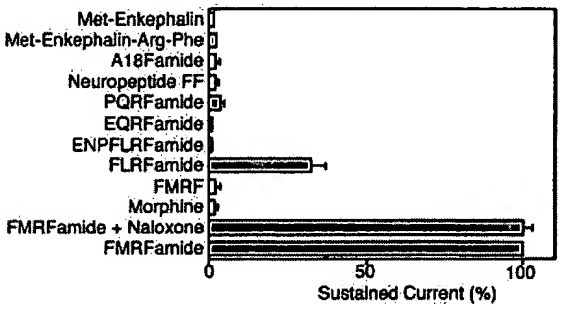

Figure 6. Effect of FMRFamide-like Peptides on ASICα Current

Oocytes expressing ASICα were exposed to indicated peptides, morphine sulphate, or naloxone prior to and during acidification to pH 5. All agents were tested at 50 μM and normalized to the response to FMRFamide (50 μM) obtained in the same cell, except for A18Famide (25 μM) and naloxone (500 μM). Naloxone was applied before the addition of FMRFamide. Data are mean ± SEM for five to eight cells assayed for each condition.

Neuropeptide FF Potentiates DRASIC Current

Differential modulation of the various acid-sensing ion channels by different peptides, and our finding that neuropeptide FF modulated DRG currents, suggested that we should test this mammalian neuropeptide on all of the acid-sensing channels. Figure 8A shows that adding neuropeptide FF prior to acidification slowed the inactivation of H^+-gated DRASIC currents. Interestingly, the kinetics of neuropeptide FF–induced potentiation were different from those induced by FMRFamide. Neuropeptide FF had subtle effects on ASICα currents, slowing inactivation but not generating appreciable sustained current (Figure 8B). ASICβ and BNC1 appeared unaffected by neuropeptide FF addition (data not shown).

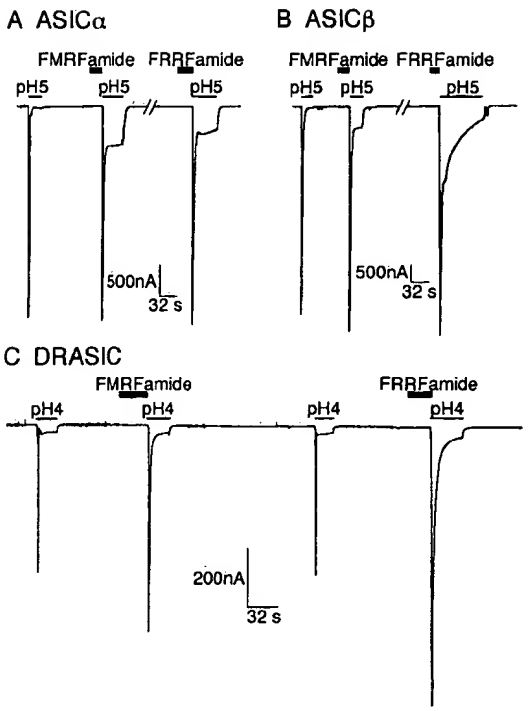

Figure 7. Effect of FMRFamide and FRRFamide on H^+-Gated DEG/ENaC Family Members Expressed in *Xenopus* Oocytes

(A and B) ASICα and ASICβ. FMRFamide (50 μM), FRRFamide (50 mM), and pH 5 solution were present in extracellular solution during time indicated by bars; n = at least 8.

(C) DRASIC. FMRFamide (100 μM), FRRFamide (100 μM), and pH 4 solution were present as indicated by bars; n = 6.

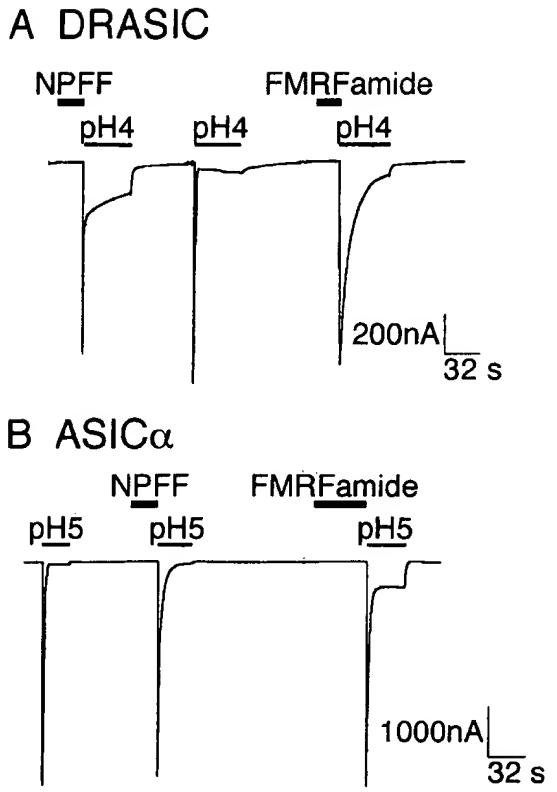

Figure 8. Effect of Neuropeptide FF on DRASIC and ASICα Expressed in *Xenopus* Oocytes

Neuropeptide FF (NPFF) (50 μM) and FMRFamide (50 μM) were present at times indicated by bars; n = 5.

Discussion

Our data indicate that FMRFamide-related neuropeptides potentiate currents from acid-sensing DEG/ENaC channels. Moreover, the localization of acid-sensing ion channels and FMRFamide-like peptides suggest the two may interact in vivo. Both DRASIC and neuropeptide FF are found in the DRG (Waldmann et al., 1997a; Chen et al., 1998; Allard et al., 1999). They are also both localized in the spinal cord and brain (Majane and Yang, 1987; Majane et al., 1989; Chen et al., 1998). Moreover, FMRFamide immunoreactivity that does not appear to be neuropeptide FF is found in DRG and brain (Ferrarese et al., 1986; Majane and Yang, 1987; Vilim et al., 1999). In this regard, it is interesting that FMRFamide was more potent than was neuropeptide FF in activating ASIC and DRG currents. We speculate that additional FMRFamide-related peptides await discovery.

Potentiation of Acid-Gated Currents by FMRFamide-Related Peptides

Earlier studies suggest that FMRFamide-like peptides can activate multiple types of receptors in mammals. These may include an opioid receptor, a G protein–coupled receptor that activates second messenger pathways, and other receptors that so far have remained unidentified (Kavaliers, 1987; Raffa and Connelly, 1992; Payza and Yang, 1993; Gherardi and Zajac, 1997; Nishimura et al., 2000). Our data indicate that mammalian members of the DEG/ENaC channel family also respond to FMRFamide-like peptides. There are at least three possible explanations. FMRFamide-related peptides might bind directly to acid-sensing channels, analogous to their interaction with FaNaCh. FMRFamide-related peptides might bind a receptor that triggers intracellular second messengers that modify the acid-sensing ion channels. Finally, FMRFamide-related peptides might bind a protein associated with acid-sensing ion channels, thereby altering their function. We favor the possibility of a direct interaction for the following reasons. First, the effect of FMRFamide was not mimicked by morphine or blocked by naloxone. Second, FMRFamide had the same effect on ASICα expressed in widely divergent cell types, *Xenopus* oocytes, and a human cell line. If the effect of FMRFamide were indirect, both cell types would have to express similar endogenous receptors coupled to similar second messenger systems. Third, in cells expressing the various individual acid-gated channels, FMRFamide, FRRFamide, and neuropeptide FF generated currents that were not only quantitatively different, but also, more importantly, qualitatively different. If these neuropeptides had different affinities for an unidentified endogenous receptor coupled to a second messenger, then only quantitative differences would be expected. Moreover, such a scenario would predict that

the quantitative effects would be similar for the different channels. This was not the case. Fourth, application of FMRFamide altered ASICα function in excised, outside-out patches of membrane. Experiments to unambiguously determine whether the effect of FMRFamide-related peptides is direct or indirect will require additional work.

The discovery that FMRFamide activated the molluscan FaNaCh showed that a peptide neurotransmitter could directly gate an ion channel (Lingueglia et al., 1995). Our data suggest that the same peptide interacts with the evolutionarily related ASIC and DRASIC channels. However, FMRFamide did not open these mammalian channels on its own; rather, it modulated the response to another agonist, protons. If FMRFamide interacts directly with the channels, these findings suggest that a FMRFamide-binding site has been at least partly conserved in these DEG/ENaC channels but that changes in structure have altered the consequences of the interaction. The alternatively spliced isoforms, ASICα and ASICβ, are identical over most of their length; however, the amino acid sequence from their N termini, through M1, and for a short distance (~100 amino acids) into the extracellular domain is not the same. Differences in the responses of ASICα and ASICβ to FMRFamide and FRRFamide suggest that the more N-terminal portions of ASIC contribute to neuropeptide modulation. That, plus the distinct interactions of FMRFamide and neuropeptide FF with FaNaCh and DRASIC, and the lack of a response with BNC1, provide a strategy and the reagents to investigate where and how these channels interact with FMRFamide and related peptides.

It is intriguing that FMRFamide should be applied before acid. We propose the following model. At pH 7.4, FMRFamide binds and is free to dissociate. However, when FMRFamide is bound at pH 7.4 and then pH is lowered, FMRFamide becomes trapped in the binding site. When the binding site is unoccupied, the channel inactivates rapidly, even in the continued presence of acid. However, when the binding site contains FMRFamide, channel inactivation is slowed and/or partially prevented. This scenario would explain two other observations. The limited ability of the peptide to alter current when applied after acidification could be explained by a conformational change at a low pH that occludes or hides the FMRFamide-binding site (Figures 4A and 4B). Trapping of FMRFamide within an occluded binding site at low pH would explain the continued generation of sustained currents, even after the peptide was removed from the bath (Figure 4D). This interpretation is consistent with our earlier observation that acid pH causes a conformational change in the related BNC1 channel that altered the extracellular solvent accessibility of a specific residue (Adams et al., 1998).

Physiologic Implications

It has been suggested that tissue ischemia and inflammation cause pain by stimulating H^+-gated cation currents (Reeh and Steen, 1996). The sustained component of those currents is thought to be particularly important (Bevan and Yeats, 1991; Lingueglia et al., 1997). Thus, the ability of neuropeptide FF and FMRFamide-related peptides to induce sustained currents suggests that such peptides and the acid-gated channels play a role in nociception. Interestingly, these peptides have been previously linked to pain perception in the spinal cord and brain. For example, chronic inflammation induces neuropeptide FF expression in the spinal cord (Kontinen et al., 1997; Vilim et al., 1999). FMRFamide-related peptides may also contribute to opiate tolerance, in which increasing amounts of opiates are required to achieve the same analgesic effect (Raffa, 1988; Roumy and Zajac, 1998). This may in part be explained by opiate-induced secretion of FMRFamide-related peptides from spinal cord neurons possibly inducing hypersensitivity of the nociceptive neurons (Tang et al., 1984).

Our data may also have implications for DEG/ENaC function in the brain. For example, intracerebroventricular injection of FMRFamide-related peptides induces a variety of physiologic responses (Mues et al., 1982; Sorenson et al., 1984; Tang et al., 1984; Kavaliers and Hirst, 1985; Yang et al., 1985; Raffa et al., 1986; Kavaliers, 1987; Thiemermann et al., 1991; Raffa and Connelly, 1992; Muthal et al., 1997; Roumy and Zajac, 1998). Recently, it was demonstrated that an amiloride analog inhibits FMRFamide-induced regulation of the brain renin–angiotensin system and hypertension (Nishimura et al., 2000). This suggests that these channels are a target of FMRFamide in the brain.

Proton-gated DEG/ENaC channels may function to integrate the response to acid and neuropeptides in the nervous system. Interestingly, another channel thought to be involved in nociception, the capsaicin receptor, also integrates multiple stimuli, heat and acidosis (Caterina et al., 1997; Tominaga et al., 1998). Thus, in neurons H^+-gated currents could vary, depending upon the type and combinations of DEG/ENaC subunits expressed and on the presence of different FMRFamide-like neuropeptides. The diversity of channel subunits and neuropeptides offers rich opportunities for interactions and new targets for pharmacotherapy.

Experimental Procedures

cDNA Constructs

Human ASICα was cloned from brain poly(A) RNA. Rat ASICβ and mouse DRASIC were cloned from DRG RNA. Human BNC1 was cloned as described (Price et al., 1996). Constructs were cloned into pMT3 for expression. The validity of the constructs was confirmed by DNA sequencing.

Cells and Expression Systems

Rat DRG neurons were cultured from Norway rats as described (Benson et al., 1999). Cells were allowed to incubate overnight at room temperature, and studies were done 1–2 days after isolation.

Expression of the cDNA constructs in *Xenopus* oocytes was accomplished by injection of plasmid DNA into the nucleus of defolliculated albino *Xenopus laevis* oocytes (Nasco, Fort Atkinson, WI) as described previously (Adams et al., 1998). Plasmids were injected at concentrations of 100 ng/μl for most experiments. Oocytes were incubated in modified Barth's solution at 18°C for 12–26 hr after injection. Cells injected with DRASIC were allowed to incubate for 24–48 hr before analysis.

HEK293T cells were a gift of Dr. Mark Stinski (University of Iowa). *ASICα* cDNA was transfected into HEK293T cells using Transfast lipid reagents (Promega, Madison, WI). To identify transfected cells, pGreenlantern vector encoding green fluorescent protein (GIBCO, Gaithersburg, MD) was cotransfected with ASICα at a ratio of 1:6; transfected cells were identified using epifluorescence microscopy. Cells were studied 1–2 days after transfection.

Electrophysiological Analysis

Whole-cell currents in oocytes were measured using two-electrode voltage-clamp as described previously (Adams et al., 1998). Oocytes were bathed in frog Ringer solution containing, in mM: NaCl, LiCl, or KCl, 116; $CaCl_2$, 0.4; $MgCl_2$, 1; and 4-(2-hydroxyethyl)-1-piperazineethanesulfonic acid (HEPES), 5 (pH 7.4). Acidic solutions were buffered with 5 mM 2-(4-morpholino)-ethanesulfonic acid (MES) instead of HEPES. Membrane voltage was held at −60 mV, unless otherwise noted. Most peptides and naloxone were obtained from Sigma (St. Louis, MO) and were added to the extracellular solution. The peptide FRRFamide was synthesized by Research Genetics (Huntsville, AL).

During whole-cell patch clamping of DRG neurons and transfected HEK293T cells, the cells were bathed with an extracellular solution that contained, in mM: NaCl, 128; $MgCl_2$, 5; $CaCl_2$, 1.8; KCl, 5.4; glucose, 5.55; and HEPES, 20 (pH 7.5 or 5). The pipette solution contained, in mM: KCl, 120; NaCl, 10; $MgCl_2$, 2; EGTA, 5; and HEPES, 10. Perfusion of cells with different solutions was done by placing the appropriate outlet in front of the cell. Data were recorded with an Axopatch 200 (Axon Instruments, Foster City, California) and stored on a digital tape recorder. Digitization was executed by acquiring data at 400 Hz using pClamp6 (Axon Instruments).

Excised, outside-out patches were obtained from transfected HEK293T cells. The bath solution contained, in mM: NaCl, 140; $MgCl_2$, 2; $CaCl_2$, 1.8; HEPES, 10 (pH 7.4), or Tris(hydroxymethyl)aminomethane (Tris) or MES (pH 5). The pipette solution contained, in mM: NMDG-Cl, 140; $MgCl_2$, 2; EGTA, 2; and HEPES, 10 (pH 7.4).

Acknowledgments

We thank Pary Weber, Ellen Tarr, Dawn Melssen, Nadia Sifri, and Theresa Mayhew for excellent assistance. We appreciate the discussions and help of Drs. Peter Snyder and Christopher Adams. We thank the University of Iowa DNA Core Facility for assistance with sequencing and oligonucleotide synthesis. This work was supported by the Howard Hughes Medical Institute; M. J. W. is an Investigator of the Howard Hughes Medical Institute.

Received January 28, 2000; revised February 28, 2000.

References

Adams, C.M., Snyder, P.M., Price, M.P., and Welsh, M.J. (1998). Protons activate brain Na^+ channel 1 by inducing a conformational change that exposes a residue associated with neurodegeneration. J. Biol. Chem. *273*, 30204–30207.

Akaike, N., and Ueno, S. (1994). Proton-induced current in neuronal cells. Prog. Neurobiol. *43*, 73–83.

Akaike, N., Krishtal, O.A., and Maruyama, T. (1990). Proton-induced sodium current in frog isolated dorsal root ganglion cells. J. Neurophysiol. *63*, 805–813.

Allard, M., Geoffre, S., Legendre, P., Vincent, J.D., and Simonnet, G. (1989). Characterization of rat spinal cord receptors to FLFQPQRFamide, a mammalian morphine modulating peptide: a binding study. Brain Res. *500*, 169–176.

Allard, M., Rousselot, P., Lombard, M.C., and Theodosis, D.T. (1999). Evidence for neuropeptide FF (FLFPQRFamide) in rat dorsal root ganglia. Peptides *20*, 327–333.

Babinski, K., Le, K.T., and Séguéla, P. (1999). Molecular cloning and regional distribution of a human proton receptor subunit with biphasic functional properties. J. Neurochem. *72*, 51–57.

Bassilana, F., Champigny, G., Waldmann, R., de Weille, J.R., Heurteaux, C., and Lazdunski, M. (1997). The acid-sensitive ionic channel subunit ASIC and the mammalian degenerin MDEG form a heteromultimeric H^+-gated Na^+ channel with novel properties. J. Biol. Chem. *272*, 28819–28822.

Benson, C.J., Eckert, S.P., and McCleskey, E.W. (1999). Acid-evoked currents in cardiac sensory neurons: a possible mediator of myocardial ischemic sensation. Circ. Res. *84*, 921–928.

Bevan, S., and Geppetii, P. (1994). Protons: small stimulants of capsaicin-sensitive sensory nerves. Trends Neurosci. *17*, 509–512.

Bevan, S., and Yeats, J. (1991). Protons activate a cation conductance in a sub-population of rat dorsal root ganglion neurones. J. Physiol. (Lond) *433*, 145–161.

Brussaard, A.B., Kits, K.S., Ter Maat, A., Mulder, A.H., and Schoffelmeer, A.N.M. (1989). Peripheral injection of DNA-RFa, a FMRFa agonist, suppresses morphine-induced analgesia in rats. Peptides *10*, 735–739.

Caterina, M.J., Schumacher, M.A., Tominaga, M., Rosen, T.A., Levine, J.D., and Juluis, D. (1997). The capasaicin receptor: a heat-activated ion channel in the pain pathway. Nature *389*, 816–824.

Chen, C.-C., England, S., Akopian, A.N., and Wood, J.N. (1998). A sensory neuron-specific, proton-gated ion channel. Proc. Natl. Acad. Sci. USA *95*, 10240–10245.

Coscoy, S., Lingueglia, E., Lazdunski, M., and Barbry, P. (1998). The Phe-Met-Arg-Phe-amide-activated sodium channel is a tetramer. J. Biol. Chem. *273*, 8317–8322.

Cottrell, G.A. (1997). The first peptide-gated ion channel. J. Exp. Biol. *200*, 2377–2386.

Davies, N.W., Lux, H.D., and Morad, M. (1988). Site and mechanism of activation of proton-induced sodium current in chick dorsal root ganglion neurones. J. Physiol. (Lond) *400*, 159–187.

Devillers, J.P., Boisserie, F., Laulin, J.P., Larcher, A., and Simonnet, G. (1995). Simultaneous activation of spinal antiopioid system (neuropeptide FF) and pain facilitatory circuitry by stimulation of opioid receptors in rats. Brain Res. *700*, 173–181.

de Weille, J.R., Bassilana, F., Lazdunski, M., and Waldmann, R. (1998). Identification, functional expression and chromosomal localisation of a sustained human proton-gated cation channel. FEBS Lett. *433*, 257–260.

Ferrarese, C., Iadarola, M.J., Yang, H.-Y.T., and Costa, E. (1986). Peripheral and central origin of Phe-Met-Arg-Phe-amide immunoreactivity in rat spinal cord. Regul. Pept. *13*, 245–252.

García-Anoveros, J., Derfler, B., Neville-Golden, J., Hyman, B.T., and Corey, D.P. (1997). BNaC1 and BNaC2 constitute a new family of human neuronal sodium channels related to degenerins and epithelial sodium channels. Proc. Natl. Acad. Sci. USA *94*, 1459–1464.

Gayton, R.J. (1982). Mammalian neuronal actions of FMRFamide and the structurally related opioid Met-enkephalin-Arg6-Phe7. Nature *298*, 275–276.

Gherardi, N., and Zajac, J.M. (1997). Neuropeptide FF receptors of mouse olfactory bulb: binding properties and stimulation of adenylate cyclase activity. Peptides *18*, 577–583.

Gouardéres, C., Sutak, M., Zajac, J.M., and Jhamandas, K. (1993). Antinociceptive effects of intrathecally administered F8Famide and FMRFamide in the rat. Eur. J. Pharm. *237*, 73–81.

Greenberg, M.J., and Price, D.A. (1992). Relationships among the FMRFamide-like peptides. Prog. Brain Res. *92*, 25–37.

Kavaliers, G.M., and Hirst, M. (1985). FMRFamide, a putative endogenous opiate antagonist: evidence from suppression of defeat-induced analgesia and feeding in mice. Neuropeptides *6*, 485–494.

Kavaliers, M. (1987). Calcium channel blockers inhibit the antagonistic effects of Phe-Met-Arg-Phe-amide (FMRFamide) on morphine- and stress-induced analgesia in mice. Brain Res. *415*, 380–384.

Kontinen, V.K., Aarnisalo, A.A., Idanpaan-Heikkila, J.J., Panula, P., and Kalso, E. (1997). Neuropeptide FF in the rat spinal cord during carrageenan inflammation. Peptides *18*, 287–292.

Kovalchuk, YuN., Krishtal, O.A., and Nowycky, M.C. (1990). The proton-activated inward current of rat sensory neurons includes a calcium component. Neurosci. Lett. *115*, 237–242.

Krishtal, O.A., and Pidoplichko, V.I. (1981). A "receptor" for protons in small neurons of trigeminal ganglia: possible role in nociception. Neurosci. Lett. *24*, 243–246.

Lindemann, B. (1996). Taste reception. Physiol. Rev. *76*, 718–766.

Lingueglia, E., Champigny, G., Lazdunski, M., and Barbry, P. (1995). Cloning of the amiloride-sensitive FMRFamide peptide-gated sodium channel. Nature *378*, 730–733.

Lingueglia, E., de Weille, J.R., Bassilana, F., Heurteaux, C., Sakai, H., Waldmann, R., and Lazdunski, M. (1997). A modulatory subunit of acid sensing ion channels in brain and dorsal root ganglion cells. J. Biol. Chem. *272*, 29778–29783.

Majane, E.A., and Yang, H.Y. (1987). Distribution and characterization of two putative endogenous opioid antagonist peptides in bovine brain. Peptides *8*, 657–662.

Majane, E.A., Panula, P., and Yang, H.Y. (1989). Rat brain regional distribution and spinal cord neuronal pathway of FLFQPQRF-NH_2, a mammalian FMRF-NH_2-like peptide. Brain Res. *494*, 1–12.

Mano, I., and Driscoll, M. (1999). DEG/ENaC channels: a touchy superfamily that watches its salt. Bioessays *21*, 568–578.

Mues, G., Fuchs, I., Wei, E.T., Weber, E., Evans, C.J., Barchas, J.D., and Chang, J.-K. (1982). Blood pressure elevation in rats by peripheral administration of Tyr-Gly-Gly-Phe-Met-Arg-Phe and the invertebrate neuropeptide, Phe-Met-Arg-Phe-NH2. Life Sciences *31*, 2555–2561.

Muthal, A.V., Mandhane, S.N., and Chopde, C.T. (1997). Central administration of FMRFamide produces antipsychotic-like effects in rodents. Neuropeptides *31*, 319–322.

Nelson, L.S., Kim, K., Memmott, J.E., and Li, C. (1998). FMRFamide-related gene family in the nematode, *Caenorhabditis elegans*. Mol. Brain Res. *58*, 103–111.

Nishimura, M., Ohtsuka, K., Takahashi, H., and Yoshimura, M. (2000). Role of FMRFamide-activated brain sodium channel in salt-sensitive hypertension. Hypertension *35*, 443–450.

Olson, T.H., Riedl, M.S., Vulchanova, L., Ortiz-Gonzalez, X.R., and Elde, R. (1998). An acid sensing ion channel (ASIC) localizes to small primary afferent neurons in rats. Neuron *9*, 1109–1113.

Payza, K., and Yang, H.Y. (1993). Modulation of neuropeptide FF receptors by guanine nucleotides and cations in membranes of rat brain and spinal cord. J. Neurochem. *60*, 1894–1899.

Perry, S.J., Huang, E.Y.K., Cronk, D., Bagust, J., Sharma, R., Walker, R.J., Wilson, S., and Burke, J.F. (1997). A human gene encoding morphine modulating peptides related to NPFF and FMRFamide. FEBS Lett. *409*, 426–430.

Price, M.P., Snyder, P.M., and Welsh, M.J. (1996). Cloning and expression of a novel human brain Na^+ channel. J. Biol. Chem. *271*, 7879–7882.

Raffa, R.B. (1988). The action of FMRFamide (Phe-Met-Arg-Phe-NH2) and related peptides on mammals. Peptides *9*, 915–922.

Raffa, R.B., and Connelly, C.D. (1992). Supraspinal antinociception produced by [D-Met2]-FMRFamide in mice. Neuropeptides *22*, 195–203.

Raffa, R.B., Heyman, J., and Porreca, F. (1986). Intrathecal FMRFamide (Phe-Met-Arg-Phe-NH2) induces excessive grooming behavior in mice. Neurosci. Lett. *65*, 94–98.

Reeh, P.W., and Steen, K.H. (1996). Tissue acidosis in nociception and pain. Prog. Brain Res. *113*, 143–151.

Roumy, M., and Zajac, J.M. (1998). Neuropeptide FF, pain and analgesia. Euro. J. Pharm. *345*, 1–11.

Schild, L., Canessa, C.M., Shimkets, R.A., Gautschi, I., Lifton, R.P., and Rossier, B.C. (1995). A mutation in the epithelial sodium channel causing Liddle disease increases channel activity in the *Xenopus laevis* oocyte expression system. Proc. Natl. Acad. Sci. USA *92*, 5699–5703.

Schneider, L.E., and Taghert, P.H. (1988). Isolation and characterization of a Drosophila gene that encodes multiple neuropeptides related to Phe-Met-Arg-Phe-NH2 (FMRFamide). Proc. Natl. Acad. Sci. USA *85*, 1993–1997.

Snyder, P.M., Price, M.P., McDonald, F.J., Adams, C.M., Volk, K.A., Zeiher, B.G., Stokes, J.B., and Welsh, M.J. (1995). Mechanism by which Liddle's syndrome mutations increase activity of a human epithelial Na^+ channel. Cell *83*, 969–978.

Sorenson, R.L., Sasek, C.A., and Elde, R.P. (1984). Phe-Met-Arg-Phe-amide (FMRF-NH2) inhibits insulin and somatostatin secretion and anti-FMRF-NH2 sera detects pancreatic polypeptide cells in the rat islet. Peptides *5*, 777–782.

Tang, J., Yang, H.Y.T., and Costa, E. (1984). Inhibition of spontaneous and opiate-modified nociception by an endogenous neuropeptide with Phe-Met-Arg-Phe-NH2-like immunoreactivity. Proc. Natl. Acad. Sci. USA *81*, 5002–5005.

Telegdy, G., and Bollók, I. (1987). Amnesic action of FMRFamide in rats. Neuropeptides *10*, 157–163.

Thiemermann, C., Al-Damluji, S., Hecker, M., and Vane, J.R. (1991). FMRF-amide and L-Arg-I-Phe increase blood pressure and heart rate in the anaesthetised rat by central stimulation of the sympathetic nervous system. Biochem. Biophys. Res. Comm. *175*, 318–324.

Tominaga, M., Caterina, M.J., Malmberg, A.B., Rosen, T.A., Gilbert, H., Skinner, K., Raumann, B.E., Basbaum, A.I., and Julius, D. (1998). The cloned capsaicin receptor integrates multiple pain-producing stimuli. Neuron *21*, 531–543.

Vilim, F.S., Aamisalo, A.A., Nieminen, M.L., Lintunen, M., Karlstedt, K., Kontinen, V.K., Kalso, E., States, B., Panula, P., and Ziff, E. (1999). Gene for pain modulatory neuropeptide NPFF: induction in spinal cord by noxious stimuli. Mol. Pharmacol. *55*, 804–811.

Waldmann, R., and Lazdunski, M. (1998). H^+-gated cation channels: neuronal acid sensors in the NaC/DEG family of ion channels. Curr. Opin. Neurobiol. *8*, 418–424.

Waldmann, R., Champigny, G., Voilley, N., Lauritzen, I., and Lazdunski, M. (1996). The mammalian degenerin MDEG, an amiloride-sensitive cation channel activated by mutations causing neurodegeneration in *Caenorhabditis elegans*. J. Biol. Chem. *271*, 10433–10436.

Waldmann, R., Bassilana, F., de Weille, J., Champigny, G., Heurteaux, C., and Lazdunski, M. (1997a). Molecular cloning of a non-inactivating proton-gated Na^+ channel specific for sensory neurons. J. Biol. Chem. *272*, 20975–20978.

Waldmann, R., Champigny, G., Bassilana, F., Heurteaux, C., and Lazdunski, M. (1997b). A proton-gated cation channel involved in acid-sensing. Nature *386*, 173–177.

Yang, H.Y.T., Fratta, W., Majane, E.A., and Costa, E. (1985). Isolation, sequencing, synthesis, and pharmacological characterization of two brain neuropeptides that modulate the action of morphine. Proc. Natl. Acad. Sci. USA *82*, 7757–7761.

Available online at www.sciencedirect.com
SCIENCE DIRECT®
Pergamon
Neuropharmacology 44 (2003) 662–671
NEURO PHARMACOLOGY
www.elsevier.com/locate/neuropharm

Effects of neuropeptide SF and related peptides on acid sensing ion channel 3 and sensory neuron excitability

E. Deval [a], A. Baron [a], E. Lingueglia [a], H. Mazarguil [b], J.-M. Zajac [b], M. Lazdunski [a,*]

[a] *Institut de Pharmacologie Moléculaire et Cellulaire, CNRS-UMR 6097, 660 route des Lucioles, Sophia Antipolis, 06560 Valbonne, France*
[b] *Institut de Pharmacologie et Biologie Structurale, CNRS-UMR 5089, 205 route de Narbonne, 31077 Toulouse Cedex, France*

Received 5 September 2002; received in revised form 4 December 2002; accepted 9 January 2003

Abstract

Acid sensing ion channel 3 (ASIC3) is a cation channel gated by extracellular protons. It is highly expressed in sensory neurons, including small nociceptive neurons and has been proposed to participate in pain perception associated with tissue acidosis and in mechanoperception. Neuropeptide FF (NPFF) and FMRFamide have been shown to potentiate proton-gated currents from cultured sensory neurons and acid sensing ion channel (ASIC) cDNA transfected cells. In this study, we report that another mammalian peptide neuropeptide SF (NPSF), derived from the same precursor, also considerably increases the amplitude of the sustained current of heterologously expressed ASIC3 (12-fold vs. 19- and nine-fold for FMRFamide and NPFF, respectively) with an EC_{50} of ~50 μM. Similar effects were also observed on endogenous ASIC3-like sustained current recorded from DRG neurons although of smaller amplitudes (two-, three- and seven-fold increase for NPSF, NPFF and FMRFamide, respectively), and essentially related to a slowing down of the inactivation rate. Importantly, this modulation induced changes in neuronal excitability in response to an electrical stimulus applied during extracellular acidification. ASIC3-mediated sustained depolarisation, and its regulation by neuropeptides, could thus be important in regulating polymodal neuron excitability particularly under inflammatory conditions where the expression levels of both NPFF precursor and ASIC3 are increased.

Keywords: ASIC3; FMRFamide-related neuropeptides; DRG neuron

1. Introduction

The Phe-Met-Arg-Phe-NH_2 (FMRFamide) and structurally related peptides are abundant in invertebrates where they might function as neurotransmitters and neuromodulators (Price and Greenberg, 1977; Roumy and Zajac, 1998). Although FMRFamide has not been isolated in mammals, endogenous mammalian FMRFamide related peptides have been identified. Neuropeptide FF (NPFF, Phe-Leu-Phe-Gln-Pro-Gln-Arg-Phe-amide) and neuropeptide AF (NPAF, Ala-Gly-Glu-Gly-Leu-Ser-Ser-Pro-Phe-Trp-Ser-Leu-Ala-Ala-Pro-Gln-Arg-Phe-amide) were first isolated from bovine brain (Yang et al., 1985), and neuropeptide SF (NPSF, Ser-Leu-Ala-Ala-Pro-Gln-Arg-Phe-amide) was isolated from the rat central nervous system (CNS) (Yang and Martin, 1995). Numerous data have accumulated about NPFF. It is released from the spinal cord following stimulation with high potassium or substance P (Zhu et al., 1992), or following opioid receptor stimulation (Devillers et al., 1995b), and it has been implicated in a variety of physiological functions, including pain modulation, opiate function and cardiovascular regulation (for reviews, see Panula et al., 1996; Roumy and Zajac, 1998).

NPFF, NPAF and NPSF derive from a common precursor, the gene of which has been cloned in human, rat, bovine and mouse (Perry et al., 1997; Vilim et al., 1999). The gene product is expressed mainly in the CNS, the dorsal spinal cord being one of the regions containing the highest concentrations (Panula et al., 1999; Vilim et al., 1999). High affinity NPFF receptors are thought to be coupled to various G-proteins (Roumy and Zajac, 2001). NPFF displays a nanomolar affinity for binding sites in the rat spinal cord whereas NPSF has a lower affinity for NPFF binding sites (28 times less than

* Corresponding author Tel.: +1-33-0-4-93-95-77-02; fax: +1-33-0-4-93-95-77-04.
E-mail address: ipmc@ipmc.cnrs.fr (M. Lazdunski).

0028-3908/03/$ - see front matter © 2003 Elsevier Science Ltd. All rights reserved.
doi:10.1016/S0028-3908(03)00047-9

NPFF). Moreover, and contrary to NPFF, NPSF does not reduce the effect of nociceptin on dorsal raphe neurons (Roumy and Zajac, 1999; Roumy et al., 2000). An enzymatic degradation product of NPFF (QRFamide, Gln-Arg-Phe-amide) has been identified, but its affinity for the NPFF receptor in rat spinal cord membranes is 1430-fold lower than that of NPFF indicating that it cannot efficiently stimulate NPFF receptors to produce a biological effect (Sol et al., 1999).

Functional ASICs (acid sensing ionic channels) are homo- or hetero-tetrameric proton-gated Na^+-permeable channels formed by the association of different subunits: ASIC1a, ASIC1b, ASIC2a, ASIC2b and ASIC3 (Chen et al., 1998; Waldmann and Lazdunski, 1998; Bassler et al., 2001). These channels are members of a super-family comprising, among others, the molluscan peptide-gated channel FaNaCh (Lingueglia et al., 1995). Proton-gated ASIC-like currents were described in sensory neurons (Krishtal and Pidoplichko, 1981b, a, c) and more recently, the expression of different ASIC subunits in these neurons has been reported (Waldmann and Lazdunski, 1998). ASIC3 (previously named DRASIC) is principally found in small and medium nociceptive sensory neurons (Voilley et al., 2001) and its expression in heterologous systems has been associated with a biphasic current comprising a fast transient component followed by a sustained phase (Waldmann et al., 1997). ASIC3 is thus a good candidate for mediating the non-adapting pain associated with tissue acidosis, and it has been implicated in acid-evoked nociception in the ischemic myocardium (Sutherland et al., 2001).

In the mollusc *Helix aspersa*, FMRFamide has been reported to directly activate the amiloride-sensitive channel FaNaCh with a micromolar concentration range (Cottrell et al., 1990; Lingueglia et al., 1995; Cottrell, 1997). The significant structural homology between FaNaCh and ASICs suggested that neuropeptides could directly activate or modulate ASIC-mediated currents. This is particularly interesting as ASIC3 expression, like that of NPFF precursor, is increased during inflammation (Vilim et al., 1999; Voilley et al., 2001). Moreover, both ASIC3 and NPFF are found in the dorsal root ganglia (Waldmann et al., 1997; Chen et al., 1998; Allard et al., 1999; Voilley et al., 2001). Recent studies have revealed that FMRFamide and NPFF modulate the homomeric ASIC1 and ASIC3 current as well as H^+-gated currents from sensory neurons (Askwith et al., 2000), and the heterologously expressed heteromeric ASIC2a + 3 current (Catarsi et al., 2001). NPFF and FMRFamide are not able to generate currents on their own, but they slow down the inactivation of ASIC1a and ASIC3 currents, inducing and/or increasing the sustained phase during acidification (Askwith et al., 2000). The sustained component of those currents is thought to be important in pain coding, but its physiological relevance is largely unknown.

This study is the first report of the effects of NPSF on ASIC3 currents expressed in a heterologous system, and on ASIC3-like currents recorded from rat cultured DRG neurons. The effects of QRFamide, and of the common C-terminal motif RFamide, are also studied, and compared to the known effects of FMRFamide and NPFF. This paper is also the first to show that the effects of these neuropeptides on the sustained phase of the ASIC3 current can be correlated with an increase in neuronal excitability associated with the increase of the ASIC current-induced sustained depolarisation.

2. Methods

2.1. Expression of ASIC channels in COS cells

COS cells at a density of 20 000 cells per 35 mm diameter petri dish were transfected with a mix of the vectors pCI-CD8 and pCI-rASIC3 (1:2 ratio) using the DEAE-Dextran method. Cells were used for electrophysiological measurements 1 to 3 days after transfection. Successfully transfected cells were recognised by their ability to fix CD8-antibody-coated beads (Dynal).

2.2. Primary culture of rat DRG neurons

Dorsal root ganglion neurons were dissected from Wistar rats (5–7 weeks) and enzymatically dissociated with 0.1% collagenase. Cells were then plated on collagen-coated 35 mm petri dishes and maintained in culture at 37 °C (95 % air/5% CO_2) in DMEM containing 5% fetal calf serum. Electrophysiological experiments were carried out 1 or 2 days after plating.

2.3. Electrophysiological measurements

The patch-clamp technique was used to measure membrane currents (voltage-clamp), and membrane potential (current-clamp) in whole-cell and outside-out configurations (Hamill et al., 1981). Currents were amplified with a RK-400 amplifier (Bio-Logic Science Instruments), digitised with a 16-bit data acquisition system (Digidata 1322A, Axon Instruments), and recorded using pClamp software (version 8.2.0.224, Axon Instruments). The data were sampled at 3.3 kHz and 20 kHz (for whole-cell and outside-out recordings, respectively), and low-pass filtered at 3–5 kHz using an eight-pole low pass filter (Bio-Logic Science Instruments). Off-line analysis of currents was performed using pClamp (Axon Instruments) and Bio-Patch (version 3.42, Bio-Logic Science Instruments). Currents obtained from outside-out patches were digitally filtered to 1 kHz using pClamp (Axon Instruments). The statistical significance of differences between sets of data was estimated using the Student *t*-test.

2.4. Solutions

The pipette solution contained (in mM): KCl 140, NaCl 5, $MgCl_2$ 2, EGTA 5, HEPES 10 (pH 7.3), and the bath solution contained (in mM): NaCl 150, KCl 5, $MgCl_2$ 2, $CaCl_2$ 2, HEPES 10 (pH 7.4). MES was used instead of HEPES to buffer bath solution pH ranging from 6 to 5. For the experiments performed on DRG neurons, the bath solution was supplemented with glucose 10 mM, CNQX 20 μM and kynurenic acid 10 μM (to inhibit glutamate-activated ionotropic currents) and the pipette solution contained (in mM): KCl 140, ATP-Na_2 2.5, $MgCl_2$ 2, $CaCl_2$ 2, EGTA 5, HEPES 10 (pH 7.3, pCa estimated to 7). 0.1 % bovine serum albumin was added in extracellular solutions containing the spider toxin PcTX1 (Escoubas et al., 2000) to prevent its adsorption to tubing and containers. The toxin was applied at least one minute before the pH drop. All the peptides were diluted in the control medium (pH 7.4) and perfused for approximately 30 s before the extracellular pH drop. Changes in extracellular pH were induced by shifting one out of eight outlets of a microperfusion system in front of the cell. Experiments were carried out at room temperature (20–22 °C). CNQX, kynurenic acid, capsaicin and FMRFamide were from Sigma.

2.5. Peptide synthesis

NPFF (Phe-Leu-Phe-Gln-Pro-Gln-Arg-Phe-amide), NPSF (Ser-Leu-Ala-Ala-Pro-Gln-Arg-Phe-amide), QRFamide (Gln-Arg-Phe-amide) and RFamide (Arg-Phe-amide) were synthesized by the solid-phase method using Fmoc amide resin chemistry with an automatic synthesiser (430A Applied Biosystem). Activation of carboxylic function of Fmoc amino-acid was obtained with 1-Hydroxy-7-azabenzotriazole and diisopropylcarbodiimide. Peptides were purified by preparative reversed phase HPLC on an Aquapore column (C8, 10 × 250 mm, 20 mm, Bronwlee Labs) and the purity determined by electro-spray ionisation mass spectrometry on a Finnigan Mat TSQ 700. The Fmoc amino acid derivatives were purchased from Bachem, France.

3. Results

3.1. Effects of NPSF and related peptides on ASIC3 currents expressed in COS cells

Fig. 1 shows the effects of mammalian NPSF and NPFF and of the molluscan FMRFamide on whole-cell ASIC3 currents recorded from transfected COS cells at −50 mV. RFamide, which represents the common C-terminal motif of those neuropeptides, and QRFamide, which has been found to be an inactive metabolite of NPFF in mouse brain (Sol et al., 1999), have also been tested. None of these peptides induced a significant change of the fast transient component of ASIC3 current (Fig. 1A). However, the peptides did induce changes of the slow sustained ASIC3 current. It should be noted that the ASIC3 sustained current, which has been shown to be half-activated at pH 3.5 (Waldmann et al., 1997), began to be detected at pH 6.3 (Fig. 1A, last trace). It represented 2 ± 1% (n = 17) and 5 ± 1% (n = 63) of the pH6.3- and pH5-induced peak current, respectively. Amplitudes of ASIC3 sustained currents, measured in the presence of each peptide, have been normalised to those measured under control conditions (Fig. 1B). As previously described (Askwith et al., 2000), FMRFamide and NPFF considerably increase the sustained current amplitude recorded at pH 5 (19- and nine-fold increases, n = 45 and 19, respectively). NPSF also increased ASIC3 sustained current amplitude with an effect slightly more potent than NPFF (12-fold increase, n = 22) whereas RFamide and QRFamide had smaller effects (only two-fold increases, n = 12 and 20, respectively). Similar results have been obtained on pH 6.3-evoked ASIC3 current, as shown in Fig. 1B (right side) for FMRFamide and NPSF (n = 11 and 8 respectively). The effects of peptides on ASIC3 inactivation rate are represented in Fig. 1C where ASIC3 current inactivation was fitted by two exponentials. FMRFamide, NPFF and QRFamide significantly increased both the slow and the fast component of ASIC3 current inactivation ($P < 0.001$, n = 16–35). These results suggest that the effects of FMRFamide, NPFF and, to a lesser extent, of QRFamide, are due to a slowing down of the ASIC3 current inactivation. Interestingly, RFamide and especially NPSF, which also increased the ASIC3 sustained phase (Fig. 1B), did not change the current inactivation time constants (Fig. 1C).

Other FMRFamide-related neuropeptides were also tested on the ASIC3 sustained phase: SQA-NPFF (Ser-Gln-Ala-NPFF), SPA-NPFF (Ser-Pro-Ala-NPFF), A-NPFF (Ala-NPFF), PA-NPFF (Pro-Ala-NPFF), SPN-NPFF (Ser-Pro-Asn-NPFF), EFW-NPSF (Glu-Phe-Trp-NPSF), QFW-NPSF (Gln-Phe-Trp-NPSF), human NPAF, human RFRP3 (Val-Pro-Asn-Leu-Pro-Gln-Arg-Phe-amide) were not able to significantly modify the rat homomeric ASIC3 sustained current (not shown).

We further characterised the effects of NPSF on the ASIC3 current, showing that its effect is concentration-dependent (Fig. 2A, inset). The effects of NPSF and NPFF were then compared to the concentration-effect curve established for FMRFamide (Fig. 2A). For each concentration of peptide, the ASIC3 sustained current increase (Isst peptide−Isst control) was normalised to the sustained current increase induced by 100 μM of peptide (Isst 100 μM−Isst control). The concentration range at which NPSF acts on ASIC3 appeared to be the same as those of FMRFamide and NPFF (EC_{50} = 49 ± 3 μM, n = 4–15, Fig. 2A).

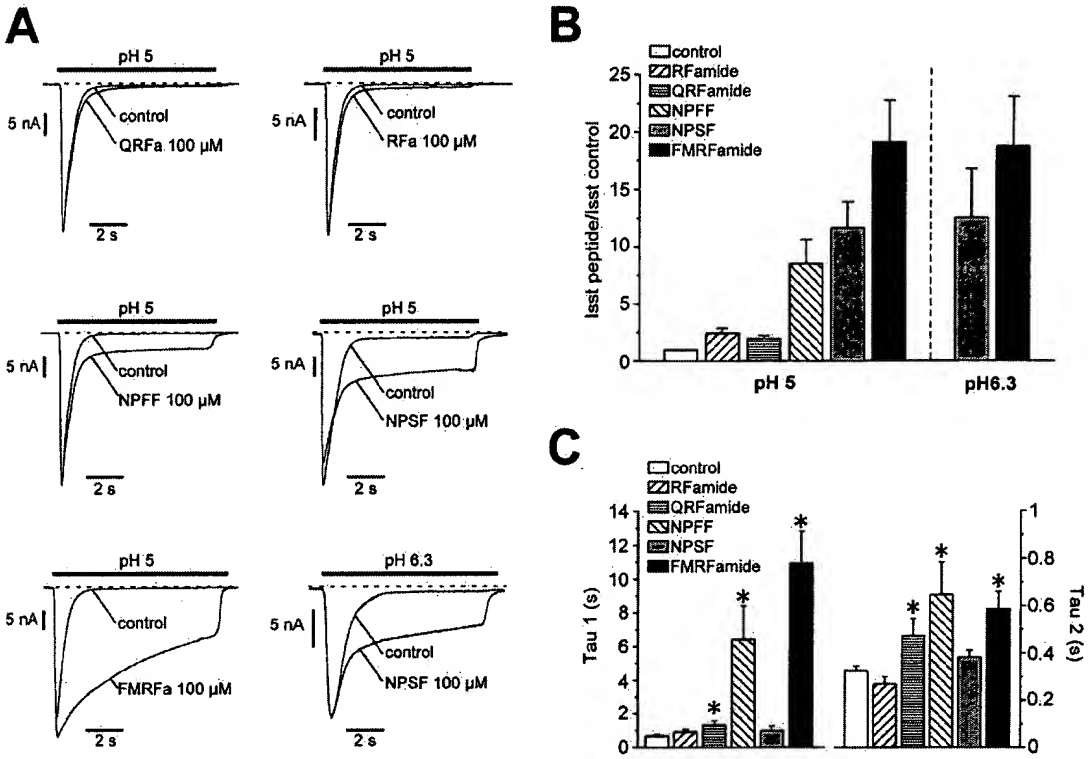

Fig. 1. Effect of FMRFamide-related peptides on homomeric ASIC3 expressed in COS cells. (A) ASIC3 currents recorded at −50 mV using the whole-cell patch-clamp technique. The dashed line represents the zero current level. The external pH acidification that elicited ASIC3 currents is indicated above each current trace. Peptides were applied 30 s before the pH drop. (B) Increase factor of ASIC3 sustained currents induced by FMRFamide-related peptides. The sustained current amplitude measured in the presence of each neuropeptide was normalised to the control currents (n = 8–45). The sustained current amplitudes were measured at the end of the pH drop. (C) Effect of neuropeptides on inactivation time constants of pH 5-evoked ASIC3 currents. ASIC3 current inactivation was fitted by a second order exponential (n = 16–35; *, $P < 0.001$).

NPSF and FMRFamide were also tested on ASIC3 currents recorded from outside-out patches (Fig. 2B). Both NPSF and FMRFamide enhanced the channel sustained activity, as previously described with whole-cell recording experiments (see Fig. 1). These data suggested that NPSF and FMRFamide might interact directly with ASIC3. Similar conclusions were previously drawn concerning the effect of the FMRFamide and NPFF peptides on ASICs (Askwith et al., 2000; Catarsi et al., 2001).

3.2. *Effects of NPSF and related peptides on endogenous ASIC3-like currents from DRG neurons*

FMRFamide-related peptides were then tested on ASIC3-like currents recorded from rat DRG cultured neurons (Fig. 3). ASIC3-like currents were selected by their insensitivity to the spider toxin PcTX1 (Escoubas et al., 2000), and by their kinetics and pH dependency. The spider toxin PcTX1 was previously shown to specifically inhibit homomeric ASIC1a channels (Escoubas et al., 2000). The method for ASIC3-like current selection has been described recently in further detail (Mamet et al., 2002). Among the recorded DRG neurons, 26.5% expressed a PcTX1-resistant ASIC3-like current. This biphasic current could either show a Na^+-specific or a cation nonspecific sustained current, probably flowing through homomeric ASIC3 or heteromeric ASIC3 + 2b channels, respectively (Lingueglia et al., 1997). As described above for homomeric ASIC3 sustained current recorded from COS cells, ASIC3-like sustained current could also be detected at pH6.3, representing 9 ± 3% (n = 11) of the peak current. It increased to 13 ± 4% (n = 27) and 17 ± 6% (n = 27) of the peak current at pH6 and pH5 respectively. ASIC3-like sustained current displayed the same pH dependency as that of homomeric ASIC3 sustained current, however, sustained current was bigger in DRG. This reinforces the idea that heteromeric ASIC3-containing channels, displaying larger sustained current (such as ASIC3 + 2b, see Lingueglia et al., 1997), are expressed in DRG. The effects of neuropeptides were similar to those previously observed with homomeric ASIC3 currents recorded in COS cells (Fig. 3A). However, increases of ASIC3-like sustained current obtained with QRFamide, NPSF, NPFF, and FMRFamide were smaller than those observed on homomeric ASIC3 currents (two-, three-, and seven-fold increases for NPSF, NPFF, and FMRFamide, respectively, n = 4–8, Fig. 3B). Both the slow and the fast components of ASIC3-like current inactivation were significantly increased by

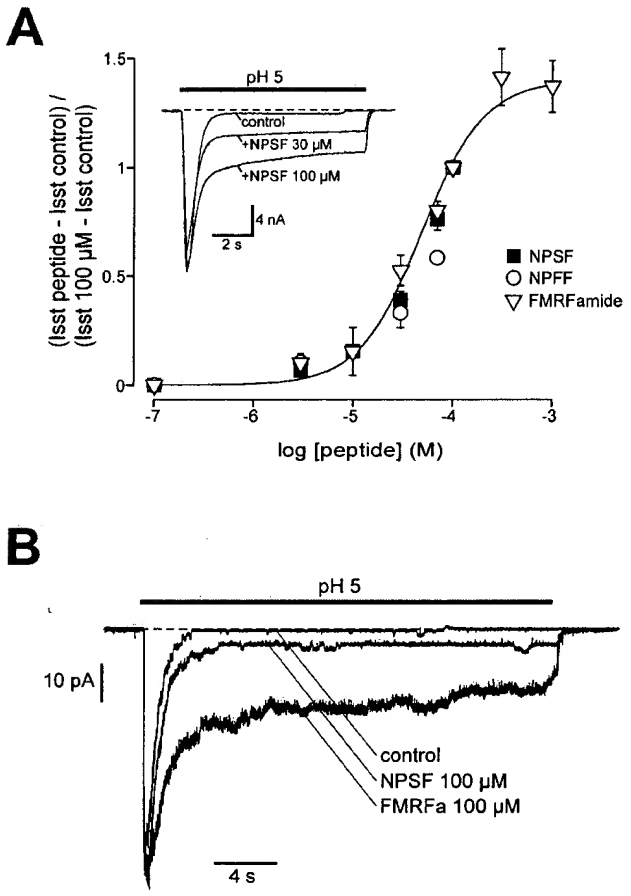

Fig. 2. Efficiency of NPSF and NPFF on homomeric ASIC3 sustained current. (A) Concentration–effect relationships representing the effect of NPSF, NPFF and FMRFamide on ASIC3 sustained current. The ASIC3 sustained current increases (Isst peptide−Isst control) were normalised to the sustained current increases induced by 100 µM of the corresponding peptide (Isst 100 µM−Isst control). A Hill equation was used to fit the FMRFamide concentration-effect relationship, and the half-maximal effect was obtained for 49 ± 3 µM (n = 4–15). It appeared that NPSF, NPFF and FMRFamide act on ASIC3 sustained current in the same concentration range. Inset: Whole-cell pH 5-evoked ASIC3 currents recorded from a single COS cell at −50 mV in the presence of different concentrations of NPSF. (B) Effect of NPSF and FMRFamide on homomeric ASIC3 current recorded from an outside-out patch. Current traces were elicited from a single patch at −50 mV, for an external acidification dropping from pH 7.4 to 5. The peptides (NPSF and FMRFamide) were applied 30 s before the pH drop.

NPSF, NPFF, and FMRFamide (Fig. 3C), suggesting that the enhancement of the ASIC3-like plateau by these peptides resulted from a slowing down of the current inactivation. It must be pointed out that the effects of neuropeptides were variable from one neuron to another, probably due to the expression of a mixture of homomeric ASIC3 channels with ASIC3-containing heteromeric channels (ASIC3 + 2a, ASIC3 + 2b, ASIC3 + 1a), which could display different regulations by FMRFamide-related peptides.

3.3. Effect of ASIC3-like current on sensory neuron excitability

Membrane potential variations were recorded in the current-clamp mode on DRG neurons expressing an ASIC3-like current. Sensory neurons had a resting potential around −55 mV (−57.4 ± 2.6 mV, n = 15) and no spontaneous action potentials (APs) were triggered. Fig. 4A shows the depolarisation induced by pH 6, 6.3 and 6.6 on a single neuron. The transient depolarisations induced by pH 6 and pH 6.3 triggered APs, shown on enlargements, whereas the threshold was not reached by the transient depolarisation induced by pH 6.6. These ASIC3-like expressing neurons displayed a mean AP threshold of −26.8 ± 1.8 mV (n = 20). Spontaneous APs were never triggered during the plateau of the depolarisation, even for small pH drops, contrary to what was reported for hippocampal neurons (Baron et al., 2002). The neuronal excitability during the plateau phase was thus studied in response to an electrical stimulus (Fig. 4B). Current pulses that did not trigger any AP at resting potential triggered several APs when applied on the sustained depolarisation induced at pH 6.6 and 6.3. However, this effect was not observed at pH 6 and below (pH 5, not shown), probably because of an inactivation of voltage-sensitive Na^+ channels that prevented AP triggering. These results show that the sustained depolarisation induced by a submaximal activation of ASIC3-like current increases the excitability of sensory neurons in response to another depolarising stimulus.

3.4. Effects of FMRFamide-related peptides on sensory neuron excitability

Fig. 5 shows voltage-clamp (Fig. 5A) and current-clamp recordings (Fig. 5B, C) from the same sensory neuron expressing an ASIC3-like current. NPSF slowed down the inactivation of the ASIC3-like current activated at pH 6.3 (Fig. 5A) or at pH 5 (not shown). In this neuron, NPSF and NPFF equally slowed down the ASIC3-like peak current inactivation and increased the sustained current (not shown). The peak current activated at pH 6.3 represented 53% of the peak current activated at pH 5, and this submaximal pH 6.3-evoked peak current induced a transient depolarisation of 22 mV (Fig. 5B) representing 55% of the depolarisation induced at pH 5 (not shown). The pH 6.3-evoked transient depolarisation was unable to induce any AP, contrary to the pH 5-induced depolarisation. As expected from the effect on ASIC3-like current, the amplitude of the initial depolarisation induced by pH 6.3 was not modified by NPSF whereas the repolarisation was slowed down (Fig. 5B). This effect on the membrane potential did not trigger any spontaneous APs. Neuronal excitability was then tested in response to an electrical stimulus (Fig. 5C). In control conditions, the current stimulus was chosen just

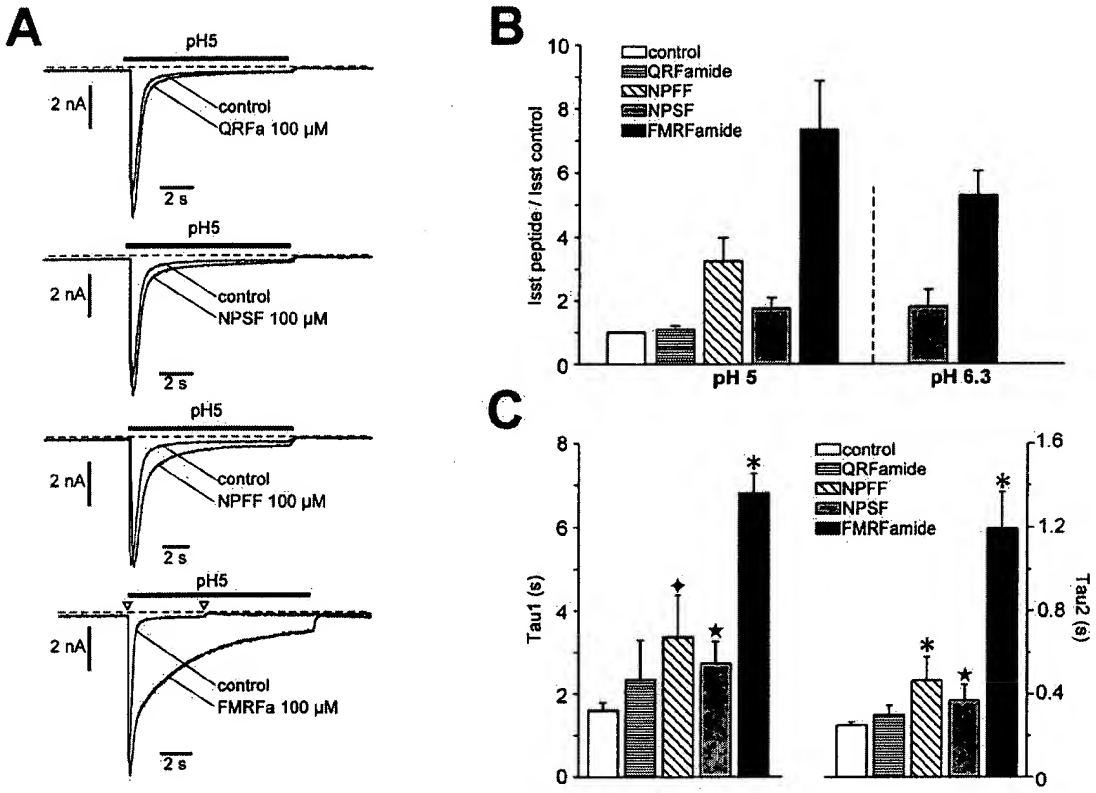

Fig. 3. Effect of FMRFamide-related peptides on ASIC3-like current from DRG neurons. (A) ASIC3-like currents recorded in whole-cell from cultured rat DRG neurons. The dashed line represents the zero current level. Currents were elicited at −50 mV following an external pH drop from pH 7.4 to 5, and peptides were applied 30 s before the pH drop. On the last trace, the control current was elicited with only a 5 s application of pH 5 (arrowheads). (B) Increase of ASIC3-like sustained currents by FMRFamide-related peptides. The sustained current amplitude measured in the presence of each neuropeptide has been normalised to the control currents (n = 3–8). The sustained current amplitudes were measured at the end of the pH drop. (C) Effect of neuropeptides on inactivation time constants of pH 5-evoked ASIC3-like currents. ASIC3-like current inactivation was fitted by a second order exponential (n = 3–20; ★, $P < 0.05$, ◆, $P < 0.01$, and ∗, $P < 0.001$).

below the threshold of AP triggering during the sustained depolarisation. Current pulses were unable to trigger any APs during the late plateau phase, but could however induce one or two APs during the initial repolarisation of the transient phase. When the ASIC3-like current activated at pH 6.3 was slowed down by 100 µM NPFF (Fig. 5C, left) or NPSF (Fig. 5C, right), the same current pulses could trigger more APs than in control conditions, because the repolarisation was slowed down after the initial transient depolarisation. This effect was not observed when the ASIC3-like current was activated at pH 6 and below, probably because of an inactivation of voltage-dependent Na^+ channels that clamped the neuron in an inexcitable state (not shown).

4. Discussion

This work describes the effects of NPSF and other mammalian FMRFamide-related neuropeptides on ASIC3, a channel which is expressed in nociceptive DRG neurons (Voilley et al., 2001) and which is thought to be involved in nociception (Lingueglia et al., 1997; Kress and Zeilhofer, 1999; Price et al., 2001; Reeh and Kress, 2001). We show that NPSF, like other RFamide-motif containing peptides, is able to drastically increase the inactivation rate and/or the sustained phase of homomeric ASIC3 currents without modifying the peak current. These data confirm and extend the results previously described by Askwith et al. (Askwith et al., 2000) for FMRFamide and NPFF. We also report that QRFamide, a degradation product of NPFF (Sol et al., 1999), and RFamide, the common C-terminal motif of FMRFamide-related peptides, slightly affect ASIC3 sustained currents. NPSF, and to a lesser degree QRFamide and RFamide, appear to be potentially interesting ASIC3-interacting peptides since they have not been implicated in G-protein mediated NPFF-receptor effects (Sol et al., 1999; Roumy et al., 2000). Surprisingly, and as previously observed for NPFF (Askwith et al., 2000), the molluscan FMRFamide peptide was more potent than NPSF. It may be that mammalian FMRFamide-related peptide(s) still to be discovered would be more potent than NPSF and NPFF.

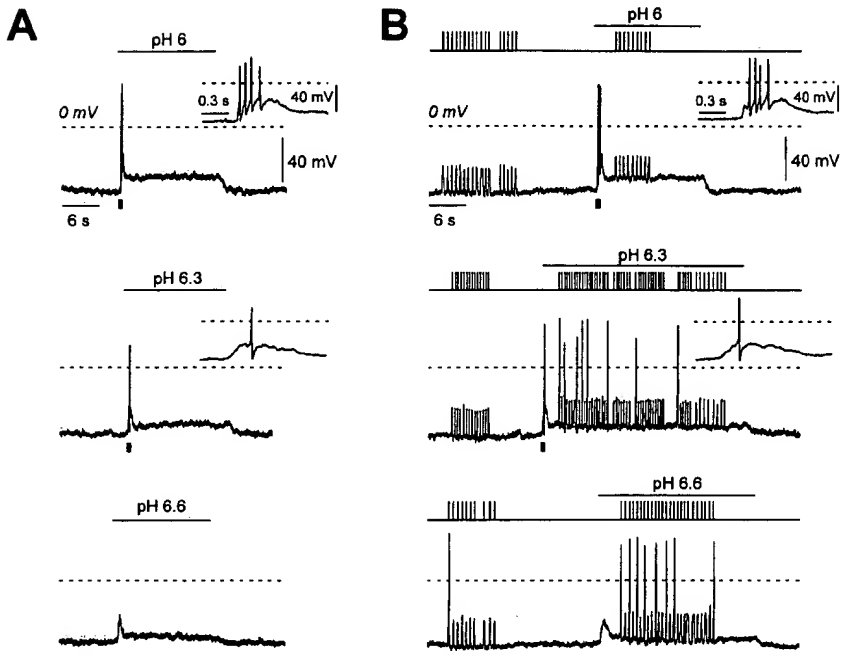

Fig. 4. Effect of ASIC3-like sustained current on sensory neuron excitability. Original current-clamp recordings from a single DRG neuron. (A) Current-clamp recording (I = 0 pA) of depolarisation induced by a pH drop from pH 7.4 to pH 6 (top), pH 6.3 (middle) and pH 6.6 (bottom). Spontaneous APs were never triggered during the plateau of the depolarisation. (B) Current-clamp recording (I = 0 pA) of depolarisation induced by a pH drop from pH 7.4 to pH 6 (top), pH 6.3 (middle) and pH 6.6 (bottom), with current pulses applied repetitively throughout the recording. The same current pulse amplitude was used for the three pH drops tested. Current pulses that did not trigger any APs at resting potential triggered several APs when applied on the sustained depolarisation induced at pH 6.6 and pH 6.3. The dashed line represents the 0 mV level. The time-lapse indicated by a black mark below the recording was enlarged in the insets, to show the APs triggered by the initial depolarisation. The same results were obtained from three different DRG neurons.

NPSF, or other related neuropeptides, were not able to generate an ASIC3 current on their own. However, NPSF (like FMRFamide) probably acts directly on the channel, although additional experiments are needed to unambiguously eliminate the possibility of an indirect interaction via membrane receptors. NPSF and the different neuropeptides exert effects on endogenous ASIC3-like sustained currents recorded from DRG neurons which are similar to the effects observed in the recombinant system. However, the effects were smaller than those observed on homomeric ASIC3 currents (two- and three-fold increases for NPSF and NPFF, and seven-fold increase for FMRFamide), and were essentially due to a slowing-down of the inactivation rate. This difference could be due to the expression of heteromeric ASIC3-containing channels in DRG neurons (Babinski et al., 1999; Alvarez de la Rosa et al., 2002; Benson et al., 2002). Effects of NPSF and other FMRFamide-related peptides on ASIC3 current occur at micromolar concentration levels which are close to the FMRFamide concentrations needed to activate the molluscan peptide-gated Na^+ channel FaNaCh (Lingueglia et al., 1995; reviewed by Cottrell, 1997). Although neuropeptides are generally considered to act at lower concentrations by binding to G-protein-coupled receptors, molluscan peptide-gated Na^+ channel has been implicated in the modulation of neurotransmission (Green et al., 1994; Lingueglia et al., 1995). In light of the effect of FMRFamide in molluscs, it can be postulated that mammalian FMRFamide-related peptides could also exert a neuromodulatory effect on sensory neurons through their direct effect on ASIC3. This would particularly be the case for NPSF which displayed a low affinity toward NPFF receptor (28 times less than NPFF), and which has been shown to be ineffective in reducing the effect of nociceptin in dorsal raphe neurons (Roumy et al., 2000).

In DRG neurons, transient depolarisations induced by small pH drops (from pH 7.4 to pH 6 or 6.3) were able to trigger APs, and were followed by a sustained depolarisation due to the plateau phase of ASIC3-like currents. No APs were spontaneously triggered during this sustained depolarisation, even for small pH drops, contrary to what was previously reported for hippocampal neurons (Baron et al., 2002). However, electrical infraliminar stimuli (i.e. that did not trigger APs at the resting membrane potential) became able to generate APs when applied during the sustained depolarisation induced at pH 6.6, pH 6.3, but not at pH 6 or below. These data show that the sustained depolarisation induced by submaximal activation of ASIC3-like current increases the excitability of sensory neurons in response to another depolarising stimulus, although effects of pH

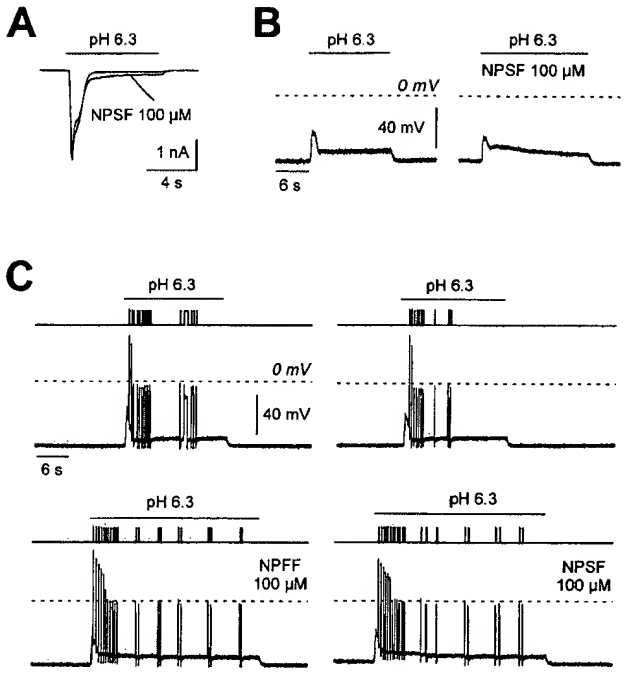

Fig. 5. Effect of FMRFamide-related peptides on sensory neuron excitability. Voltage-clamp and current-clamp recordings from a single DRG neuron expressing an ASIC3-like current. (A) Voltage-clamp recordings showing the effect of NPSF (100 µM) on the ASIC3-like current induced by a pH drop from pH 7.4 to pH 6.3. Holding potential: −50 mV. (B) Current-clamp recordings (I = 0) of the depolarisation induced by a pH drop from pH 7.4 to pH 6.3 before and after a 30 s application of NPSF 100 µM (right). The dashed line represents the 0 mV level. (C) Effect of 100 µM NPFF (left) and NPSF (right) on neuronal excitability. Current-clamp recordings (I = 0) of the depolarisation induced by a pH drop from pH 7.4 to pH 6.3 with current pulses applied repetitively throughout the pH drop. The same current pulse amplitude was used for the four recordings shown. After a 30 s application of 100 µM NPFF (left, bottom) or 100 µM NPSF (right, bottom), the same current pulses could trigger more APs than in control conditions (upper traces). The dashed line represents the 0 mV level. The same results were obtained from three different DRG neurons.

on other channels (K^+, VR1) cannot be ruled out. However, the proportion of neurons expressing the different current types (ASIC and VR1 currents) has recently been described (Mamet et al., 2002). Indeed, in the present study, effects of neuropeptides have only been tested on DRG neurons expressing an ASIC3-like current. Moreover, several studies described the pH-sensitivity of the vanilloid receptor VR1 (Tominaga et al., 1998; Jerman et al., 2000; Welch et al., 2000), with a half activation of the channel at pH values below 5. Under these circumstances, it can be proposed that there is no, or only a minor, contribution of VR1 to the acid-evoked sustained current elicited at pH 6 and 6.3. Furthermore, we performed experiments in COS cells expressing rat VR1 (not shown) showing that NPSF, NPFF and FMRFamide (100µM) have no effect on the acid-evoked VR1 current.

DRG neurons form a physically and functionally heterogeneous population that expresses different mixes of voltage-gated Na^+ channels. It has been shown that both TTX-sensitive (TTX-S) and TTX-resistant (TTX-R) currents were expressed by small DRG neurons from adult rats (Rush et al., 1998). At least 95% of TTX-S channels appeared to be inactivated by potentials more positive than −40 mV, whereas more than 90% of TTX-R channels were available at −40 mV. TTX-R currents were thus the best candidates to support firing under conditions of chronic depolarisation. It can then be proposed that the initial APs observed during an external pH acidification would result from the activation of both TTX-S and TTX-R Na^+ channels. This hypothesis is supported by the mean AP threshold measured during our experiments on sensory neurons (-26.8 ± 1.8 mV, $n = 20$). Then, the APs electrically triggered during the sustained depolarisation would be related to the activation of TTX-R channels. This conclusion is supported by a recent study (Rola et al., 2002) which suggests that AP triggering in cardiac DRG neurons during membrane depolarisation, is mostly due to TTX-R current. However, the TTX-R channels would be inactivated when the acid-evoked sustained depolarisation is too high (i.e. for pH 6 and below), and the neuron would then become inexcitable. This property could be important in coding sustained pain, when the neuron is stimulated by several painful stimuli, and modulators of this plateau phase, such as NPSF or NPFF, could thus play a major role in various physiopathological conditions.

To conclude, we have shown that NPSF, like other FMRFamide-related peptides, acts on heterologously expressed ASIC3 currents by increasing the slow sustained phase. This effect led us to investigate the role of ASIC3 sustained current in DRG neuron excitability. We have reported that ASIC3-induced sustained depolarisation modulates the neuronal excitability in response to other stimuli. The neuronal excitability could be either increased when the membrane potential reached during the sustained depolarisation is just below the activation threshold of the voltage-dependent TTX-R channels, or decreased by a higher sustained depolarisation that leads to inactivation of these Na^+ channels. Regulation of ASIC3-induced sustained depolarisation by NPSF and FMRFamide-related peptides could thus constitute a fine tuning of nociceptive neuron excitability in coding sustained pain, particularly under inflammatory conditions where the expression levels of both the NPFF precursor (Vilim et al., 1999) and of the ASIC3 subunit (Voilley et al., 2001) are increased.

Acknowledgements

We are grateful to N. Voilley, J. Mamet, and M. Salinas for helpful discussion, to M. Jodar and N. Leroudier for excellent technical assistance and to V. Lopez

for secretarial assistance. L. Rash is gratefully acknowledged for proofreading the manuscript. The rat VR1 construct was kindly provided by Dr N. Voilley. This work was supported by the Centre National de la Recherche Scientifique, the Institut National de la Santé et de la Recherche Médicale, the Association Française contre les Myopathies, the Association pour la Recherche sur le Cancer (A. B.), Astra Zeneca AB Research Area CNS/Pain, and the Ministère de la Recherche (ACI: Molécules et Cibles Thérapeutiques).

References

Allard, M., Rousselot, P., Lombard, M.C., Theodosis, D.T., 1999. Evidence for neuropeptide FF (FLFQRFamide) in rat dorsal root ganglia. Peptides 20, 327–333.

Alvarez de la Rosa, D., Zhang, P., Shao, D., White, F., Canessa, C.M., 2002. Functional implications of the localization and activity of acid- sensitive channels in rat peripheral nervous system. Proceedings National Academy of Sciences of the USA 99, 2326–2331.

Askwith, C.C., Cheng, C., Ikuma, M., Benson, C., Price, M.P., Welsh, M.J., 2000. Neuropeptide FF and FMRFamide potentiate acid-evoked currents from sensory neurons and proton-gated DEG/ENaC channels. Neuron 26, 133–141.

Babinski, K., Le, K.T., Seguela, P., 1999. Molecular cloning and regional distribution of a human proton receptor subunit with biphasic functional properties. J Neurochem 72, 51–57.

Baron, A., Waldmann, R., Lazdunski, M., 2002. ASIC-like, proton-activated currents in rat hippocampal neurons. Journal of Physiology 539, 485–494.

Bassler, E.L., Ngo-Anh, T.J., Geisler, H.S., Ruppersberg, J.P., Grunder, S., 2001. Molecular and functional characterization of acid-sensing ion channel (ASIC) 1b. Journal of Biological Chemistry 11, 11.

Benson, C.J., Xie, J., Wemmie, J.A., Price, M.P., Henss, J.M., Welsh, M.J., Snyder, P.M., 2002. Heteromultimers of DEG/ENaC subunits form H^+-gated channels in mouse sensory neurons. Proceedings National Academy of Sciences of the USA 99, 2338–2343.

Catarsi, S., Babinski, K., Seguela, P., 2001. Selective modulation of heteromeric ASIC proton-gated channels by neuropeptide FF. Neuropharmacology 41, 592–600.

Chen, C.C., England, S., Akopian, A.N., Wood, J.N., 1998. A sensory neuron-specific, proton-gated ion channel. Proceedings of the National Academy of Sciences of the USA 95, 10240–10245.

Cottrell, G.A., 1997. The first peptide-gated ion channel. Journal of Experimental Biology 200, 2377–2386.

Cottrell, G.A., Green, K.A., Davies, N.W., 1990. The neuropeptide Phe-Met-Arg-Phe-NH2 (FMRFamide) can activate a ligand-gated ion channel in Helix neurons. Pflugers Archives 416, 612–614.

Devillers, J.P., Boisserie, F., Laulin, J.P., Larcher, A., Simonnet, G., 1995b. Simultaneous activation of spinal antiopioid system (neuropeptide FF) and pain facilitatory circuitry by stimulation of opioid receptors in rats. Brain Research 700, 173–181.

Escoubas, P., De Weille, J.R., Lecoq, A., Diochot, S., Waldmann, R., Champigny, G., Moinier, D., Menez, A., Lazdunski, M., 2000. Isolation of a tarantula toxin specific for a class of proton-gated Na^+ channels. Journal of Biological Chemistry 275, 25116–25121.

Green, K.A., Falconer, S.W., Cottrell, G.A., 1994. The neuropeptide Phe-Met-Arg-Phe-NH2 (FMRFamide) directly gates two ion channels in an identified Helix neurone. Pflugers Archives 428, 232–240.

Hamill, O.P., Marty, A., Neher, E., Sakmann, B., Sigworth, F.J., 1981. Improved patch-clamp techniques for high-resolution current recording from cells and cell-free membrane patches. Pflugers Archives 391, 85–100.

Jerman, J.C., Brough, S.J., Prinjha, R., Harries, M.H., Davis, J.B., Smart, D., 2000. Characterization using FLIPR of rat vanilloid receptor (rVR1) pharmacology. British Journal of Pharmacology 130, 916–922.

Kress, M., Zeilhofer, H.U., 1999. Capsaicin, protons and heat: new excitement about nociceptors. Trends in Pharmacological Sciences 20, 112–118.

Krishtal, O.A., Pidoplichko, V.I., 1981a. Receptor for protons in the membrane of sensory neurons. Brain Research 214, 150–154.

Krishtal, O.A., Pidoplichko, V.I., 1981b. A receptor for protons in the membrane of sensory neurons may participate in nociception. Neuroscience 6, 2599–2601.

Krishtal, O.A., Pidoplichko, V.I., 1981c. A 'receptor' for protons in small neurons of trigeminal ganglia: possible role in nociception. Neuroscience Letters 24, 243–246.

Lingueglia, E., Champigny, G., Lazdunski, M., Barbry, P., 1995. Cloning of the amiloride-sensitive FMRFamide peptide-gated sodium channel. Nature 378, 730–733.

Lingueglia, E., De Weille, J.R., Bassilana, F., Heurteaux, C., Sakai, H., Waldmann, R., Lazdunski, M., 1997. A modulatory subunit of acid sensing ion channels in brain and dorsal root ganglion cells. Journal of Biological Chemistry 272, 29778–29783.

Mamet, J., Baron, A., Lazdunski, M., Voilley, N., 2002. Proinflammatory mediators, stimulators of sensory neuron excitability via the expression of acid-sensing ion channels. Journal of Neuroscience 22/24, 10662–10670.

Panula, P., Aarnisalo, A.A., Wasowicz, K., 1996. Neuropeptide FF, a mammalian neuropeptide with multiple functions. Progress in Neurobiology 48, 461–487.

Panula, P., Kalso, E., Nieminen, M., Kontinen, V.K., Brandt, A., Pertovaara, A., 1999. Neuropeptide FF and modulation of pain. Brain Research 848, 191–196.

Perry, S.J., Yi-Kung Huang, E., Cronk, D., Bagust, J., Sharma, R., Walker, R.J., Wilson, S., Burke, J.F., 1997. A human gene encoding morphine modulating peptides related to NPFF and FMRFamide. FEBS Letters 409, 426–430.

Price, D.A., Greenberg, M.J., 1977. Structure of a molluscan cardioexcitatory neuropeptide. Science 197, 670–671.

Price, M.P., Mcilwrath, S.L., Xie, J., Cheng, C., Qiao, J., Tarr, D.E., Sluka, K.A., Brennan, T.J., Lewin, G.R., Welsh, M.J., 2001. The DRASIC cation channel contributes to the detection of cutaneous touch and acid stimuli in mice. Neuron 32, 1071–1083.

Reeh, P.W., Kress, M., 2001. Molecular physiology of proton transduction in nociceptors. Current Opinion in Pharmacology 1, 45–51.

Rola, R., Szulczyk, B., Szulczyk, P., Witkowski, G., 2002. Expression and kinetic properties of Na(+) currents in rat cardiac dorsal root ganglion neurons. Brain Research 947, 67–77.

Roumy, M., Gouarderes, C., Mazarguil, H., Zajac, J.M., 2000. Are neuropeptides FF and SF neurotransmitters in the rat? Biochemical and Biophysical Research Communications 275, 821–824.

Roumy, M., Zajac, J.M., 1998. Neuropeptide FF, pain and analgesia. European Journal of Pharmacology 345, 1–11.

Roumy, M., Zajac, J., 1999. Neuropeptide FF selectively attenuates the effects of nociceptin on acutely dissociated neurons of the rat dorsal raphe nucleus. Brain Research 845, 208–214.

Roumy, M., Zajac, J.M., 2001. Neuropeptide FF receptors couple to a cholera toxin-sensitive G-protein in rat dorsal raphe neurones. European Journal of Pharmacology 417, 45–49.

Rush, A.M., Brau, M.E., Elliott, A.A., Elliott, J.R., 1998. Electrophysiological properties of sodium current subtypes in small cells from adult rat dorsal root ganglia. Journal of Physiology 511, 771–789.

Sol, J.C., Roussin, A., Proto, S., Mazarguil, H., Zajac, J.M., 1999. Enzymatic degradation of neuropeptide FF and SQA-neuropeptide FF in the mouse brain. Peptides 20, 1219–1227.

Sutherland, S.P., Benson, C.J., Adelman, J.P., Mccleskey, E.W., 2001.

Acid-sensing ion channel 3 matches the acid-gated current in cardiac ischemia-sensing neurons. Proceedings National Academy of Sciences of the USA 98, 711–716.

Tominaga, M., Caterina, M.J., Malmberg, A.B., Rosen, T.A., Gilbert, H., Skinner, K., Raumann, B.E., Basbaum, A.I., Julius, D., 1998. The cloned capsaicin receptor integrates multiple pain-producing stimuli. Neuron 21, 531–543.

Vilim, F.S., Aarnisalo, A.A., Nieminen, M.L., Lintunen, M., Karlstedt, K., Kontinen, V.K., Kalso, E., States, B., Panula, P., Ziff, E., 1999. Gene for pain modulatory neuropeptide NPFF: induction in spinal cord by noxious stimuli. Molecular Pharmacology 55, 804–811.

Voilley, N., De Weille, J., Mamet, J., Lazdunski, M., 2001. Nonsteroid anti-inflammatory drugs inhibit both the activity and the inflammation-induced expression of acid-sensing ion channels in nociceptors. Journal of Neuroscience 21, 8026–8033.

Waldmann, R., Bassilana, F., De Weille, J.R., Champigny, G., Heurteaux, C., Lazdunski, M., 1997. Molecular cloning of a non-inactivating proton-gated Na^+ channel specific for sensory neurons. Journal of Biological Chemistry 272, 20975–20978.

Waldmann, R., Lazdunski, M., 1998. H(+)-gated cation channels: neuronal acid sensors in the NaC/DEG family of ion channels. Current Opinion in Neurobiology 8, 418–424.

Welch, J.M., Simon, S.A., Reinhart, P.H., 2000. The activation mechanism of rat vanilloid receptor 1 by capsaicin involves the pore domain and differs from the activation by either acid or heat. Proceedings National Academy of Sciences of the U S A 97, 13889–13894.

Yang, H.Y., Fratta, W., Majane, E.A., Costa, E., 1985. Isolation, sequencing, synthesis, and pharmacological characterization of two brain neuropeptides that modulate the action of morphine. Proceedings National Academy of Sciences of the USA 82, 7757–7761.

Yang, H.Y., Martin, R.M., 1995. Isolation and characterization of a neuropeptide FF-like peptide from brain and spinal cord rat. Society of Neurosciences Abstract 21, 760.

Zhu, J., Jhamandas, K., Yang, H.Y., 1992. Release of neuropeptide FF (FLFQPQRF-NH2) from rat spinal cord. Brain Research 592, 326–332.

THE JOURNAL OF BIOLOGICAL CHEMISTRY
Vol. 276, No. 38, Issue of September 21, pp. 35361–35367, 2001
Printed in U.S.A.

Zn^{2+} and H^+ Are Coactivators of Acid-sensing Ion Channels*

Received for publication, June 6, 2001, and in revised form, July 6, 2001
Published, JBC Papers in Press, July 16, 2001, DOI 10.1074/jbc.M105208200

Anne Baron‡, Lionel Schaefer‡, Eric Lingueglia‡, Guy Champigny, and Michel Lazdunski§

From the Institut de Pharmacologie Moléculaire et Cellulaire, CNRS, UMR 6097, 660 route des Lucioles, Sophia Antipolis, 06560 Valbonne, France

Acid-sensing ion channels (ASICs) are cationic channels activated by extracellular protons. They are expressed in sensory neurons, where they are thought to be involved in pain perception associated with tissue acidosis. They are also expressed in brain. A number of brain regions, like the hippocampus, contain large amounts of chelatable vesicular Zn^{2+}. This paper shows that Zn^{2+} potentiates the acid activation of homomeric and heteromeric ASIC2a-containing channels (*i.e.* ASIC2a, ASIC1a+2a, ASIC2a+3), but not of homomeric ASIC1a and ASIC3. The EC_{50} for Zn^{2+} potentiation is 120 and 111 μM for the ASIC2a and ASIC1a+2a current, respectively. Zn^{2+} shifts the pH dependence of activation of the ASIC1a+2a current from a $pH_{0.5}$ of 5.5 to 6.0. Systematic mutagenesis of the 10 extracellular histidines of ASIC2a leads to the identification of two residues (His-162 and His-339) that are essential for the Zn^{2+} potentiating effect. Mutation of another histidine residue, His-72, abolishes the pH sensitivity of ASIC2a. This residue, which is located just after the first transmembrane domain, seems to be an essential component of the extracellular pH sensor of ASIC2a.

Acid-sensing ionic channels (ASICs)[1] are H^+-gated cation channels expressed in sensory neurons and in neurons of the central nervous system. Four different genes encoding six polypeptides have been identified so far: ASIC1a (1) and ASIC1b (2), ASIC2a (3–6) and ASIC2b (7), ASIC3 (8–10), and ASIC4 (11, 12). Functional ASICs are thought to be tetrameric assemblies of ASIC subunits (13, 14). Both homomeric and heteromeric ASICs can be formed, which exhibit different kinetics, external pH sensitivities, and tissue distribution (7, 14–17). The recently identified ASIC4 subunit does not seem to form a H^+-activated channel on its own (11, 12).

ASIC1a is present in brain and sensory neurons, whereas its splice variant ASIC1b is found only in sensory neurons. Both ASIC1a and ASIC1b mediate fast inactivating currents upon modest but rapid acidification of the external medium. ASIC2a is substantially expressed in the brain, whereas its variant ASIC2b is present in both brain and sensory neurons. ASIC2b has no activity on its own but can form functional heteromers with other ASIC subunits and particularly ASIC3 (7). ASIC3 is specifically found in the small nociceptive sensory neurons and generates a biphasic current with a fast inactivating phase, followed by a sustained component (10). All the ASIC subunits share the same topological organization with intracellular N and C termini and two putative transmembrane domains flanking a large cysteine-rich extracellular loop (16).

In sensory neurons, ASIC currents are thought to play an important role in nociception during a tissue acidosis, for instance in muscle and cardiac ischemia (18–23) and in inflammation (24). It has been also proposed that some might participate in touch sensation (25, 26). Their function in the central nervous system is less documented. An important role of ASICs in signal transduction associated with local pH variations during normal neuronal activity has been proposed (27, 28). They might also be involved in pathological situations such as brain ischemia and epilepsy that produce significant extracellular acidification.

Some ASICs are expressed in brain regions that contain large amounts of chelatable Zn^{2+}. For instance, presynaptic vesicles of glutamatergic hippocampal terminals contain Zn^{2+} in up to millimolar concentrations (29, 30). Zn^{2+} corelease with the neurotransmitter results in a transient increase of the local synaptic Zn^{2+} concentration up to 100–300 μM from resting levels below 500 nM (31–35), and has the potential to alter the behavior of various membrane channels and neurotransmitter receptors (35–37).

Here we show that Zn^{2+} potentiates the activation of ASIC2a-containing channels. We have used site-directed mutagenesis to investigate the structural determinants of Zn^{2+} coactivation in the extracellular loop of the ASIC2a subunit. We have identified two histidine residues, His-162 and His-339, that are essential for the Zn^{2+} potentiating effect, but also another histidine residue, His-72, which causes a large shift in pH sensitivity of ASIC2a when mutated and could be an important component of the pH sensor.

EXPERIMENTAL PROCEDURES

Expression of ASIC Currents in Xenopus oocytes—*Xenopus laevis* were purchased from CRBM (Montpellier, France). Pieces of the ovary were surgically removed, and individual oocytes were dissected in a saline solution (ND96) containing 96 mM NaCl, 2 mM KCl, 1.8 mM $CaCl_2$, 2 mM $MgCl_2$, and 5 mM HEPES (pH 7.4 with NaOH). Stage V and VI oocytes were treated for 2 h with collagenase (1 mg/ml, type Ia, Sigma) in ND96 to remove follicular cells. cRNA of rat ASIC1a, WT and mutated ASIC2a and ASIC3 were synthesized with the mCAP RNA capping kit from Stratagene and injected (0.15–2.5 ng/oocyte) using a pressure microinjector. The oocytes were kept at 19 °C in the ND96 saline solution supplemented with penicillin (6 μg/ml) and streptomycin (5 μg/ml). Oocytes were studied within 1–3 days following injection. In a 0.3-ml perfusion chamber, a single oocyte was impaled with two standard glass microelectrodes (1–2.5-megohm resistance) filled with 3 M KCl and maintained under voltage clamp using a Dagan TEV 200 amplifier. Currents were sampled at 100 Hz and low pass-filtered at 500 Hz. Data acquisition and analysis were performed using pClamp software (Axon Instruments). All experiments were performed at room temperature (20–22 °C) in ND96 bathing solution. For measurements

* This work was supported by CNRS, INSERM, the Association Française contre les Myopathies (AFM), and the Association pour la Recherche sur le Cancer (ARC). The costs of publication of this article were defrayed in part by the payment of page charges. This article must therefore be hereby marked "*advertisement*" in accordance with 18 U.S.C. Section 1734 solely to indicate this fact.

‡ These authors should be considered equally as first author.

§ To whom correspondence should be addressed. Tel.: 33-4-93-95-77-02 or -03; Fax: 33-4-93-95-77-04; E-mail: ipmc@ipmc.cnrs.fr.

[1] The abbreviations used are: ASIC, acid-sensing ion channel; MES, 4-morpholinoethanesulfonic acid; MTSET, (2-(trimethylammonium)-ethyl)methanethiosulfonate bromide; WT, wild type.

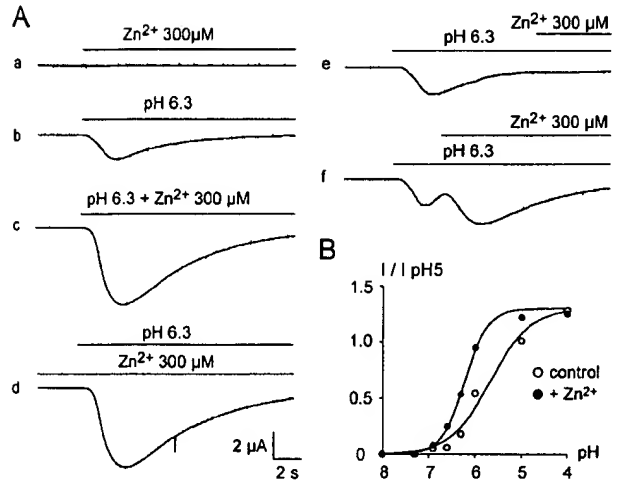

FIG. 1. **Typical experiment showing the potentiation by Zn^{2+} of the heteromeric ASIC1a+2a current expressed in *Xenopus* oocytes.** *A*, 300 μM Zn^{2+} could not activate any ASIC current at pH 7.4 (*a*), but increased the amplitude of ASIC current induced by pH 6.3 (*b*), whether it was applied simultaneously (*c*) or before the pH step (*d*). Zn^{2+} did not reactivate the ASIC current when fully inactivated by pH 6.3 (*e*) but increased the not fully inactivated current (*f*). *B*, On the same oocyte, Zn^{2+} (300 μM) induced a left shift of the current activation curve associated with an increase in the Hill coefficient (○, control; ●, + Zn^{2+}). The current amplitude is expressed as a fraction of the current induced by pH 5 ($I/I_{pH\,5}$). Holding potential, −70 mV.

of ASIC currents, changes in extracellular pH were induced by rapid perfusion of the experimental chamber. Depending on the pH range, acidic solutions were buffered with HEPES (pH > 6), MES (pH between 6 and 5), or acetate (pH < 5).

Expression of ASIC Currents in COS Cells—COS cells, at a density of 20,000 cells/35-mm diameter Petri dish, were transfected with a mix of pCI-CD8 and the following plasmids: pCI-rASIC1a, pCI-rASIC2a, or pCI-rASIC3 (1:5 ratio) using the DEAE-dextran method. Cells were used for electrophysiological measurements 1–3 days after transfection. Successfully transfected cells were recognized by their ability to fix CD8 antibody-coated beads (Dynal). Ion currents were recorded using the whole cell patch-clamp technique (38). Data were sampled at 500 Hz and low pass-filtered at 3 kHz using pClamp8 software (Axon Instruments). The statistical significance of differences between sets of data was estimated by single-sided Student's t test. The pipette solution contained (in mM): KCl 140, NaCl 5, $MgCl_2$ 2, EGTA 5, HEPES 10 (pH 7.35); and the bath solution contained (in mM): NaCl 150, KCl 5, $MgCl_2$ 2, $CaCl_2$ 2, HEPES 10 (pH 7.45). MES or acetate were used instead of HEPES to buffer bath solution pH ranging from 6 to 5, and from 4.5 to 3, respectively. $ZnCl_2$ was added to the bath solution at concentration ranging from 1 μM to 10 mM. Changes in extracellular pH were induced by shifting one out of six outlets of a microperfusion system in front of the cell. Experiments were carried out at room temperature (20–22 °C).

Site-directed Mutagenesis—Mutants were prepared by polymerase chain reaction using a modification of the method of gene splicing by overlap extension (39) or using the GeneEditor *in vitro* site-directed mutagenesis system from Promega. The amplified products were digested by *Eco*RI and *Xho*I and subcloned into the pBSK-SP6-globin vector specially designed for *Xenopus* oocyte expression (5). cRNA were synthetized from the *Not*I-digested vector using the mCAP RNA capping kit from Stratagene.

RESULTS

Effect of Zn^{2+} on the Heteromeric ASIC1a+2a Current—The extensive colocalization of the ASIC1a and ASIC2a subunits in central neurons (3, 15) led us to first study the effect of Zn^{2+} on the heteromeric ASIC1a+2a channel expressed in *Xenopus* oocytes. The properties of the current recorded after coinjection of equal quantities of both ASIC1a and ASIC2a cRNA were in good agreement with those already described for a heteromeric ASIC1a+2a current (15). However, in the presence of 300 μM Zn^{2+}, the submaximal ASIC current induced by pH 6.3 was increased ~3-fold (Fig. 1*A*, *b* and *c*), whereas Zn^{2+} alone at pH 7.4 could not activate any current (Fig. 1*A*, *a*). The same Zn^{2+}-potentiated ASIC current could be recorded when Zn^{2+} was applied either before the acidic pH jump (tested up to 3 min; Fig. 1*A*, *d*) or simultaneously (Fig. 1*A*, *c*). When the ASIC current was fully inactivated (after 5 s at pH 6.3; Fig. 1*A*, *e*), it could not be reactivated by the addition of Zn^{2+}. However, application of Zn^{2+} in the course of the inactivation process was still able to increase the fraction of the ASIC current that was not inactivated (Fig. 1*A*, *f*). Based on these results, Zn^{2+} was applied simultaneously with the pH drop in all subsequent experiments.

Zn^{2+} (300 μM) induced a left shift of the ASIC1a+2a half-maximal activation from pH 5.5 to pH 6, and an increase in the Hill coefficient from 1.05 to 1.4 (Fig. 1*B*, typical experiment; Fig. 2*A*, mean results), whereas the maximal current induced at pH 4 was not modified. Fig. 2*B* shows the mean factor by which the ASIC1a+2a current amplitude was increased by 300 μM Zn^{2+} at different pH values. The potentiation by Zn^{2+} depended on the extracellular pH, with greater effects between pH 6.9 and 6.3 than between pH 6 and pH 5. The relative Zn^{2+}-induced increases in current amplitude reached 4.00 ± 1.06-fold (n = 6) the control current, for pH 6.6. Zn^{2+} has no effect on the pH-dependent ASIC1a+2a current inactivation (Fig. 2*C*). Zn^{2+} concentrations between 1 μM and 10 mM were tested on ASIC1a+2a currents activated at pH 6.3 (Fig. 2*D*). The Zn^{2+} concentration producing the half-maximal increase in current amplitude was 111 μM with a Hill coefficient of 0.8. A Zn^{2+} concentration of 300 μM was used in all further experiments.

Effect of Zn^{2+} on Homomeric ASIC1a and ASIC2a Currents—To determine which ASIC subunit was responsible for the Zn^{2+} potentiation of the heteromeric ASIC1a+2a current, we have tested the effects of Zn^{2+} on homomeric ASIC1a and ASIC2a currents expressed in *Xenopus* oocytes. ASIC2a requires rather low extracellular pH for activation ($pH_{0.5}$ = 4.34, Fig. 3*A*) (6, 15). When applied simultaneously with acid, 300 μM Zn^{2+} increased the amplitude of the ASIC2a current only in the first half of the activation curve, between pH 6.3 and pH 4.5 (Fig. 3*A*). Even if the effect of Zn^{2+} on the ASIC2a activation curve seems moderate, the relative increases in current amplitude reached 1.21 ± 0.04-fold (n = 11) to 7.00 ± 1.89-fold (n = 4) the control current, for pH 4.5 and 6.3, respectively (Fig. 3*B*). Zn^{2+} coactivated the homomeric ASIC2a current induced by pH 5.7 with an EC_{50} of 120 μM and a Hill slope factor of 1.44 (Fig. 3*B*, *inset*).

In contrast to ASIC2a, ASIC1a current is not potentiated by Zn^{2+} (Fig. 3*C*). Zn^{2+} instead exerted a very small inhibition on the ASIC1a current, but this effect was not significant. Fig. 3*D* illustrates that the effects of 300 μM Zn^{2+} on the ASIC1a, ASIC2a, and ASIC1a+2a currents induced by pH 6 and 5 are similar after expression in COS cells (transfection) or *Xenopus* oocytes (cRNA injection).

Effect of Zn^{2+} on Heteromeric ASIC2a+3 and Homomeric ASIC3 Currents—Since the Zn^{2+}-induced potentiation of ASIC currents seemed to be linked to the presence of the ASIC2a subunit, we tested the effect of Zn^{2+} on the heteromeric ASIC2a+3 channel expressed in *Xenopus* oocytes. Such an association has been characterized by Babinski *et al.* (17). The ASIC3 current was not potentiated but rather slightly inhibited by 300 μM Zn^{2+} (Fig. 4*A*). However, when ASIC2a was coexpressed with ASIC3, Zn^{2+} potentiated both the peak and the plateau phases of the current (Fig. 4*B*). Fig. 4*C* illustrates the relative Zn^{2+}-induced increase of ASIC3, ASIC2a+3, and ASIC1a+2a currents activated at pH 6, 5, and 4. The potentiation of the ASIC2a+3 current by Zn^{2+} was similar to that of the ASIC1a+2a current.

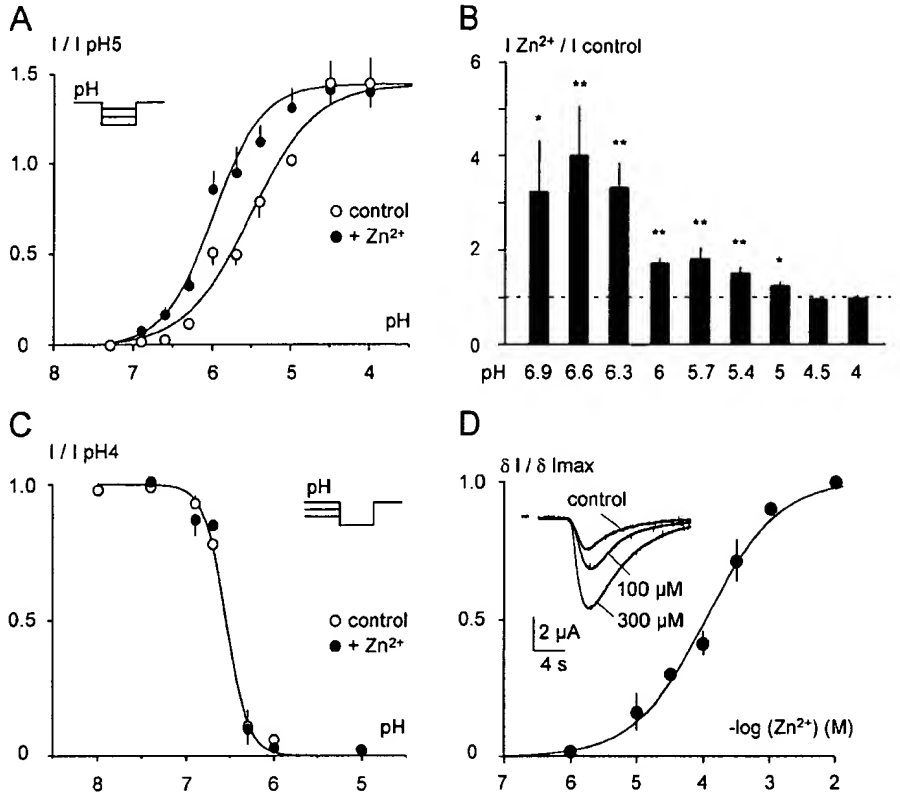

FIG. 2. **Effect of Zn^{2+} on the heteromeric ASIC1a+2a current expressed in *Xenopus* oocytes.** *A*, effect of Zn^{2+} on the activation of the ASIC1a+2a current. The current amplitude is expressed as a fraction of the current induced by pH 5 ($I/I_{pH\,5}$). Zn^{2+} (300 μM) induced a left shift of the mean activation curve, the $pH_{0.5}$ being shifted to 6.0 (●) from a control value at 5.5 (○), associated with an increase of the Hill coefficient reaching 1.4 from the control value of 1.05. *B*, relative effect of 300 μM Zn^{2+} for each pH value. The ratio between the current amplitude in presence and in absence of Zn^{2+} ($I_{Zn}{}^{2+}/I_{control}$) was calculated for each pH value and plotted as mean ± S.E. (n = 4–11). *, $p < 0.05$; **, $p < 0.005$, significantly different from pH 4 ratio. *C*, effect of Zn^{2+} on the pH-dependent inactivation of heteromeric ASIC1a+2a current. The current was induced by pH 4 from a resting pH value ranging from 8 to 5, normalized to the current induced from pH 7.4 ($I/I_{pH\,7.4}$), and expressed as mean ± S.E. as a function of resting pH value (n = 3–21). ○, control; ●, +300 μM Zn^{2+}. *D*, dose-response curve of Zn^{2+} potentiation of ASIC1a+2a current. Currents were activated by pH 6.3 in absence and presence of Zn^{2+} concentrations ranging from 1 μM to 10 mM. The current amplitude increase (δI) was normalized to its maximal value ($\delta I/\delta I_{max}$) and plotted as mean ± S.E. as a function of Zn^{2+} concentration (n = 3–12). *Inset*, original current traces showing the effect of 100 μM and 300 μM Zn^{2+}. Holding potential, −70 mV.

Involvement of Extracellular Histidines in the Coactivation of ASIC2a by Zn^{2+}—ASIC2a appears as the major subunit conferring Zn^{2+} sensitivity to ASICs. We used site-directed mutagenesis to investigate the structural determinants of Zn^{2+} coactivation in the extracellular loop of the ASIC2a subunit. Amino acids found at Zn^{2+} binding sites in proteins include histidine, cysteine, and occasionally aspartate or glutamate (40). When charged water-soluble sulfhydryl reactive reagents like MTSET, a cationic methanethiosulfonate, were applied extracellularly, they had no effect on the ASIC2a current, making unlikely that a cysteine residue interact with extracellularly applied Zn^{2+} (data not shown). On the other hand, diethylpyrocarbonate that reacts with several amino acid side chains, including the imidazole group side of histidine residues (41), suppressed the Zn^{2+} activation of the ASIC2a current (Fig. 5*B*) and of the ASIC1a+2a current (data not shown), suggesting a possible involvement of histidine residues in the Zn^{2+} coactivating effect. We systematically replaced the 10 histidine residues in the extracellular loop of ASIC2a by alanine and checked the Zn^{2+} sensitivity of the mutants (Table I). All mutants were still functional with no significant modifications of their $pH_{0.5}$ except the H72A mutant that had lost its ability to be activated by acidic pH down to pH 3. The expected potentiation of the ASIC2a current by zinc (up to 2 times at pH 5.5) was observed for the wild-type channel and for several mutants, but two of them, H162A and H339A, displayed no apparent potentiation, with little if any modification of their properties (Table I and Fig. 5, *C* and *D*). Each of these mutants lacked the potentiating effect of 300 μM Zn^{2+}, which could be as high as an 8-fold increase compared with the wild-type current amplitude at pH 6 (Fig. 5*E*). The absence of effect is not due to a shift in the pH dependence since the $pH_{0.5}$ of the two mutants (H162A, $pH_{0.5}$ = 4.71; H339A, $pH_{0.5}$ = 4.74) was not significantly modified compared with the wild-type channel ($pH_{0.5}$ = 4.72) (Table I).

Effect of Zn^{2+} on Heteromeric ASIC Currents Involving Mutated ASIC2a Subunits—We coexpressed wild type ASIC2a or H162A and H339A mutants with ASIC1a. The pH sensitivity of the ASIC1a+2a heteromeric currents was similar whether the ASIC2a subunit was mutated or not (Fig. 6*B*). Surprisingly, the ASIC1a+ASIC2a H162A current remained highly sensitive to zinc, whereas the ASIC1a+ASIC2a H339A current was practically insensitive (Fig. 6*A*). Even if the pH dependence found for the heteromeric ASIC1a+ASIC2a H339A current ($pH_{0.5}$ = 5.7, Fig. 6*B*) was intermediate between that of homomeric ASIC1a ($pH_{0.5}$ = 6.4) and ASIC2a ($pH_{0.5}$ = 4.7), this did not completely exclude a mixture of the two different homomeric currents. To confirm the heteromeric association of the ASIC1a and ASIC2a H339A subunits, we have used the G430V mutant of ASIC1a, which displays a low basal amiloride-sensitive current and is not activated by acidification (15). Co-expression of this mutant with ASIC2a H339A induced a proton-activated current with a $pH_{0.5}$ significantly different from that of the ASIC2a H339A channel alone, indicating that a heteromultimeric channel was indeed formed by association of both subunits (Fig. 6*C*). This confirmed that the ASIC2a H339A mutation was responsible for the lack of Zn^{2+} coactivation on the heteromeric channel formed with ASIC1a.

We coexpressed wild type or H162A and H339A mutants of ASIC2a with ASIC3. The pH sensitivity of the heteromeric ASIC2a+3 current was similar whether the ASIC2a subunit was mutated or not (Fig. 6*E*). When coexpressed with ASIC3, the H162A and the H339A mutated forms of ASIC2a decreased the effect of Zn^{2+} on both transient and sustained current. The decrease in zinc effect was more pronounced for the H339A mutation than for the H162A mutation (Fig. 6*D*), as observed previously with the ASIC1a+2a current.

Involvement of Extracellular Histidines in the Activation of ASIC2a by Protons—The ASIC2a H72A mutant is not activated by increasing the external H^+ concentration (Table I). This can reflect a loss of the capability of the channel to sense extracellular pH. However, this could also be due to a disrup-

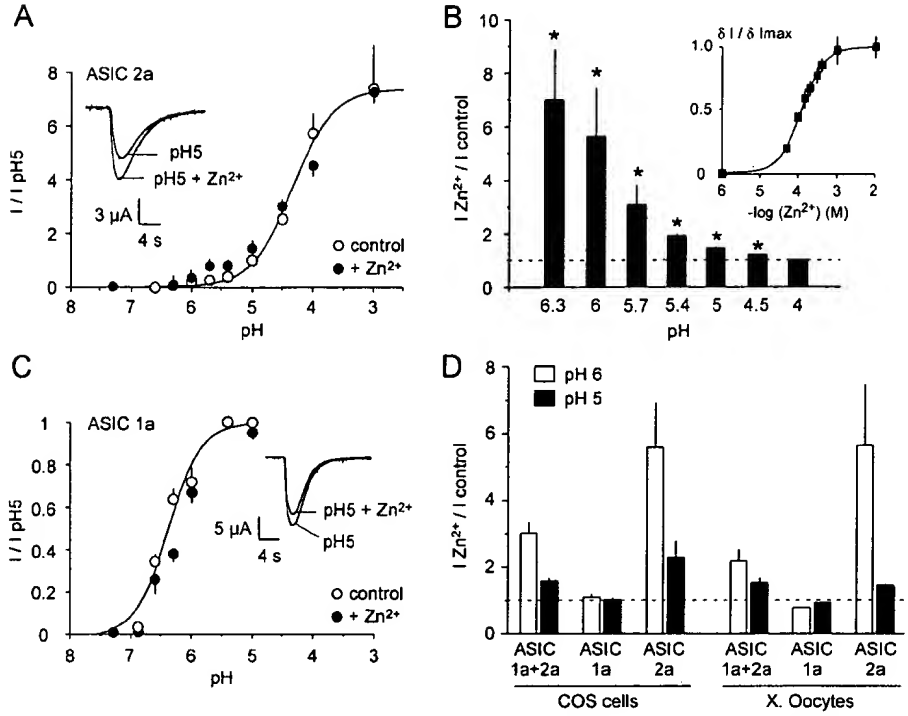

FIG. 3. **Effects of Zn^{2+} on homomeric ASIC1a and ASIC2a currents.** *A*, effect of Zn^{2+} on the pH-dependent activation of the ASIC2a current expressed in *Xenopus* oocytes. Current amplitude was expressed as a fraction of the current induced by pH 5 ($I/I_{pH\ 5}$), and plotted as mean ± S.E. (n = 3–22). The control curve (○) showed a half-maximal activation at $pH_{0.5}$ = 4.34 and a Hill coefficient of 1.3. Zn^{2+} 300 µM (●) increased the amplitude of ASIC2a currents activated by pH values under the $pH_{0.5}$ value. *Inset*, current traces showing the effect of Zn^{2+} on ASIC2a current activated at pH 5. Holding potential, −70 mV. *B*, relative effect of Zn^{2+} on ASIC2a current expressed in *Xenopus* oocytes for each pH value. The ratio between the current amplitude in presence and in absence of Zn^{2+} 300 µM ($I_{Zn}{}^{2+}/I_{control}$) was plotted as mean ± S.E. (n = 3–22). *, significantly different from the pH 4 ratio ($p < 0.005$). *Inset*, dose-response curve of Zn^{2+} potentiation of ASIC2a current. Currents were activated by pH 5.7 in absence and presence of Zn^{2+} concentrations ranging from 1 µM to 10 mM. The current amplitude increase was normalized to its maximal value ($\delta I/\delta I_{max}$) and plotted as mean ± S.E. as a function of Zn^{2+} concentration (n = 8–12). The calculated Hill coefficient is 1.44. *C*, effect of Zn^{2+} on the pH-dependent activation of the ASIC1a current expressed in *Xenopus* oocytes. Current amplitude was expressed as a fraction of the current induced by pH 5 ($I/I_{pH\ 5}$), and plotted as mean ± S.E. (n = 3–9). The control activation curve (○) showed a half-maximal activation at $pH_{0.5}$ = 6.37 and a Hill slope factor of 1.64. Zn^{2+} at 300 µM (●) did not increase ASIC1a current. *Inset*, current traces showing ASIC1a currents activated at pH 5 in absence and presence of Zn^{2+}. Holding potential, −70 mV. *D*, relative effect of Zn^{2+} on ASIC1a+2a, ASIC1a, and ASIC2a currents activated at pH 6 (*white bars*) and pH 5 (*black bars*), expressed in COS cells (*left*) or *Xenopus* oocytes (*right*). The ratio between the current amplitude in presence and in absence of Zn^{2+} 300 µM ($I_{Zn}{}^{2+}/I_{control}$) was calculated for each pH value and plotted as mean ± S.E. (n = 4–22).

tion of the necessary association with other subunits to form a homomeric channel. Analysis of the pH sensor of ASICs is complicated by the absence of other modes of activation, such as capsaicin and/or temperature for the VR1 channel (42). To analyze in more detail the effect of the H72A mutation on the ASIC2a properties, we have used a previously described gain-of-function mutant of ASIC2a that displays a medium to high amiloride-sensitive basal current and retains the property to be activated by external protons (5, 6). This mutant corresponds to the change of one amino acid, Gly-430, located in a region preceding the second transmembrane domain of ASIC2a. This residue plays a key role in the gating of the channel (6, 43). The G430T mutant has a large basal current and a $pH_{0.5}$ of 6.6 for protons activation (Fig. 7*B* and Ref. 6). The H72A mutation has been introduced in this mutant, and the properties of the double mutant have been analyzed. Interestingly, the double mutant was functional (Fig. 7*A*), demonstrating that the H72A mutation is not a loss-of-function mutation and that subunit association was not disrupted. Like the single gain-of-function mutant (6), the double mutant showed a large constitutive current, which remained activated by low pH with no apparent inactivation (Fig. 7*A*), but the pH dependence was largely modified, shifted toward more acidic pH by almost 2 orders of magnitude ($pH_{0.5}$ = 4.9; Fig. 7*B*). This drastic modification of the pH sensitivity of ASIC2a by the H72A mutation could explain the lack of activation of the single H72A mutant

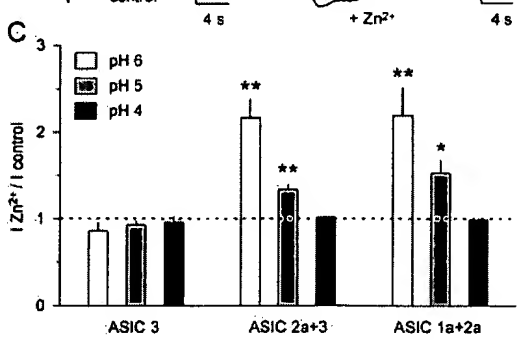

FIG. 4. **Effects of Zn^{2+} on homomeric ASIC3 and heteromeric ASIC2a+3 currents expressed in *Xenopus* oocytes.** Current traces showing the effect of Zn^{2+} (300 µM) on ASIC3 (*A*) and ASIC2a+3 (*B*) current activated by pH 5 and recorded at −70 mV. *C*, relative effect of Zn^{2+} on ASIC 3, ASIC2a+3, and ASIC1a+2a currents activated at pH 6 (*white bars*), pH 5 (*gray bars*), and pH 4 (*black bars*). The ratio between the current amplitude in presence and in absence of Zn^{2+} 300 µM ($I_{Zn}{}^{2+}/I_{control}$) was calculated for each pH value and plotted as mean ± S.E. (n = 5–10). *, $p < 0.05$; **, $p < 0.005$, significantly different from pH 4 ratio.

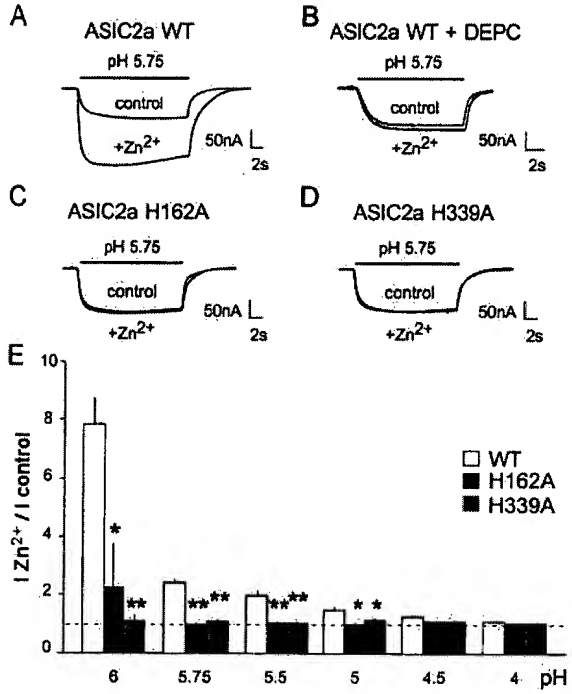

FIG. 5. **Alanine substitution of His-162 and His-339 in ASIC2a abolished the effect of Zn^{2+} on homomeric ASIC2a current.** *A*, Zn^{2+} (300 μM) increases the amplitude of homomeric ASIC2a current activated by pH 5.75. *B*, effect of Zn^{2+} is suppressed after application of 0.6 mM diethylpyrocarbonate (DEPC) for 10 min, suggesting an involvement of histidine residues in this effect. H162A (*C*) and H339A (*D*) mutations abolish the Zn^{2+} coactivation of ASIC2a current. *E*, effect of Zn^{2+} on the activity of WT, H162A, and H339A ASIC2a currents stimulated by pH ranging from 6 to 4. The Zn^{2+} effect is expressed as the ratio between the current amplitude in presence and in absence of Zn^{2+} 300 μM ($I_{Zn}{}^{2+}/I_{control}$) calculated from current traces as in *A–D*. Data are shown as mean ± S.E. (n = 4–15). *, $p < 0.05$; **, $p < 0.005$, significantly different from wild type channel. Holding potential for *A–E*, −70 mV.

TABLE I

Alanine substitution of ASIC2a extracellular histidines and effect on zinc coactivation activity

Schematic representation of the ASIC2a subunit showing the mutated histidines in the extracellular loop and the two membrane-associated domains (M1 and M2) is shown on the left. The pH for half-maximal activation ($pH_{0.5}$) and the effect of co-application of Zn^{2+} with acidic pH (pH 5.5) calculated as the ratio between the current amplitude in presence and in absence of 300 μM Zn^{2+} ($I_{Zn}{}^{2+}/I_{Ctr}$) were determined for each mutant at a holding potential of −70 mV. Means ± S.E. are shown (n = 3–10). **, $p < 0.005$, significantly different from wild type ASIC2a (unpaired t test). NA, nonactivated by acidic pH.

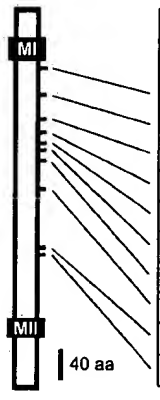

Mutant	$pH_{0.5}$	I Zn^{2+}/I Ctr (pH5.5)	
WT	4.72 ± 0.12	1.98 ± 0.04	
H72A	NA	NA	
H109A	4.72 ± 0.32	1.63 ± 0.14	
H127A	4.96 ± 0.40	1.43 ± 0.07	
H145A	4.51 ± 0.29	1.76 ± 0.27	
H158A	4.52 ± 0.34	1.48 ± 0.13	
H162A	4.71 ± 0.18	1.07 ± 0.05	**
H180A	4.48 ± 0.11	2.00 ± 0.19	
H249A	4.43 ± 0.24	1.74 ± 0.15	
H326A	4.90 ± 0.31	1.44 ± 0.03	
H339A	4.74 ± 0.19	1.05 ± 0.06	**

because shifting the $pH_{0.5}$ of the wild-type ASIC2a channel ($pH_{0.5}$ = 4.7) to more acidic values by several pH units would lead to a channel virtually insensitive to proton activation.

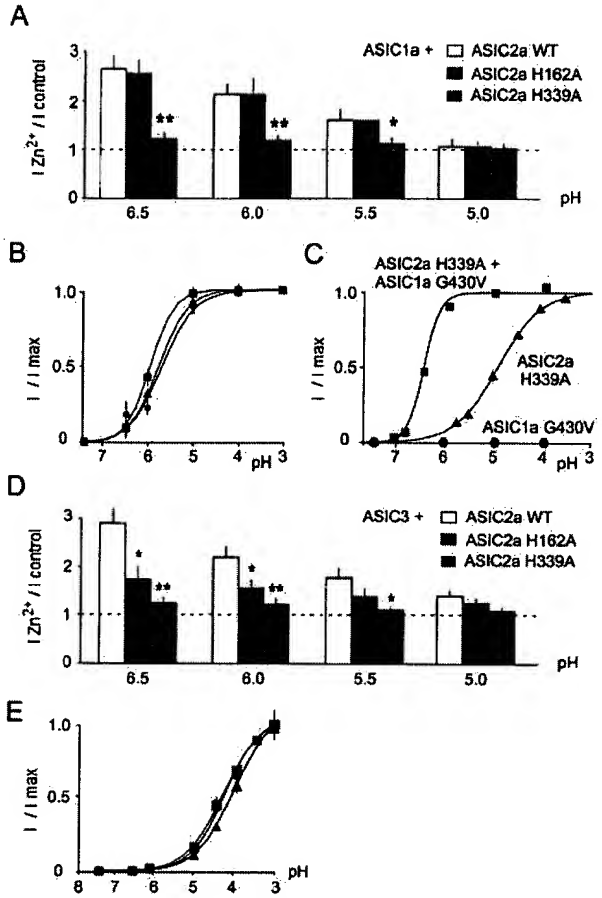

FIG. 6. **Effect of ASIC2a H162A and H332A mutations on the Zn^{2+} coactivation of heteromeric ASIC1a+2a and ASIC2a+3 channels.** *A*, Zn^{2+} effect on heteromeric channels containing ASIC1a and the mentioned ASIC2a subunit at different pH. Representation and experimental procedures are the same as in Fig. 5*E*. Data correspond to mean ± S.E. (n = 7–11). *, $p < 0.05$; **, $p < 0.005$, significantly different from WT channel (unpaired t test). *B*, pH dependence of heteromeric channels containing WT or mutated ASIC2a subunits. The $pH_{0.5}$ of channels containing WT (●), H162A (■), and H339A (▲) ASIC2a subunits are 5.8, 6.0, and 5.7, respectively. Current amplitude was expressed as a fraction of the current induced by pH 3.0 (I/I_{max}). Each *point* corresponds to mean ± S.E. of 8–12 oocytes. *C*, pH dependence of homomeric ASIC2a H339A (▲), ASIC1a G430V (●), and heteromeric ASIC2a H339A+ASIC1a G430V (■) channels was established. Each *point* represents the mean ± S.E. of 8–12 oocytes. Currents were recorded at a holding potential of −70 mV. The ASIC1a G430V mutant is not activated by increasing the H^+ concentration, as described previously (15). The $pH_{0.5}$ of the heteromeric channel is largely shifted toward more alkaline pH compared with the ASIC2a H339A mutant alone, demonstrating an association of this mutant with ASIC1a. *D*, Zn^{2+} effect on heteromeric channels containing ASIC3 and the mentioned ASIC2a subunit at different pH. Data correspond to mean ± S.E. (n = 6–14). *, $p < 0.05$; **, $p < 0.005$, significantly different from WT channel (unpaired t test). *E*, the H162A and H339A mutations in ASIC2a were without effect on the pH dependence of the ASIC2a+3 peak current. $pH_{0.5}$ values were, respectively, 4.3, 4.1, and 4.3 for channels containing WT (■), H162A (▲), and H339A (●) ASIC2a subunits. Each *point* corresponds to mean ± S.E. of 6–9 oocytes. Current amplitude was expressed as a fraction of the current induced by pH 3 (I/I_{max}). Holding potential for *A–E*, −70 mV.

DISCUSSION

Coactivation of ASIC Currents by Zn^{2+}—Zn^{2+} is known to exert a variety of inhibitory effects on ion channels, but stimulatory effects are rare. For instance, potentiation by Zn^{2+} has been described for the activation of purinergic $P2X_2$, $P2X_3$, and $P2X_4$ channels by ATP (44–46).

We show that both homomeric ASIC2a channels and heteromeric ASIC2a-containing channels are potentiated when Zn^{2+}

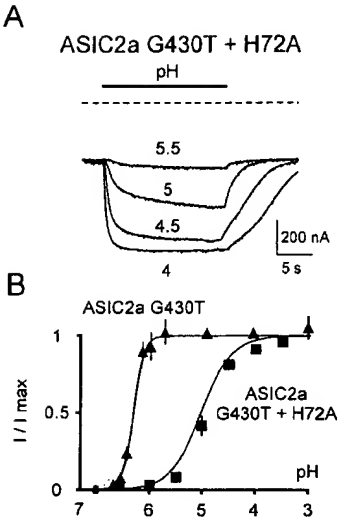

FIG. 7. **The H72A mutation modifies the pH dependence of homomeric ASIC2a current.** *A*, the G430T mutation is associated with a basal amiloride-sensitive current (5), but the mutated channel is still activated by acidic pH with modified pH sensitivity compared with wild-type channel (6). Introduction of the H72A mutation in the G430T ASIC2a mutant does not eliminate the basal activity and the activation by acidic pH. The H72A mutation is therefore not loss-of-function, but it drastically alters the pH dependence of ASIC2a. The *bar* above the current recordings represents the pH pulse, value being indicated for each trace. The zero current base line is indicated by a *dotted line*. *B*, effect of the ASIC2a H72A mutation on the pH dependence of the ASIC2a G430T gain-of-function current. The $pH_{0.5}$ of the G430T mutant is 6.6 (▲). The double mutant H72A+G430T has a $pH_{0.5}$ of 4.9 (■), although the H72A simple mutant is not activated by pH down to pH 3.0. Current amplitude was expressed as a fraction of the current induced by pH 3.0 (I/I_{max}). Each *point* represents the mean ± S.E. of 5–8 oocytes. Holding potential for *A* and *B*, −70 mV.

is coapplied with acidic pH. Zn^{2+} alone could not activate the ASIC1a+2a current, in good agreement with the results obtained by Adams *et al.* (47) on ASIC2a current. The potentiating effect of Zn^{2+} on either homomeric or heteromeric ASIC2a-containing channels only appeared between pH 6.9 and pH 5, independent of the pH dependence of the current, suggesting the involvement of titrable residues that would less efficiently chelate Zn^{2+} as pH decreases.

Physiological Significance of ASIC Current Coactivation by Zn^{2+}—The Zn^{2+} concentrations that potentiate the ASIC2a-containing channels (EC_{50} = 111 μM for ASIC1a+2a current and EC_{50} = 120 μM for ASIC2a) are compatible with the physiological concentration of synaptically released Zn^{2+} (100–300 μM) (31–35). Our results suggest that ASICs might be a physiological target for Zn^{2+}. Some ASICs that are expressed in the CNS (*e.g.* ASIC1a+2a, $pH_{0.5}$ = 5.5, Fig. 2*A*) require rather acidic pH for activation. The coactivation by Zn^{2+} shifts the pH dependence of the ASIC1a+2a channel closer to physiological pH values and strongly augments the activity of the heteromeric ASIC1a+2a and the homomeric ASIC2a channel at pH values just below neutral. The native ASIC-like current of rat primary cultured hippocampal neurons are indeed also coactivated by Zn^{2+} (data not shown).[2] The potentiation by Zn^{2+} of the hippocampal ASIC current could participate in the modulation of neuronal excitability by increasing the membrane depolarization induced by small pH changes.

Extracellular Histidines of ASIC2a Are Involved in Zn^{2+} Effect—The effect of zinc is immediate and does not necessitate any pre-application, suggesting a direct interaction with a zinc-binding site located in the extracellular domain of the channel. The side chain of histidine has been involved in the zinc-binding sites of numerous metalloproteins (40). Alanine substitution of each of the 10 histidine residues present in the extracellular loop of ASIC2a demonstrates that His-162 and His-339 are involved in the Zn^{2+} effect. Replacement of His-162 or His-339 completely abolished the sensitivity of ASIC2a to 300 μM Zn^{2+}. The simplest interpretation of our results is that His-162 and His-339 are part of the Zn^{2+} binding site on ASIC2a. However, it should be kept in mind that the mutagenesis alone does not provide a definite demonstration of such direct participation. All ASICs containing the ASIC2a subunit, *i.e.* homomeric ASIC2a and heteromeric ASIC1a+2a or ASIC2a+3, are sensitive to Zn^{2+}. The data presented here using co-expression of mutated ASIC2a subunits with ASIC1a or ASIC3 definitely demonstrate that Zn^{2+} sensitivity in heteromeric channels is carried by the ASIC2a subunit. A comparison between sequences of ASIC1a, ASIC2a, and ASIC3 shows that, although His-162 is highly conserved in all these subunits, His-339 is specific of ASIC2a (Fig. 8). Because ASIC2a is the main subunit responsible for the Zn^{2+} sensitivity of ASICs, it is then tempting to assign to His-339 a predominant role in this property. However, the selective replacement of His-162 by alanine can also completely abolish the Zn^{2+} sensitivity of the homomeric ASIC2a channel, whereas it has moderate or no effect on heteromeric channels. This could reflect some difference between the Zn^{2+} binding sites of homomeric and heteromeric channels comprising the ASIC2a subunit.

FIG. 8. **Alignments of rat acid-sensing ion channels in the regions surrounding the histidine residues important for Zn^{2+} regulation and pH sensing.** *Asterisks* indicate the position of His-72, His-162, and His-339 in ASIC2a. Identical and similar residues are printed *white* on *black/dark gray* and *black* on *gray*, respectively. The Clustal program was used to generate the alignments. Accession numbers for rat ASIC1a, ASIC2a, and ASIC3 are U94403, U53211, and AF013598, respectively.

His-72 Is Involved in the pH Sensor of ASIC2a—Titrable histidine residues are major determinants of pH modulation in many ion channels (48, 49), whereas glutamate residues have also been shown to be important for acid sensing as for the capsaicin receptor VR1 (42). The His-72 residue adjacent to the first transmembrane domain of ASIC2a (Table I) drastically changes its pH sensitivity since the ASIC2a H72A channel has become insensitive to acidic pH. However, it is not the unique determinant of the pH sensitivity because the ASIC2a G430T+H72A double mutant remains activable by low pH (Fig. 7). Other positions have been shown previously to be involved in the pH dependence of ASIC2a like the Gly-430 residue situated just before the second transmembrane segment (6) and the region preceding the first transmembrane domain (50). The His-72 residue of ASIC2a is conserved in ASIC1a and ASIC3 (Fig. 8). These positions have been mutated in both ASIC1a and ASIC3, but in that case no modification of the pH dependence of the mutant channels was observed, with $pH_{0.5}$ = 6.5 and 6.1 for the ASIC1a H73A and ASIC3 H73A peak currents, respectively, compared with $pH_{0.5}$ values of 6.4 for ASIC1a and 6.3 for ASIC3 (data not shown). There is a precedent for such a situation with two-P domain K^+ channels (48, 51); His-98 has been shown to be important for the pH dependence of TASK-3 near physiological pH, but TWIK-1, which also contains a histidine residue at the equivalent position, does not display a pH dependence in the same pH range.

In summary, the present study has revealed interesting structural features of acid-sensing ion channels, with special

[2] A. Baron, R. Waldmann, and M. Lazdunski, manuscript in preparation.

emphasis on ASIC2a, which is coactivated both by external Zn^{2+} and extracellular acidification. Several histidines have been identified as candidate electron donors to the Zn^{2+} coordination site, and another histidine residue is a candidate for the pH sensor. However, there are clearly other residues directly or indirectly involved in pH sensing that will also need to be identified.

Acknowledgments—We thank M. Jodar, N. Leroudier, and V. Friend for excellent technical assistance and V. Lopez for secretarial assistance. We thank N. Voilley and J. Mamet for helpful comments. We are particularly grateful to Dr. R. Waldmann for the ASIC clones and for the important role he played at the beginning of this work.

REFERENCES

1. Waldmann, R., Champigny, G., Bassilana, F., Heurteaux, C., and Lazdunski, M. (1997) *Nature* **386,** 173–177
2. Chen, C. C., England, S., Akopian, A. N., and Wood, J. N. (1998) *Proc. Natl. Acad. Sci. U. S. A.* **95,** 10240–10245
3. Garcia-Anoveros, J., Derfler, B., Neville-Golden, J., Hyman, B. T., and Corey, D. P. (1997) *Proc. Natl. Acad. Sci. U. S. A.* **94,** 1459–1464
4. Price, M. P., Snyder, P. M., and Welsh, M. J. (1996) *J. Biol. Chem.* **271,** 7879–7882
5. Waldmann, R., Champigny, G., Voilley, N., Lauritzen, I., and Lazdunski, M. (1996) *J. Biol. Chem.* **271,** 10433–10436
6. Champigny, G., Voilley, N., Waldmann, R., and Lazdunski, M. (1998) *J. Biol. Chem.* **273,** 15418–15422
7. Lingueglia, E., de Weille, J. R., Bassilana, F., Heurteaux, C., Sakai, H., Waldmann, R., and Lazdunski, M. (1997) *J. Biol. Chem.* **272,** 29778–29783
8. Babinski, K., Le, K. T., and Seguela, P. (1999) *J. Neurochem.* **72,** 51–57
9. de Weille, J. R., Bassilana, F., Lazdunski, M., and Waldmann, R. (1998) *FEBS Lett.* **433,** 257–260
10. Waldmann, R., Bassilana, F., de Weille, J., Champigny, G., Heurteaux, C., and Lazdunski, M. (1997) *J. Biol. Chem.* **272,** 20975–20978
11. Akopian, A. N., Chen, C. C., Ding, Y., Cesare, P., and Wood, J. N. (2000) *Neuroreport* **11,** 2217–2222
12. Grunder, S., Geissler, H. S., Bassler, E. L., and Ruppersberg, J. P. (2000) *Neuroreport* **11,** 1607–1611
13. Coscoy, S., Lingueglia, E., Lazdunski, M., and Barbry, P. (1998) *J. Biol. Chem.* **273,** 8317–8322
14. Waldmann, R., Champigny, G., Lingueglia, E., De Weille, J. R., Heurteaux, C., and Lazdunski, M. (1999) *Ann. N. Y. Acad. Sci.* **868,** 67–76
15. Bassilana, F., Champigny, G., Waldmann, R., de Weille, J. R., Heurteaux, C., and Lazdunski, M. (1997) *J. Biol. Chem.* **272,** 28819–28822
16. Waldmann, R., and Lazdunski, M. (1998) *Curr. Opin. Neurobiol.* **8,** 418–424
17. Babinski, K., Catarsi, S., Biagini, G., and Seguela, P. (2000) *J. Biol. Chem.* **275,** 28519–28525
18. Pan, H. L., Longhurst, J. C., Eisenach, J. C., and Chen, S. R. (1999) *J. Physiol. (Lond.)* **518,** 857–866
19. Kress, M., and Zeilhofer, H. U. (1999) *Trends Pharmacol. Sci.* **20,** 112–118
20. Olson, T. H., Riedl, M. S., Vulchanova, L., Ortiz-Gonzalez, X. R., and Elde, R. (1998) *Neuroreport* **9,** 1109–1113
21. Benson, C. J., Eckert, S. P., and McCleskey, E. W. (1999) *Circ. Res.* **84,** 921–928
22. Sutherland, S. P., Benson, C. J., Adelman, J. P., and McCleskey, E. W. (2000) *Proc. Natl. Acad. Sci. U. S. A.* **98,** 711–716
23. Sutherland, S. P., Cook, S. P., and McCleskey, E. W. (2000) *Prog. Brain Res.* **129,** 21–38
24. Reeh, P. W., and Steen, K. H. (1996) *Prog. Brain Res.* **113,** 143–151
25. Garcia-Anoveros, J., Samad, T. A., Woolf, C. J., and Corey, D. P. (2001) *J. Neurosci.* **21,** 2678–2686
26. Price, M. P., Lewin, G. R., McIlwrath, S. L., Cheng, C., Xie, J., Heppenstall, P. A., Stucky, C. L., Mannsfeldt, A. G., Brennan, T. J., Drummond, H. A., Qiao, J., Benson, C. J., Tarr, D. E., Hrstka, R. F., Yang, B., Williamson, R. A., and Welsh, M. J. (2000) *Nature* **407,** 1007–1011
27. Krishtal, O. A., Osipchuk, Y. V., Shelest, T. N., and Smirnoff, S. V. (1987) *Brain Res.* **436,** 352–356
28. Chesler, M., and Kaila, K. (1992) *Trends Neurosci.* **15,** 396–402
29. Slomianka, L. (1992) *Neuroscience* **48,** 325–352
30. Frederickson, C. J. (1989) *Int. Rev. Neurobiol.* **31,** 145–238
31. Budde, T., Minta, A., White, J. A., and Kay, A. R. (1997) *Neuroscience* **79,** 347–358
32. Assaf, S. Y., and Chung, S. H. (1984) *Nature* **308,** 734–736
33. Howell, G. A., Welch, M. G., and Frederickson, C. J. (1984) *Nature* **308,** 736–738
34. Weiss, J. H., Sensi, S. L., and Koh, J. Y. (2000) *Trends Pharmacol. Sci.* **21,** 395–401
35. Smart, T. G., Xie, X., and Krishek, B. J. (1994) *Prog. Neurobiol.* **42,** 393–341
36. Vogt, K., Mellor, J., Tong, G., and Nicoll, R. (2000) *Neuron* **26,** 187–196
37. Harrison, N. L., and Gibbons, S. J. (1994) *Neuropharmacology* **33,** 935–952
38. Hamill, O. P., Marty, A., Neher, E., Sakmann, B., and Sigworth, F. J. (1981) *Pflugers Arch.* **391,** 85–100
39. Horton, R. M., Ho, S. N., Pullen, J. K., Hunt, H. D., Cai, Z., and Pease, L. R. (1993) *Methods Enzymol.* **217,** 270–279
40. Berg, J. M., and Shi, Y. (1996) *Science* **271,** 1081–1085
41. Miles, E. W. (1977) *Methods Enzymol.* **47,** 431–442
42. Jordt, S. E., Tominaga, M., and Julius, D. (2000) *Proc. Natl. Acad. Sci. U. S. A.* **97,** 8134–8139
43. Adams, C. M., Snyder, P. M., Price, M. P., and Welsh, M. J. (1998) *J. Biol. Chem.* **273,** 30204–30207
44. Wildman, S. S., King, B. F., and Burnstock, G. (1998) *Br. J. Pharmacol.* **123,** 1214–1220
45. Wildman, S. S., King, B. F., and Burnstock, G. (1999) *Br. J. Pharmacol.* **128,** 486–492
46. Wildman, S. S., King, B. F., and Burnstock, G. (1999) *Br. J. Pharmacol.* **126,** 762–768
47. Adams, C. M., Snyder, P. M., and Welsh, M. J. (1999) *J. Biol. Chem.* **274,** 15500–15504
48. Rajan, S., Wischmeyer, E., Xin Liu, G., Preisig-Muller, R., Daut, J., Karschin, A., and Derst, C. (2000) *J. Biol. Chem.* **275,** 16650–16657
49. Clarke, C. E., Benham, C. D., Bridges, A., George, A. R., and Meadows, H. J. (2000) *J. Physiol. (Lond.)* **523,** 697–703
50. Coscoy, S., de Weille, J. R., Lingueglia, E., and Lazdunski, M. (1999) *J. Biol. Chem.* **274,** 10129–10132
51. Kim, Y., Bang, H., and Kim, D. (2000) *J. Biol. Chem.* **275,** 9340–9347

THE JOURNAL OF BIOLOGICAL CHEMISTRY
Vol. 275, No. 33, Issue of August 18, pp. 25116–25121, 2000
Printed in U.S.A.

Isolation of a Tarantula Toxin Specific for a Class of Proton-gated Na^+ Channels*

Received for publication, April 28, 2000, and in revised form, May 16, 2000
Published, JBC Papers in Press, May 26, 2000, DOI 10.1074/jbc.M003643200

Pierre Escoubas‡, Jan R. De Weille‡, Alain Lecoq§, Sylvie Diochot‡, Rainer Waldmann‡, Guy Champigny‡, Danielle Moinier‡, André Ménez§, and Michel Lazdunski‡¶**

*From the ‡Institut de Pharmacologie Moléculaire et Cellulaire, Centre National de la Recherche Scientifique, 660 route des Lucioles, Sophia-Antipolis, 06560 Valbonne, France, **the Université Pierre et Marie Curie, Paris 75006, France, and the §Département d'Ingéniérie des protéines, CEA, Saclay 91130, France*

Acid sensing is associated with nociception, taste transduction, and perception of extracellular pH fluctuations in the brain. Acid sensing is carried out by the simplest class of ligand-gated channels, the family of H^+-gated Na^+ channels. These channels have recently been cloned and belong to the acid-sensitive ion channel (ASIC) family. Toxins from animal venoms have been essential for studies of voltage-sensitive and ligand-gated ion channels. This paper describes a novel 40-amino acid toxin from tarantula venom, which potently blocks (IC_{50} = 0.9 nM) a particular subclass of ASIC channels that are highly expressed in both central nervous system neurons and sensory neurons from dorsal root ganglia. This channel type has properties identical to those described for the homomultimeric assembly of ASIC1a. Homomultimeric assemblies of other members of the ASIC family and heteromultimeric assemblies of ASIC1a with other ASIC subunits are insensitive to the toxin. The new toxin is the first high affinity and highly selective pharmacological agent for this novel class of ionic channels. It will be important for future studies of their physiological and physio-pathological roles.

Proton-gated Na^+-permeable channels are the simplest form of ligand-gated channels. They are present in many neuronal cell types throughout the central nervous system (1–5), suggesting an important function of these channels in signal transduction associated with local pH variations during normal neuronal activity. These channels might also play an important role in pathological situations such as brain ischemia or epilepsy, which produce significant extracellular acidification. They are also present in nociceptive neurons (1–3, 5, 6) and are thought to be responsible for the sensation of pain that accompanies tissue acidosis in muscle and cardiac ischemia (7, 8), corneal injury (9), and inflammation and local infection (10, 11). It is only very recently that the first proton-gated channel, acid-sensitive ion channel (ASIC)[1] was cloned (12). The ASICs belong to a superfamily that includes amiloride-sensitive epithelial Na^+ channels (13, 14), the FMRFamide-gated Na^+ channel (15), and the nematode degenerins (DEGs), which probably correspond to mechano-sensitive Na^+-permeable channels (16). Several ASIC subunits have now been described: ASIC1a (12), ASIC1b (17), ASIC2a (18–21), ASIC2b (22), and ASIC3 (23–25). The different subunits produce channels with different kinetics, external pH sensitivities, and tissue distribution. They can form functional homomultimers as well as heteromultimers (21, 22, 26). ASIC1a and ASIC1b both mediate rapidly inactivating currents following rapid and modest acidification of the external pH. However, although ASIC1a is present in both brain and afferent sensory neurons, its splice variant ASIC1b is found only in sensory neurons (17). ASIC2a forms an active H^+-gated channel and is abundant in the brain but essentially absent in sensory neurons, whereas its splice variant ASIC2b is present in both brain and sensory neurons and is inactive as an homomultimer. ASIC2b can form functional heteromultimers with other ASIC subunits and particularly ASIC3 (21). ASIC3 is found exclusively in small sensory neurons that act as nociceptors. Its expression in various heteromultimeric systems generates a biphasic current with a fast inactivating phase followed by a sustained component (22). The association of ASIC2b with ASIC3 forms an heteromultimer with properties (time course and ionic selectivity) similar to those of a native sustained H^+-sensitive channel, which is present in dorsal root ganglion cells and appears to play a particularly important role in pain sensation (6).

Venoms from snakes, scorpions, sea anemones, marine snails, and spiders are rich sources of peptide toxins that have proven of great value in the functional exploration of voltage-sensitive and ligand-gated ion channels. This report describes the discovery and characterization from the venom of the South American tarantula *Psalmopoeus cambridgei*, of psalmotoxin 1 (PcTX1), the first potent and specific blocker of this new class of ASIC channels.

EXPERIMENTAL PROCEDURES

Venom and Toxin Purification—P. cambridgei (Araneae Theraphosidae) venom was obtained by electrical stimulation of anesthetized spiders (Invertebrate Biologics). Freeze-dried crude venom was resuspended in distilled water, centrifuged (14,000 rpm, 4 °C, 20 min), filtered on 0.45-μm microfilters (SJHVL04NS, 4-mm diameter; Millipore), and stored at −20 °C prior to analysis. Crude venom diluted to 10 times the initial volume was fractionated by C8 reversed-phase high pressure liquid chromatography (RP-HPLC) (10 × 250 mm, 5C8MS; Nacalai Tesque) using a linear gradient of acetonitrile/water in constant 0.1% trifluoroacetic acid. A second purification step used cation exchange chromatography on a Tosoh SP5PW column (4.6 × 70 mm) (Tosoh), with a linear gradient of ammonium acetate in water (20 mM to 2 M). A total of 160 μl of venom was purified in two separate batches (10 and 150 μl). All solvents used were of HPLC grade. Separation was conducted on a Hewlett-Packard HP1100 system coupled to a diode array detector and a microcomputer running the Chemstation® software.

* This work was supported by the Center National de la Recherche Scientifique and the Association Française contre les Myopathies. The costs of publication of this article were defrayed in part by the payment of page charges. This article must therefore be hereby marked "*advertisement*" in accordance with 18 U.S.C. Section 1734 solely to indicate this fact.

¶ To whom correspondence should be addressed. Tel.: 33-4-93-95-77-02; Fax: 33-4-93-95-77-04p; E-mail: ipmc@ipmc.cnrs.fr.

[1] The abbreviations used are: ASIC, acid-sensitive ion channel; PcTX1, psalmotoxin 1; RP, reversed-phase; HPLC, high pressure liquid chromatography; DRG, dorsal root ganglion; Fmoc, *N*-(9-fluorenyl)-methoxycarbonyl.

Monitoring of the elution was done at 215 and 280 nm.

Peptide Characterization—Samples were hydrolyzed in a Waters Pico-Tag station, with 6 N HCl (0.6% phenol) at 110 °C, under vacuum for 20 h. Hydrolyzed peptides were derivatized with phenylisothiocyanate, and the derivatized amino acid mixtures were analyzed by C18 RP-HPLC using a gradient of 60% acetonitrile in 50 mM phosphate buffer (100 mM $NaClO_4$). The peptide was reduced and alkylated by 4-vinyl-pyridine, desalted by C8 RP-HPLC, and submitted to automated N-terminal sequencing on an Applied Biosystems model 477A gas phase sequencer.

Reduced-alkylated toxin was submitted to the following treatments: (*a*) tosylphenylalanyl chloromethyl ketone-treated Trypsin (Sigma), 2% w/w at 37 °C for 14 h in 100 mM ammonium bicarbonate, 0.1 mM $CaCl_2$ pH 8.1; (*b*) V8 protease at 37 °C for 24 h in 50 mM ammonium bicarbonate, pH 7.8, in 10% acetonitrile; and (*c*) BNP-skatole (2-(nitrophenylsulfenyl)-3-methyl-3-bromoindolenine) at 37 °C for 24 h in 75% acetic acid. Resulting peptides were separated by RP-HPLC using a linear gradient of acetonitrile/water in constant 0.1% trifluoroacetic acid.

Mass spectra of native PcTX1 dissolved in α-cyano-4-hydroxycinnamic acid matrix were recorded on a MALDI-TOF Perseptive Voyager Elite spectrometer (Perseptive Biosystems), in positive ion linear mode using an internal calibration method with a mixture of β-insulin (3495.9 Da) and bovine insulin (5733.5 Da). Data were analyzed using the GRAMS386 software. Theoretical molecular masses and pI values were calculated from sequence data using the GPMAW protein analysis software. Synthetic PcTX1 was analyzed on a Micromass Platform II electrospray system (Micromass, Altrincham, UK), in positive mode (cone voltage 20kV, temperature 60 °C).

Sequence homologies were determined using sequences obtained from a search of nonredundant protein data bases *via* the BLAST server. Sequence alignments and percentages of similarity were calculated with ClustalW.

Peptide Synthesis and Refolding—The synthesis of native PcTX1 was performed using the Fmoc/*tert*-butyl and maximal temporary protection strategy on an Applied Biosystems 433A synthesizer. The chemical procedure used 0.05 nM of Fmoc-Thr(OtBu)-4-hydroxymethylphenoxy resin (0.39 mmol/g), a 20-fold excess of each amino acid, and dicyclohexylcarbodiimide/1-hydroxy-7-azabenzotriazole activation. Deprotection (1.5 h) and cleavage (200 mg of peptide + resin) were achieved using 10 ml of a mixture trifluoroacetic acid/triisopropylsilane/water (9.5/0.25/0.25, v/v/v). The acidic mixture was then precipitated twice in 100 ml of cold diethylether. The solid was dissolved in 50 ml of 10% aqueous acetic acid and freeze-dried. The crude reduced toxin was purified by RP-HPLC on a C18 semi-preparative column (21 × 250 mm, Jupiter) using a 40-min gradient of acetonitrile/water in 0.1% trifluoroacetic acid (0–18% B in 4 min, 30% B in 30 min, and 100% B in 6 min, where B is 90% acetonitrile/H_2O/0.1%trifluoroacetic acid).

Oxidation of the reduced toxin was achieved at 0.1 mg/10 ml in degassed potassium phosphate buffer (100 mM, pH 7.8) using the redox couple reduced glutathione (5 mM)/oxidized glutathione (0.5 mM). The disappearance of the reduced peptide was monitored by RP-HPLC on a C18 analytical column (10 × 15 mm, Vydac) using a 40-min gradient (0–18% B in 8 min, 30% B in 18 min, and 60% B in 14 min).

Expression in Xenopus Oocytes—Cloning of cDNA and synthesis of complementary RNA were done as described previously (26). *Xenopus laevis* were purchased from Centre de Recherches en Biochimie Macromoléculaire (Montpellier, France). Pieces of the ovary were surgically removed, and individual oocytes were dissected in a saline solution (ND96) containing 96 mM NaCl, 2 mM KCl, 1.8 mM $CaCl_2$, 2 mM $MgCl_2$, and 5 mM HEPES (pH 7.4 with NaOH). Stage V and VI oocytes were treated for 2 h with collagenase (1 mg/ml, type Ia; Sigma) in ND96 to remove follicular cells. cRNA (ASIC1a, ASIC2a, Kv2.1, and Kv2.2) or DNA (ASIC1b, ratASIC3, Kv4.2, and Kv4.3) solutions were injected (5–10 ng/μl for cRNA and 50–100 ng/μl for DNA, 50 nl/oocyte) using a pressure microinjector. The oocytes were kept at 19 °C in the ND96 saline solution supplemented with gentamycin (5 μg/ml). Oocytes were studied within 2–4 days following injection. In a 0.3-ml perfusion chamber, a single oocyte was impaled with two standard glass microelectrodes (1–2.5 MΩ resistance) filled with 3 M KCl and maintained under voltage clamp using a Dagan TEV 200 amplifier. Stimulation of the preparation, data acquisition, and analysis were performed using the pClamp software (Axon Instruments). All experiments were performed at room temperature (21–22 °C) in ND96. 0.1% bovine serum albumine was added in solutions containing PcTX1 to prevent its adsorption to tubing and containers. For measurements of ASIC currents, changes in extracellular pH were induced by rapid perfusion, with or without PcTX1, near the oocyte. Test solutions with a pH of 4 or 5 were buffered with MES rather than HEPES. Voltage-dependent K^+ channels were activated by depolarization tests to +10 mV from a holding potential of −80 mV, and the toxin solutions were applied externally by gently puffing 100 μl near the oocyte.

In the initial screening, 1-μl aliquots of crude venoms were tested at a 1:1000 dilution in ND96 solution. During the fractionation process aliquots (1:20) of chromatographic fractions were dried, redissolved in ND96, and applied to the oocyte by perfusion.

Expression in COS Cells—COS cells, at a density of 20.000 cells/35-mm diameter Petri dish, were transfected with a mix of CD8 and one of the following plasmids: pCI-ASIC1a, pCI-ASIC1b, pCI-ASIC2a, and pCI-ASIC3 (1:5) using the DEAE-Dextran method. Cells were used for electrophysiological measurements 1–3 days after transfection. Successfully transfected cells were recognized by their ability to fix CD8 antibody-coated beads (Dynal, Norway).

DRG Neurons Cultures and Cerebellar Granule Cell Cultures—DRG of 2–3-day-old Wistar rats were mechanically dissociated and maintained in culture in Eagle's medium supplemented with 100 ng/ml nerve growth factor. Cells were used for electrophysiological recordings 2 or 3 days after plating.

Cerebella of 4–8-day-old mice were dissected, mechanically dissociated, and cultured as described previously (27). Cells were used for electrophysiological recordings 10–14 days after plating.

Electrophysiology on COS Cells and Neurons—Ion currents were recorded using either the whole cell or outside-out patch clamp technique, and results were stored on hard disc. Data analysis was carried out using the Serf freeware. Statistical significance of differences between sets of data was estimated by the single-sided Student test. The pipette solution contained 140 mM KCl, 2 mM $MgCl_2$, 5 mM EGTA, and 10 mM HEPES (pH 7.2). The bath solution contained 140 mM NaCl, 5 mM KCl, 2 mM $MgCl_2$, 2 mM $CaCl_2$, and 10 mM HEPES (pH 7.3). Changes in extracellular pH were induced by shifting one of six outlets of a microperfusion system in front of the cell or patch. Experiments were carried out at room temperature (20–24 °C).

RESULTS

Purification—The screening of several tarantula venoms was carried out against cloned ASIC channels expressed in *Xenopus* oocytes. It singled out *P. cambridgei* venom as containing a potent inhibitor of the ASIC1a proton-gated current. A diluted solution of 1 μl of crude venom (1:1000) applied to the oocyte provoked a 90% block of the ASIC1a current. Bioassay-guided fractionation of the venom by reversed-phase and cation exchange chromatography led to the purification of the minor venom constituent Psalmotoxin 1 (PcTX1), in a two-step process (Fig. 1, *A* and *B*). PcTX1 is a 40-amino acid peptide, possessing 6 cysteines linked by three disulfide bridges. Its full sequence was established by N-terminal Edman degradation of the reduced alkylated toxin and of several cleavage fragments (Fig. 1*D*). The calculated molecular mass (4689.40 Da average) was in accordance with the measured molecular mass (4689.25 Da) and suggested a free carboxylic acid at the C-terminal extremity.

PcTX1 has limited overall homology to other spider venom toxins identified to date (Fig. 1*E*). However, it shares a conserved cysteine distribution (Fig. 1*F*) found both in spider venom and cone snails polypeptide toxins (28, 29). It is a basic polypeptide (pI 10.38 for the native form with disulfide bridges bonded) comprising a large number of basic residues (9 residues, including 4 arginines) but also of acidic residues (6 residues).

Synthesis—The chemical synthesis of PcTX1-OH unambiguously confirmed the structure of PcTX1. The purified refolded synthetic toxin (PcTX1 s) and the native form have identical measured molecular mass, and when co-injected in two separate experiments using reversed-phase and cation exchange HPLC, native and synthetic PcTX1 were indistinguishable in their migration and co-eluted in both systems (Fig. 1*C*). Most electrophysiological experiments were therefore conducted with the synthetic toxin.

Selective Block of ASIC1a—The effect of PcTX1 on the activity of ASIC1a, ASIC1b, ASIC2a, and ASIC3 channels expressed in *X. laevis* oocytes is shown in Fig. 2. The natural as well as

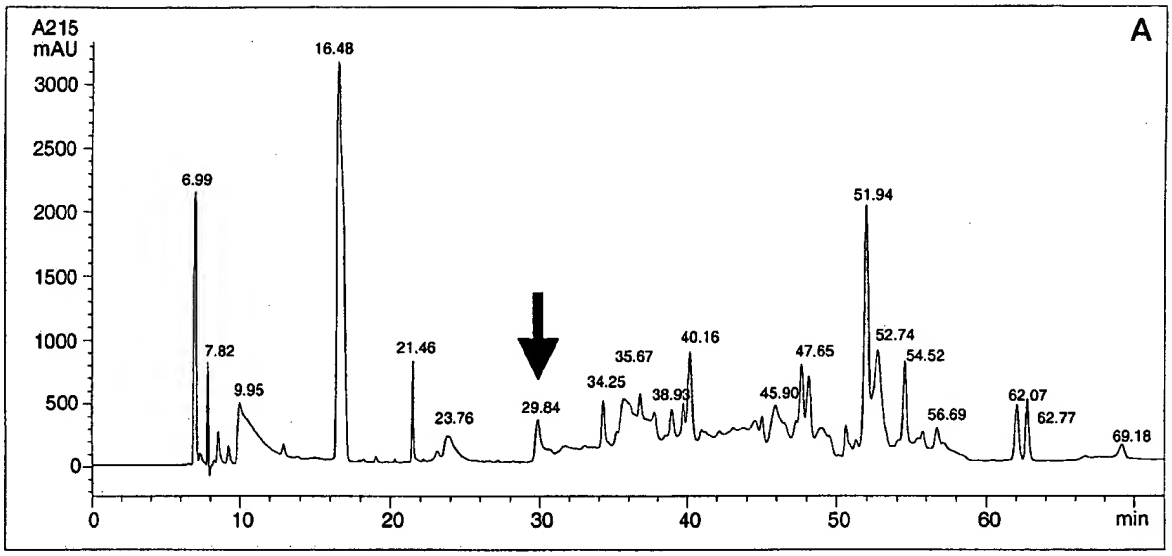

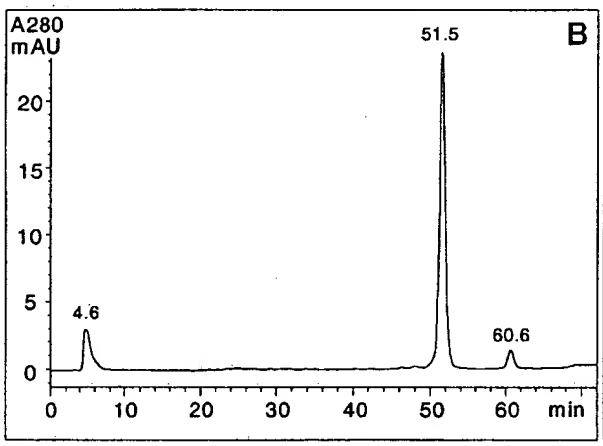

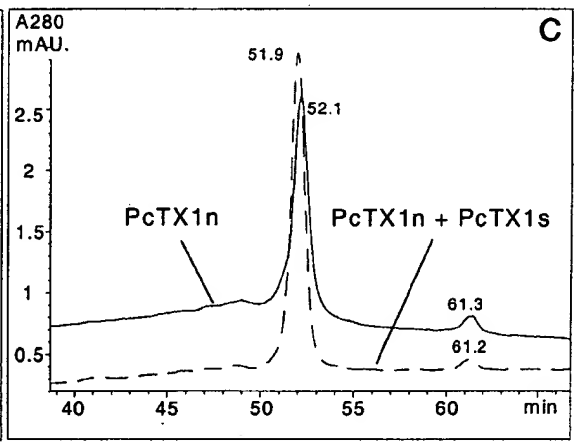

D

```
PcTX1          EDCIPKWKGCVNRHGDCCEGLECWKRRRSFEVCVPKTPKT
Edman          --------------------------------X----->
BNP-skatole                                KRRRSFEVCVPKTPKT
Trypsin No7                                   XXEVCVP
V8                                               VCVPKTPKT
```

E

		% Sim	Activity
PcTX1	----EDCIPKWKGCVNRHG-DCCEGLECWKRRRSFEVCVPKTPKT-		ASIC1a
HpTX2	----DDCGKLRSGCDTNA--DCCEGYVCRL------WCKLDW----	59.5	Kv4.2
HaTX1	-----ECRYLAGGCKTTS--DCCKHLGCKFR---DKYCAWDFTFS-	59.8	Kv2.1
SNX482	GVDKAGCRYMFGGCSVND--DCCPRLGCHSL---FSYCAWDLTFSD	60.0	VSCC (R)
GsTXSIA	-----DCVRFWGKCSQTS--DCCPHLACKSKW-PRNICVWDGSV--	68.9	VSCC (P/N)
PaTX1	-----YCQKWMWTCDSAR--KCCEGLVCRL------WCKKII----	55.6	Kv4.2/4.3

F

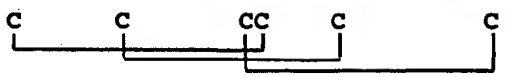

FIG. 1. **Purification and characterization of PcTX1.** *A*, RP-HPLC separation of crude *P. cambridgei* venom (10 μl) with a linear gradient of water/acetonitrile in 0.1% aqueous trifluoroacetic acid. The *arrow* indicates fraction 10, which containing PcTX1. *B*, cation exchange chromatography of fraction 10 with a linear gradient of ammonium acetate (20 mM to 2 M in 88 min). *C*, co-elution experiments with the native toxin (PcTX1n, *solid trace*) injected alone (100 pmol) and co-injected with the synthetic toxin (PcTX1n + PcTX1 s, *dotted trace*, 100 pmol each) by cation exchange HPLC. *D*, PcTX1 sequence determination by automated Edman degradation of reduced-alkylated peptide and proteolytic cleavage fragments. *E*,

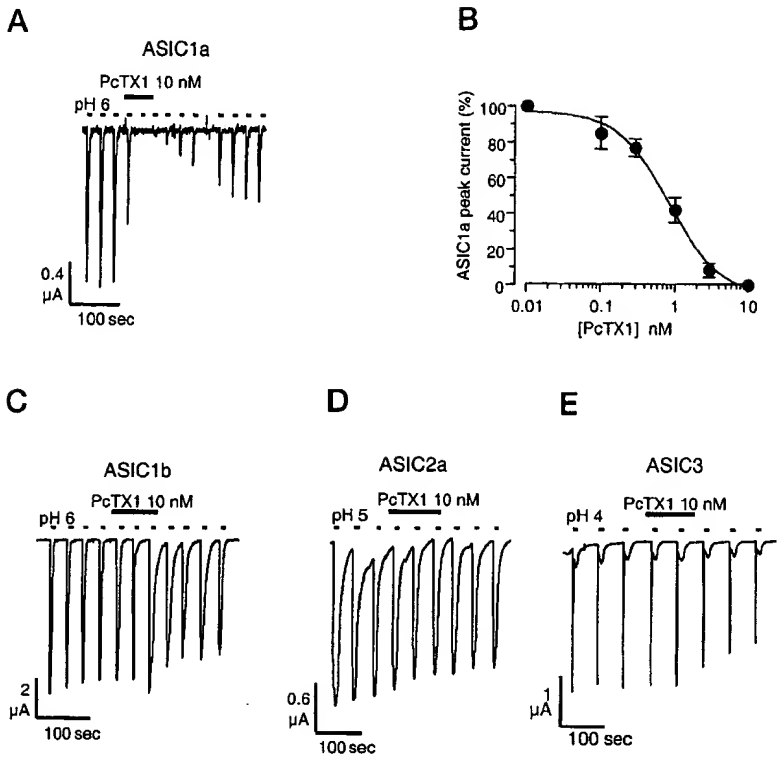

FIG. 2. **PcTX1 selectively blocks H^+-gated channels expressed in oocytes.** *A*, complete inhibition of the ASIC1a current by 10 nM PcTX1. Oocytes were clamped at −60 mV, and currents were activated by a pH drop from pH 7.4 to pH 6 (*short bars*) every 30 s. The reversibility of the blockade was observed during extensive washout. *B*, dose-response curve for synthetic PcTX1 block of the ASIC1a current activated by a pH drop from pH 7.4 to pH 6. Points represent the means ± S.E. (4–7 experiments). IC_{50} = 0.9 nM, n_H (Hill coefficient) = 1.2. *C*, the ASIC1b current was activated by a pH drop from pH 7.4 to pH 6 every 30 s. The *black bar* indicates a 2-min perfusion of PcTX1 (10 nM, n = 5). The incomplete reversibility is due to a rundown of the Na^+ current, which is observed under repetitive stimulations by consecutive pH drops at 30-s intervals. *D*, ASIC2a current activated by a drop to pH 5 every 45 s. The *black bar* indicates a 2 min perfusion of PcTX1 (10 nM, n = 9). *E*, the rapid and slow components of the ASIC3 current are activated at pH 4 every min. The *black bar* indicates a 2-min perfusion of PcTX1 (10 nM, n = 3).

the synthetic toxin block the ASIC1a current recorded at pH 6, with an IC_{50} of 0.9 nM (Fig. 2, *A* and *B*). The blockade is rapid and reversible. PcTX1 at 10 nM also completely blocks the ASIC1a current activated by a pH drop to pH 5 or pH 4 (not shown). PcTX1 is highly selective. Neither the native nor the synthetic PcTX1 (10 nM or 100 nM) blocked ASIC1b currents activated at pH 6 (Fig. 2*C*). Similarly, the ASIC2a channel activated by a pH drop to pH 5 was insensitive to the action of PcTX1 at 10 nM (Fig. 2*D*) or 100 nM (not shown). The rapid and slow components of the ASIC3 channel were also insensitive to the perfusion of PcTX1 at 10 nM (Fig. 2*E*) and 100 nM (not shown). The toxin was also tested on the epithelial Na^+ channel formed by the assembly of α, β, and γ subunits (30), and no inhibition occurred with concentrations of 10 nM or 100 nM PcTx1 (n = 3, not shown).

Sequence homologies of PcTX1 with other spider toxins that block different subtypes of voltage-dependent K^+ channels such as hanatoxins (Kv2.1) (31), heteropodatoxins (Kv4.2) (32), and phrixotoxins (Kv4.2, Kv4.3) (33) (Fig. 1*E*) prompted us to test its effects against Kv2.1, Kv2.2, Kv4.2, and Kv4.3 channels expressed in *Xenopus* oocytes. These channels were not affected by 10 or 100 nM PcTX1 (not shown).

Experiments carried out with the same ASIC channels expressed in COS cells confirmed the results obtained in oocytes. ASIC1a was completely inhibited by 10 nM PcTX1, whereas ASIC1b, ASIC2a, and ASIC3 were insensitive (n = 10 for each channel) to a higher toxin concentration of 50 nM (not shown).

PcTX1 was then assayed on heteromultimers of the ASIC1a subunit (Fig. 3). Co-expression of ASIC1a and ASIC3 in COS cells produces a rapidly inactivating H^+-gated current (τ = 0.19 ± 0.01 s at pH 6, n = 5) that is insensitive to PcTX1 (n = 10) (Fig. 3*C*), whereas ASIC1a homomultimers produce a current that inactivates more slowly at the same pH (τ = 2.10 ± 0.30 s, n = 10) but that is completely blocked by PcTX1 (10 nM) (Fig. 3*A*). ASIC1a/ASIC2a heteromultimers were also insensitive to PcTX1 (Fig. 3*B*).

The ASIC1a channel can also be blocked by amiloride, but the IC_{50} is 10 μM (12), *i.e.* 10^4 times lower in affinity than PcTX1. Moreover amiloride is not selective. It blocks the transient current generated by ASIC1a (12), ASIC1b (17), ASIC2a (18, 19), and ASIC3 (23).

Activity of PcTX1 on Native Proton-gated Currents—Small DRG neurons isolated from 2-day-old rats were voltage clamped at −60 mV and stimulated by a pH drop from pH 7.3 to pH 6. As previously observed in small sensory neurons from trigeminal ganglia (1), this pH change evoked three different types of responses that are presented in Fig. 4 (*A–C*). Currents presented in Fig. 4*A* were blocked by 3–10 nM of the toxin PcTX1, whereas H^+-evoked currents in other neurons were insensitive to the toxin (Fig. 4, *B–C*). DRG neurons express at least two subpopulations of transient currents as judged by their constants of inactivation (Fig. 4, *A*, *B*, and *D*). One population inactivates very rapidly with a time constant of inactivation below 0.5 s, whereas the other one has time constants between 1 and 3 s, the average time constant of inactivation being 1.95 ± 0.14 s (n = 23). The data clearly indicate that the most rapidly inactivating currents with an average time constant of inactivation of 0.24 ± 0.03 s (n = 22) are insensitive to PcTX1. Only the more slowly inactivating H^+-gated channels are highly sensitive to PcTX1.

The dose-response curve presented in Fig. 4*E* was obtained from the PcTX1-sensitive population of neurons. The IC_{50}

multiple sequence alignment of PcTX1 and short spider peptides of similar structure and known mode of action. *% Sim*, percentage of similarity, identical + homologous residues. *Black boxes* indicate conserved residues, and *gray boxes* indicate functionally homologous residues. *X* indicates undetermined residues, and *bold type* indicates residues confirmed by cleavage peptide sequencing. *F*, conserved cysteine positions and disulfide bridges arrangement by homology to known toxins. Sequences are from Ref. 32 (HpTX2), Ref. 37 (SNX482), Ref. 33 (PaTX1), Ref. 31 (HaTX1), and Ref. 38 (GsTXSIA). *VSCC*, voltage-sensitive calcium channels; *Kv*, voltage-dependent potassium channels. All peptides except HpTX2 are from tarantula venoms.

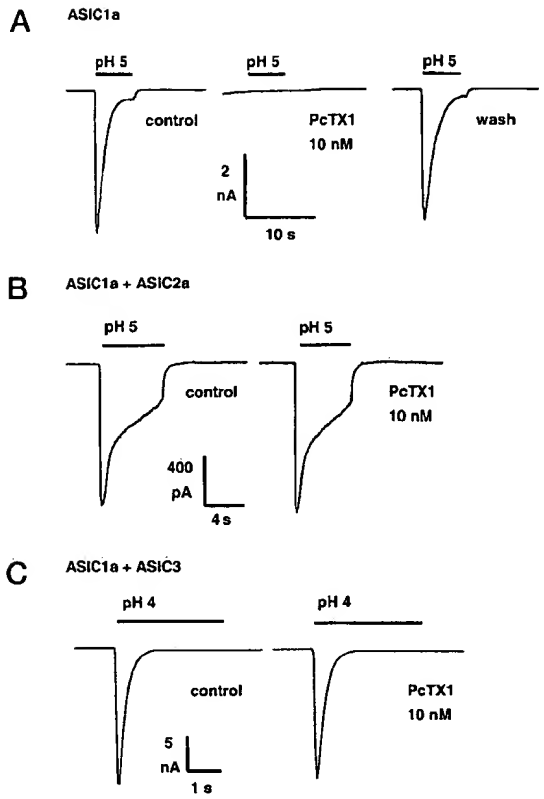

FIG. 3. **Effect of PxTX1 on ASIC homomultimers and heteromultimers.** PcTX1 blocks ASIC1a homomultimers and is inactive on ASIC1a/ASIC2a and ASIC1a/ASIC3 heteromultimers. COS cells transfected with ASIC1a, ASIC1a + ASIC2a, or ASIC1a + ASIC3 were voltage clamped at −60 mV and subjected to a pH drop as indicated (n = 10). Although ASIC1a homomultimers were inhibited by 10 nM PcTX1 (*A*), none of the heteromultimers were sensitive to the toxin (*B* and *C*). Note that the sustained component produced by ASIC3 homomultimers (Fig. 2*E*) is absent in the ASIC1a + ASIC3 heteromultimer (*C*).

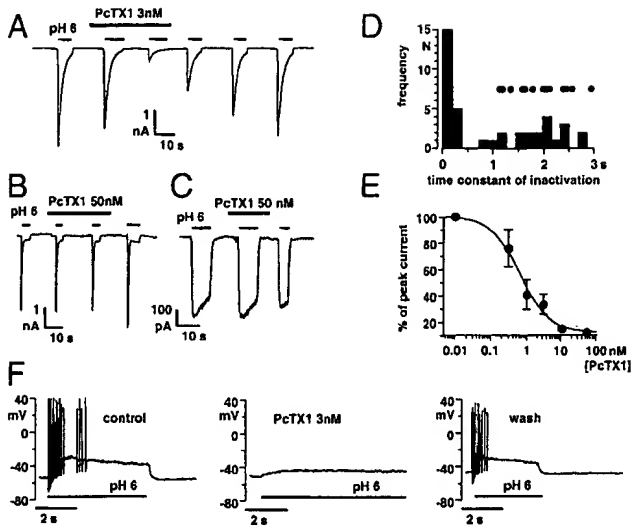

FIG. 4. **Effect of PxTX1 on DRG neurones.** PcTX1 inhibits a subpopulation of H^+-gated currents in dorsal root ganglion neurons. H^+-gated currents were recorded from DRG neurons in the whole cell voltage clamp configuration. Neurons were clamped at −60 mV, and currents were evoked by rapid jumps in pH from pH 7.3 to pH 6 (*short bars* above the traces in *A–C*). In 23 of 48 H^+-responsive neurons PcTX1 inhibited the H^+-gated current (*A*), whereas very rapidly inactivating or very slowly inactivating currents recorded in 25 other H^+-responsive neurons were resistant to 50 nM of the toxin (*B* and *C*). Current inactivation in each cell expressing either H^+-gated currents as in *A* or *B* was fitted with a single exponential, and the profile showing the distribution of time constants in the different cells is shown in *D*. The time constants of the currents that could be inhibited by PcTX1 are shown in the same graph as *filled circles*. *E*, dose inhibition curve obtained from cells expressing the PcTX1-sensitive channels (as in *A*), IC_{50} = 0.7 nM. *F*, DRG neurons (in current clamp) respond to a drop in extracellular pH from pH 7.3 to pH 6, with a burst of spike activity, which is suppressed by PcTX1.

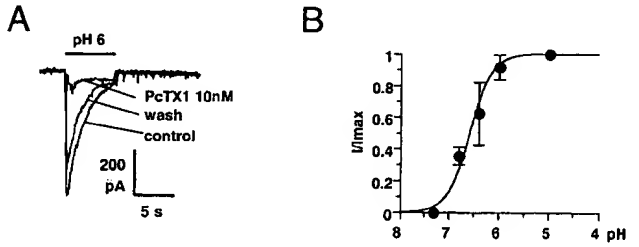

FIG. 5. **PcTX1 inhibits the H^+-gated current in cerebellar granule cells.** Mouse cerebellar granule cells were voltage clamped at −60 mV and subjected to a drop in pH from pH 7.3 to pH 6. Almost all of the current is inhibited by 10 nM PcTX1 (*A*). The pH dependence of the proton-gated current in cerebellar cells is shown in *B*.

value for half-maximum inhibition is 0.7 nM, very similar to the value of 0.9 nM obtained for ASIC1a channels expressed in *Xenopus* oocytes.

Fig. 4*F* shows that a change of the extracellular pH from pH 7.3 to pH 6 in neurons that express the channel type shown in Fig. 4*A* evokes a rapid depolarization resulting in a train of action potentials. This effect is blocked by very low concentrations of PcTX1, and this inhibition is reversible.

ASIC channel subunits are highly expressed in cerebellum and particularly in granular cells (12, 34). This is why we have used these cells to analyze the properties of these channels in central nervous system neurons (Fig. 5). Cerebellar granule cells in culture all responded to a pH drop from pH 7.3 to pH 6 with a transient Na^+ inward current characterized by a time constant of inactivation of 2.06 ± 0.17 s (n = 10) (Fig. 5*A*). Both the rate of inactivation and the pH dependence of this H^+-gated Na^+ channel ($pH_{0.5}$ 6.6 *versus* $pH_{0.5}$ 6.4) are very similar to those of the ASIC1a channel (Ref. 12 and this work) (Fig. 5*B*). H^+-gated Na^+ channels with the same properties have been recently identified in cortical neurons (35). The transient H^+-gated Na^+ channel expressed by granule cells was completely inhibited by 10 nM PcTX1 (n = 10) (Fig. 5*A*).

DISCUSSION

PcTX1 is a novel toxin from tarantula venom that is a potent and specific blocker of one class of H^+-gated Na^+ channels. The molecular scaffold of PcTX1 is likely to be similar to that previously described for both cone snail and spider toxins (28, 36). It comprises a triple-stranded antiparallel β-sheet structure reticulated by three disulfide bridges and tightly folded into the "knottin" fold pattern (29). PcTX1 is characterized by the unusual quadruplet Lys^{25}-Arg^{26}-Arg^{27}-Arg^{28}, which probably forms a strongly positive "patch" at the surface of the toxin molecule, constituting an area that is a strong candidate for receptor recognition.

It is particularly intriguing to observe (*a*) that PcTX1 is absolutely specific for ASIC1a and can distinguish between the two ASIC1 splice variants ASIC1a and ASIC1b, although they only differ in their N-terminal sequence (17); (*b*) that PcTX1 can also distinguish between ASIC1a, ASIC2 and ASIC3; and (*c*) that PcTX1 looses its capacity to block ASIC1a as soon as this subunit is associated with another member of the family, be it ASIC2a or ASIC3.

An important site of the interaction of ASIC1a with PcTX1 is probably located in the extracellular stretch of 113 amino acids

situated immediately after the first transmembrane domain. This is the only extracellular site where the splice variants ASIC1a and ASIC1b are different. They are identical in extracellular regions except for the 113-residue region immediately C-terminal to the first transmembrane domain.

ASIC1a is present in the central nervous system (notably in the hippocampus and the cerebellar granular layer) as well as in DRG neurons (12). Electrophysiological experiments have shown that both cerebellar granule cells and a subpopulation of DRG neurons possess H^+-gated currents that inactivate at pH 6 with time constants of 1.95–2.06 s, very similar if not identical to the time constant of inactivation (2.10 ± 0.30 s) of the homomultimeric ASIC1a current expressed in COS cells. The H^+-gated currents in these neurons are inhibited by very low concentrations of PcTX1. The resemblance in the inactivation kinetics and pH dependence, in the selective block of the current by PcTX1 and the near identity of the IC_{50} values for the blockade of ASIC1a channels (IC_{50} = 0.9 nM) and of native channels (IC_{50} = 0.7 nM) strongly suggest that the H^+-gated current with a τ_{inact} of ~2 s in both DRG cells and cerebellar granular cells is mediated by an homomultimeric assembly of ASIC1a. This view is strengthened by the fact that none of the heteromultimeric channels tested (ASIC1a/ASIC2a and ASIC1a/ASIC3) is sensitive to the toxin.

DRG neurons also express H^+-gated currents with time constants of inactivation that are either faster or slower than the time constant of inactivation of the homomultimeric ASIC1a current. A class of these proton-sensitive channels inactivates at a fast rate (τ_{inact} = 0.24 ± 0.03 s), which turns out, as shown in this work, to be very similar to the rate of inactivation of the ASIC1a/ASIC3 channel expressed in COS cells (τ_{inact} = 0.19 ± 0.01 s). This rapidly inactivating current, like the current generated by ASIC1a/ASIC3 heteromultimers, is insensitive to PcTX1.

The ASIC3 channel alone or in association with ASIC2b (22) probably corresponds to the sustained current recorded in DRG cells (6). ASIC3 homomultimers, ASIC3/ASIC2b heteromultimers, and the native noninactivating H^+-gated channels are not blocked by PcTX1. It is hoped that further studies will provide other toxins specifically active on these maintained channels that are thought to play an important role in pain (6).

Spider venoms are mixtures of neuroactive peptides capable of incapacitating the prey through a myriad of molecular mechanisms. PcTX1 is a potent tool that now opens the way to a more detailed analysis of the physiological function of the important class of H^+-gated Na^+ channels.

Acknowledgments—We are grateful to M. Jodar, Y. Benhamou and V. Lopez for technical assistance and to E. Lingueglia for the epithelial Na^+ channel and ASIC2b clones and very helpful discussions. The support of Dr. T. Nakajima and the Suntory Institute for Bioorganic Research (Osaka, Japan) is gratefully acknowledged.

REFERENCES

1. Krishtal, O. A., and Pidoplichko, V. I. (1981) *Neurosci. Lett.* **24,** 243–246
2. Krishtal, O. A., and Pidoplichko, V. I. (1981) *Brain Res.* **214,** 150–154
3. Krishtal, O. A., and Pidoplichko, V. I. (1981) *Neuroscience* **6,** 2599–2601
4. Davies, N. W., Lux, H. D., and Morad, M. (1988) *J. Physiol. (Lond.)* **400,** 159–187
5. Akaike, N., and Ueno, S. (1994) *Prog. Neurobiol.* **43,** 73–83
6. Bevan, S., and Yeats, J. (1991) *J. Physiol. (Lond.)* **433,** 145–161
7. Benson, C. J., Eckert, S. P., and McCleskey, E. W. (1999) *Circ. Res.* **84,** 921–928
8. Pan, H. L., Longhurst, J. C., Eisenach, J. C., and Chen, S. R. (1999) *J. Physiol. (Lond.)* **518,** 857–866
9. Chen, X., Gallar, J., and Belmonte, C. (1997) *Invest. Ophthalmol. Vis. Sci.* **38,** 1944–1953
10. Kress, M., and Zeilhofer, H. U. (1999) *Trends Pharmacol. Sci.* **20,** 112–118
11. McCleskey, E. W., and Gold, M. S. (1999) *Annu. Rev. Physiol.* **61,** 835–856
12. Waldmann, R., Champigny, G., Bassilana, F., Heurteaux, C., and Lazdunski, M. (1997) *Nature* **386,** 173–177
13. Lingueglia, E., Voilley, N., Waldmann, R., Lazdunski, M., and Barbry, P. (1993) *FEBS Lett.* **318,** 95–99
14. Canessa, C. M., Horisberger, J. D., and Rossier, B. C. (1993) *Nature* **361,** 467–470
15. Lingueglia, E., Champigny, G., Lazdunski, M., and Barbry, P. (1995) *Nature* **378,** 730–733
16. Huang, M., and Chalfie, M. (1994) *Nature* **367,** 467–470
17. Chen, C. C., England, S., Akopian, A. N., and Wood, J. N. (1998) *Proc. Natl. Acad. Sci. U. S. A.* **95,** 10240–10245
18. Waldmann, R., Champigny, G., Voilley, N., Lauritzen, I., and Lazdunski, M. (1996) *J. Biol. Chem.* **271,** 10433–10436
19. Price, M. P., Snyder, P. M., and Welsh, M. J. (1996) *J. Biol. Chem.* **271,** 7879–7882
20. Garcia-Anoveros, J., Derfler, B., Neville-Golden, J., Hyman, B. T., and Corey, D. P. (1997) *Proc. Natl. Acad. Sci. U. S. A.* **94,** 1459–1464
21. Champigny, G., Voilley, N., Waldmann, R., and Lazdunski, M. (1998) *J. Biol. Chem.* **273,** 15418–15422
22. Lingueglia, E., de Weille, J. R., Bassilana, F., Heurteaux, C., Sakai, H., Waldmann, R., and Lazdunski, M. (1997) *J. Biol. Chem.* **272,** 29778–29783
23. Waldmann, R., Bassilana, F., de Weille, J., Champigny, G., Heurteaux, C., and Lazdunski, M. (1997) *J. Biol. Chem.* **272,** 20975–20978
24. De Weille, J. R., Bassilana, F., Lazdunski, M., and Waldmann, R. (1998) *FEBS Lett.* **433,** 257–260
25. Babinski, K., Le, K. T., and Seguela, P. (1999) *J. Neurochem.* **72,** 51–57
26. Bassilana, F., Champigny, G., Waldmann, R., de Weille, J. R., Heurteaux, C., and Lazdunski, M. (1997) *J. Biol. Chem.* **272,** 28819–28822
27. Lauritzen, I., De Weille, J., Adelbrecht, C., Lesage, F., Murer, G., Raisman-Vozari, R., and Lazdunski, M. (1997) *Brain Res.* **753,** 8–17
28. Narasimhan, L., Singh, J., Humblet, C., Guruprasad, K., and Blundell, T. (1994) *Nat. Struct. Biol.* **1,** 850–852
29. Norton, R. S., and Pallaghy, P. K. (1998) *Toxicon* **36,** 1573–1583
30. Canessa, C. M., Merillat, A. M., and Rossier, B. C. (1994) *Am. J. Physiol.* **267,** C1682–C1690
31. Swartz, K. J., and Mackinnon, R. (1995) *Neuron* **15,** 941–949
32. Sanguinetti, M. C., Johnson, J. H., Hammerland, L. G., Kelbaugh, P. R., Volkmann, R. A., Saccomano, N. A., and Mueller, A. L. (1997) *Mol. Pharmacol.* **51,** 491–498
33. Diochot, S., Drici, M. D., Moinier, D., Fink, M., and Lazdunski, M. (1999) *Br. J. Pharmacol.* **126,** 251–263
34. Waldmann, R., and Lazdunski, M. (1998) *Curr. Opin. Neurobiol.* **8,** 418–424
35. Varming, T. (1999) *Neuropharmacology* **38,** 1875–1881
36. Pallaghy, P. K., Nielsen, K. J., Craik, D. J., and Norton, R. S. (1994) *Protein Sci.* **3,** 1833–1839
37. Newcomb, R., Szoke, B., Palma, A., Wang, G., Chen, X., Hopkins, W., Cong, R., Miller, J., Urge, L., Tarczy-Hornoch, K., Loo, J. A., Dooley, D. J., Nadasdi, L., Tsien, R. W., Lemos, J., and Miljanich, G. (1998) *Biochemistry* **37,** 15353–15362
38. Lampe, R. A., Defeo, P. A., Davison, M. D., Young, J., Herman, J. L., Spreen, R. C., Horn, M. B., Mangano, T. J., and Keith, R. A. (1993) *Mol. Pharmacol.* **44,** 451–460

1: Genes Chromosomes Cancer. 2002 Aug;34(4):428-36. Related Articles, Link

Breakpoint position on 17q identifies the most aggressive neuroblastoma tumors.

Lastowska M, Cotterill S, Bown N, Cullinane C, Variend S, Lunec J, Strachan T, Pearson AD, Jackson MS.

Institute of Human Genetics, International Centre for Life, University of Newcastle upon Tyne, Central Parkway, Newcastle upon Tyne NE1 3BZ, UK. m.a.lastowska@ncl.ac.uk

Gain of chromosome arm 17q is a powerful prognostic factor in neuroblastoma and the distribution of 17q breakpoints suggests that the dosage of one or more genes in 17q22-23 to 17qter is critical for tumor progression. To identify the smallest region of 17q gain, we used eight probes to map translocation breakpoints in 48 primary neuroblastoma tumors. We identified at least five different breakpoints, all localized within the proximal part of 17q (from D17Z to MPO). The shortest region of gain identified by these probes extends from MPO (17q23.1) to 17qter. Surprisingly, we found that breakpoints localized proximal to ERBB2 (17q12) were associated with significantly better patient survival than breakpoints localized distal to ERBB2. Breakpoints localized distal to ERBB2 identified patients with a particularly poor prognosis, higher mitotic karyorrhectic index, and stage 4 disease. This implies that breakpoint position on 17q is a discriminative factor within this prognostically poor group of patients. This result also suggests that the biological effect of 17q gain durin neuroblastoma progression has a complex basis. We propose that this involves dosage alterations of genes localized on both sides of the 17q breakpoints, with a gene or genes mapping between 17cen and 17q12 acting to suppress progression, and a gene or genes mapping between 17q23.1 and 17qter acting t promote tumor progression.

PMID: 12112532 [PubMed - indexed for MEDLINE]

Cell, Vol. 118, 687–698, September 17, 2004, Copyright ©2004 by Cell Press

Neuroprotection in Ischemia: Blocking Calcium-Permeable Acid-Sensing Ion Channels

Zhi-Gang Xiong,[1,*] Xiao-Man Zhu,[1,7] Xiang-Ping Chu,[1,7] Manabu Minami,[1] Jessica Hey,[1] Wen-Li Wei,[2] John F. MacDonald,[2] John A. Wemmie,[3,4,5] Margaret P. Price,[5] Michael J. Welsh,[5] and Roger P. Simon[1,6]

[1]Robert S. Dow Neurobiology Laboratories
Legacy Research
Portland, Oregon 97232
[2]Department of Physiology
University of Toronto
Toronto, Ontario M5S 1A8
Canada
[3]Department of Psychiatry
University of Iowa
[4]Department of Veterans Affairs Medical Center
[5]Department of Internal Medicine and
Howard Hughes Medical Institute
University of Iowa
Iowa City, Iowa 52242
[6]Department of Neurology, Physiology, and Pharmacology
Oregon Health and Science University
Portland, Oregon 97239

Summary

Ca^{2+} toxicity remains the central focus of ischemic brain injury. The mechanism by which toxic Ca^{2+} loading of cells occurs in the ischemic brain has become less clear as multiple human trials of glutamate antagonists have failed to show effective neuroprotection in stroke. Acidosis is a common feature of ischemia and is assumed to play a critical role in brain injury; however, the mechanism(s) remain ill defined. Here, we show that acidosis activates Ca^{2+}-permeable acid-sensing ion channels (ASICs), inducing glutamate receptor-independent, Ca^{2+}-dependent, neuronal injury inhibited by ASIC blockers. Cells lacking endogenous ASICs are resistant to acid injury, while transfection of Ca^{2+}-permeable ASIC1a establishes sensitivity. In focal ischemia, intracerebroventricular injection of ASIC1a blockers or knockout of the ASIC1a gene protects the brain from ischemic injury and does so more potently than glutamate antagonism. Thus, acidosis injures the brain via membrane receptor-based mechanisms with resultant toxicity of $[Ca^{2+}]_i$, disclosing new potential therapeutic targets for stroke.

Introduction

Intracellular Ca^{2+} overload is essential for neuronal injury associated with neuropathological syndromes, including brain ischemia (Choi, 1995, 1988a). Excessive Ca^{2+} in the cell activates a cascade of cytotoxic events leading to activation of enzymes that break down proteins, lipids, and nucleic acids. NMDA receptors, the most important excitatory neurotransmitter receptors in the central nervous system (McLennan, 1983; Dingledine et al., 1999), have long been considered the main target responsible for Ca^{2+} overload in the ischemic brain (Simon et al., 1984; Rothman and Olney, 1986; Choi, 1988b; Meldrum, 1995). However, recent clinical efforts to prevent brain injury through the therapeutic use of NMDA receptor antagonists have been disappointing (Lee et al., 1999; Wahlgren and Ahmed, 2004). Although multiple factors, including difficulty in early initiation of treatment, may have contributed to trial failures, it is likely that glutamate receptor-independent Ca^{2+} toxicity might also be responsible for ischemic brain injury.

The normal brain requires complete oxidation of glucose to fulfill its energy requirements. During ischemia, oxygen depletion forces the brain to switch to anaerobic glycolysis. Accumulation of lactic acid as a byproduct of glycolysis and protons produced by ATP hydrolysis causes pH to fall in the ischemic brain (Rehncrona, 1985; Siesjo et al., 1996). Consequently, tissue pH typically falls to 6.5–6.0 during ischemia under normoglycemic conditions and can fall below 6.0 during severe ischemia or under hyperglycemic conditions (Nedergaard et al., 1991; Rehncrona, 1985; Siesjo et al., 1996). Nearly all in vivo studies indicate that acidosis aggravates ischemic brain injury (Tombaugh and Sapolsky, 1993; Siesjo et al., 1996). However, the mechanisms of this process remain unclear, although a host of possibilities has been suggested (Siesjo et al., 1996; McDonald et al., 1998; Swanson et al., 1995; Ying et al., 1999).

Acid-sensing ion channels (ASICs), a newly described class of ligand-gated channels (Waldmann et al., 1997a; Krishtal, 2003), have been shown to be expressed throughout neurons of mammalian central and peripheral nervous systems (Waldmann et al., 1997a, 1999; Waldmann and Lazdunski, 1998; Krishtal, 2003; Alvarez de la Rosa et al., 2002, 2003). They are members of the degenerin/epithelial sodium channel (Deg/ENaC) superfamily (Benos and Stanton, 1999; Bianchi and Driscoll, 2002; Krishtal, 2003). Pertinent to ischemia, ASICs may also flux Ca^{2+} (Waldmann et al., 1997a; Chu et al., 2002; Yermolaieva et al., 2004).

To date, six ASIC subunits have been cloned. Four of these subunits can form functional homomultimeric channels that are activated by acidic pH to conduct a sodium-selective, amiloride-sensitive, cation current. The pH of half-maximal activation ($pH_{0.5}$) of these channels differs: ASIC1a (or ASIC1), $pH_{0.5}$ = 6.2 (Waldmann et al., 1997a); ASIC1β, a splice variant of ASIC1a with a unique N-terminal, $pH_{0.5}$ = 5.9 (Chen et al., 1998); ASIC2a, $pH_{0.5}$ = 4.4 (Waldmann et al., 1999); and ASIC3, $pH_{0.5}$ = 6.5 (Waldmann et al., 1997b). Neither ASIC2b nor ASIC4 can form functional homomeric channel (Akopian et al., 2000; Grunder et al., 2000; Lingueglia et al., 1997), but ASIC2b has been shown to associate with other subunits and modulate their activity (Lingueglia et al., 1997). In addition to Na^+ permeability, homomeric ASIC1a can flux Ca^{2+} (Waldmann et al., 1997a; Chu et al., 2002; Yermolaieva et al., 2004). Although the exact

*Correspondence: zxiong@downeurobiology.org
[7]These authors contributed equally to this work.

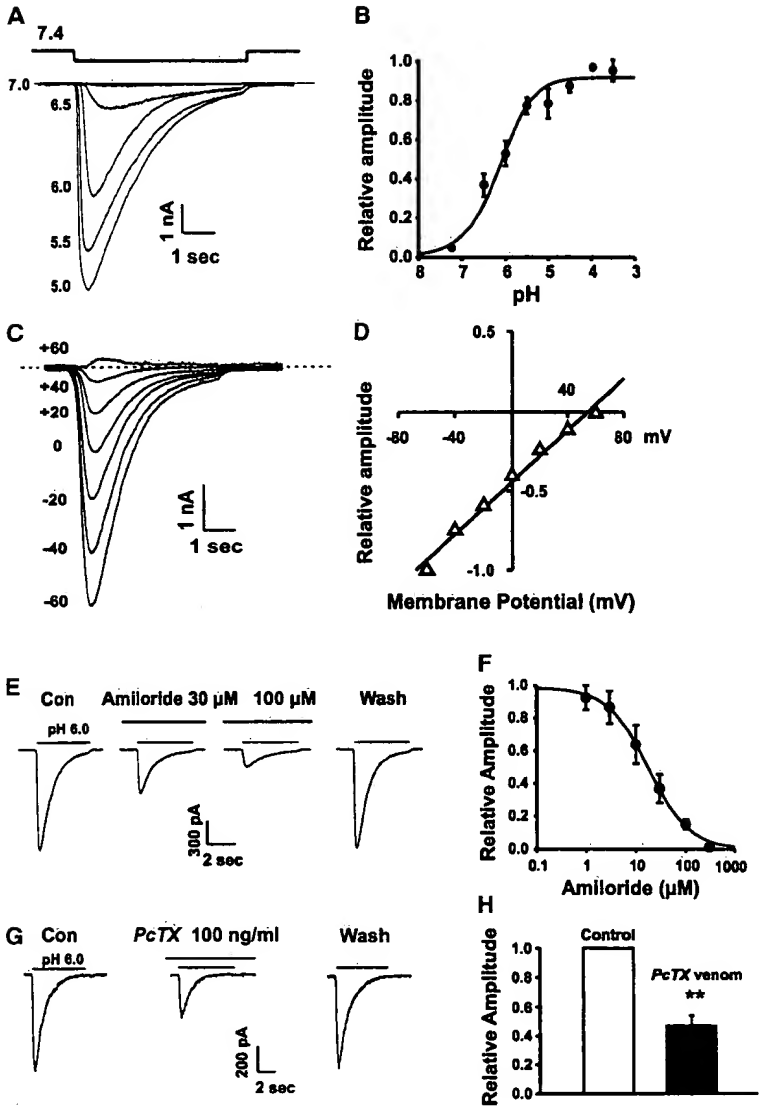

Figure 1. Electrophysiology and Pharmacology of ASICs in Cultured Mouse Cortical Neurons

(A and B) pH dependence of ASIC currents activated by pH drop from 7.4 to values indicated. Dose-response curves were fit to Hill equation with an average $pH_{0.5}$ of 6.18 ± 0.06 (n = 10).

(C and D) Current-voltage relationship of ASICs (n = 5). The amplitudes of ASIC current at various voltages were normalized to that recorded at −60 mV.

(E and F) Dose-dependent blockade of ASIC currents by amiloride. IC_{50} = 16.4 ± 4.1 µM, n = 8.

(G and H) Blockade of ASIC currents by *PcTX* venom. **p < 0.01.

subunit composition of ASICs in native neurons has not been determined, both ASIC1a and ASIC2a subunits have been shown to be abundant in the brain (Price et al., 1996; Bassilana et al., 1997; Wemmie et al., 2002; Alvarez de la Rosa et al., 2003).

Detailed functions of ASICs in both peripheral and central nervous systems remain to be determined. In peripheral sensory neurons, ASICs have been implicated in mechanosensation (Price et al., 2000, 2001) and perception of pain during tissue acidosis (Bevan and Yeats, 1991; Krishtal and Pidoplichko, 1981; Ugawa et al., 2002; Sluka et al., 2003; Chen et al., 2002), particularly in ischemic myocardium where ASICs likely transduce anginal pain (Benson et al., 1999). The presence of ASICs in the brain, which lacks nociceptors, suggests that these channels have functions beyond nociception. Indeed, recent studies have indicated that ASIC1a is involved in synaptic plasticity, learning/memory, and fear conditioning (Wemmie et al., 2002, 2003). Here, using a combination of patch-clamp recording, Ca^{2+} imaging, receptor subunit transfection, in vitro cell toxicity assays, and in vivo ischemia models combined with gene knockout, we demonstrate activation of Ca^{2+}-permeable ASIC1a as largely responsible for glutamate-independent, acidosis-mediated, and ischemic brain injury.

Results

Acidosis Activates ASICs in Mouse Cortical Neurons

We first recorded ASIC currents in cultured mouse cortical neurons, a preparation commonly used for cell toxicity studies (Koh and Choi, 1987; Sattler et al., 1999). At a holding potential of −60 mV, a rapid reduction of extracellular pH (pH_e) to below 7.0 evoked large transient inward currents with a small steady-state component in the majority of neurons (Figure 1A). The amplitude of inward current increased in a sigmoidal fashion as pH_e decreased, yielding a $pH_{0.5}$ of 6.18 ± 0.06 (n = 10, Figure 1B). A linear I-V relationship and a reversal close to the Na^+ equilibrium potential were obtained (n = 6, Figures

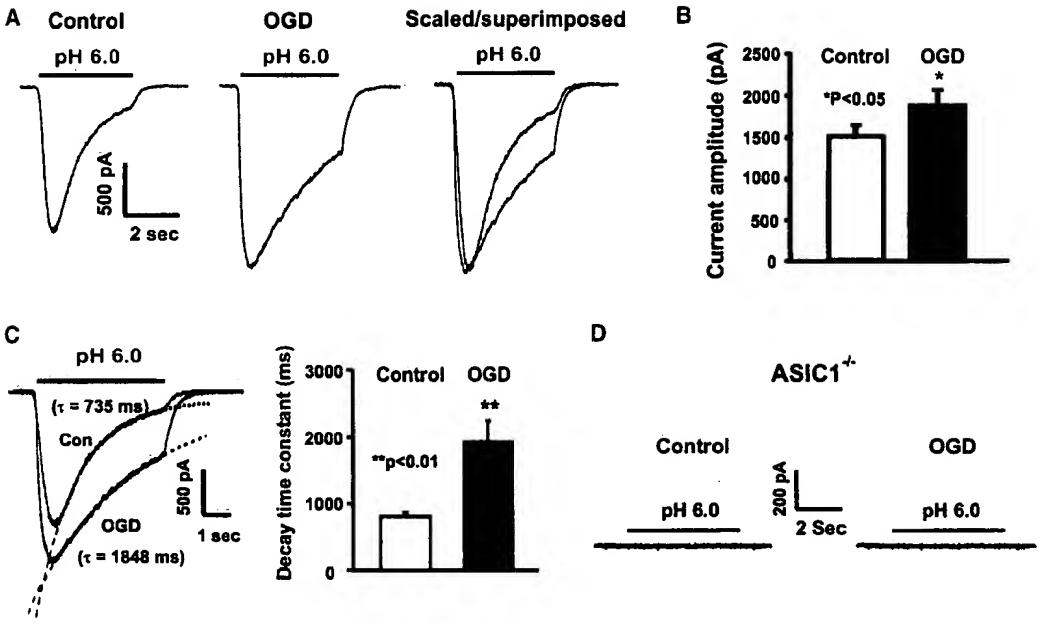

Figure 2. Modeled Ischemia Enhances Activity of ASICs

(A) Representative traces showing increase in amplitude and decrease in desensitization of ASIC currents following 1 hr OGD.

(B) Summary data of increase of ASIC current amplitude in OGD neurons. n = 40 and 44, *p < 0.05.

(C) Representative traces and summary data showing decreased ASIC current desensitization in OGD neurons. n = 6, **p < 0.01.

(D) Representative traces showing lack of acid-activated current at pH 6.0 in ASIC1$^{-/-}$ neurons, in control condition, and following 1 hr OGD (n = 12 and 13).

1C and 1D). These data demonstrate that lowering pH_o activates typical ASICs in mouse cortical neurons.

We then tested the effect of amiloride, a nonspecific blocker of ASICs (Waldmann et al., 1997a), on the acid-activated currents. Similar to previous studies, mainly in sensory neurons (Waldmann et al., 1997a; Benson et al., 1999; Chen et al., 1998; Varming, 1999), amiloride dose-dependently blocked ASIC currents in cortical neurons with an IC_{50} of 16.4 ± 4.1 μM (n = 8, Figures 1E and 1F). Psalmotoxin 1 (or PcTX1) from venom of the tarantula *Psalmopoeus cambridgei* (*PcTX* venom) has been shown to be a specific ASIC1a blocker (Escoubas et al., 2000). Our studies show that, at a protein concentration of 25 ng/ml, *PcTX* venom itself also blocks the current mediated by homomeric ASIC1a expressed in COS-7 cells by ~70% (n = 4, see Supplemental Figure S1 at http://www.cell.com/cgi/content/full/118/6/687/DC1). However, it does not affect currents mediated by heteromeric ASIC1a/2a, homomeric ASIC2a, or ASIC3 channels at 500 ng/ml (n = 4–6). In addition, at 500 ng/ml, *PcTX* venom does not affect the currents through known voltage- and ligand-gated channels, further indicating its specificity for homomeric ASIC1a (n = 4–5, Supplemental Figure S2, and Supplemental Data).

We then tested the effect of *PcTX* venom on acid-activated current in cortical neurons. At 100 ng/ml, *PcTX* venom reversibly blocked the peak amplitude of ASIC current by 47% ± 7% (n = 15, Figures 1G and 1H), indicating significant contributions of homomeric ASIC1a to total acid-activated currents. Increasing *PcTX* concentration did not induce further reduction in the amplitude of ASIC current in the majority of cortical neurons (n = 8, data not shown), indicating coexistence of *PcTX*-insensitive ASICs (e.g., heteromeric ASIC1a/2a) in these neurons.

ASIC Response Is Potentiated by Modeled Ischemia

Since acidosis is a central feature of brain ischemia, we determined whether ASICs are activated in ischemic conditions and whether ischemia modifies the properties of these channels. We recorded ASIC currents in neurons following 1 hr oxygen glucose deprivation (OGD), a common model of in vitro ischemia (Goldberg and Choi, 1993). One set of cultures was washed three times with glucose-free extracellular fluid (ECF) and subjected to OGD, while control cultures were subjected to washes with glucose containing ECF and incubation in a conventional cell culture incubator. OGD was terminated after 1 hr by replacing glucose-free ECF with Neurobasal medium and incubating cultures in the conventional incubator. ASIC current was then recorded 1 hr following the OGD when there was no morphological alteration of neurons. OGD treatment induced a moderate increase of the amplitude of ASIC currents (1520 ± 138 pA in control group, n = 44; 1886 ± 185 pA in neurons following 1 hr OGD, n = 40, p < 0.05, Figures 2A and 2B). More importantly, OGD induced a dramatic decrease in ASIC desensitization as demonstrated by an increase in time constant of the current decay (814.7 ± 58.9 ms in control neurons, n = 6; 1928.9 ± 315.7 ms in neurons following OGD, n = 6, p < 0.01, Figures 2A and 2C). In cortical neurons cultured from ASIC1$^{-/-}$ mice, reduction of pH from 7.4 to 6.0 did not activate any inward current (n = 52), similar to a previous study in hippocampal neurons (Wemmie et al., 2002). In

these neurons, 1 hr OGD did not activate or potentiate acid-induced responses (Figure 2D, n = 12 and 13).

Acidosis Induces Glutamate-Independent Ca^{2+} Entry via ASIC1a

Using a standard ion-substitution protocol (Jia et al., 1996) and the fura-2 fluorescent Ca^{2+}-imaging technique (Chu et al., 2002), we determined whether ASICs in cortical neurons are Ca^{2+} permeable. With bath solutions containing 10 mM Ca^{2+} (Na^+ and K^+-free) as the only charge carrier and at a holding potential of −60 mV, we recorded inward currents larger than 50 pA in 15 out of 18 neurons, indicating significant Ca^{2+} permeability of ASICs in the majority of cortical neurons (Figure 3A). Consistent with activation of homomeric ASIC1a channels, currents carried by 10 mM Ca^{2+} were largely blocked by both the nonspecific ASIC blocker amiloride and the ASIC1a-specific blocker *PcTX* venom (Figure 3B). The peak amplitude of Ca^{2+}-mediated current was decreased to 26% ± 2% of control by 100 μM amiloride ($n = 6$, $p < 0.01$) and to 22% ± 0.9% by 100 ng/ml *PcTX* venom ($n = 5$, $p < 0.01$). Ca^{2+} imaging, in the presence of blockers of other major Ca^{2+} entry pathways (MK801 10 μM and CNQX 20 μM for glutamate receptors; nimodipine 5 μM and ω-conotoxin MVIIC 1 μM for voltage-gated Ca^{2+} channels), demonstrated that 18 out of 20 neurons responded to a pH drop with detectable increases in the concentration of intracellular Ca^{2+} ($[Ca^{2+}]_i$) (Figure 3C). In general, $[Ca^{2+}]_i$ remains elevated during prolonged perfusion of low pH solutions. In some cells, the $[Ca^{2+}]_i$ increase lasted even longer than the duration of acid perfusion (Figure 3C). Long-lasting Ca^{2+} responses suggest that ASIC response in intact neurons is less desensitized than in whole-cell recordings or that Ca^{2+} entry through ASICs induces subsequent Ca^{2+} release from intracellular stores. Preincubation of neurons with 1 μM thapsigargin partially inhibited the sustained component of Ca^{2+} increase, suggesting that Ca^{2+} release from intracellular stores may also contribute to acid-induced intracellular Ca^{2+} accumulation ($n = 6$, data not shown). Similar to the current carried by Ca^{2+} ions (Figure 3B), both peak and sustained increases in $[Ca^{2+}]_i$ were largely inhibited by amiloride and *PcTX* venom (Figures 3C and 3D, n = 6–8), consistent with involvement of homomeric ASIC1a in acid-induced $[Ca^{2+}]_i$ increase. Knockout of the ASIC1 gene eliminated the acid-induced $[Ca^{2+}]_i$ increase in all neurons without affecting NMDA receptor-mediated Ca^{2+} response (Figure 3E, n = 8). Patch-clamp recordings demonstrated lack of acid-activated currents at pH 6.0 in 52 out of 52 of the $ASIC1^{-/-}$ neurons, consistent with absence of ASIC1a subunits. Lowering pH to 5.0 or 4.0, however, activated detectable current in 24 out of 52 $ASIC1^{-/-}$ neurons, indicating the presence of ASIC2a subunits in these neurons (Figure 3F). Further electrophysiological studies demonstrated that $ASIC1^{-/-}$ neurons have normal responses for various voltage-gated channels and NMDA, GABA receptor-gated channels (data not shown).

ASIC Blockade Protects against Acidosis-Induced, Glutamate-Independent Neuronal Injury

Acid-induced injury was studied on neurons grown on 24-well plates incubated in either pH 7.4 or 6.0 ECF containing MK801, CNQX, and nimodipine. Cell injury was assayed by the measurement of lactate dehydrogenase (LDH) release (Koh and Choi, 1987) at various time points (Figures 4A and 4B) and by fluorescent staining of alive/dead cells (Figure 4C). Compared to neurons treated at pH 7.4, 1 hr acid incubation (pH 6.0) induced a time-dependent increase in LDH release (Figure 4A). After 24 hr, 45.7% ± 5.4% of maximal LDH release was induced (n = 25 wells). Continuous treatment at pH 6.0 induced greater cell injury (Figure 4B, n = 20). Consistent with the LDH assay, alive/dead staining with fluorescein diacetate (FDA, blue) and propidium iodide (PI, red) showed similar increases in cell death by 1 hr acid treatment (Figure 4C, and Supplemental Figure S3 on the *Cell* web site). One hour incubation with pH 6.5 ECF also induced significant but less LDH release than with pH 6.0 ECF (n = 8 wells, data not shown).

To determine whether activation of ASICs is involved in acid-induced glutamate receptor-independent neuronal injury, we tested the effect of amiloride and *PcTX* venom on acid-induced LDH release. Addition of either 100 μM amiloride or 100 ng/ml *PcTX* venom 10 min before and during the 1 hr acid incubation significantly reduced LDH release (Figure 4D). At 24 hr, LDH release was decreased from 45.3% ± 3.8% to 31.1% ± 2.5% by amiloride and to 27.9% ± 2.6% by *PcTX* venom (n = 20–27, $p < 0.01$). Addition of amiloride or *PcTX* venom in pH 7.4 ECF for 1 hr did not affect baseline LDH release, although prolonged incubation (e.g., 5 hr) with amiloride alone increased LDH release (n = 8, data not shown).

Activation of Homomeric ASIC1a Is Responsible for Acidosis-Induced Injury

To determine whether Ca^{2+} entry plays a role in acid-induced injury, we treated neurons with pH 6.0 ECF in the presence of normal or reduced $[Ca^{2+}]_o$. Reducing Ca^{2+} from 1.3 to 0.2 mM inhibited acid-induced LDH release (from 40.0% ± 4.1% to 21.9% ± 2.5%), as did ASIC1a blockade with *PcTX* venom ($n = 11–12$, $p < 0.01$; Figure 5A). Ca^{2+}-free solution was not tested, as a complete removal of $[Ca^{2+}]_o$ activates large inward currents through a Ca^{2+}-sensing cation channel, which may otherwise complicate data interpretation (Xiong et al., 1997). Inhibition of acid injury by both amiloride and *PcTX*, nonspecific and specific ASIC1a blockers, and by reducing $[Ca^{2+}]_o$ strongly suggests that activation of Ca^{2+}-permeable ASIC1a is involved in acid-induced neuronal injury.

To provide additional evidence that activation of ASIC1a is involved in acid injury, we studied acid injury of nontransfected and ASIC1a transfected COS-7 cells, a cell line commonly used for expression of ASICs due to its lack of endogenous channels (Chen et al., 1998; Immke and McCleskey, 2001; Escoubas et al., 2000). Following confluence (36–48 hr after plating), cells were treated with either pH 7.4 or 6.0 ECF for 1 hr. LDH release was measured 24 hr after acid incubation. Treatment of nontransfected COS-7 cells with pH 6.0 ECF did not induce increased LDH release when compared with pH 7.4-treated cells (10.3% ± 0.8% for pH 7.4, and 9.4% ± 0.7% for pH 6.0, n = 19 and 20 wells; $p > 0.05$, Figure 5B). However, in COS-7 cells stably transfected with ASIC1a, 1 hr incubation at pH 6.0 significantly increased

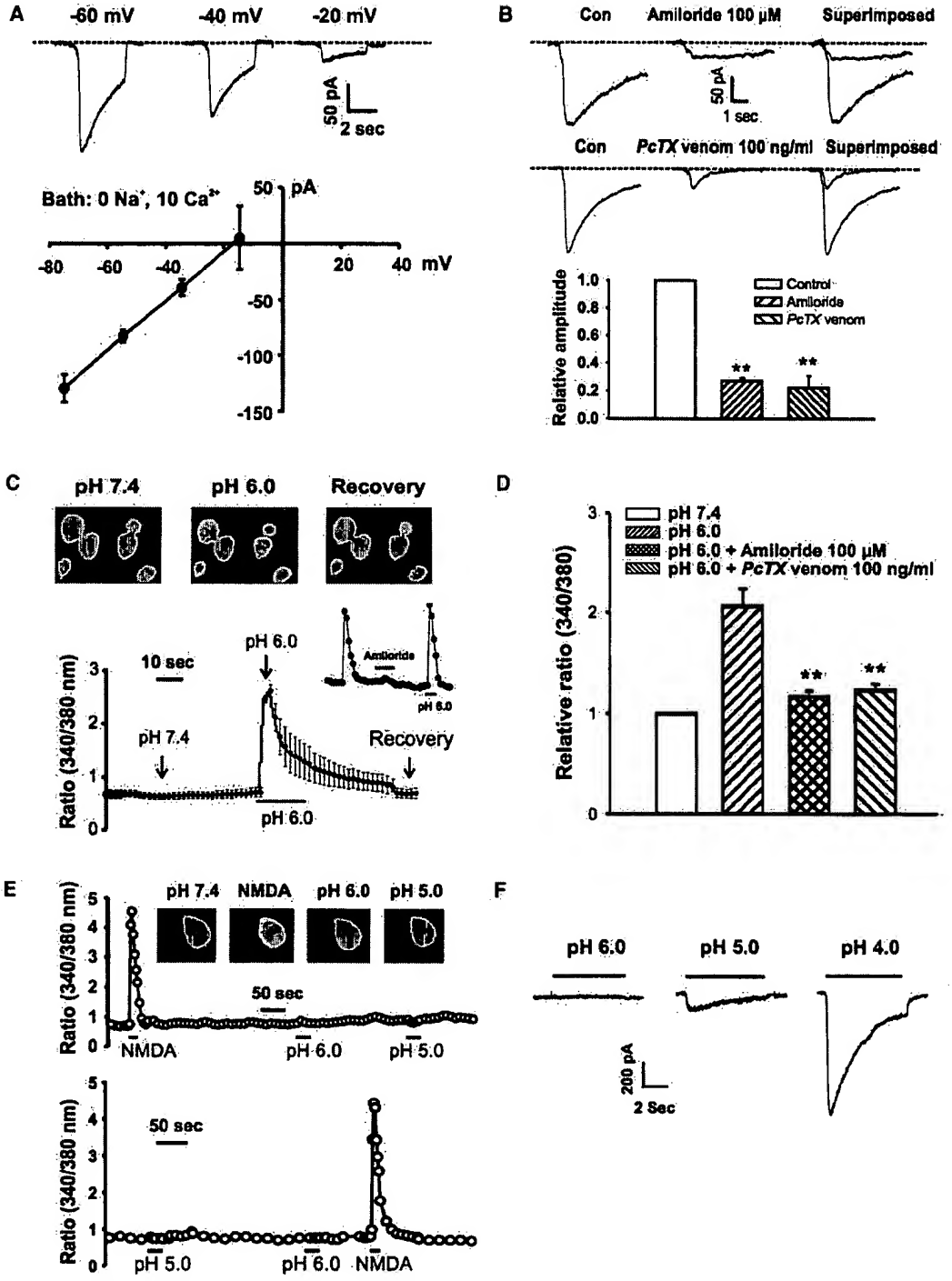

Figure 3. ASICs in Cortical Neurons Are Ca^{2+} Permeable, and Ca^{2+} Permeability Is ASIC1a Dependent

(A) With Na^{+}-free ECF containing 10 mM Ca^{2+} as the only charge carrier, inward currents were recorded at pH 6.0. The average reversal potential is ~−17 mV after correction of liquid junction potential (n = 5).

(B) Representative traces and summary data showing blockade of Ca^{2+}-mediated current by amiloride and *PcTX* venom. The peak amplitude of Ca^{2+}-mediated current decreased to 26% ± 2% of control value by 100 μM amiloride (n = 6, $p < 0.01$) and to 22% ± 0.9% by 100 ng/ml *PcTX* venom (n = 5, $p < 0.01$).

(C) Representative images and 340/380 ratios showing increase of $[Ca^{2+}]_i$ by pH drop to 6.0. Neurons were bathed in normal ECF containing 1.3 mM $CaCl_2$ with blockers for voltage-gated Ca^{2+} channels (5 μM nimodipine and 1 μM ω-conotoxin MVIIC) and glutamate receptors (10 μM MK801 and 20 μM CNQX). (Inset) Inhibition of acid-induced increase of $[Ca^{2+}]_i$ by 100 μM amiloride.

(D) Summary data showing inhibition of acid-induced increase of $[Ca^{2+}]_i$ by amiloride and *PcTX* venom. n = 6–8, $^{**}p < 0.01$ compared with pH 6.0 group.

(E) Representative image and 340/380 ratio demonstrating lack of acid-induced increase of $[Ca^{2+}]_i$ in ASIC1$^{-/-}$ neurons; neurons had a normal response to NMDA (n = 8).

(F) Representative traces showing lack of acid-activated current at pH 6.0 in ASIC1$^{-/-}$ neurons.

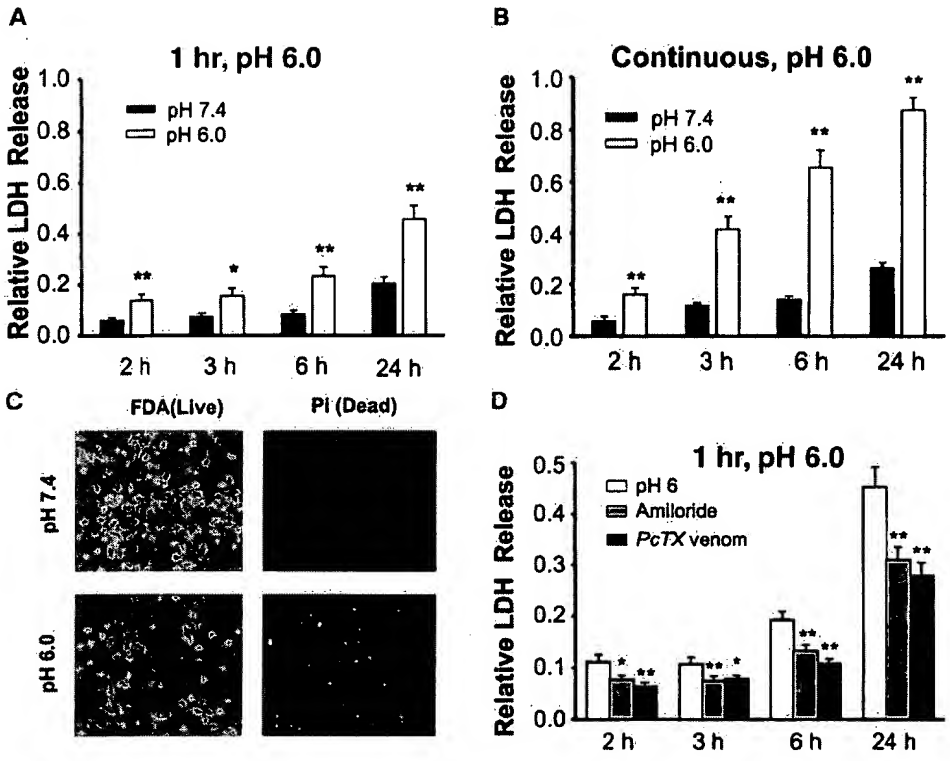

Figure 4. Acid Incubation Induces Glutamate Receptor-Independent Neuronal Injury Protected by ASIC Blockade

Time-dependent LDH release induced by 1 hr (A) or 24 hr incubation (B) of cortical neurons in pH 7.4 (solid bars) or 6.0 ECF (open bars). n = 20–25 wells, $^{*}p < 0.05$, and $^{**}p < 0.01$, compared to pH 7.4 group at same time points. (C) Analysis of acid-induced neuronal injury with fluorescein diacetate (FDA) staining of cell bodies of alive neurons and propidium iodide (PI) staining of nuclei of dead neurons. (D) Inhibition of acid-induced LDH release by 100 μM amiloride or 100 ng/ml *PcTX* venom (n = 20–27, $^{*}p < 0.05$, and $^{**}p < 0.01$). MK801, CNQX, and nimodipine were present in ECF for all experiments (A–D).

LDH release from 15.5% ± 2.4% to 24.0% ± 2.9% (n = 8 wells, $p < 0.05$). Addition of amiloride (100 μM) inhibited acid-induced LDH release in these cells (Figure 5B).

We also studied acid injury of CHO cells transiently transfected with cDNAs encoding GFP alone or GFP plus ASIC1a. After the transfection (24–36 hr), cells were incubated with acidic solution (pH 6.0) for 1 hr, and cell injury was assayed 24 hr following the acid incubation. As shown in Supplemental Figure S4, 1 hr acid incubation largely reduced surviving GFP-positive cells in GFP/ASIC1a group but not in the group transfected with GFP alone (n = 3 dishes in each group).

To further demonstrate an involvement of ASIC1a in acidosis-induced neuronal injury, we performed cell toxicity experiments on cortical neurons cultured from $ASIC^{+/+}$ and $ASIC1^{-/-}$ mice (Wemmie et al., 2002). Again, 1 hr acid incubation of $ASIC^{+/+}$ neurons at 6.0 induced substantial LDH release that was reduced by amiloride and *PcTX* venom (n = 8–12). One hour acid treatment of $ASIC1^{-/-}$ neurons, however, did not induce significant increase in LDH release at 24 hr (13.8% ± 0.9% for pH 7.4 and 14.2% ± 1.3% for pH 6.0, n = 8, $p > 0.05$), indicating resistance of these neurons to acid injury (Figure 5C). In addition, knockout of the ASIC1 gene also eliminated the effect of amiloride and *PcTX* venom on acid-induced LDH release (Figure 5C, n = 8 each), further suggesting that the inhibition of acid-induced injury of cortical neurons by amiloride and *PcTX* venom (Figure 4D) was due to blockade of ASIC1 subunits. In contrast to acid incubation, 1 hr treatment of $ASIC1^{-/-}$ neurons with 1 mM NMDA + 10 μM glycine (in Mg^{2+}-free [pH 7.4] ECF) induced 84.8% ± 1.4% of maximal LDH release at 24 hr (n = 4, Figure 5C), indicating normal response to other cell injury processes.

Modeled Ischemia Enhances Acidosis-Induced Glutamate-Independent Neuronal Injury via ASICs

As the magnitude of ASIC currents is potentiated by cellular and neurochemical components of brain ischemia—cell swelling, arachidonic acid, and lactate (Allen and Attwell, 2002; Immke and McCleskey, 2001)—and, more importantly, the desensitization of ASIC currents is dramatically reduced by modeled ischemia (see Figures 2A and 2C), we expected that activation of ASICs in ischemic conditions should produce greater neuronal injury. To test this hypothesis, we subjected neurons to 1 hr acid treatment under oxygen and glucose deprivation (OGD). MK801, CNQX, and nimodipine were added to all solutions to inhibit voltage-gated Ca^{2+} channels and glutamate receptor-mediated cell injury associated with OGD (Kaku et al., 1991). One hour incubation with pH 7.4 ECF under OGD conditions induced only 27.1% ± 3.5% of maximal LDH release at 24 hr (n = 5, Figure 5D). This finding is in agreement with a previous report that 1 hr OGD does not induce substantial cell injury with the blockade of glutamate receptors and voltage-

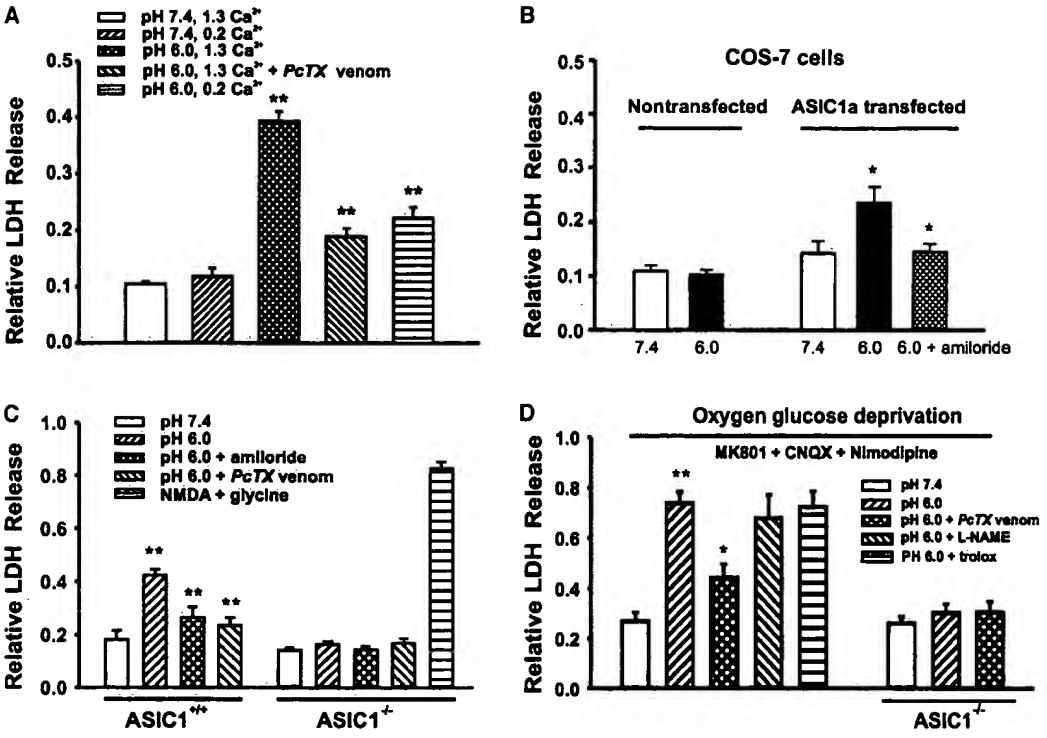

Figure 5. Involvement of ASIC1a in Acid-Induced Injury In Vitro

(A) Inhibition of acid-induced LDH release by reducing $[Ca^{2+}]_o$ (n = 11–12, **p < 0.01 compared with pH 6.0, 1.3 Ca^{2+}).

(B) Acid incubation induced increase of LDH release in ASIC1a-transfected but not nontransfected COS-7 cells (n = 8–20). Amiloride (100 μM) inhibited acid-induced LDH release in ASIC1a-transfected cells. *p < 0.05 for 7.4 versus 6.0 and 6.0 versus 6.0 + amiloride.

(C) Lack of acid-induced injury and protection by amiloride and *PcTX* venom in ASIC1$^{-/-}$ neurons (n = 8 in each group, p > 0.05).

(D) Acid-induced increase of LDH release in cultured cortical neurons under OGD (n = 5). LDH release induced by combined 1 hr OGD/acidosis was not inhibited by trolox and L-NAME (n = 8–11). OGD did not potentiate acid-induced LDH release in ASIC1$^{-/-}$ neurons. **p < 0.01 for pH 7.4 versus pH 6.0 and *p < 0.05 for pH 6.0 versus 6.0 + *PcTX* venom. MK801, CNQX, and nimodipine were present in ECF for all experiments (A–D).

gated Ca^{2+} channels (Aarts et al., 2003). However, 1 hr OGD, combined with acidosis (pH 6.0), induced 73.9% ± 4.3% of maximal LDH release (n = 5, Figure 5D, p < 0.01), significantly larger than acid-induced LDH release in the absence of OGD (see Figure 4A, p < 0.05). Addition of the ASIC1a blocker *PcTX* venom (100 ng/ml) significantly reduced acid/OGD-induced LDH release to 44.3% ± 5.3% (n = 5, p < 0.05, Figure 5D).

We also performed the same experiment with cultured neurons from the ASIC1$^{-/-}$ mice. Unlike in ASIC1 containing neurons, however, 1 hr treatment with combined OGD and acid only slightly increased LDH release in ASIC1$^{-/-}$ neurons (from 26.1% ± 2.7% to 30.4% ± 3.5%, n = 10–12, Figure 5D). This finding suggests that potentiation of acid-induced injury by OGD is largely due to OGD potentiation of ASIC1-mediated toxicity.

Aarts et al. (2003) have recently studied ischemia molded by prolonged OGD (2 hr) but without acidosis. In this model system, they demonstrated activation of a Ca^{2+}-permeable nonselective cation conductance activated by reactive oxygen/nitrogen species resulting in glutamate receptor-independent neuronal injury. The prolonged OGD-induced cell injury modeled by Aarts et al. is dramatically reduced by agents either scavenging free radicals directly (e.g., trolox) or reducing the production of free radicals (e.g., L-NAME) (Aarts et al., 2003). To determine whether combined short duration OGD and acidosis induced neuronal injury involves a similar mechanism, we tested the effect of trolox and L-NAME on OGD/acid-induced LDH release. As shown in Figure 5D, neither trolox (500 μM) nor L-NAME (300 μM) had significant effect on combined 1 hr OGD/acidosis-induced neuronal injury (n = 8–11). Additional experiments demonstrated that the ASIC blockers amiloride and *PcTX* venom had no effect on the conductance of TRPM7 channels reported to be responsible for prolonged OGD-induced neuronal injury by Aarts et al. (2003) (Supplemental Figure S5). Together, these findings strongly suggest that activation of ASICs but not TRPM7 channels is largely responsible for combined 1 hr OGD/acidosis-induced neuronal injury in our studies.

Activation of ASIC1a in Ischemic Brain Injury In Vivo

To provide evidence that activation of ASIC1a is involved in ischemic brain injury in vivo, we first tested the protective effect of amiloride and *PcTX* venom in a rat model of transient focal ischemia (Longa et al., 1989). Ischemia (100 min) was induced by transient middle cerebral artery occlusion (MCAO). A total of 6 μl artificial CSF (aCSF) alone, aCSF-containing amiloride (1 mM), or *PcTX* venom (500 ng/ml) was injected intracerebroven-

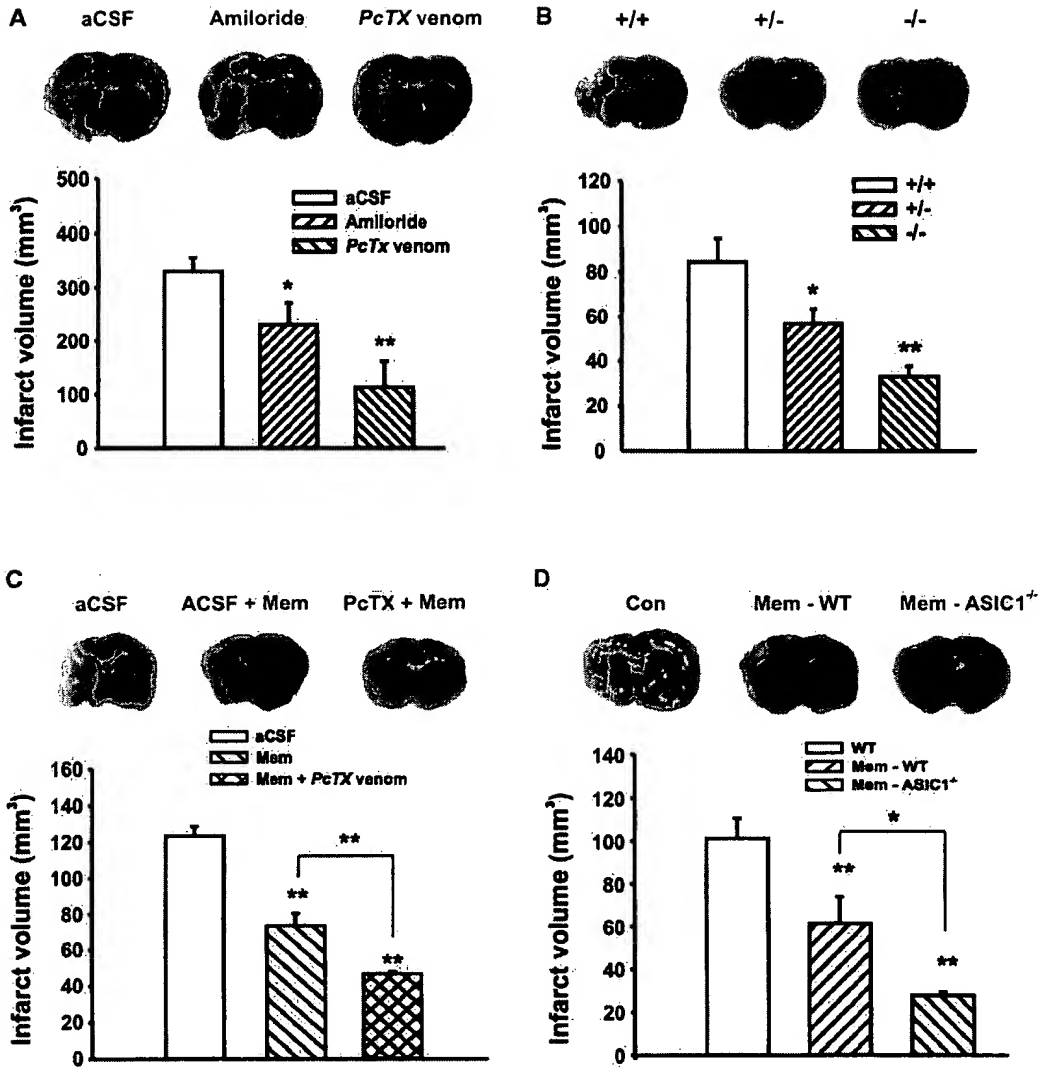

Figure 6. Neuroprotection by ASIC1 Blockade and ASIC1 Gene Knockout in Brain Ischemia In Vivo

(A) TTC-stained brain sections show infarct area (image) and volume (bar graph) in brains from aCSF (n = 7), amiloride (n =11), or *PcTX* venom (n = 5) injected rats. *$p < 0.05$ and **$p < 0.01$ compared with aCSF injected group.

(B) Reduction in infarct volume in brains from ASIC1$^{-/-}$ mice (n = 6 for each group). *$p < 0.05$ and **$p < 0.01$ compared with +/+ group.

(C) Reduction in infarct volume in brains from mice i.p. injected with 10 mg/kg memantine (Mem) or i.p. injection of memantine accompanied by i.c.v. injection of *PcTX* venom (500 ng/ml). **$p < 0.01$ compared with aCSF injection and between memantine and memantine plus *PcTX* venom (n = 5 in each group).

(D) Reduction in infarct volume in brains from either ASIC1$^{+/+}$ (wt) or ASIC1$^{-/-}$ mice i.p. injected with memantine (n = 5 in each group). *$p < 0.05$, and **$p < 0.01$.

tricularly 30 min before and after the ischemia. Based on the study by Westergaard (1969), the volume for cerebral ventricular and spinal cord fluid for 4-week-old rats is estimated to be ~60 μl. Assuming that the infused amiloride and *PcTX* were uniformly distributed in the CSF, we would expect a concentration of ~100 μM for amiloride and ~50 ng/ml for PcTX, which is a concentration found effective in our cell culture experiments. Infarct volume was determined by TTC staining (Bederson et al., 1986) at 24 hr following ischemia. Ischemia (100 min) produced an infarct volume of 329.5 ± 25.6 mm^3 in aCSF-injected rats (n = 7) but only 229.7 ± 41.1 mm^3 in amiloride-injected (n = 11, $p < 0.05$) and 130.4 ± 55.0 mm^3 (~60% reduction) in *PcTX* venom-injected rats (n = 5, $p < 0.01$) (Figure 6A).

We next used ASIC1$^{-/-}$ mice to further demonstrate the involvement of ASIC1a in ischemic brain injury in vivo. Male ASIC1$^{+/+}$, ASIC1$^{+/-}$, and ASIC1$^{-/-}$ mice (~25 g, with congenic C57Bl6 background) were subjected to 60 min MCAO as previously described (Stenzel-Poore et al., 2003). Consistent with the protection by pharmacological blockade of ASIC1a (above), −/− mice displayed significantly smaller (~61% reduction) infarct volumes (32.9 ± 4.7 mm^3, n = 6) as compared to +/+ mice (84.6 ± 10.6 mm^3, n = 6, $p < 0.01$). +/− mice also showed reduced infarct volume (56.9 ± 6.7 mm^3, n = 6, $p < 0.05$) (Figure 6B).

We then determined whether blockade of ASIC1a channels or knockout of the ASIC1 gene could provide additional protection in vivo in the setting of glutamate

receptor blockade. We selected the uncompetitive NMDA receptor antagonist memantine, as it has been recently used in successful clinical trials (Tariot et al., 2004). Memantine (10 mg/kg) was injected intraperitoneally (i.p.) into C57Bl6 mice immediately following 60 min MCAO and accompanied by intracerebroventricular injection (i.c.v.) of a total volume of 0.4 μl aCSF alone or aCSF containing *PcTX* venom (500 ng/ml) 15 min before and following ischemia. In control mice with i.p. injection of saline and i.c.v. injection of aCSF, 60 min MCAO induced an infarct volume of 123.6 ± 5.3 mm^3 (n = 5, Figure 6C). In mice with i.p. injection of memantine and i.c.v. injection of aCSF, the same duration of ischemia induced an infarct volume of 73.8 ± 6.9 mm^3 (n = 5, $p < 0.01$). However, in mice injected with memantine and *PcTX* venom, an infarct volume of only 47.0 ± 1.1 mm^3 was induced (n = 5, $p < 0.01$ compared with both control and memantine groups, Figure 6C). These data strongly suggest that blockade of homomeric ASIC1a can provide additional protection in in vivo ischemia in the setting of NMDA receptor blockade. Additional protection was also observed in $ASIC1^{-/-}$ mice treated with pharmacologic NMDA blockade (Figure 6D). In $ASIC^{+/+}$ mice i.p. injected with saline or 10 mg/kg memantine, 60 min MCAO induced an infarct volume of 101.4 ± 9.4 mm^3 or 61.6 ± 12.7 mm^3, respectively (n = 5 in each group, Figure 6D). However, in $ASIC1^{-/-}$ mice injected with memantine, the same ischemia duration induced an infarct volume of 27.7 ± 1.6 mm^3 (n = 5), significantly smaller than the infarct volume in $ASIC1^{+/+}$ mice injected with memantine ($p < 0.05$).

Discussion

Despite enormous recent progress defining cellular and molecular responses of the brain to ischemia, there is no effective treatment for stroke patients. Most notable are the failures of multicenter clinical trials of glutamate antagonists (Lee et al., 1999; Wahlgren and Ahmed, 2004). Here we demonstrate a new mechanism of ischemic brain injury and the role of ischemic acidosis in this biology. We show that ischemic injury in the setting of acidosis occurs via activation of Ca^{2+}-permeable ASICs, a newly described class of ligand-gated channels (Waldmann et al., 1997a; Waldmann and Lazdunski, 1998). This Ca^{2+} toxicity is independent of glutamate receptors or voltage-gated Ca^{2+} channels.

Using whole-cell patch-clamp recording in mixed cortical cultures, we demonstrate activation of ASIC currents in the range of pH_e that occurs commonly in ischemia. With Fura-2 fluorescent imaging and ion substitution protocols, we show ASICs flux Ca^{2+} in cortical neurons and do so in the presence of NMDA, AMPA, and voltage-gated Ca^{2+} channel blockade. Using in vitro cell toxicity models, we demonstrate that acidosis induces glutamate-independent neuronal injury, which is reduced by both nonspecific and specific ASIC1a antagonists, and by lowering $[Ca^{2+}]_e$. In addition, we show that neurons and COS-7 cells lacking ASIC1a are resistant to acid injury, while transfection of COS-7 cells with Ca^{2+}-permeable ASIC1a results in acid sensitivity. Using in vivo focal ischemia models, we demonstrate that pharmacologic blockade of ASIC1a channels and ASIC1a gene knockout both protected the brain from ischemic injury and do so in the presence of NMDA blockade.

Local $[H^+]$ is the agonist for ASICs functioning during normal synaptic transmission in the brain (Wemmie et al., 2002). This signaling is not injurious. However, ASICs respond also to the global, marked pH declines occurring in the ischemic brain. Within 1 min of global ischemia, pH_e falls from 7.2 to 6.5 (Simon et al., 1985), a level sufficient to activate ASIC1a channels, which have a $pH_{0.5}$ at 6.2. Remarkably, ischemia itself, modeled in vitro, markedly enhances the magnitude of ASIC response at a given level of acidosis, thus potentiating toxic Ca^{2+} loading in ischemic neurons. Furthermore, ischemia dramatically reduces desensitization of ASIC currents, signifying a possibility of long-lasting activity of ASICs during prolonged ischemic acidosis in vivo.

It has been shown in intact animals that brief global reductions of brain pH to 6.5 alone do not produce brain injury (Litt et al., 1985), nor does hypoxia alone (Miyamoto and Auer, 2000; Pearigen et al., 1996). However, our in vitro data suggest that the combination of ischemia (hypoxia) with acidosis (ischemic acidosis), as occurs in vivo, may cause marked brain injury through ischemia enhancing the toxic effect of ASIC1a channels. This argument is strongly supported by the finding that both ASIC1a blockade and ASIC1a gene knockout produce substantial (~60%) reduction in infarct volume.

Acidosis, apart from affecting ischemic brain injury via ASICs, affects the function of other channels as well. Particularly pertinent in ischemia is the acid blockade of the NMDA channels (Tang et al., 1990; Traynelis and Cull-Candy, 1990), which is protective against in vitro ischemic neuronal injury (Kaku et al., 1993; Giffard et al., 1990). This NMDA blockade in the ischemic brain by acidosis might in part explain the failure of NMDA antagonists in human stroke trials. Treatment of stroke with ASIC1a blockade could be particularly effective, as ischemic acidosis is serving as an additional therapy by blocking NMDA function.

As our in vitro studies showing a protective effect of ASIC1a blockade were performed in the presence of antagonists of NMDA, AMPA, and voltage-gated Ca^{2+} channels, the findings reported here may offer a new and robust neuroprotective strategy for stroke, either alone or in combination with other therapies (MacGregor et al., 2003). Further, we demonstrate in vivo that pharmacologic ASIC1a blockade or ASIC1a gene deletion offer more potent neuroprotection against stroke than NMDA antagonism.

Together, our studies suggest that activation of Ca^{2+}-permeable ASIC1a is a novel, glutamate-independent biological mechanism underlying ischemic brain injury. As the regulation of other potentially protective ASIC subunits also occurs in the ischemic brain (Johnson et al., 2001), these findings may help the design of novel therapeutic neuroprotective strategies for brain ischemia.

Experimental Procedures

Neuronal Culture

Following anesthesia with halothane, cerebral cortices were dissected from E16 Swiss mice or P1 $ASIC1^{+/+}$ and $ASIC1^{-/-}$ mice and incubated with 0.05% trypsin-EDTA for 10 min at 37°C. Tissues were then triturated with fire-polished glass pipettes and plated on poly-L-ornithine-coated 24-well plates or 25 × 25 mm glass coverslips at a density of 2.5×10^5 cells per well or 10^6 cells per coverslip. Neurons were cultured with MEM supplemented with 10% horse

serum (for E16 cultures) or Neurobasal medium supplemented with B27 (for P1 cultures) and used for electrophysiology and toxicity studies after 12 days. Glial growth was suppressed by addition of 5-fluoro-2-deoxyuridine and uridine, yielding cultured cells with ~90% neurons as determined by NeuN and GFAP staining (data not shown).

Electrophysiology

ASIC currents were recorded with whole-cell patch-clamp and fast-perfusion techniques. The normal extracellular solution (ECF) contained (in mM) 140 NaCl, 5.4 KCl, 25 HEPES, 20 glucose, 1.3 $CaCl_2$, 1.0 $MgCl_2$, 0.0005 TTX (pH 7.4), 320–335 mOsm. For low pH solutions, various amounts of HCl were added. For solutions with pH < 6.0, MES instead of HEPES was used for more reliable pH buffering. Patch electrodes contained (in mM) 140 CsF, 2.0 $MgCl_2$, 1.0 $CaCl_2$, 10 HEPES, 11 EGTA, 4 MgATP (pH 7.3), 300 mOsm. The Na^+-free solution consisted of 10 mM $CaCl_2$, 25 mM HEPES with equiosmotic NMDG or sucrose substituting for NaCl (Chu et al., 2002). A multibarrel perfusion system (SF-77B, Warner Instrument Co.) was employed for rapid exchange of solutions.

Cell Injury Assay—LDH Measurement

Cells were washed three times with ECF and randomly divided into treatment groups. MK801 (10 μM), CNQX (20 μM), and nimodipine (5 μM) were added in all groups to eliminate potential secondary activation of glutamate receptors and voltage-gated Ca^{2+} channels. Following acid incubation, neurons were washed and incubated in Neurobasal medium at 37°C. LDH release was measured in culture medium using the LDH assay kit (Roche Molecular Biochemicals). Medium (100 μl) was transferred from culture wells to 96-well plates and mixed with 100 μl reaction solution provided by the kit. Optical density was measured at 492 nm 30 min later, utilizing a microplate reader (Spectra Max Plus, Molecular Devices). Background absorbance at 620 was subtracted. The maximal releasable LDH was obtained in each well by 15 min incubation with 1% Triton X-100 at the end of each experiment.

Ca^{2+} Imaging

Cortical neurons grown on 25 × 25 mm glass coverslips were washed three times with ECF and incubated with 5 μM fura-2-acetoxymethyl ester for 40 min at 22°C, washed three times, and incubated in normal ECF for 30 min. Coverslips were transferred to a perfusion chamber on an inverted microscope (Nikon TE300). Cells were illuminated using a xenon lamp and observed with a 40× UV fluor oil-immersion objective lens, and video images were obtained using a cooled CCD camera (Sensys KAF 1401, Photometrics). Digitized images were acquired and analyzed in a PC controlled by Axon Imaging Workbench software (Axon Instruments). The shutter and filter wheel (Lambda 10-2) were controlled by the software to allow timed illumination of cells at 340 or 380 nm excitation wavelengths. Fura-2 fluorescence was detected at emission wavelength of 510 nm. Ratio images (340/380) were analyzed by averaging pixel ratio values in circumscribed regions of cells in the field of view. The values were exported to SigmaPlot for further analysis.

Fluorescein-Diacetate Staining and Propidium Iodide Uptake

Cells were incubated in ECF containing fluorescein-diacetate (FDA) (5 μM) and propidium iodide (PI) (2 μM) for 30 min followed by wash with dye-free ECF. Alive (FDA-positive) and dead (PI-positive) cells were viewed and counted on a microscope (Zeiss) equipped with epifluorescence at 580/630 nm excitation/emission for PI and 500/550 nm for FDA. Images were collected using an Optronics DEI-730 camera equipped with a BQ 8000 sVGA frame grabber and analyzed using computer software (Bioquant, TN).

Transfection of COS-7 Cells

COS-7 cells were cultured in MEM with 10% HS and 1% PenStrep (GIBCO). At ~50% confluence, cells were cotransfected with cDNAs for ASICs and GFP in pc^{DNA3} vector using FuGENE6 transfection reagents (Roche Molecular Biochemicals). DNA for ASICs (0.75 μg) and 0.25 μg of DNA for GFP were used for each 35 mm dish. GFP-positive cells were selected for patch-clamp recording 48 hr after transfection. For stable transfection of ASIC1a, 500 μg/ml G418 was added to culture medium 1 week following the transfection. The surviving G418-resistant cells were further plated and passed for >5 passages in the presence of G418. Cells were then checked with patch-clamp and immunofluorescent staining for the expression of ASIC1a.

Oxygen-Glucose Deprivation

Neurons were washed three times and incubated with glucose-free ECF at pH 7.4 or 6.0 in an anaerobic chamber (Model 1025, Forma Scientific) with an atmosphere of 85% N_2, 10% H_2, and 5% CO_2 at 35°C. Oxygen-glucose deprivation (OGD) was terminated after 1 hr by replacing the glucose-free ECF with Neurobasal medium and incubating the cultures in a normal cell culture incubator. With HEPES-buffered ECF used, 1 hr OGD slightly reduced pH from 7.38 to 7.28 (n = 3) and from 6.0 to 5.96 (n = 4).

Focal Ischemia

Transient focal ischemia was induced by suture occlusion of the middle cerebral artery (MCAO) in male rats (SD, 250–300 g) and mice (with congenic C57Bl6 background, ~25 g) anesthetized using 1.5% isoflurane, 70% N_2O, and 28.5% O_2 with intubation and ventilation. Rectal and temporalis muscle temperature was maintained at 37°C ± 0.5°C with a thermostatically controlled heating pad and lamp. Cerebral blood flow was monitored by transcranical LASER doppler. Animals with blood flow not reduced below 20% were excluded.

Animals were killed with chloral hydrate 24 hr after ischemia. Brains were rapidly removed, sectioned coronally at 1 mm (mice) or 2 mm (rats) intervals, and stained by immersion in vital dye (2%) 2,3,5-triphenyltetrazolium hydrochloride (TTC). Infarction area was calculated by subtracting the normal area stained with TTC in the ischemic hemisphere from the area of the nonischemic hemisphere. Infarct volume was calculated by summing infarction areas of all sections and multiplying by slice thickness. Rat intraventricular injection was performed by stereotaxic technique using a microsyringe pump with cannula inserted stereotactically at 0.8 mm posterior to bregma, 1.5 mm lateral to midline, and 3.8 mm ventral to the dura. All manipulations and analyses were performed by individuals blinded to treatment groups.

Acknowledgments

Supported by NIH grants, the American Heart Association, the Good Samaritan Foundation, the VA Research Career Development Award, and the Howard Hughes Medical Institute Biomedical Research Program. We thank Ms. Natasha Close for technical support, Drs. R. Waldmann and M. Lazdunski (Institut de Pharmacologie Moleculaire et Cellulaire, CNRS Valbonne, France) for ASIC clones, Dr. E.W. McCleskey (Vollum Institute, Portland) for COS-7 and CHO cells, and Dr. A. Scharenberg (University of Washington, Seattle) for Flag murine TRPM7/pCDNA4-TO cDNA.

Received: March 13, 2004
Revised: July 14, 2004
Accepted: July 26, 2004
Published: September 16, 2004

References

Aarts, M., Iihara, K., Wei, W.L., Xiong, Z.G., Arundine, M., Cerwinski, W., MacDonald, J.F., and Tymianski, M. (2003). A key role for TRPM7 channels in anoxic neuronal death. Cell *115*, 863–877.

Akopian, A.N., Chen, C.C., Ding, Y., Cesare, P., and Wood, J.N. (2000). A new member of the acid-sensing ion channel family. Neuroreport *11*, 2217–2222.

Allen, N.J., and Attwell, D. (2002). Modulation of ASIC channels in rat cerebellar Purkinje neurons by ischemia-related signals. J. Physiol. *543*, 521–529.

Alvarez de la Rosa, D., Zhang, P., Shao, D., White, F., and Canessa, C.M. (2002). Functional implications of the localization and activity of acid-sensitive channels in rat peripheral nervous system. Proc. Natl. Acad. Sci. USA *99*, 2326–2331.

Alvarez de la Rosa, D., Krueger, S.R., Kolar, A., Shao, D., Fitzsimonds, R.M., and Canessa, C.M. (2003). Distribution, subcellular localization and ontogeny of ASIC1 in the mammalian central nervous system. J. Physiol. *546*, 77–87.

Bassilana, F., Champigny, G., Waldmann, R., De Weille, J.R., Heurteaux, C., and Lazdunski, M. (1997). The acid-sensitive ionic channel subunit ASIC and the mammalian degenerin MDEG form a heteromultimeric H+-gated Na+ channel with novel properties. J. Biol. Chem. *272*, 28819–28822.

Bederson, J.B., Pitts, L.H., Germano, S.M., Nishimura, M.C., Davis, R.L., and Bartkowski, H.M. (1986). Evaluation of 2,3,5-triphenyltetrazolium chloride as a stain for detection and quantification of experimental cerebral infarction in rats. Stroke *17*, 1304–1308.

Benos, D.J., and Stanton, B.A. (1999). Functional domains within the degenerin/epithelial sodium channel (Deg/ENaC) superfamily of ion channels. J. Physiol. *520*, 631–644.

Benson, C.J., Eckert, S.P., and McCleskey, E.W. (1999). Acid-evoked currents in cardiac sensory neurons: a possible mediator of myocardial ischemic sensation. Circ. Res. *84*, 921–928.

Bevan, S., and Yeats, J. (1991). Protons activate a cation conductance in a sub-population of rat dorsal root ganglion neurones. J. Physiol. *433*, 145–161.

Bianchi, L., and Driscoll, M. (2002). Protons at the gate: DEG/ENaC ion channels help us feel and remember. Neuron *34*, 337–340.

Chen, C.C., England, S., Akopian, A.N., and Wood, J.N. (1998). A sensory neuron-specific, proton-gated ion channel. Proc. Natl. Acad. Sci. USA *95*, 10240–10245.

Chen, C.C., Zimmer, A., Sun, W.H., Hall, J., Brownstein, M.J., and Zimmer, A. (2002). A role for ASIC3 in the modulation of high-intensity pain stimuli. Proc. Natl. Acad. Sci. USA *99*, 8992–8997.

Choi, D.W. (1988a). Calcium-mediated neurotoxicity: relationship to specific channel types and role in ischemic damage. Trends Neurosci. *11*, 465–469.

Choi, D.W. (1988b). Glutamate neurotoxicity and diseases of the nervous system. Neuron *1*, 623–634.

Choi, D.W. (1995). Calcium: still center-stage in hypoxic-ischemic neuronal death. Trends Neurosci. *18*, 58–60.

Chu, X.P., Miesch, J., Johnson, M., Root, L., Zhu, X.M., Chen, D., Simon, R.P., and Xiong, Z.G. (2002). Proton-gated channels in PC12 cells. J. Neurophysiol. *87*, 2555–2561.

Dingledine, R., Borges, K., Bowie, D., and Traynelis, S.F. (1999). The glutamate receptor ion channels. Pharmacol. Rev. *51*, 7–61.

Escoubas, P., De Weille, J.R., Lecoq, A., Diochot, S., Waldmann, R., Champigny, G., Moinier, D., Menez, A., and Lazdunski, M. (2000). Isolation of a tarantula toxin specific for a class of proton-gated Na+ channels. J. Biol. Chem. *275*, 25116–25121.

Giffard, R.G., Monyer, H., Christine, C.W., and Choi, D.W. (1990). Acidosis reduces NMDA receptor activation, glutamate neurotoxicity, and oxygen-glucose deprivation neuronal injury in cortical cultures. Brain Res. *506*, 339–342.

Goldberg, M.P., and Choi, D.W. (1993). Combined oxygen and glucose deprivation in cortical cell culture: calcium-dependent and calcium-independent mechanisms of neuronal injury. J. Neurosci. *13*, 3510–3524.

Grunder, S., Geissler, H.S., Bassler, E.L., and Ruppersberg, J.P. (2000). A new member of acid-sensing ion channels from pituitary gland. Neuroreport *11*, 1607–1611.

Immke, D.C., and McCleskey, E.W. (2001). Lactate enhances the acid-sensing Na+ channel on ischemia-sensing neurons. Nat. Neurosci. *4*, 869–870.

Jia, Z., Agopyan, N., Miu, P., Xiong, Z., Henderson, J., Gerlai, R., Taverna, F.A., Velumian, A., MacDonald, J., Carlen, P., et al. (1996). Enhanced LTP in mice deficient in the AMPA receptor GluR2. Neuron *17*, 945–956.

Johnson, M.B., Jin, K., Minami, M., Chen, D., and Simon, R.P. (2001). Global Ischemia induces expression of acid-sensing ion channel 2a in rat brain. J. Cereb. Blood Flow Metab. *21*, 734–740.

Kaku, D.A., Goldberg, M.P., and Choi, D.W. (1991). Antagonism of non-NMDA receptors augments the neuroprotective effect of NMDA receptor blockade in cortical cultures subjected to prolonged deprivation of oxygen and glucose. Brain Res. *554*, 344–347.

Kaku, D.A., Giffard, R.G., and Choi, D.W. (1993). Neuroprotective effects of glutamate antagonists and extracellular acidity. Science *260*, 1516–1518.

Koh, J.Y., and Choi, D.W. (1987). Quantitative determination of glutamate mediated cortical neuronal injury in cell culture by lactate dehydrogenase efflux assay. J. Neurosci. Methods *20*, 83–90.

Krishtal, O. (2003). The ASICs: signaling molecules? Modulators? Trends Neurosci. *26*, 477–483.

Krishtal, O.A., and Pidoplichko, V.I. (1981). A receptor for protons in the membrane of sensory neurons may participate in nociception. Neuroscience *6*, 2599–2601.

Lee, J.M., Zipfel, G.J., and Choi, D.W. (1999). The changing landscape of ischaemic brain injury mechanisms. Nature Suppl. *399*, A7–14.

Lingueglia, E., De Weille, J.R., Bassilana, F., Heurteaux, C., Sakai, H., Waldmann, R., and Lazdunski, M. (1997). A modulatory subunit of acid sensing ion channels in brain and dorsal root ganglion cells. J. Biol. Chem. *272*, 29778–29783.

Litt, L., Gonzalez-Mendez, R., Severinghaus, J.W., Hamilton, W.K., Shuleshko, J., Murphy-Boesch, J., and James, T.L. (1985). Cerebral intracellular changes during supercarbia: an in vivo 31P nuclear magnetic resonance study in rats. J. Cereb. Blood Flow Metab. *5*, 537–544.

Longa, E.Z., Weinstein, P.R., Carlson, S., and Cummins, R. (1989). Reversible middle cerebral artery occlusion without craniectomy in rats. Stroke *20*, 84–91.

MacGregor, D.G., Avshalumov, M.V., and Rice, M.E. (2003). Brain edema induced by in vitro ischemia: causal factors and neuroprotection. J. Neurochem. *85*, 1402–1411.

McDonald, J.W., Bhattacharyya, T., Sensi, S.L., Lobner, D., Ying, H.S., Canzoniero, L.M., and Choi, D.W. (1998). Extracellular acidity potentiates AMPA receptor-mediated cortical neuronal death. J. Neurosci. *18*, 6290–6299.

McLennan, H. (1983). Receptors for the excitatory amino acids in the mammalian central nervous system. Prog. Neurobiol. *20*, 251–271.

Meldrum, B.S. (1995). Excitatory amino acid receptors and their role in epilepsy and cerebral ischemia. Ann. N Y Acad. Sci. *757*, 492–505.

Miyamoto, O., and Auer, R.N. (2000). Hypoxia, hyperoxia, ischemia, and brain necrosis. Neurology *54*, 362–371.

Nedergaard, M., Kraig, R.P., Tanabe, J., and Pulsinelli, W.A. (1991). Dynamics of interstitial and intracellular pH in evolving brain infarct. Am. J. Physiol. *260*, R581–R588.

Pearigen, P., Gwinn, R., and Simon, R.P. (1996). The effects in vivo of hypoxia on brain injury. Brain Res. *725*, 184–191.

Price, M.P., Snyder, P.M., and Welsh, M.J. (1996). Cloning and expression of a novel human brain Na+ channel. J. Biol. Chem. *271*, 7879–7882.

Price, M.P., Lewin, G.R., McIlwrath, S.L., Cheng, C., Xie, J., Heppenstall, P.A., Stucky, C.L., Mannsfeldt, A.G., Brennan, T.J., Drummond, H.A., et al. (2000). The mammalian sodium channel BNC1 is required for normal touch sensation. Nature *407*, 1007–1011.

Price, M.P., McIlwrath, S.L., Xie, J., Cheng, C., Qiao, J., Tarr, D.E., Sluka, K.A., Brennan, T.J., Lewin, G.R., and Welsh, M.J. (2001). The DRASIC cation channel contributes to the detection of cutaneous touch and acid stimuli in mice. Neuron *32*, 1071–1083.

Rehncrona, S. (1985). Brain acidosis. Ann. Emerg. Med. *14*, 770–776.

Rothman, S.M., and Olney, J.W. (1986). Glutamate and the pathophysiology of hypoxic-ischemic brain damage. Ann. Neurol. *19*, 105–111.

Sattler, R., Xiong, Z., Lu, W.Y., Hafner, M., MacDonald, J.F., and Tymianski, M. (1999). Specific coupling of NMDA receptor activation to nitric oxide neurotoxicity by PSD-95 protein. Science *284*, 1845–1848.

Siesjo, B.K., Katsura, K., and Kristian, T. (1996). Acidosis-related damage. Adv. Neurol. *71*, 209–233.

Simon, R.P., Swan, J.H., Griffiths, T., and Meldrum, B.S. (1984).

Blockade of N-methyl-D-aspartate receptors may protect against ischemic damage in the brain. Science *226*, 850–852.

Simon, R.P., Benowitz, N., Hedlund, R., and Copeland, J. (1985). Influence of the blood-brain pH gradient on brain phenobarbital uptake during status epilepticus. J. Pharmacol. Exp. Ther. *234*, 830–835.

Sluka, K.A., Price, M.P., Breese, N.M., Stucky, C.L., Wemmie, J.A., and Welsh, M.J. (2003). Chronic hyperalgesia induced by repeated acid injections in muscle is abolished by the loss of ASIC3, but not ASIC1. Pain *106*, 229–239.

Stenzel-Poore, M.P., Stevens, S.L., Xiong, Z., Lessov, N.S., Harrington, C.A., Mori, M., Meller, R., Rosenzweig, H.L., Tobar, E., Shaw, T.E., et al. (2003). Effect of ischaemic preconditioning on genomic response to cerebral ischaemia: similarity to neuroprotective strategies in hibernation and hypoxia-tolerant states. Lancet *362*, 1028–1037.

Swanson, R.A., Farrell, K., and Simon, R.P. (1995). Acidosis causes failure of astrocyte glutamate uptake during hypoxia. J. Cereb. Blood Flow Metab. *15*, 417–424.

Tang, C.M., Dichter, M., and Morad, M. (1990). Modulation of the N-methyl-D-aspartate channel by extracellular H+. Proc. Natl. Acad. Sci. USA *87*, 6445–6449.

Tariot, P.N., Farlow, M.R., Grossberg, G.T., Graham, S.M., McDonald, S., and Gergel, I. (2004). Memantine treatment in patients with moderate to severe Alzheimer disease already receiving donepezil: a randomized controlled trial. JAMA *291*, 317–324.

Tombaugh, G.C., and Sapolsky, R.M. (1993). Evolving concepts about the role of acidosis in ischemic neuropathology. J. Neurochem. *61*, 793–803.

Traynelis, S.F., and Cull-Candy, S.G. (1990). Proton inhibition of N-methyl-D-aspartate receptors in cerebellar neurons. Nature *345*, 347–350.

Ugawa, S., Ueda, T., Ishida, Y., Nishigaki, M., Shibata, Y., and Shimada, S. (2002). Amiloride-blockable acid-sensing ion channels are leading acid sensors expressed in human nociceptors. J. Clin. Invest. *110*, 1185–1190.

Varming, T. (1999). Proton-gated ion channels in cultured mouse cortical neurons. Neuropharmacology *38*, 1875–1881.

Wahlgren, N.G., and Ahmed, N. (2004). Neuroprotection in cerebral ischaemia: facts and fancies—the need for new approaches. Cerebrovasc. Dis. Supp. *17*, 153–166.

Waldmann, R., and Lazdunski, M. (1998). H(+)-gated cation channels: neuronal acid sensors in the NaC/DEG family of ion channels. Curr. Opin. Neurobiol. *8*, 418–424.

Waldmann, R., Champigny, G., Bassilana, F., Heurteaux, C., and Lazdunski, M. (1997a). A proton-gated cation channel involved in acid-sensing. Nature *386*, 173–177.

Waldmann, R., Bassilana, F., de Weille, J., Champigny, G., Heurteaux, C., and Lazdunski, M. (1997b). Molecular cloning of a non-inactivating proton-gated Na+ channel specific for sensory neurons. J. Biol. Chem. *272*, 20975–20978.

Waldmann, R., Champigny, G., Lingueglia, E., De Weille, J., Heurteaux, C., and Lazdunski, M. (1999). H(+)-gated cation channels. Ann. N Y Acad. Sci. *868*, 67–76.

Wemmie, J.A., Chen, J., Askwith, C.C., Hruska-Hageman, A.M., Price, M.P., Nolan, B.C., Yoder, P.G., Lamani, E., Hoshi, T., Freeman, J.H., and Welsh, M.J. (2002). The acid-activated ion channel ASIC contributes to synaptic plasticity, learning, and memory. Neuron *34*, 463–477.

Wemmie, J.A., Askwith, C.C., Lamani, E., Cassell, M.D., Freeman, J.H., Jr., and Welsh, M.J. (2003). Acid-sensing ion channel 1 is localized in brain regions with high synaptic density and contributes to fear conditioning. J. Neurosci. *23*, 5496–5502.

Westergaard, E. (1969). The cerebral ventricles of the rat during growth. Acta Anat. (Basel) *74*, 405–423.

Xiong, Z., Lu, W., and MacDonald, J.F. (1997). Extracellular calcium sensed by a novel cation channel in hippocampal neurons. Proc. Natl. Acad. Sci. USA *94*, 7012–7017.

Yermolaieva, O., Leonard, A.S., Schnizler, M.K., Abboud, F.M., and Welsh, M.J. (2004). Extracellular acidosis increases neuronal cell calcium by activating acid-sensing ion channel 1a. Proc. Natl. Acad. Sci. USA *101*, 6752–6757.

Ying, W., Han, S.K., Miller, J.W., and Swanson, R.A. (1999). Acidosis potentiates oxidative neuronal death by multiple mechanisms. J. Neurochem. *73*, 1549–1556.

Spider venom helps researchers elucidate role of acidosis in stroke

The roles of NMDA receptors and calcium-ion influx in stroke are well established, but researchers have now discovered a new link between acid-sensitive ion channels (ASICs) and ischaemia-induced brain injury. ASICs, like NMDA receptors, have been implicated in neuronal plasticity.

"Our findings that the ASIC1a blockers and gene knockout can dramatically reduce the amount of brain injury suggest that targeting these channels may prove to be an effective stroke therapy", says lead author Zhigang Xiong (Robert S Dow Neurobiology Laboratories, Portland, OR, USA). Rona Giffard (Stanford University, CA, USA) comments "This report is the first to demonstrate the possibility that calcium influx via ASIC channels can contribute to neuronal ischaemic death".

Xiong and co-workers studied the role of ASICs in vitro and in animal models. The researchers found that acidosis activates ASICs in vitro, causing an influx of calcium ions into neurons. This influx of calcium could be blocked by amiloride, a non-specific ASIC blocker, and by *PcTX* venom (from the tarantula *Psalmopoeus cambridgei*), a blocker specific to the ASIC1a subunit. Xiong's team also report that oxygen glucose deprivation

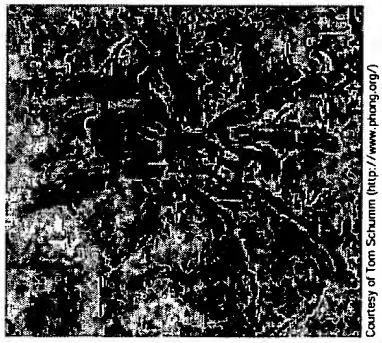

Courtesy of Tom Schumm (http://www.phang.org/)

Psalmopoeus cambridgei

increases ASIC currents in neurons and enhances acidosis-induced neuronal injury. This response was absent in transgenic mice lacking ASIC1a.

The researchers went on to investigate the effects of amiloride and *PcTX* in a rat model of stroke. Both compounds were injected intracerebroventricularly 30 mins before and after ischaemia, and both reduced infarct volume. Furthermore, the researchers found that infarct volumes were larger in wild-type mice compared with transgenic mice lacking the ASIC1a subunit. Finally, they compared the effects of the NMDA antagonist memantine with *PcTX* venom. Interestingly, a combination of the two compounds produced the largest reduction in infarct volume (*Cell* 2004; **118**: 687–98).

According to John Wood (University College London, UK), these results are important for two reasons. "Firstly, non-toxic molecules such as amiloride can be rapidly assessed for their utility as neuroprotectants", says Wood. "Second, a possible synergy between NMDA blockers and ASIC1a blockers may be important for the development of more effective neuroprotective strategies".

"The identification of a new anti-ischaemic target is exciting", says Giffard, "but the possibility that it can be developed into an efficacious treatment for stroke at this point must remain a hopeful future possibility".

Rebecca Love

Good fats prevent dendritic damage in mouse model of AD

A diet deficient in docosahexaenoic acid (DHA), a polyunsaturated fatty acid (PFA), may increase the risk of Alzheimer's disease (AD) by depleting postsynaptic proteins, thus causing dendritic and cognitive dysfunction, according to research in a strain of transgenic mice (Tg2576) expressing the human APP protein. "The omega-3 fatty acid, DHA, protects against Alzheimer-gene induced dramatic loss of postsynaptic dendritic spine protein, drebrin, that helps regulate actin dynamics", says senior author Greg Cole (University of California, Los Angeles, CA, USA).

Cole and colleagues examined protein expression in Tg2576 mice and in post-mortem brain tissue from patients with AD and found depletion of drebrin in both cases. In addition, drebrin loss was greater in old Tg2576 mice than in young mice. The researchers went on to investigate the effects of depleting omega-3 PFAs in the diet of Tg2576 mice. They found that drebrin and PSD-95, another postsynaptic protein, were depleted, but presynaptic proteins were unaffected. Adding DHA back in to the diet abolished the depletion of drebrin. Both drebrin and PSD-95 are known to have important roles in cognitive function.

DHA prevents caspase activity by activation of the PI3-kinase–Akt pathway. Therefore, the authors hypothesise, reduced DHA may increase caspase cleavage of actin, resulting in dendritic dysfunction. Indeed, dietary restriction of omega-3 PFAs resulted in a 95% reduction in a PI3-kinase subunit in the brains of Tg2576 mice. Again, this deficiency could be partly restored by feeding the mice DHA (*Neuron* 2004; **43**: 633–45).

What are the cognitive consequences of a PFA-restricted diet in these mice? When Cole's team tested Tg2576 mice on the restricted diet in the Morris water maze test, which assesses memory function, their performance was significantly impaired.

"Because of epidemiological data on fish and DHA as factors associated with reduced risk for AD, the likelihood that our results in mice with a human AD gene are clinically relevant is higher than would be expected with agents with support only from in vitro and animal model studies", Cole concludes. "For those who wish to hedge their bets . . . ", write Lennart Mucke and Robert Pitas in an accompanying commentary (*Neuron* 2004; **43**: 596–99). ". . . eat more fish".

Rebecca Love

CLINICAL IMPLICATIONS OF BASIC RESEARCH

Limiting Stroke-Induced Damage by Targeting an Acid Channel

Morris Benveniste, Ph.D., and Raymond Dingledine, Ph.D.

Why are brain neurons so much more susceptible to ischemic injury than, say, muscle or skin tissue? A clue is provided by work showing that the activation of neuronal acid-sensing ion channel 1 (ASIC1) can lead to neuronal death.[1-3] A recent study by Xiong et al.[3] places this observation in the context of stroke by showing that the activation of ASIC1 during the metabolic acidosis accompanying experimental stroke contributes substantially to subsequent brain injury.

Excessive loading of calcium into neurons through *N*-methyl-D-aspartate (NMDA) receptors and voltage-dependent calcium channels is thought to be one of the triggers of neuronal injury after ischemic stroke. ASIC1 contributes to this process and is a member of the family of epithelial sodium channels located in the brain. Protein subunits (e.g., the ASIC1 splice variant ASIC1a) assemble as multimeric complexes to form voltage-insensitive, amiloride-sensitive channels in the surface membrane. In contrast to many calcium-permeable neurotransmitter-receptor channels, such as nicotinic acetylcholine receptors and glutamate receptors, which are inhibited as pH falls, acid-sensing ion channels are activated as pH falls. ASIC1a begins to open when the pH falls below approximately 7.0, and its activation is half maximal at a pH of 6.2 — a pH range that should occur within the penumbra

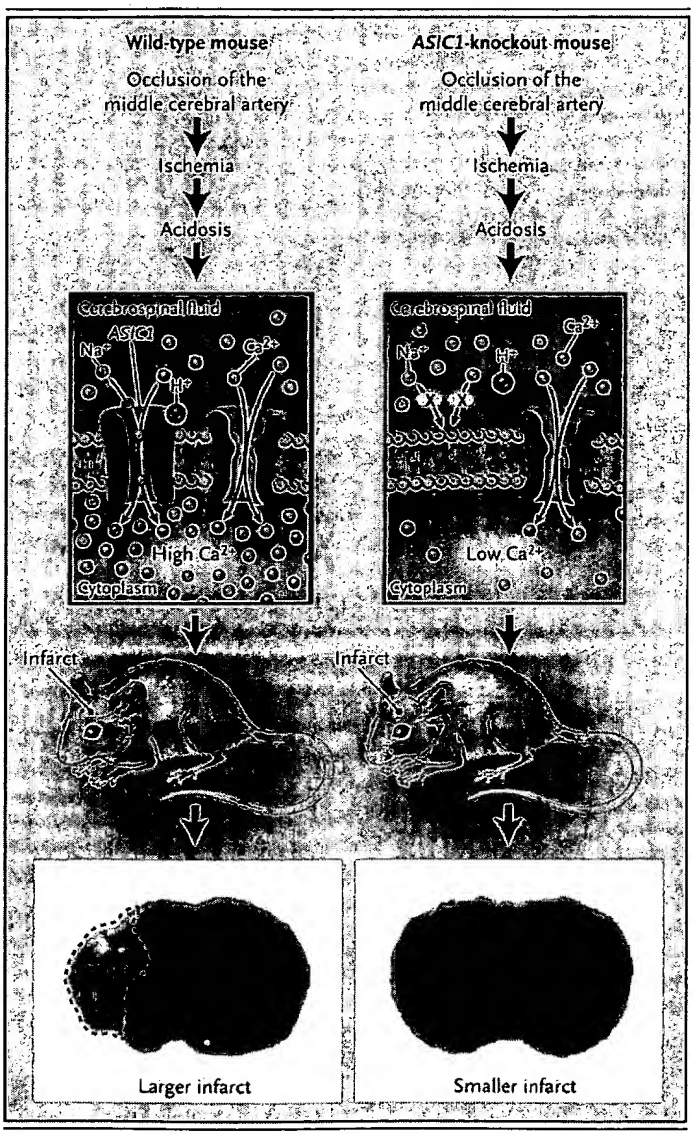

Figure 1. Involvement of the *ASIC1* Channel during Stroke.

In a recent study, Xiong et al.[3] used a mouse model of ischemic stroke, in which occlusion of the middle cerebral artery leads to ischemia, acidosis, and ultimately, stroke, to evaluate the influence of an acidosis-sensitive ion channel on the size of the resulting infarct. The middle cerebral artery of wild-type mice or mice in which the *ASIC1* gene had been knocked out was occluded for 1 hour, and the volume of the infarct was assayed 24 hours later by staining coronal sections (bottom panels) with a vital dye. Wild-type mice had larger infarcts than the *ASIC1*-knockout mice. Other evidence obtained by Xiong et al.[3] suggests that neurotoxicity is partially mediated through the activation of ASIC1a, which, in turn, causes an increase in intracellular calcium concentrations, possibly through the acid-sensing ion channel itself, with or without the assistance of other calcium-permeable channels (middle panels). CSF denotes cerebrospinal fluid.

and core of an infarct. Moreover, the activation of acid-sensing ion channels is promoted by stretching of the membrane, the release of arachidonic acid, the production of lactate,[1,4] or a drop in extracellular calcium concentrations[5] — conditions that occur within an infarct as cells swell, calcium-dependent phospholipases are activated, and calcium influx occurs.

Xiong et al.[3] used both in vitro and in vivo methods to determine whether acidosis or an ischemic insult could cause the calcium-dependent death of neurons through ASIC1. Using the release of lactate dehydrogenase to measure the incidence of neuronal death in cortical cultures, they showed that the neurotoxic effect of exposure to a medium with a pH of 6.0 was inhibited by both amiloride and the ASIC1a-specific antagonist psalmotoxin 1 (PcTX1), a component of the venom of a Trinidad Chevron tarantula. Acid-mediated neurotoxicity was absent in mice deficient in the *ASIC1* gene. Taken together, these results suggest that ASIC1 can cause a clinically significant incidence of calcium-mediated death of neurons in the presence of acidosis in vitro.

Excess influx of calcium is known to trigger neuronal degeneration, but whether ASIC1 itself is an important portal for the entry of calcium is a matter of controversy. We know that acidosis induces a cytoplasmic increase in calcium concentrations in ASIC1-transfected cells.[2] Xiong et al.[3] show that brief exposure of cortical neurons to a medium with a pH of 6.0 in the presence of a cocktail of glutamate and calcium-channel blockers leads to an increase in calcium concentrations within the cytoplasm that can be blocked by exposure to amiloride or PcTX1. The acidosis-triggered increase in calcium was absent in neurons isolated from mice that were deficient in ASIC1. The authors conclude that calcium enters directly through the acid-sensing ion channels under acidic conditions, although other routes of calcium entry are probably also involved.

Finally, using genetic and pharmacologic strategies, Xiong et al.[3] showed that ASIC1 mediates neuronal death in vivo in a mouse model of stroke (Fig. 1). The volume of infarcts caused by transient occlusion of the middle cerebral artery could be reduced by intraventricular injections of amiloride or PcTX1 and was also smaller in mice lacking the *ASIC1* gene than in wild-type mice. The addition of PcTX1 or a deficiency of ASIC1 conferred additional neuroprotection in mice treated with memantine (which blocks the NMDA receptor), suggesting that ASIC1 has a direct role in mediating neurotoxicity.

The report by Xiong et al.[3] points the way to a neuroprotective strategy for stroke — namely, to develop a small-molecule inhibitor of ASIC1 or its components. The current treatment of stroke relies on the use of thrombolytic agents, which are of demonstrable value only if delivered within three hours after the onset of stroke. Although potential side effects must be considered, a small-molecule inhibitor of acid-sensing ion channels could be an attractive option, because these channels should be relatively quiescent under nonacidotic conditions. The context-dependent activation of ASIC1 with acidification makes this cation channel a particularly intriguing target for new stroke therapies.

Dr. Dingledine reports holding equity in NeurOp.

From the Department of Physiology and Pharmacology, Sackler School of Medicine, Tel Aviv University, Tel Aviv, Israel (M.B.); and the Department of Pharmacology, Emory University School of Medicine, Atlanta (M.B., R.D.).

1. Allen NJ, Attwell D. Modulation of ASIC channels in rat cerebellar Purkinje neurons by ischaemia-related signals. J Physiol 2002; 543:521-9.
2. Yermolaieva O, Leonard AS, Schnizler MK, Abboud FM, Welsh MJ. Extracellular acidosis increases neuronal cell calcium by activating acid-sensing ion channel 1a. Proc Natl Acad Sci U S A 2004;101: 6752-57.
3. Xiong ZG, Zhu XM, Chu XP, et al. Neuroprotection in ischemia: blocking calcium-permeable acid-sensing ion channels. Cell 2004; 118:687-98.
4. Immke DC, McCleskey EW. Lactate enhances the acid-sensing Na+ channel on ischemia-sensing neurons. Nat Neurosci 2001;4: 869-70.
5. *Idem.* Protons open acid-sensing ion channels by catalyzing relief of Ca2+ blockade. Neuron 2003;37:75-84.